Investigation of the immunological cross-reactivity between *Plasmodium vivax* Duffy Binding Protein and *Plasmodium falciparum* VAR2CSA for vaccine development

by

Catherine J. Mitran

A thesis submitted in partial fulfillment of the requirements for the degree of

Doctor of Philosophy

in

Public Health

School of Public Health
University of Alberta

Abstract

Worldwide, an estimated 30 million pregnancies are at risk of malaria infection each year. In pregnancy, *Plasmodium falciparum* parasites express a protein called VAR2CSA that mediates adherence of infected red blood cells (iRBCs) to chondroitin sulfate A (CSA) in the placenta. VAR2CSA antibodies are acquired during infection in pregnancy and are associated with protection from placental malaria, which can cause pre-term birth, low birth weight, spontaneous abortion, maternal anemia and even infant and maternal mortality. We previously observed that men and children in Colombia had antibodies to VAR2CSA, but the origin of these antibodies was unknown. We hypothesized that infection with *P. vivax* elicited antibodies to epitopes that are conserved across the structurally related Duffy Binding-like (DBL) domains found in the *P. vivax* antigen, PvDBP, and VAR2CSA.

We analyzed sera from nonpregnant Colombians and Brazilians exposed to *P. vivax* and monoclonal antibodies raised against the DBL domain of PvDBP (DBPII). We found that over 50% of individuals had antibodies that recognized VAR2CSA. Affinity-purified DBPII human antibodies and a DBPII monoclonal antibody, called 3D10, recognized VAR2CSA, showing that PvDBP exposure can give rise to cross-reactive antibodies. Importantly 3D10 also inhibited parasite binding to CSA, which is the primary *in vitro* correlate of protection against placental malaria. These data suggest that PvDBP induces antibodies that recognize VAR2CSA and can block parasite adhesion to CSA, revealing a novel mechanism of cross-species immune recognition to falciparum malaria.

Next, we investigated the cross-reactive epitopes in PvDBP and VAR2CSA. We determined that the epitope which elicits cross-reactive antibodies in PvDBP is contained within the subdomain 1 (SD1) region. Notably, human antibodies affinity purified against a synthetic SD1

peptide blocked parasite adhesion to CSA *in vitro.* The epitope in SD1 is subdominant and highly conserved in PvDBP, and in turn, SD1 antibodies target cryptic epitopes in *P. falciparum* VAR2CSA. The epitopes in VAR2CSA that are recognized by vivax-derived cross-reactive antibodies are distinct from those recognized by VAR2CSA immune serum.

We then attempted to exploit this cross-reactivity to develop a peptide vaccine against against VAR2CSA based on the epitope that generated 3D10. We mapped the minimal binding epitope for 3D10 to a peptide in SD1. However, this peptide did not elicit cross-reactive VAR2CSA antibodies in mice. When we tested 3D10 against a broader, overlapping peptide array spanning SD1, we found that it recognized a discontinuous epitope consisting of three segments of SD1. To preserve the native structure of the epitope as much as possible, we used a synthetic scaffold to conformationally-constrain the SD1 peptide and coupled it to a carrier protein. Immunizations with this peptide, $SD1_{CLIPS,}$ elicited antibodies in mice and a rabbit that cross-reacted with VAR2CSA. However, the cross-reactive antibodies were at low titre in the sera and bound to VAR2CSA with low avidity. We then affinity purified the cross-reactive IgG from the anti-$SD1_{CLIPS}$ rabbit serum on a column coated with VAR2CSA. The cross-reactive IgG recognized native VAR2CSA on the surface of RBCs infected with three different strains of *P. falciparum*. However, the antibodies did not block parasite adhesion to CSA or mediate opsonic phagocytosis of iRBCs, *in vitro*.

We then tried several approaches to enhance the cross-reactive antibody response elicited by $SD1_{CLIPS}$ immunizations. First, we compared three different adjuvants and found that formulation with GLA-SE elicited a higher titre of cross-reactive antibodies in mice, compared to either GLA-LSQ or Complete Freund's Adjuvant. Next, we employed a heterologous prime/boost strategy, in which mice received a boost with recombinant VAR2CSA following immunizations

with SD1$_{CLIPS}$. However, compared to control mice, a VAR2CSA boost did not enhance the cross-reactive antibody response. We also tested whether exposure to native VAR2CSA on the surface of iRBCs would boost the cross-reactive antibodies generated through SD1$_{CLIPS}$ immunizations. But, similar to the heterologous recombinant protein boost, injection with iRBCs expressing VAR2CSA did not boost the cross-reactive antibodies in mice.

SD1$_{CLIPS}$ is not a viable vaccine candidate in its current state. However, this work has laid a foundation for further immunization studies with second generation SD1$_{CLIPS}$-based vaccine candidates. The fact that immunizations with a peptide from PvDBP elicited antibodies in a rabbit that cross-reacted with native VAR2CSA from three different strains of *P. falciparum*, shows the potential of targeting conserved epitopes to elicit strain-transcending immune responses.

Preface

Portions of Chapter 1 and 6 have previously been published as Mitran CJ, Yanow SK. The Case for Exploiting Cross-Species Epitopes in Malaria Vaccine Design. *Front Immunol.* 2020 Feb 27;11:335 (doi: 10.3389/fimmu.2020.00335). S.K. Yanow and I jointly wrote this manuscript.

The research presented in Chapters 2, 3, 4 and 5 of this thesis was undertaken as part of an international collaboration led by my supervisor, Dr. Stephanie Yanow. Chapter 2 was published as Gnidehou S, Mitran CJ, Arango E, Banman S, Mena A, Medawar E, Lima BAS, Doritchamou J, Rajwani J, Jin A, Gavina K, Ntumngia F, Duffy P, Narum D, Ndam NT, Nielsen MA, Salanti A, Kano FS, Carvalho LH, Adams JH, Maestre A, Good MF, Yanow SK. Cross-Species Immune Recognition Between *Plasmodium vivax* Duffy Binding Protein Antibodies and the *Plasmodium falciparum* Surface Antigen VAR2CSA. *J Infect Dis.* 2019. 219(1):110-120 (doi: 10.1093/infdis/jiy467). I performed ELISAs, IBAs, affinity purifications, parasite culture, flow cytometry and contributed to data analysis and preparation of the manuscript. S. Gnidehou performed ELISAs and contributed to data analysis, conceptualization of the study and preparation of the manuscript. E. Arango and A.E. Maestre provided human sera samples from Colombia and F.S. Kano and L.H. Carvalho provided human sera samples from Brazil. S. Banman performed ELISAs and IF assays. B.A.S. Lima performed ELISAs. J. Rajwani performed sequence alignments. E. Medawar and A. Jin produced recombinant DBL5ε protein and D. Narum produced recombinant DBL4ε protein. J. Doritchamou performed SPR experiments under the supervision of P. Duffy. F. Ntumngia, N.T. Ndam, M.A. Nielsen, A. Salanti and J.H. Adams contributed reagents. M.F. Good contributed to the conceptualization of

the study and S.K. Yanow contributed to the conceptualization of the study and preparation of the manuscript.

Chapter 3 was published as Mitran CJ, Mena A, Gnidehou S, Banman S, Arango E, Lima BAS, Lugo H, Ganesan A, Salanti A, Mbonye AK, Ntumngia F, Barakat K, Adams JH, Kano FS, Carvalho LH, Maestre AE, Good MF, Yanow SK. Antibodies to Cryptic Epitopes in Distant Homologues Underpin a Mechanism of Heterologous Immunity between *Plasmodium vivax* PvDBP and *Plasmodium falciparum* VAR2CSA. *mBio*. 2019. 10(5):e02343-19 (doi: 10.1128/mBio.02343-19). I prepared structural models in PyMol, performed ELISAs, parasite culture, affinity purifications, IBAs and animal immunizations (performed at the University of Alberta), contributed to data analysis, and jointly conceived the study and wrote the manuscript with M.F. Good and S.K. Yanow. A. Mena performed ELISAs, affinity purifications, IBAs and contributed to data analysis. S. Banman and S. Gnidehou performed ELISAs. E. Arango and A.E. Maestre provided human sera samples from Colombia and F.S. Kano and L.H. Carvalho provided human sera samples from Brazil. B.A.S Lima and H. Lugo performed ELISAs. A. Ganesan performed structural analysis and prepared structural models in PyMol under the supervision of K. Barakat. F. Ntumngia, A. Salanti and J.H. Adams contributed key reagents. A.K. Mbonye contributed to sample collection in Uganda.

Some of Chapter 4 was published as Mitran CJ, Higa LM, Good MF, Yanow SK. Generation of a Peptide Vaccine Candidate against Falciparum Placental Malaria Based on a Discontinuous Epitope. *Vaccines.* 2020. 8(3):392 (doi: 10.3390/vaccines8030392). I prepared protein structure images in PyMol, performed mouse immunizations, ELISAs, affinity purifications, flow cytometry, IBAs, opsonic phagocytosis experiments and data analysis and

jointly conceived the study and wrote the manuscript with S.K. Yanow. L.M. Higa performed ELISAs and M.F. Good contributed to study conceptualization.

Data in Chapter 5 has not been published. I performed animal immunizations, ELISAs, flow cytometry and data analysis and jointly conceived the study with S.K. Yanow and M.F. Good. L.M. Higa also performed ELISAs.

This work is dedicated to the memory of my beloved friend, Dr. Farah Elawar. Farah was incomparably kind, outrageously funny, a brilliant scientist and an absolute force of nature.

"There are some who bring a light so great to the world that even after they have gone the light remains."

— Unknown

Acknowledgements

First and foremost, I would like to thank my supervisor, Dr. Stephanie Yanow. You are an absolutely brilliant scientist and an even better mentor and friend. Working in your lab I learned so much about malaria and scientific research in general, but most importantly I discovered a passion for infectious disease research that will guide my career for years to come. You gave me the independence and encouragement to follow many of my research tangents, but always stopped me from going too far down the rabbit hole. I can never thank you enough for the incredible opportunities, experiences and support that you have given me over the past 5 years.

Secondly, I want to thank my committee members, Dr. Michael Hawkes and Dr. Patrick Hanington. Your guidance and encouragement throughout this program have been invaluable. To Dr. Michael Good, I cannot thank you enough for your advice and support. Your wisdom and knowledge are only matched by your dedication and enthusiasm, and I am so fortunate to have had the chance to get to know you. Thank you to our collaborators in Uganda and Colombia: Dr. Anthony Mbonye, Dr. Eliana Arango and Dr. Amanda Maestre. Without your contributions, this research would not have been possible.

I would also like to thank the many incredible people that I have met throughout this journey. From the people that I was fortunate enough to share lab space with, to the friends that I made halfway around the world; you all made this a wild ride. Dr. Sedami Gnidehou, Dr. Ken Gavina, Dr. Brian Taylor, Farah Elawar, Hannah Brooks, Jessica Dooley, Jamie-Lee Mills, Angie Mena, Dr. Ninad Mehta, Maddy Wiebe, and many more, thank you for all the knowledge you shared with me and the laughs along the way. Also, thank you to everyone in the MMI Department for making the last 5 years so enjoyable and to the HSLAS staff who worked tirelessly to ensure that my mice were happy and healthy.

Finally, I want to thank the funders, without whom this work would not have been possible. Thank you to the University of Alberta Li Ka Shing Institute of Virology, NSERC, NIH and CIHR for supporting this work and to CIHR, NSERC, Alberta Innovates, WCHRI and the University of Alberta for providing me with funding.

Table of Contents

List of tables

List of figures

Chapter 1

Chapter 2

Chapter 3

Chapter 4

Chapter 5

Chapter 6

List of Abbreviations

ABTS - 2,2′-azino-di-3-ethylbenzthiazoline sulfonate
AMA-1 - apical membrane antigen 1
Aoa - aminooxyacetic acid
API - annual parasitic index (number of malaria cases/1,000 inhabitants)
ARDS - acute respiratory distress syndrome
AU – arbitrary unit
BSA – bovine serum albumin
CD36 – cluster of differentiation 36
CFA - complete Freund's adjuvant
CLIPS - Chemical Linkage of Peptides onto Scaffolds
CSA – chondroitin sulfate A
CSP - circumsporozoite surface protein
CSPGs - chondroitin sulfate proteoglycans
DAPI – 4',6-diamidino-2-phenylindole
DARC – Duffy Receptor for Chemokines
DBL – Duffy binding-like
DMF - dimethylformamide
DNA – deoxyribonucleic acid
DT - diphtheria toxoid
DTT - dithiothreitol
EBA - erythrocyte binding antigen
EBP2 - erythrocyte binding protein 2
ELISA – enzyme-linked immunosorbent assay
EtBr - ethidium bromide
GLA-LSQ - glucopyranosyl lipid adjuvant liposomal formulation containing QS-21/saponin
GLA-SE - GLA-stable emulsion
HEPES – 4-(2-hydroxyethyl)-1-perazineethanesulfonic acid
HRP - horse radish peroxidase
HSP - heat shock protein
IBA – inhibition of binding assay
ICAM-1 - Intercellular Adhesion Molecule 1
ID - interdomain
IF - immunofluorescence
IF assay - incomplete Freund's adjuvant
IgG - immunoglobulin G
IL - interleukin

iRBC – infected RBC
kDa - kilodalton
KLH - keyhole limpet hemocyanin
mAb - monoclonal antibody
MiP – malaria in pregnancy
MSP - merozoite surface protein
NaSCN - sodium thiocyanate
NK - natural killer
NLRP3 - NLR family pyrin domain containing 3
OD - optical density
PBS – phosphate-buffered saline
PfEMP1 - *Plasmodium falciparum* erythrocyte membrane protein 1
PfRBHs - *Plasmodium falciparum* reticulocyte-binding homologues
PvDBP - *Plasmodium vivax* Duffy binding protein
qPCR - quantitative polymerase chain reaction
RBC - red blood cell
RPMI – Roswell Park Memorial Institute buffer
RSV - respiratory syncytial virus
RT – room temperature
RT-PCR - reverse transcription polymerase chain reaction
SARS-CoV-2 - severe acute respiratory syndrome coronavirus 2
SEM - standard error of the mean
SD – standard deviation
SMI – submicroscopic infection
TMB - 3,3',5,5'-Tetramethylbenzidine
TNF - tumor necrosis factor
T_{RM} cells - tissue-resident memory T cells
uRBC - uninfected RBC
VSA – variant surface antigen

Chapter 1. Introduction

Portions of this Chapter have been previously published (1).

1.1 Malaria epidemiology

The world has seen unprecedented progress in malaria control over the past two decades. In 2019 malaria caused an estimated 409,000 deaths worldwide, compared to 736,000 in the year 2000 (2). The World Health Organization estimates that since the year 2000, 7.6 million malaria-related deaths and 1.5 billion malaria cases have been averted, thanks to advances in surveillance, prevention, diagnosis and treatment. However, despite continued elimination efforts there has been a plateau in progress in recent years and malaria remains one of the most important human parasitic diseases in the world. There are a number of biological threats to malaria eradication, including the emergence of insecticide resistance in the *Anopheles* mosquitoes that transmit malaria, deletion of the *pfhrp2/3* gene(s) which encode the antigens that are detected by most rapid diagnostic tests, and mutations in the *PfKelch13* gene that confer resistance to first-line antimalarial treatments (2). Furthermore, the on-going SARS-CoV-2 pandemic has caused significant interruptions to malaria control efforts in many endemic countries, leading to predictions that malaria morbidity and mortality will increase in the coming years.

There are six species of *Plasmodium* that cause malaria in humans: *P. falciparum, P. vivax, P. malariae, P. knowlesi, P. ovae curtisi* and *P. ovale wallikeri* (3, 4). *P. falciparum* is the most virulent malaria species and is responsible for the majority of deaths, most of which occur in children under the age of five in sub-Saharan Africa (2). In this region, *P. falciparum* is the major malaria-causing species (Figure 1.1A). *P. vivax* was historically thought to be absent from most of sub-Saharan Africa, with the exception of the Horn of Africa and Madagascar. However, recent

studies have reported widespread *P. vivax* infections in all regions of Africa (Figure 1.1B and C) (Reviewed in (5)).

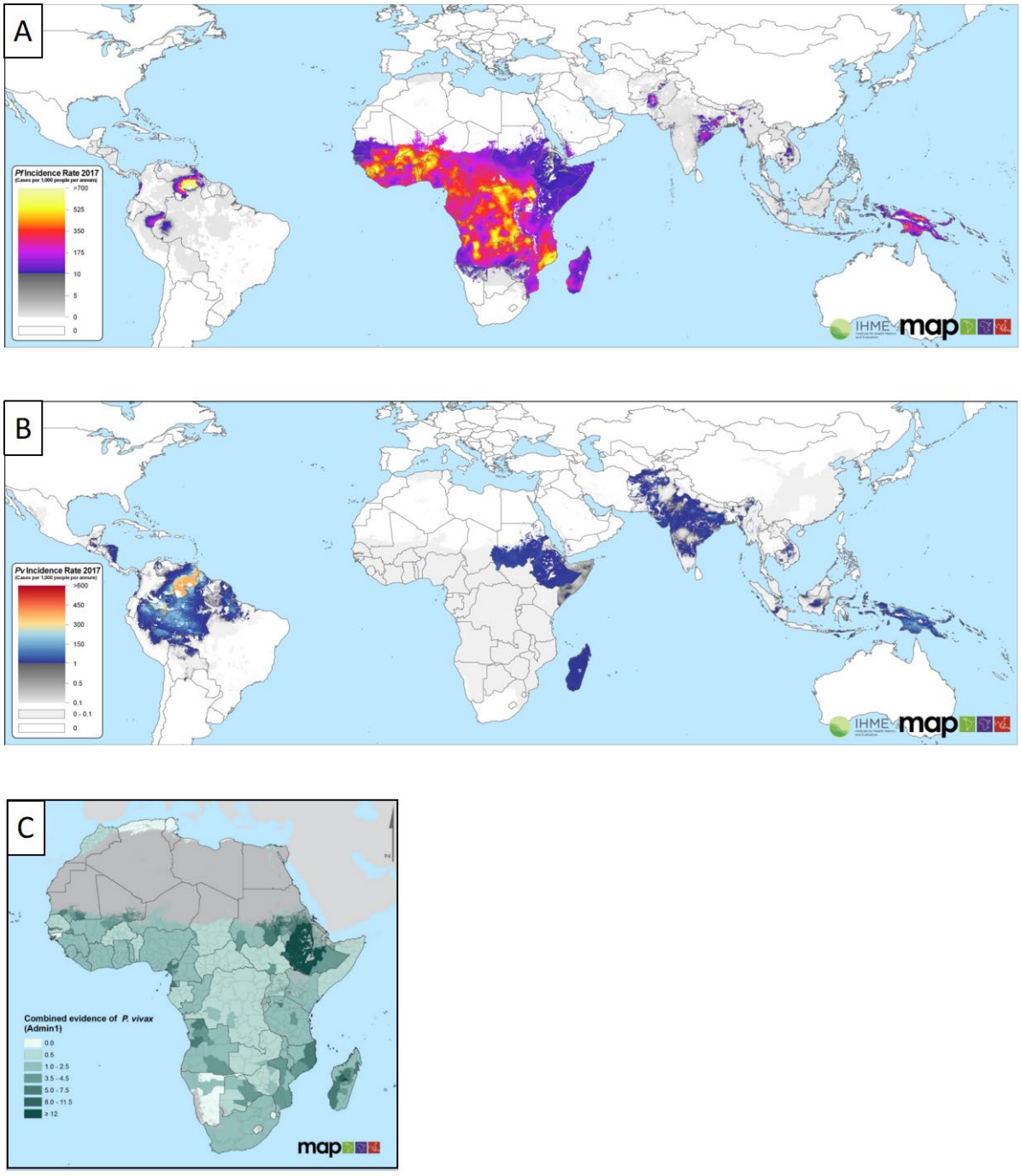

Figure 1.1. Worldwide distribution of *Plasmodium falciparum and P. vivax.* (A) *P. falciparum* and (B) *P. vivax* incidence rates in 2017. Data are cases per 1000 people per year. Images adapted from (6). (C) A composite evidence map detailing indications of the presence of *P. vivax* in Africa. Evidence from vector data, community surveys, clinical case reports, serology and traveller infections were weighted and combined. Darker shading signifies greater evidence of *P.vivax* presence, white signifies no evidence and grey indicates unsuitable environmental conditions for *P. vivax.* Image adapted from (5).

1.2 Malaria lifecycle

The malaria parasite is transmitted to humans through the bite of an infected female *Anopheles* mosquito (7, 8). When an infected mosquito takes a blood meal, sporozoites in the saliva are injected into the skin and make their way into the bloodstream (Figure 1.2). The sporozoites travel to the liver, colonize hepatocytes and undergo multiple rounds of mitosis to form multinuclear cells, called schizonts (9). Upon rupture, tens of thousands of merozoites are released into the bloodstream and invade red blood cells (RBCs). Once in the RBCs, the parasites again undergo several rounds of mitosis to form schizonts. The infected RBCs (iRBCs) then rupture and the merozoites invade new RBCs and continue the asexual erythrocytic cycle of the parasite.

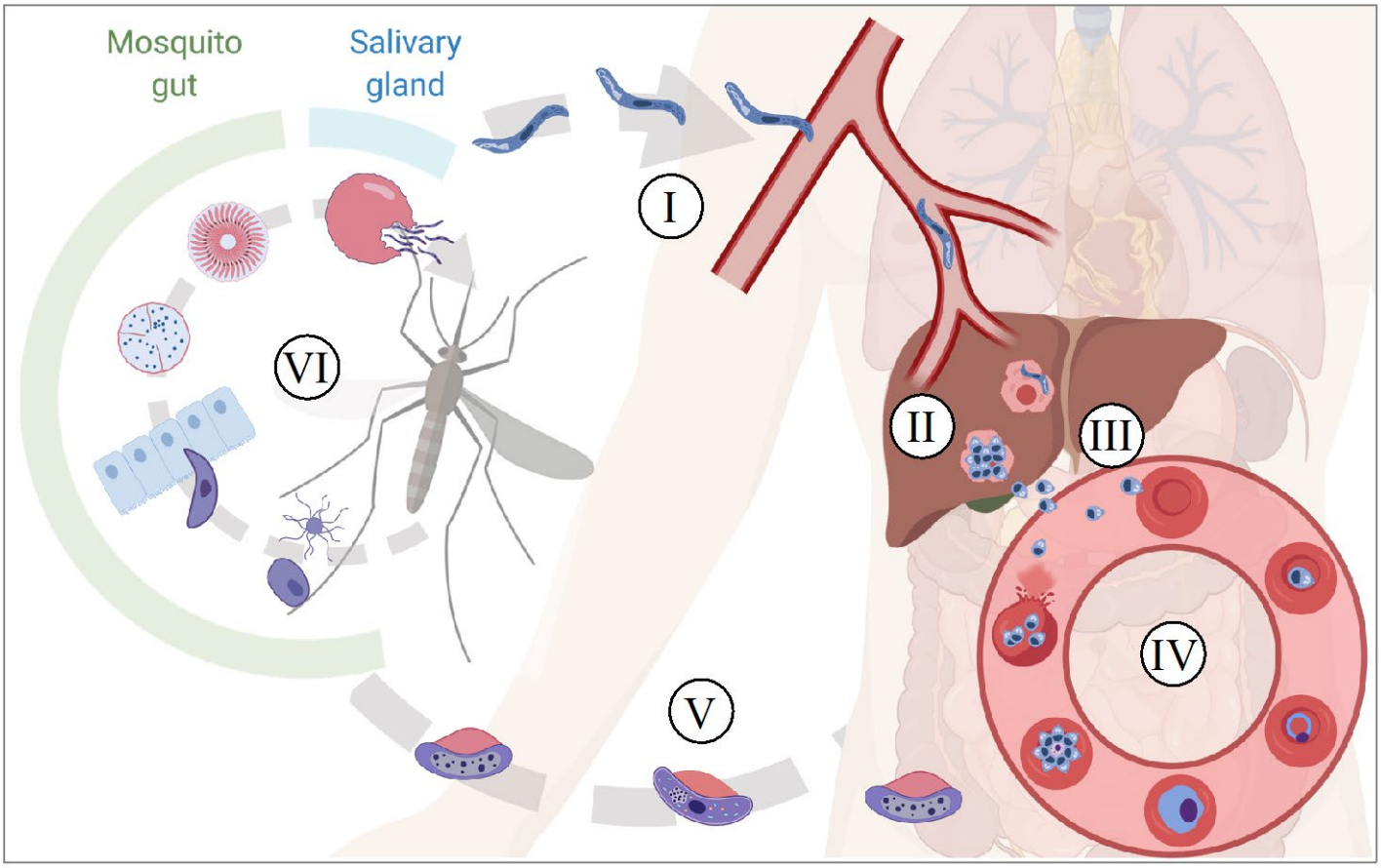

Figure 1.2. *Plasmodium* lifecycle. (I) *Plasmodium* sporozoites are injected into the host in the saliva of an infected female *Anopheles* mosquito. The sporozoites then make their way into the bloodstream, where they travel to the liver. (II) Following invasion into hepatocytes, the sporozoites undergo many rounds of mitosis, forming thousands of merozoites. (III) The merozoites are released into the bloodstream, where they invade red blood cells (RBCs). (IV) In the RBC the parasite will again undergo several rounds of asynchronous mitosis to form schizonts, which release merozoites that can invade new RBCs. (V) During the erythrocytic cycle, some parasites will differentiate into sexual stages of the parasite, called gametocytes. These gametocytes are then taken up by mosquitoes during a blood meal. (VI) The gametocytes undergo sexual reproduction in the midgut of the mosquito, eventually forming sporozoites that can be transmitted to another host. Made with BioRender.com.

Invasion into RBCs is a well-orchestrated, sensitive process that relies on specific interactions between particular parasite antigens and host proteins. For instance, PvDBP is a protein that mediates irreversible binding between *P. vivax* merozoites and the Duffy Antigen Receptor for Chemokines (DARC) on the RBC membrane during invasion (10, 11). The PvDBP protein is approximately 140 kDa and is comprised of six extracellular domains, with a Duffy-binding like (DBL) domain (region II) that binds DARC (12-14). When the invasion process has been initiated and PvDBP has been secreted from the merozoite micronemes, it forms a dimer, which allows it to bind to a DARC dimer on the RBC surface, mediating invasion (Figure 1.3). The specificity of these parasite ligand-host receptor interactions are thought to underpin the RBC tropism displayed by malaria parasites (15). Not only do they restrict the parasites to specific hosts, but they also restrict the parasites to RBCs of specific ages in the host. *P. vivax* and *P. ovale* are restricted to the youngest RBCs, reticulocytes, while *P. malariae* parasites are only found in the oldest RBCs and both *P. knowlesi* and *P. falciparum* can invade RBCs of any age.

During the erythrocytic cycle, some of the parasites undergo sexual differentiation to form male and female gametocytes. After sequestration and maturation in the bone marrow, the gametocytes circulate in the bloodstream of the host and are taken up by mosquitoes during a blood meal (16-18). The gametocytes undergo sexual reproduction in the midgut of the mosquito, eventually forming sporozoites that can be transmitted to another host. In *P. ovale* and *P. vivax* infections, a small number of parasites form hypnozoites in the liver, which remain dormant for long periods of time and cause relapsing infections if left untreated (19, 20).

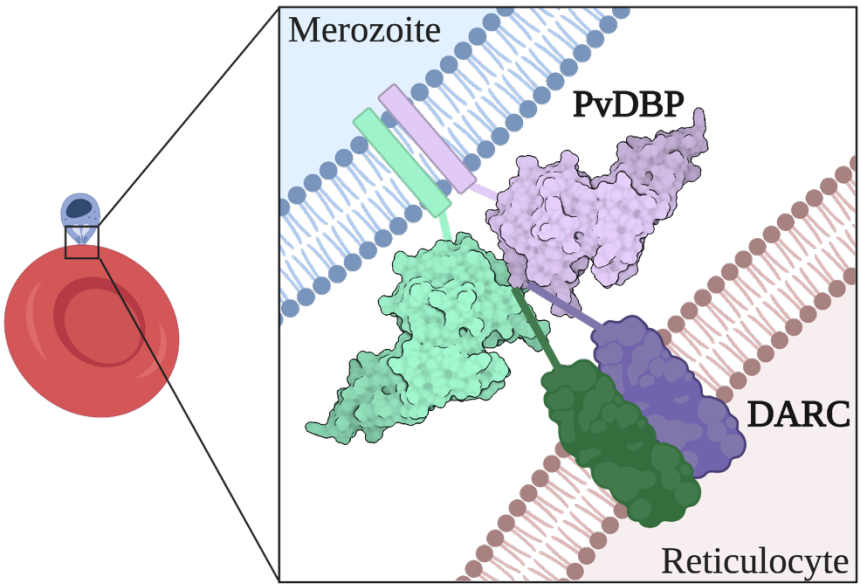

Figure 1.3. PvDBP binding to DARC. The DBL domains of two PvDBP proteins are shown in dimer form binding to a dimer of DARC on the reticulocyte membrane. Based on a figure from (21). Created with BioRender.com

The complicated, multi-stage lifecycle of the malaria parasite likely plays a key role in the parasites' success, as it considerably impairs the host immune response to the parasite. The parasites express a unique set of antigens at each stage in the lifecycle, with very little antigenic overlap between stages (22). This likely contributes to the fact that sterile immunity is rarely observed in vaccinated or naturally exposed populations.

1.3 Malaria disease

The liver stage of malaria is asymptomatic, and symptoms of the disease are only observed during the erythrocytic cycle. The classical presentation of uncomplicated malaria is a cyclic pattern of fever, chills and sweating, the timing of which is defined by the parasites' replication cycle. *P. knowlesi* replicates every 24 hours, *P. falciparum* and *P. vivax* replicate every 48 hours, *P. ovale* replicates every 50 hours and *P. malariae* replicates every 72 hours (23). Because of these differences, *P. falciparum, P. vivax* and *P. ovale* were historically referred to as "tertian" parasites, as symptoms occurred every second day in these infections. *P. malariae* was known as the "quartan" parasite because infection with this parasite causes symptoms every three days. Despite being accepted as the "classic" presentation of malarial disease, these well-defined cyclic symptoms are rarely observed. Rather, patients often present with a combination of fever, chills, sweat, headaches, nausea and vomiting, body aches and general malaise (8).

Severe malaria is a life-threatening disease most commonly caused by *P. falciparum* but is also observed in *P. vivax* and *P. knowlesi* infections. Clinical manifestations of severe malaria are diverse and can involve cerebral malaria (symptoms include seizures, coma or other neurological abnormalities), severe anemia, hemoglobinuria, acute respiratory distress syndrome (ARDS), acute kidney injury, metabolic acidosis and abnormalities in blood coagulation (8). Children living in high-endemic areas are at highest risk for severe malaria under the age of 5, but generally acquire

immunity to severe malaria by the time they reach adolescence (24). However, sterile immunity is rarely observed (25). Subsequent malaria infections are usually not lethal in these individuals but are still associated with significant morbidity. In endemic areas it is also common for people to have chronic low-parasitemia infections that remain asymptomatic. These infections often remain undetected and therefore untreated and are an important source of onward transmission (26, 27).

The biological mechanisms underlying the progression from uncomplicated to severe malaria is complex and challenging to delineate. This is likely due to the fact that the host immune response plays a vital role in the pathogenesis of severe malaria and disease progression is dependent on host, as well as parasite factors. The situation is further complicated by the large number of cytokines involved and the fact that their effects are often context and concentration dependent. A balance must be maintained between proinflammatory and anti-inflammatory cytokines for an effective anti-malaria response that does not endanger the host. Excessive proinflammatory cytokine production can result in host tissue damage, severe disease and even death, while an insufficient proinflammatory response can result in unregulated parasite growth. For instance, tumor necrosis factor (TNF) is protective at moderate serum concentrations. However, if the TNF levels are dysregulated and become too high, they are associated with severe disease (28, 29). Cytokine-mediated pathologies are often prevented by immunoregulatory components of the immune system, such as interleukin 10 (IL-10). The immunomodulatory effects of IL-10 are primarily exerted through suppressed production of proinflammatory cytokines, such as TNF-α, by monocytes and macrophages (Reviewed in (30)). This suppression helps to ensure a balance is maintained to facilitate parasite clearance while minimizing tissue damage. As is the case with all cytokines, too much IL-10 can impair the parasite-killing functions of innate immune cells, resulting in unchecked parasite growth and host death. The importance of maintaining this

delicate balance has been observed with many other cytokines, including IFN-γ, IL-1β, IL-6 and IL-12 (31, 32).

Importantly, there are also specific cytokine profiles that have been associated with different clinical syndromes (33). For example, low IL-10 levels have been associated with severe malarial anemia (34), whereas high IL-10 levels are observed in patients with respiratory distress (35). These studies, and many others, revealed the complex and delicate balance between pro- and anti-inflammatory host responses that must be maintained during malaria infection. However, it is important to note that parasite virulence factors also play a central role in dictating disease severity.

1.4 Malaria vaccines and host immunity

A malaria vaccine would have a tremendous impact on vulnerable populations, with the potential to save nearly half a million lives annually and prevent over 200 million cases (36). Yet the development of an efficacious vaccine remains elusive. As mentioned above, the parasite expresses antigens that are largely stage-specific during its lifecycle and no single defining vaccine target or even whole organism vaccine can protect against all stages. Despite this, there are multiple opportunities for vaccines to interrupt the parasite lifecycle (37). A vaccine that prevents sporozoite colonization of hepatocytes could protect individuals from *Plasmodium* infection, while a vaccine targeting blood stage antigens could curb the clinical manifestations of disease, and a gametocyte-targeting vaccine could block transmission to mosquitoes.

P. falciparum causes the largest burden of disease worldwide, which is why much of the research and vaccine development efforts have focused specifically on this species. As a result, most of what is known about immune responses to the parasite and vaccine candidates is from studies of *P. falciparum.* Thus, the following discussion focuses primarily on *P. falciparum* immunity.

It is generally accepted that innate and adaptive cellular immune mechanisms are largely responsible for the protection against sporozoites and intrahepatic parasites, whereas the humoral arm of the immune system is the primary defender against the intracellular blood stage parasites. However, there is evidence that both humoral and cell-mediated immunity play roles in the immune response against all stages of the parasitic infection. For example, complement-fixing antibodies targeting a sporozoite antigen were associated with protection against clinical *P. falciparum* infection in children (38). Although overall the high level of these antibodies associated with protection were only observed in a subset of sera samples (20%). It should also be noted that results from studies investigating the contribution of anti-sporozoite antibodies to clinical protection have been inconsistent. This is likely because the sporozoites travel from the skin to the liver within minutes where they invade hepatocytes and become inaccessible to antibodies. Therefore, it is probable that a high concentration of specific immunoglobulin would need to be present in the bloodstream at the time of infection to offer antibody-mediated immunity. This likely explains why anti-sporozoite antibodies are often reported to be effective *in vitro* but are inconsistently associated with clinical protection to malaria in naturally-exposed populations.

T cell mediated immune responses are thought to be primarily responsible for pre-erythrocytic immunity. The importance of T cells, particularly CD8+ T cells, to pre-erythrocytic immunity has been underscored by a number of studies using experimental animal models (39-41). Infected hepatocytes present parasite-derived antigens on their surface using MHC class I and II molecules, which are recognized by CD8+ and CD4+ T cells, respectively (42). Studies in animal models suggested that once the T cells are activated, they produce interferon-γ (IFNγ) that kills the intrahepatic parasites (43). However, there is limited evidence for naturally-acquired T cell mediated immunity in human populations (Reviewed in (22)). This is likely a result of the

relatively low number of sporozoites that are injected by infected mosquitoes (10-100), which may not provide sufficient antigen to generate a strong immune response. Therefore, much of our knowledge about pre-erythrocytic immunity in humans comes from vaccine studies.

In fact, immunizations with whole inactivated or attenuated sporozoites have yielded promising results in human trials. For instance, intravenous injection of attenuated whole sporozoites conferred a high degree of protection in human challenge experiments with homologous *P. falciparum* strains (44-51). In a recent phase 1 trial of the whole sporozoite vaccine candidate, PfSPZ, in Mali, the vaccine was safe, well tolerated and offered some protection against natural *P. falciparum* infection (hazard ratio: 0.517, 95% CI 0.313–0.856) (52). Although the high levels of sterile immunity that were reported in some experimental human challenge models were not observed in this trial, the vaccine protected a significant proportion of vaccinees over an entire malaria season. Unfortunately, there are a number of challenges that these vaccine candidates must overcome before they could ever be implemented at scale. These include cold-chain storage (in some cases liquid nitrogen is required), intravenous inoculation and manufacturing scale-up (53).

Nevertheless, these studies provide important insight into the human immune response against pre-erythrocytic malaria parasites. In many of these studies, the levels of vaccine-induced cytotoxic CD4+ T cells in peripheral circulation were associated with protection (46-51). Interestingly, both the induction of CD8+ T cells and the associated protection were less consistent in these trials. For instance, following vaccination with PfSPZ, vaccine-specific CD8+ T cells were observed in the peripheral blood of some protected individuals, yet were completely absent in others (49). However, studies in nonhuman primates may offer an explanation for these findings. Following immunizations with PfSPZ, the levels of vaccine-specific CD8+ T cells were 3-4 log units higher in the liver than in peripheral blood samples (Reviewed in (54)). These data have led

to the hypothesis that following vaccination, the CD8+ T cells are primed in secondary lymphoid organs and immediately migrate to the liver, often preventing their detection in peripheral blood samples.

In support of this hypothesis, there is accumulating evidence for the importance of liver tissue-resident memory T cells (T_{RM} cells) in the immune response to malaria. T_{RM} cells are highly specialized CD8+ T cells that withdraw from circulation in the liver, where they patrol sinusoids for specific pathogens (Reviewed in (54)). These cells were found to be potent mediators of protection against intrahepatic malaria parasites following immunizations with attenuated sporozoites in mice (55, 56). As a result, studies are currently underway using a vaccination strategy aimed at specifically inducing a T_{RM} cell response in the liver. However, given that these cells are, by definition, not present in peripheral blood, accurately measuring their levels in human immunization trials could be a significant hurdle to the progress of these vaccines.

In addition to immunizations with whole sporozoites, a number of subunit vaccines targeting pre-erythrocytic parasites have been developed. In fact the only licenced malaria vaccine, called RTS,S, which is currently undergoing pilot rollout in three African countries, is based on the circumsporozoite surface protein (CSP) antigen from *P. falciparum* sporozoites (57). Unfortunately, this vaccine offers only partial protection that wanes significantly over time (58, 59). This is likely because the RTS,S vaccine primarily elicits an antibody response targeting the CSP antigen, which displays a high degree of natural polymorphisms in different *P. falciparum* strains (60). RTS,S also does not contain the N terminal region of CSP that was reported to be the target of protective immunity in children (61) and evidence suggests that there is limited boosting of antibodies against pre-erythrocytic antigens following natural infection (25). Furthermore, the RTS,S vaccine induces limited T cell responses (62, 63), which, as discussed previously, were

important mediators of vaccine-induced pre-erythrocytic immunity. New CSP-based vaccine candidates have been designed in an attempt to overcome the aforementioned challenges and several have entered clinical trials, along with a number of novel subunit vaccines that are based on different sporozoite antigens (Reviewed in (54)).

In the erythrocytic stage of malaria, immunity is assumed to be primarily mediated by antibodies; however, there are contributions from the innate immune system as well. In a seminal study on erythrocytic immunity, pooled IgG from adults living in a malaria-endemic region of Africa was passively transferred to children with malaria, resulting in significant reductions in parasitemia (64). Although these findings have been repeated in other studies of human and murine malaria, it has proven challenging to define individual antigenic correlates of protection. Antibody responses in naturally-exposed individuals are directed against many asexual antigens, which complicates the process of deciphering protective responses from markers of infection (65). There are a number of *in vitro* assays that are used to evaluate the function of different antibodies, including opsonic phagocytosis, complement fixation, inhibition of binding assays, antibody-mediated cellular cytotoxicity and growth inhibition assays. However, there is inconsistent evidence that the results of these assays correlate with clinical protection (Reviewed in (66)).

Although data from studies of blood-stage immunity have not always been consistent, putative antigenic targets of protective antibodies have been identified. For instance, a systematic review of several longitudinal studies found that IgG responses against invasion ligands, including merozoite surface protein 1 ($MSP1_{19}$), MSP3 and apical membrane antigen 1 (AMA-1) were associated with protection against clinical malaria (67). Additional studies pointed to protective antibodies targeting *P. falciparum* reticulocyte-binding homologues (PfRHs) and antigens in the erythrocyte binding antigen (EBA) family (68-70). There have been several clinical trials of

vaccine candidates based on merozoite surface antigens, but they have shown limited efficacy. For instance, in a phase IIb trial of AMA-1, protection against homologous *P. falciparum* strains was observed, but not against heterologous strains (71). Furthermore, the protection was not correlated with antibody function.

Antibodies that target parasite antigens on the iRBC membrane have also been correlated with protection in longitudinal studies (Reviewed in (72)). The main targets of these antibodies were identified as the variant surface antigens (VSAs) that are expressed by *P. falciparum* parasites and displayed on the surface of iRBCs. These antigens are members of the *P. falciparum* erythrocyte membrane protein-1 (PfEMP1) family that mediate iRBC binding to host tissues, a specific interaction that the protective antibodies are assumed to disrupt (discussed further in Chapter 1, Section 1.5). As in other stages of malaria infection, achieving strain-transcending immunity to blood-stage infection is a significant challenge that both naturally-acquired and vaccine-induced immunity must overcome (73).

In addition to antibodies, γδ T cells have recently been recognized as important mediators of immunity to blood-stage malaria (74-77). Two mechanisms were described by which γδ T cells may mediate immunity to blood-stage parasites: opsonic phagocytosis of iRBCs and direct killing of iRBCs (77). Direct killing was initiated when γδ T cell antigen receptors (TCR) recognized parasite antigens, which triggered them to released granulysin through degranulation, lysing the infected erythrocyte. Interestingly, this is similar to the mechanism by which CD8+ T cells kill *P. vivax*-infected reticulocytes (76). This mechanism of action does not play a significant role in *P. falciparum* iRBC clearance, because *P. falciparum* parasites are not restricted to reticulocytes, as is the case with *P. vivax*. The majority of *P. falciparum* parasites infect mature RBCs, which do not express MHC class I or II molecules, prohibiting detection by CD8+ or CD4+ T cells,

respectively. Although studies of γδ T cells have offered key insights into malarial immunity, further study is needed to determine their clinical relevance.

1.5 Immune evasion strategies

Plasmodium parasites have evolved eloquent mechanisms to avoid destruction by the host immune system and ensure onward transmission. A key mechanism employed by the parasites is antigenic polymorphism, which inhibits the host from acquiring strain-transcending immunity. A primary example of this are antigens in the PfEMP1 family, which are encoded by *var* genes. Each *var* gene contains two exons separated by a single intron. Exon 1, which displays high nucleotide variation between *var* genes, encodes the extracellular portion of the PfEMP1 protein, while the more conserved exon 2 encodes the intracellular portion of the protein. High variation in exon 1 and thus, the extracellular portion of the PfEMP1 proteins, is observed within the same parasite genome and between the genomes of different *P. falciparum* parasites (78). Although this strategy has been most thoroughly described in *P. falciparum* parasites, high rates of polymorphisms are seen in immunodominant antigens from many *Plasmodium* species. In fact, polymorphisms in the merozoite invasion ligands of *P. vivax*, such as PvDBP, present a significant hurdle to the development of strain-transcending immunity (79-81).

Proteins in the PfEMP1 family also mediate another very important immune-evasion strategy: withdrawal from the peripheral blood through sequestration in host tissues (82). PfEMP1 proteins contain structurally conserved DBL domains that mediate binding to different host receptors including CD36, ICAM-1 and chondroitin sulfate A (CSA) (83-85). Sequestration of iRBCs is an important survival strategy for the parasites, as it allows them to withdraw from circulation and avoid being cleared by the spleen. When the parasite matures in the RBC from ring

stage to trophozoite and schizont stages, the iRBC membrane becomes increasingly stiff. This loss of deformability has been attributed to the stiffness of the parasite itself, changes in the RBC membrane architecture mediated by exported parasite proteins and modification and depletion of RBC membrane proteins (reviewed in (86)). As a result, the stiff RBCs infected with mature parasites are at greater risk of being filtered out by the spleen (87). Therefore, sequestration in a variety of host tissues, including the placenta, is important for parasite survival and onward transmission. It is likely that the high degree of polymorphisms observed in PfEMP1 proteins is a strategy used by the parasites to prevent host immunity from targeting these vital binding antigens.

Another way that *P. falciparum* parasites ensure sequestration in host tissues is, as mentioned above, to bind to a number of different host ligands. This requires that the parasite genome encode a repertoire of different PfEMP1 proteins capable of binding to diverse host ligands. This strategy is called antigenic variation. Approximately 60 *var* genes encode the PfEMP1 proteins in the haploid *P. falciparum* genome (88-90). All members of the *var* gene family are expressed in a mutually exclusive manner, meaning that each parasite will only express one of the 60 *var* genes at a time. However, through a mechanism known as *var* gene switching, successive generations of parasites may express a different member of the *var* multigene family (91).

The mechanism of *var* gene switching involves several distinct steps: *var* gene silencing, transcription and switching to transcription of a different *var* gene. By default, all *var* genes are silenced in the parasite genome, which is thought to be achieved through reversible histone modifications (92-94) and tethering at the nuclear periphery (95-97). A single *var* gene is then transcribed for approximately 10-14 hours following merozoite invasion of an erythrocyte (98, 99). Transcription of this *var* gene ceases in the later blood stage, but it remains in the 'poised'

state, marked for reactivation in the next erythrocytic cycle. This mechanism results in epigenetic memory, which ensures that the same *var* gene will be expressed in the subsequent erythrocytic cycle in the vast majority of parasites (100, 101). However, in approximately 2% of parasites (estimated using *in vitro* studies), the previously transcribed *var* gene returns to the silenced state rather than the poised state (102). This results in the transcription of a different *var* gene in the next erythrocytic cycle, leading to *var* gene switching.

The mechanisms underlying the regulation of *var* gene silencing and activation are not well understood, but host factors are thought to play an important role. Early studies using long term *P. knowlesi* infection in nonhuman primate models, which is how antigenic variation in *Plasmodium* was first discovered, suggested an essential role for the spleen (103). In this model, expression of variant surface antigens on iRBCs stops when the parasites are passaged in a splenectomized monkey, but expression of these antigens returns upon passage in an intact host (104, 105). However, the molecular mechanisms underlying the role of the spleen remains a mystery.

Despite the current ambiguity surrounding the *var* gene switching mechanism, selection for dominant phenotypes during infection is quite well described. Interestingly, all *var* genes are silenced in sporozoites when they are introduced into the human from the salivary glands of the mosquito (106). Following egress from hepatocytes, *var* gene transcription was demonstrated to be highly variable during the early stages of the erythrocytic cycle. Studies using experimentally infected individuals found that at the onset of blood stage infection almost all *var* genes were transcribed (107, 108). However, in subsequent generations, specific *var* genes began to dominate, which was attributed to immune pressure exerted by antibodies directed against some of the PfEMP1 antigens. It is important to note that both of these studies used malaria naïve, non-immune volunteers. The findings may have been different in individuals living in malaria-endemic regions

who had previously developed partial immunity. Nevertheless, these studies provide important information about epigenetic memory involved in *var* gene transcription and suggest that it may be 'reset' during transmission. This memory reset may allow the malaria parasite to selectively express the PfEMP1 antigen that will ensure the greatest fitness in each host.

1.6 Malaria in pregnancy

P. falciparum infection in pregnancy can cause a number of deleterious health outcomes. These include pre-term birth, low birth weight, intrauterine growth restriction, spontaneous abortion, still birth, maternal hypertension, maternal anemia, infant and maternal mortality and even long-term cognitive defects in children born to mothers with placental malaria (109-119). Parasitized RBC sequestration in the placenta mediates much of the pathology associated with malaria in pregnancy (MiP). When *P. falciparum* infects a pregnant woman, the parasites express a protein in the PfEMP1 family, called VAR2CSA. VAR2CSA is exported to the surface of the iRBC and mediates binding to a low-sulfated glycosaminoglycan, called CSA, present on chondroitin sulfate-proteoglycans (CSPGs) expressed in the intervillous space of the placenta (Figure 1.4A) (83, 120-130). With the exception of some malignant tumors, the unique form of CSA modification that VAR2CSA binds to is only found in the placenta (131). CSA has been associated with placental trophoblast invasion of uterine tissue and the rapid cell proliferation that occurs during the placental implantation process (132). Given that invasion of surrounding tissues and rapid cell proliferation are hallmarks of cancerous tumors, it is not surprising that placental-like CSA is a ubiquitous modification on proteoglycans expressed by cancer cells (131). In fact, recombinant VAR2CSA moieties are now being investigated for their ability to detect cancer and deliver targeted anti-tumor treatments (131, 133-138).

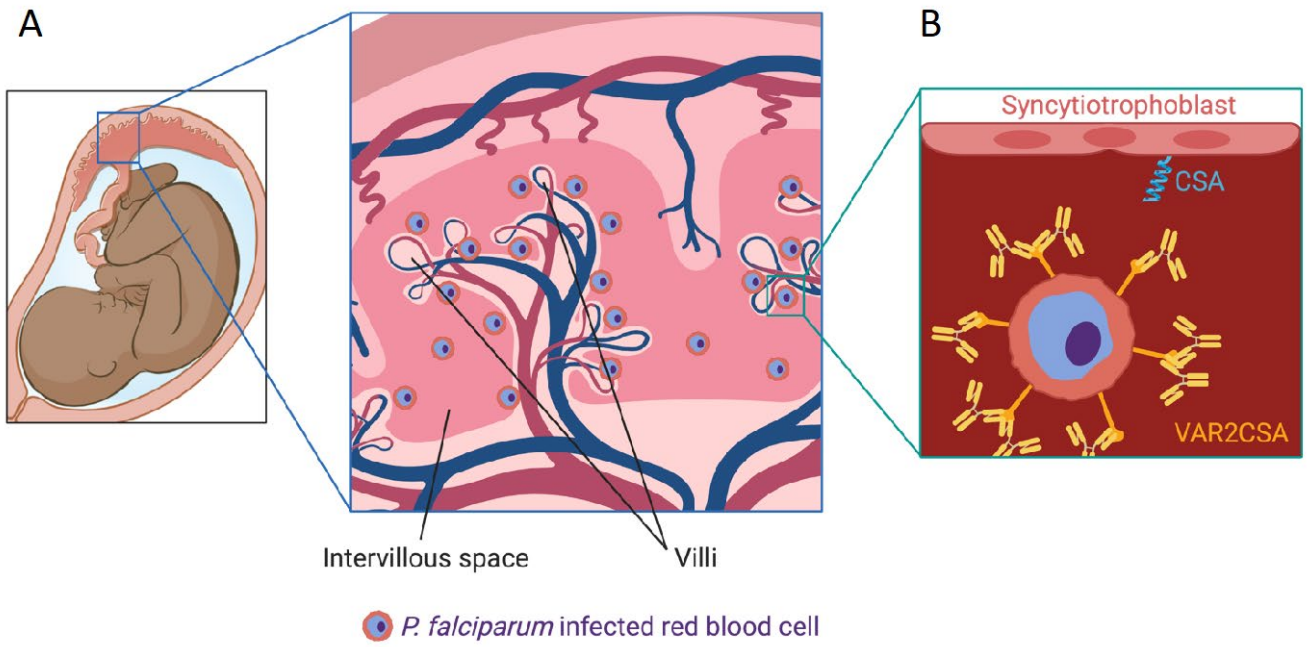

Figure 1.4. Placental malaria and maternal immunity. (A) In pregnancy, *P. falciparum* express VAR2CSA on the surface of infected red blood cells (iRBCs), which mediates adherence to chondroitin sulfate A (CSA) in the placenta. This sequestration results in a massive accumulation of iRBCs in the intervillous space of the placenta. (B) When a woman has had multiple *P. falciparum* infections in pregnancy, she will develop protective anti-VAR2CSA antibodies that block iRBC binding to CSA. Made using BioRender.com.

Sequestration in the placenta allows the iRBCs to avoid being cleared by the spleen, making the CSA-VAR2CSA interaction a key target for host immunity. In fact, once a woman has had several malaria infections in pregnancy, she develops protective anti-VAR2CSA antibodies in a parity-dependent manner (Figure 1.4B) (139-145). In pregnant women in Cameroon, the presence of moderate and high avidity anti-VAR2CSA antibodies during the fifth and sixth months of pregnancy reduced the risk of placental malaria 2.3-fold (95% CI, 1.0-4.9) and 7.6-fold (95% CI: 1.2-50.0), respectively (145). In a more recent study on MiP in Benin, antibodies against the VAR2CSA-based vaccine candidate, PAMVAC, were associated with better health outcomes (146). The authors reported that elevated levels of anti-VAR2CSA total IgG and specifically IgG3 during pregnancy were associated with higher birth weights, while levels of anti-VAR2CSA IgG4 were associated with a lower risk of placental malaria (146). Studies evaluating the function of these protective antibodies have found that they offer protection by mediating opsonic phagocytosis of iRBCs and blocking sequestration to CSA (147-152). For instance, in Benin, an increase in CSA binding inhibition activity in plasma, between inclusion into the study and delivery, was associated with protection from placental infection, low birth weight and preterm birth (147). However, a recent systematic review suggested that anti-VAR2CSA antibodies are markers of infection rather than measures of protection (153). Nevertheless, it is likely that the antibodies that are protective function by blocking parasite adhesion to CSA and/or mediating opsonic phagocytosis.

The parity-dependent pattern of anti-VAR2CSA antibody acquisition has been described in many populations living in sub-Saharan Africa, where *P. falciparum* is the primary malaria-causing species (2). However, fewer studies have investigated anti-VAR2CSA antibodies in populations living in areas co-endemic for *P. falciparum* and *P. vivax*. In cross-sectional studies

of non-pregnant populations and a longitudinal study in pregnancy in Colombia, where *P. falciparum* and *P. vivax* co-circulate, we observed an unusual pattern of anti-VAR2CSA antibody acquisition (154, 155). Primigravid women and non-pregnant populations, such as men and children, had antibodies that recognized VAR2CSA. In the pregnant population, about a quarter of the women were infected at some point in pregnancy but these were nearly all submicroscopic infections (SMIs). Women were not treated with antimalarials or on intermittent preventative therapy (IPT) yet there were very few negative health outcomes associated with these SMIs in pregnancy. Furthermore, in the women that became infected, the ability of antibodies to block parasite adhesion to CSA *in vitro* correlated positively with maternal hemoglobin levels, suggesting they could be protective (152). These findings are in contrast to studies in Africa that have reported poor health outcomes associated with SMIs in pregnancy (156-161).

Evidence of protection against sub-microscopic *P. falciparum* infections in pregnancy has been observed in other studies in locations that are co-endemic for *P. falciparum* and *P. vivax.* Another study in Colombia reported that SMI at delivery was not associated with any poor birth outcomes, despite evidence of placental damage (162). However, women who had a microscopically detected malaria infection at some point during pregnancy gave birth to babies that had significantly lower birth weight than uninfected women. Consistent with these findings, a cross-sectional study from the same group reported significant histopathological changes in the placenta of women with submicroscopic *P. falciparum* (and *P. vivax*) infections at delivery, but no poor birth outcomes (163). Although the observation of placental damage with no associated adverse birth outcomes may seem contradictory, it has been reported that low birth weight may be more related to the acute insult of the malaria infection than to irreversible placental changes (164).

Consistent with the findings from Colombia, a cross-sectional study performed in Peru found that asymptomatic *P. falciparum* and *P. vivax* infections were associated with increased monocytes in the placenta and pigmented monocytes in placental vessels (165). However, no adverse health outcomes were associated with SMI in pregnancy. A study in Papua New Guinea, where *P. falciparum* and *P. vivax* also co-circulate, found that higher proportion of low birth weight deliveries among women who had SMIs at delivery compared to uninfected women (the authors did not differentiate between *P. falciparum* and *P. vivax* infection) (166). However, this difference was not statistically significant (OR 2.41; CI 0.99-5.89; p = 0.054) and there was no difference in the mean birth weight of babies born to infected mothers compared to uninfected mothers. A cross-sectional study from India also found that microscopically detected, but not SMIs, were associated with maternal anemia and low birth weight (167). Furthermore, a multicenter prospective cohort study investigating MiP in Colombia, Guatemala, Brazil, India and Papua New Guinea also reported that submicroscopic *P. falciparum* infections were not associated with maternal anemia or low birth weight (168).

Considered together, the majority of these results suggest that in regions where *P. falciparum* and *P. vivax* co-circulate, a patent *P. falciparum* infection in pregnancy is still associated with significant health risks, but when the infections are submicroscopic this association is not observed. These findings contradict studies on falciparum MiP in Africa, where submicroscopic *P. falciparum* infections are associated with poor health outcomes (156-161).

As discussed previously, our studies of MiP in Colombia suggest that, in this population, protection against the poor health outcomes associated with SMI in pregnancy may be a result of anti-VAR2CSA antibodies (152, 154). Interestingly, in this population, there was evidence of pregnancy-independent acquisition of anti-VAR2CSA antibodies. Non-pregnant populations, such

as men and children, were found to have anti-VAR2CSA antibodies that were able to block parasite adhesion to CSA *in vitro*. Furthermore, acute *P. vivax* infection or past exposure to *P. vivax* was associated with anti-VAR2CSA antibodies. This led us to suggest that there may be genotypic or phenotypic differences in parasites in this region, owing to co-endemicity of *P. falciparum* and *P. vivax*, or that there was immunological cross-reactivity between VAR2CSA and a *P. vivax* antigen.

1.7 Immunological cross-reactivity between *Plasmodium* species

Rather unexpectedly, insight into the immunological basis of cross-reactivity first emerged from attempts to develop species-specific diagnostic tests. In testing the specificity of a complement fixation assay for malaria diagnosis, Kingsbury detected cross-reactivity between *P. vivax* and *P. falciparum* antigens (169). Sera from 6 of 12 individuals with acute *P. vivax* infection reacted to *P. falciparum* antigens in a precipitin test, and likewise, 5 of 16 sera from patients infected with *P. falciparum* reacted to *P. vivax* antigens. However, a later paper by Mayer and Heildelberger (1946) suggested that the specificity of the test was compromised by reactivity of sera with human stromata in the antigen preparations (170). In a different precipitin test developed by Taliaferro et al., sera from patients in Honduras infected with *P. vivax* reacted with antigens prepared from a *P. falciparum*-infected placenta (171, 172). Surprisingly, heterologous reactions were as strong as the homologous ones. These findings were replicated in two separate studies in Honduras with over 500 sera but not in a later study in Puerto Rico with antigens prepared in the same manner (173). The results from the Puerto Rico study were deemed inconclusive and the inconsistency attributed to the generally poor performance of the precipitin test at that time. Serological cross-reactivity was later observed against *P. falciparum* and *P. vivax* crude antigens

prepared from short-term culture of parasites isolated from infected patients, but the homologous reactions were more intense than the heterologous reactions (174).

With the advent of techniques to fluorescently label antibodies, their recognition of antigens from distinct malaria species could be directly observed under the microscope with the immunofluorescence (IF) assay. In one of the first records of this method applied to the study of human malaria, fluorescently-labeled immunoglobulin from a patient with a long-standing *P. vivax* infection recognized RBCs infected with the simian malaria species *P. cynomolgi* (although not *P. berghei*) (175). This finding was replicated in another study where sera from *P. vivax*-infected patients (n=4) recognized thin blood smears made from monkeys infected with *P. cynomolgi* (176). Homologous parasites were recognized much more strongly than heterologous parasites, but cross-reactivity in this case was reciprocal: serum from 5 volunteers infected with *P. cynomolgi* recognized two strains of *P. vivax* (Chesson and Venezuelan strains) by IF assay using thin blood smears made from infected patients (176). Similarly, antibodies from a laboratory worker following an accidental *P. cynomolgi* infection recognized thin smears of *P. vivax* iRBCs as strongly as those infected with *P. cynomolgi* (175).

Immunological cross-reactivity between *P. vivax* and *P. falciparum* was also demonstrated with sera from naturally infected individuals (177). Sera from 9 out of 29 individuals with a *P. vivax* infection recognized *P. falciparum* iRBCs, while sera from 11 out of 21 individuals with a *P. falciparum* infection recognized *P. vivax* iRBCs. In this same study, cross-reactivity was also observed in individuals deliberately infected with *P. vivax* or *P. falciparum*. Based on the antibody titers against homologous versus heterologous iRBCs, *P. vivax* sera were more cross-reactive against *P. falciparum* iRBCs than the converse.

In Guatemala, sera from individuals naturally exposed to *P. vivax* strongly cross-reacted with asexual *P. falciparum* antigens by enzyme-linked immunosorbent assay (ELISA) (20/43 positive), IF assay (35/36 positive) and by immunoprecipitation assays (32/32 positive) (178). In order to rule out past *P. falciparum* infection as the source of these antibodies (despite >99% prevalence of *P. vivax*), the sera were also tested against the *P. falciparum* CSP and heat shock protein (HSP) 70 kD-like-molecule repeat peptides by ELISA. Only 2 out of 36 sera samples recognized the PfCSP repeat peptide and 1 out of 33 sera samples recognized the *P. falciparum* HSP70 kD-like-molecule repeat peptide (179), suggesting the antibodies were truly cross-reactive. In this study, serological recognition of a HSP70 peptide was used to rule out antibodies specific to *P. falciparum* infection, but this family of proteins contains other epitopes that are shared across *Plasmodium* species (180). Given their ubiquitous nature, it is possible that these and other conserved housekeeping antigens underpinned some of the cross-reactivity discussed previously. While these may be viable targets of cross-reactive antibodies, their validity as vaccine candidates would depend on whether they elicit functional antibodies.

IF assay was also useful to validate the interactions between the different species of rodent malaria and to develop a model of antigenic similarity among these parasites (181). Hyperimmune sera generated by infecting mice three times with either *P. berghei, P. yoelii, P. chabaudi* or *P. vinckei* revealed that the four species were serologically indistinguishable by IF assay. Sera from rabbits immunized with soluble antigens from these parasites gave similar results. These findings form the basis of a proposed model of antigenic conservation between the four murine malaria species whereby certain antigens are shared among all four species, some antigens are shared only between the most similar pairs of parasites and then others are specific to each species.

Cellular immunity is also likely to play a role in cross-species immunity and may underpin the protective clinical effects (reduced symptoms and disease severity) - yet there is scant data on the potential contribution of T cells to this immune mechanism. In rodent models, antibody-independent mechanisms clearly influenced susceptibility to heterologous challenge (182). For example, B cell deficient mice chronically infected with *P. yoelii* were resistant to lethal challenge with *P. chabaudi* (182). Cross-reactive T cell responses are also vital to the heterologous immunity observed in murine malaria models of attenuated sporozoite vaccination. Immunization with radiation-attenuated *P. berghei* sporozoites protected 79% of mice challenged with *P. yoelii* sporozoites and immunization with *P. yoelii* sporozoites protected 63% of mice challenged with *P. berghei* sporozoites (183). Heterologous protection was dependent on $CD8^+$ T cells whereas antibodies from immunized mice only recognized homologous, but not heterologous, sporozoites. In another study, 100% of mice immunized with genetically-attenuated *P. yoelii* sporozoites were protected against *P. berghei* sporozoite challenge (184). The authors suggested that late-liver stage arresting sporozoites elicited a broadly protective $CD8^+$ T cell response.

There are few reports of species-transcending T cells in humans. The most definitive study showed that T-cells isolated from volunteers immunized with attenuated blood stage *P. falciparum* parasites proliferated *in vitro* in response to *P. knowlesi* iRBCs (185). Whether these T cells have functional activity to protect against heterologous challenge is not known, but this data could provide important insight for vaccine development.

1.8 Challenges in placental malaria vaccine development

There are two recombinant protein vaccine candidates based on the minimal CSA-binding domains of two different alleles of *var2csa* that recently underwent evaluation in phase Ia/Ib

clinical trials. PRIMVAC consists of the DBL1X-ID1-DBL2X domains of the 3D7 allele of VAR2CSA and the PAMVAC vaccine candidate consists of the ID1-DBL2X-ID2a domains of the FCR3 allele (Figure 1.5) (186, 187). After eliciting high titres of strain-transcending antibodies in pre-clinical small animal studies (188-191), both candidates advanced to clinical trials. The candidates elicited strong antibody responses against the same strain of parasite that the vaccine was based on; however, recognition of different *P. falciparum* strains was limited (186, 187). Likewise, sera from vaccinees were able to block homologous parasite strains from binding to CSA *in vitro*, but when sera from volunteers who had received PRIMVAC were tested against heterologous parasite strains, no blocking was observed (187). No data was reported from the PRIMVAC clinical trial from inhibition of binding assays using heterologous parasite strains. However, a recent review by the authors involved in these studies referred to the lack of strain-transcending inhibition observed with both candidates (192).

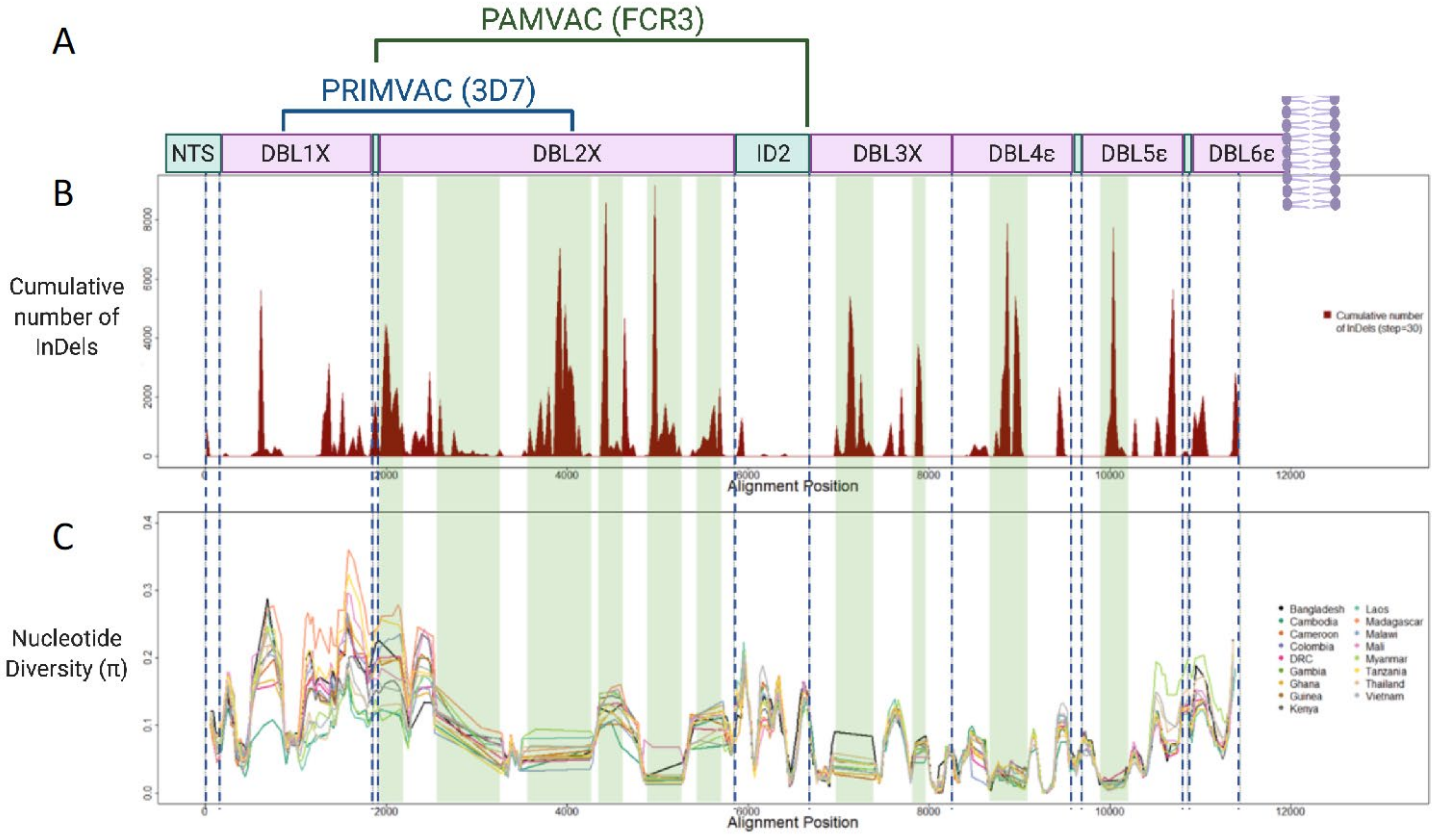

Figure 1.5. VAR2CSA vaccine candidates and sequence diversity. (A) The schematic view of VAR2CSA consists of the N-terminal sequence (NTS), six Duffy binding-like (DBL) domains, interdomain regions (turquoise boxes), transmembrane sequence and the acidic terminal segment (not shown). The PRIMVAC vaccine candidate consists of the DBL1X-ID1-DBL2X domains of the 3D7 allele of VAR2CSA. The PAMVAC vaccine candidate consists of the ID1-DBL2X-ID2a domains of the FCR3 allele of VAR2CSA. Sequence diversity across the first 5 DBL domains from 1,249 field isolates was determined in (193). (B) The accumulation of unique insertions and deletions (InDels) are indicated in red. (C) The nucleotide diversity across the *var2csa* genes is indicated with lines coloured according to the geographic origin of the isolates. Green shading indicates low levels of nucleotide diversity. Figure was adapted from (193) and was made using BioRender.com.

Given the considerable polymorphisms that exist between VAR2CSA antigens from different parasite strains, strain-transcending immunity is a significant, yet vital hurdle that these vaccines must overcome (193). For instance, a recent study evaluating ID1-DBL2 polymorphisms identified 95 distinct variants in Malawi and 57 in Benin (194). There was often more than one variant detected in a single clinical isolate and the authors estimated that approximately 30% of the residues in this region were polymorphic. Unfortunately, this high degree of antigenic polymorphism is not unique to VAR2CSA and the lack of strain-transcending immune responses reported in these studies highlights a common challenge faced by malaria vaccines.

The limitations of current experimental vaccines may reflect a shortcoming in the traditional approach to antigen discovery (195). Candidates, particularly blood stage antigens, are often identified as targets of neutralizing antibodies in immune sera; but the corollary is that this strategy selects for immunodominant epitopes that are under strong immune selection, and consequently, are highly polymorphic. Incorporating conserved and cryptic epitopes (epitopes not normally exposed to the immune system) into vaccines may overcome these challenges.

Based on the immunological cross-reactivity data presented above, we propose that epitopes conserved across species can be exploited in vaccine design. This idea may seem heretical given the absence of sterile immunity following lifelong exposure to a single species, and our understanding that the immune response to malaria is largely considered strain-specific. In fact, cross-species immunity has doubtlessly been selected *against* due to the co-circulation of multiple *Plasmodium* species competing for the same human host. Competition between parasites likely resulted in the evolution of different virulence and lifecycle strategies as a form of mutual adaptation, and within these species-specific adaptations arose antigenic diversity in virulence genes of that parasite. Nevertheless, the shared evolutionary history among the six species of

Plasmodium purports that many proteins will be homologous in origin, with common structures and/or functions. As such, it is likely that there are subdominant or even immunologically cryptic epitopes that remain conserved across multiple species. As a vaccine strategy, this presents an opportunity to direct the immune response against these conserved epitopes and exploit them in a cross-species malaria vaccine.

1.9 Research objectives

The overarching goal of this research was to investigate immunological cross-reactivity between PvDBP and VAR2CSA that is elicited through natural infection and immunization, and to apply this knowledge to rational vaccine design. In Chapter 2, I describe the cross-reactive anti-VAR2CSA antibodies that are elicited in populations naturally exposed to *P. vivax* and through PvDBP immunizations in mice. In Chapter 3, I investigated the nature of the epitopes in PvDBP and VAR2CSA that mediate the cross-reactivity between these antigens. In Chapter 4, I discuss attempts to develop a vaccine candidate based on the putative cross-reactive epitope in PvDBP, with the goal of eliciting cross-reactive antibodies that target VAR2CSA. Finally, in Chapter 5, I show the results from two different approaches to optimize our immunization strategy with hopes of focusing and strengthening the immune response against the cross-reactive epitope(s).

Chapter 2: Cross-species immune recognition between *Plasmodium vivax* Duffy Binding Protein antibodies and the *Plasmodium falciparum* surface antigen VAR2CSA

Data from this Chapter have been previously (155).

2.1 Introduction

Malaria in pregnancy is responsible for 200,000 infant deaths and 10,000 maternal deaths annually (196). Most deaths occur in sub-Saharan Africa and are caused by infection with *P. falciparum*. Morbidity and mortality from MiP is largely attributed to sequestration of parasites in the placenta, whereby iRBCs adhere to the syncytiotrophoblast, resulting in stillbirth, fetal growth restriction, low birth weight and maternal anemia (109, 197).

Sequestration is a common mechanism used by *P. falciparum* to evade host immune defenses and clearance from the spleen. The surface antigen, VAR2CSA, plays a central role in the pathogenesis of placental malaria. Expression of this protein on the surface of iRBCs mediates binding to CSA and parasite accumulation in the placental intervillous space (121). Antibodies targeting VAR2CSA protect women from placental malaria and are associated with improved birth outcomes (198). Protective antibodies typically arise in response to placental infection and as a result, antibodies are acquired in a parity-dependent manner. Primigravid women, who have lower levels of antibodies, have the greatest risk of complications from MiP whereas multigravid women have acquired protective antibodies (199).

VAR2CSA is a member of the PfEMP1 family of proteins and contains six DBL domains and three inter-domain regions (200). It was discovered as an antigen that is upregulated in *P. falciparum* parasites from pregnant women (129) and in parasite strains selected *in vitro* for adhesion to CSA (121). Although most studies report that antibodies to VAR2CSA are confined to pregnant populations, antibodies against the full-length protein or individual domains were

reported in non-pregnant populations (in men and children)(143, 154, 201-203). We previously observed a high frequency of antibodies in non-pregnant populations from Colombia (154). Over 50% of men and children with acute infection with *P. falciparum* or *P. vivax* had antibodies that recognized the ID1-ID2, DBL3X and DBL5ε domains of VAR2CSA. VAR2CSA-specific antibodies were also observed in pregnant women but were independent of parity. We further showed that antibodies from sera of pregnant and non-pregnant Colombians functionally inhibited parasite adhesion to CSA (154).

Neither the origin of these VAR2CSA cross-reactive antibodies nor their role in protecting against placental malaria is known. One hypothesis is that antibodies against VAR2CSA acquired outside of pregnancy could originate from exposure to *P. vivax*, which co-circulates with *P. falciparum* in this region of Colombia. While there is no direct homologue of VAR2CSA in *P. vivax*, two proteins (PvDBP and EBP2) contain DBL domains structurally similar to the six domains in VAR2CSA (204-206). Little is known about the function of EBP2. PvDBP interacts with the DARC on reticulocytes (207) and antibodies to PvDBP are observed in sera of patients exposed to *P. vivax* (208).

Here we demonstrate that men and children from Colombia and Brazil who were exposed to *P. vivax* have antibodies to full-length VAR2CSA. We show that cross-reactive antibodies can originate from exposure to PvDBP during infection and in mice following immunization with the DBPII. We show that the mouse DBPII monoclonal antibody recognizes the surface of VAR2CSA-expressing parasites and inhibits parasite binding to CSA *in vitro*, supporting a role for functional cross-recognition of *P. vivax* PvDBP antibodies against VAR2CSA.

2.2 Methods

2.2.1 Ethical considerations

Study approval was granted by the Health Research Ethics Board of the University of Alberta in Canada (Pro00041720), the Comité de Ética of Instituto de Investigaciones Médicas of Universidad de Antioquia in Colombia (Approval Numbers: 009-2013, 002-2015, 009-2016), the Ethics Committee of FIOCRUZ, Brazilian Ministry of Health and the Ethical Committee of Research on Human beings from the CPqRR/Fiocruz (Reports No. 07/2009 and No. 26/2013; CAEE:50522115.7.0000.5091/ 05/2016), the Comité Consultatif de Déontologie et d'Ethique of the Research Institute for Development in France, the ethical committee of the Faculty of Health Science in Benin, and the Higher Degrees, Research and Ethics Committee in Uganda (HDREC 368). All participants provided voluntary written consent.

2.2.2 Study region and study design

Samples from individuals in two Latin American countries (Colombia and Brazil) were included in this study (Table 2.1). Both symptomatic and asymptomatic men and children exposed to malaria were recruited in Colombia between 2013 and 2016, in the municipality of Puerto Libertador in the Department of Córdoba (7°53′17″N 75°40′18″W; mean altitude 66 m.a.s.l.). The symptomatic population included patients who presented to the clinic with suspected malaria. Sera from the community were collected during a cross-sectional survey. Epidemiologic characteristics of this region are described elsewhere (209). Briefly, the transmission intensity is low and stable, with no marked fluctuations in the number of malaria cases during the year; the entomological inoculation rate ranges from 3.5 to 4.8 infective bites per person per year (210). From 2013-2016, the annual parasitic index (API; number of malaria cases/1,000 inhabitants) in our study region

ranged from 1.2 to 2.7 for *P. vivax*, and 0.1 to 0.7 for *P. falciparum* (Instituto Nacional de Salud, Colombia). Fifty sera from residents of Medellín, where there is no malaria, were included as unexposed controls.

Table 2.1. Study population

Country	Town	Malaria status	Participants, No.	Sex (M:F)
Colombia				
	Puerto Libertador	Exposed to *Pf* and *Pv*	156[a]	154:2[b]
	Medellín	No exposure	50	25:25
Brazil				
	Rio Pardo	Exposed to *Pv*	41	41:0
	Belo Horizonte	No exposure	10	4:6
Canada				
	Edmonton	No exposure	21	5:16

Abbreviations: *Pf, Plasmodium falciparum*; *Pv, P. vivax*
[a]Includes 9 men and children whose sera were used for affinity purification.
[b]Females were ≤ 12 years old.

In Brazil, malaria-exposed participants were recruited in the agricultural settlement of Rio Pardo (1º 46'S-1º54'S, 60º22'W-60º10W), Presidente Figueiredo municipality, northeast Amazonas State in the Brazilian Amazon area. The study site and malaria transmission patterns were described elsewhere (211). A population-based open cohort study was initiated in November 2008, where 541 inhabitants were enrolled at baseline, and after six and twelve months, two similar cross-sectional surveys were carried out. The API in 2008-2009 ranged from 199.0 to 307.6 for *P. vivax* and from 6.5 to 26.2 for *P. falciparum* (211, 212). In addition, plasma samples from malaria-unexposed Brazilian adults were collected in the region of Belo Horizonte, Minas Gerais state.

Positive controls included pooled sera from pregnant women from Benin and Uganda who participated in other studies. Additional unexposed controls included sera from 21 Canadian

residents (five men and 16 women), with no history of travel to malaria-endemic countries. These samples were collected in a previous study (154).

2.2.3 Sample collection

Blood samples from Colombian participants (<5 mL) were collected by venipuncture. Thick and thin blood films were prepared, stained with Giemsa and diagnosed by microscopy. Total nucleic acid was extracted from red blood cell pellets and malaria diagnosis was performed by RT-qPCR as described elsewhere (213). Whole blood and plasma from Brazilian participants was collected as described previously (214) and malaria diagnosis was performed by qPCR (215).

2.2.4 ELISA

The specific levels of antibodies (IgG) were measured in serum samples using an enzyme-linked immunosorbent assay (ELISA) as described elsewhere (154). PfMSP1 and PvMSP1 were purchased commercially (CTK Biotech, USA). VAR2CSA DBL domains (FCR3 allele) and *IT4var07* CIDRα1.4 were produced in *E. coli* as described (216). Full-length VAR2CSA (FCR3 allele) was produced as described (217). The DBPII region of the PvDBP DBL domain was expressed and purified as described (218). Plates were coated with 0.5 µg/mL of each antigen. Optical density (OD) values were converted to arbitrary units (AU) (219) relative to a pool of sera from multigravid women from Benin that was run on each plate, according to the formula: AU= ($OD_{test\ sera}$-background)/$OD_{Benin\ pool}$-background)*100. Background was the OD value of the antigen with secondary antibody alone. Cut-off values for each antigen were determined based on the mean OD of individual Canadian sera (19-21 sera) plus 2 standard deviations and converted to AU against the Beninese multigravid control on the same plate. Two mouse monoclonal antibodies

(mAbs), 3D10 and 2D10 (both IgG1), were developed following immunization with the DBPII domain of PvDBP (218) and compared with a commercial isotype control (Invitrogen, USA).

2.2.6 Affinity purification

Recombinant PvDBP (DBPII region; 3 mg) was loaded onto a HiTrap NHS-Activated HP column (GE Healthcare Life Sciences). Sera from nine Colombian men and children with antibodies to PvDBP were pooled, loaded onto the column, and eluted. Total IgG was purified further using a HiTrap Protein G HP column (GE Healthcare Life Sciences) and quantified using a Nanodrop. The elution fractions containing IgG were concentrated and the buffer was exchanged with 1X PBS, using an Amicon ® Ultra-4 centrifugal filter (Merck Millipore Ltd).

2.2.7 *P. falciparum* culture

P. falciparum CS2 strain (FCR3 allele of VAR2CSA), NF54-CSA (3D7 allele of VAR2CSA), and a placental isolate (220) were cultured *in vitro*, as described previously (221). Parasites were selected on CSA (C9819, Sigma-Aldrich) to enrich for parasites expressing VAR2CSA. Mature parasites were magnet-purified using the VarioMACS according to the manufacturer's instructions (Miltenyl Biotec).

2.2.8 Immunofluorescence (IF) assay

Thin smears of magnet-purified *P. falciparum* CS2 iRBCs were fixed with methanol, washed in 1xPBS, blocked in 3% BSA/1xPBS for 1 h at RT and placed in a humidified chamber at 4°C overnight with primary antibody at 1/100 in 1%BSA/1xPBS. Slides were washed and secondary antibody (Alexa555 goat anti-mouse or Alexa647 goat anti-rabbit; Molecular Probes)

was diluted 1/500 in 1%BSA/1xPBS and incubated for 2 h at RT. Prolong® Gold Antifade reagent containing DAPI (Molecular Probes) was applied and slides mounted with a no. 1.5 cover glass. Image data were collected using a Leica SP5 laser scanning confocal microscope equipped with a 100x/1.44 oil-immersion lens. A Gaussian filter was applied with a kernel size of 5 using Leica LASAF software. Figures were compiled using Image J.

2.2.9 Flow cytometry

Mature parasites ($1x10^5$ cells) from *P. falciparum* strains CS2 and NF54-CSA, and a placental isolate were incubated for 1 h at 4°C with the 3D10 mAb or isotype control (143 µg/mL). Mouse antibodies were preabsorbed on uninfected RBCs and detected with Alexa Fluor 647 conjugated goat anti-mouse IgG (dilution 1:500, Life Technologies). Rabbit anti-VAR2CSA or normal rabbit serum was preabsorbed on uninfected RBCs, incubated with iRBCs at 1:40, and detected with Alexa Fluor 647 conjugated goat anti-rabbit IgG (1:500, Life Technologies). Parasite DNA was stained with 5 µg/mL of DAPI. Uninfected RBCs were excluded based on DAPI staining. DAPI-positive iRBCs (>11,000 cells) were quantified by flow cytometry (Fortessa X20) and data analyzed with FlowJo version 7.6 (TreeStar, Ashland, USA). For fluorescent flow microscopy, CS2 iRBCs were stained as described above. Images of individual iRBCs were captured using the ImageStream^X Mark II Imaging Flow Cytomoter (Inspire v6.2, Amnis Corporation, Seattle, WA) and analyzed using Ideas software (v6.2, Amnis Corporation, Seattle, WA).

2.2.10 Inhibition of Binding Assay (IBA)

The ability of antibodies to interfere with CSA adhesion of iRBCs was assessed by a modified static IBA protocol (154). Total IgG was purified from sera of Colombian men and

children positive for antibodies to PvMSP1 and VAR2CSA, but negative for antibodies to PfMSP1 (sera from Figure 1B that had an AU for VAR2CSA above the cut-off), using a HiTrap Protein G HP column (GE Healthcare Life Sciences) and quantified using a Nanodrop. The control total IgG was purified from a pool of sera from Colombian men and women living in Medellín. IgGs were tested in the IBA at a concentration of 4 mg/mL. The mouse DBPII monoclonal 3D10 and the IgG1 isotype control were tested in the IBA at a concentration of 100 µg/mL. Following incubation with antibodies and iRBCs, the entire CSA spot was imaged with a 4X objective using an EVOS FL Auto microscope (Invitrogen) equipped with a 4X/0.13 lens and the number of bound iRBCs on each spot was quantified using Image J. All experiments included replicates across multiple plates and strains and were performed at least twice. The percent inhibition was based on the number of parasites bound per spot after incubation with the test sera or IgG divided by the control, with the sCSA counts as 100% maximum inhibition.

2.2.11 Statistical analyses

Data were plotted using Prism software (version 7; GraphPad). A D'Agostino-Pearson test was used to determine if data sets for the serology data (Figure 1A) followed a normal distribution. Comparisons of VAR2CSA AU data were made using a Kruskal-Wallis test and Dunn's multiple comparisons test. Comparisons of parasite counts in IBAs were made using Student's *t* test (Figures 2.1C and 2.5).

2.3 Results

2.3.1 Populations exposed to *P. vivax* have VAR2CSA antibodies

We first tested whether non-pregnant populations living in a malaria-endemic region of Colombia have VAR2CSA antibodies (Figure 2.1A). Negative controls included Canadians and

non-exposed Colombians living in Medellín where there is no malaria (all were confirmed negative for malaria infection by qPCR). In the negative controls, few had antibodies to VAR2CSA (Figure 2.1A). In contrast, 50/94 men and children who presented to the clinic in Puerto Libertador (Table 2.2) had VAR2CSA antibodies (49% of men and 61% of children; Figure 2.1A). Asymptomatic men and children from the community (53 in total, all PCR negative; Table 2.2) also had VAR2CSA antibodies (40% of the men and 64% of the children; Figure 2.1A). These results are consistent with our published data that Colombian men and children had antibodies recognizing the recombinant VAR2CSA domains ID1-ID2, DBL3X and DBL5ε (154). Given that the full-length protein has a higher affinity for CSA than the individual domains (222), we focused on the cross-reactivity to the entire folded protein rather than the individual domains.

Table 2.2 Nonpregnant Populations from Puerto Libertador, Colombia, Tested for Serum Reactivity to the *Plasmodium falciparum* Surface Antigen VAR2CSA

Group, Recruitment Site	Participants, No.	Species, No.
Men (n = 105)		
Clinic	63	…
Positive	30	*P. vivax* (22), *P. falciparum* (8)
Negative	33	None
Community	42	…
Negative	42	None
Children[a] (n = 42)		
Clinic	31	…
Positive	15	*P. vivax* (9), *P. falciparum* (6)
Negative	16	None
Community	11	…
Negative	11	None

[a]Includes 2 girls ≤12 years of age

We hypothesized that VAR2CSA antibodies acquired outside of pregnancy arose from exposure to *P. vivax*. To determine whether Colombian men and children were exposed to different

species of *Plasmodium*, serology was performed using PfMSP1 and PvMSP1. Negative PfMSP1 serology suggests lack of recent exposure to *P. falciparum* based on the long antibody half-life (7.6 years in similar low transmission settings) (223) and the findings that PfMSP1 antibodies were reported to occur in 80% of individuals recently infected with *P. falciparum* (224). We identified 28 sera reactive only to PvMSP1. Forty-six percent of sera had antibodies that recognized VAR2CSA (Figure 2.1B). While lack of antibodies to PfMSP1 does not definitively exclude prior exposure to *P. falciparum*, we subsequently identified a population in the Brazilian Amazon with no documented infection with *P. falciparum* during the five years prior to sample collection, according to the Brazil Epidemiological Surveillance Information System (SIVEP). After screening by serology, sera from 41 men and children were positive for antibodies to PvMSP1 and negative against PfMSP1. Of these, 31 had antibodies that recognized VAR2CSA (76%; Figure 2.1B), consistent with the high frequency of cross-reactive antibodies in our Colombian population.

To test whether VAR2CSA antibodies in the *P. vivax*-exposed populations are functional, total IgG was purified from the Colombian sera that were positive for VAR2CSA, pooled, and tested in triplicate in the inhibition of binding assay (IBA) in which iRBCs are incubated with antibody prior to being added to CSA adsorbed to plastic. These IgGs blocked binding to CSA of a *P. falciparum* placental isolate (adapted to *in vitro* culture) by 24% relative to total IgG purified from a pool of sera from Medellín where there is no malaria (Figure 2.1C). This experiment was repeated with the CS2 strain with both purified IgG and total serum, with similar results. The mean percent inhibition across all experiments and strains (n=5 independent experiments) was 22.3% ± 3.9% SEM.

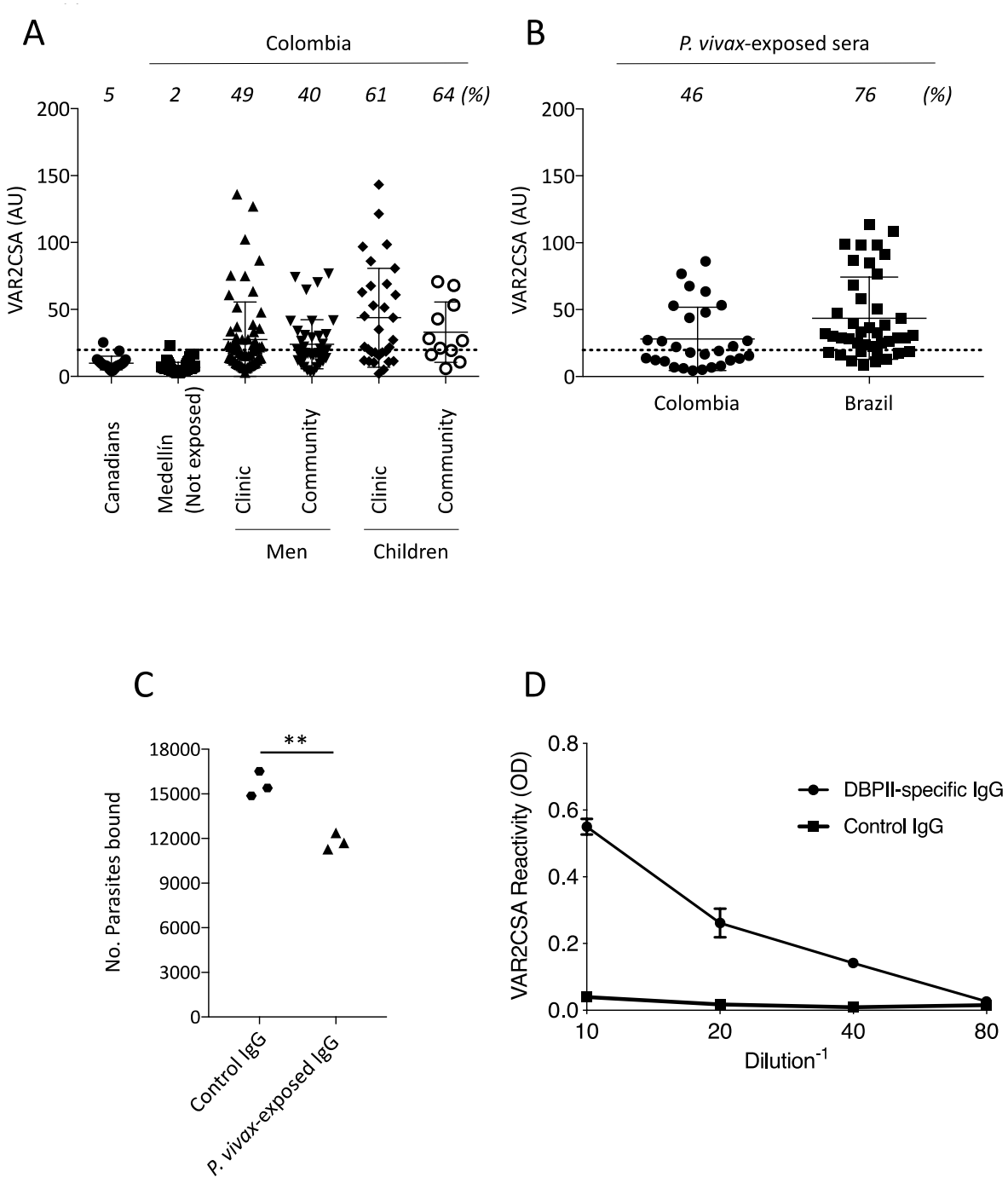

Figure 2.1. Human antibodies to DBPII recognize VAR2CSA. (A) Sera from different populations in Colombia were tested for reactivity to full-length VAR2CSA (FCR3 allele) by ELISA (dilution 1/1000). Values are expressed as arbitrary units (AU) relative to a positive control on each plate, with mean and SD. A cut-off value (stippled line) was determined for each antigen based on the mean OD values for individual sera from the Canadian population plus 2 SD. The percentage of samples with an AU above the cut-off is indicated for each population (%). AU values of the sera from the malaria-exposed groups in the clinic and community were significantly

different from the unexposed group from Medellín using a Dunn's multiple comparisons test ($p<0.0001$ for all comparisons between groups). (B) VAR2CSA reactivity in sera positive against PvMSP1 and negative against PfMSP1. Samples are from Colombia and Brazil, and analysed against VAR2CSA as in (A). (C) Colombian sera from (B) that were seropositive against VAR2CSA and with *P. vivax* exposure were pooled and IgG was purified. Total IgG was tested in the inhibition of binding assay against a placental isolate that was adapted to *in vitro* culture. Total IgG was purified from the pooled sera of unexposed Colombians as control IgG. Results are expressed as the number of parasites bound to CSA from triplicates of a representative experiment. Significance was determined using a Student's *t* test comparing unexposed Control IgG and *P. vivax*-exposed IgG for each experiment. ** $p < 0.01$. (D) DBPII antibodies were affinity-purified from a pool of sera from Colombian men and children previously exposed to *P. vivax* and titrated against VAR2CSA (FCR3) by ELISA, with an initial concentration of 12 µg/mL IgG (1/10 dilution on the x-axis). IgG of unexposed Colombians served as the control. Data are mean OD values ± SD.

2.3.2 PvDBP and VAR2CSA share common epitopes

DBL domains in VAR2CSA and PvDBP share structural similarities (206) and 16-21% sequence identity (Figure 2.2). We therefore asked whether PvDBP antibodies in *P. vivax*-exposed individuals would cross-react with VAR2CSA, thus identifying a potential source for these antibodies. We affinity-purified DBPII IgG from pooled sera from Colombian men and children and found that DBPII-specific human antibodies reacted with VAR2CSA with an endpoint titre of 3 µg/mL (Figure 2.1D). Total IgG purified from Medellín sera was used as a negative control. These data suggest that exposure to PvDBP following *P. vivax* infection is one possible source of antibodies that recognize VAR2CSA.

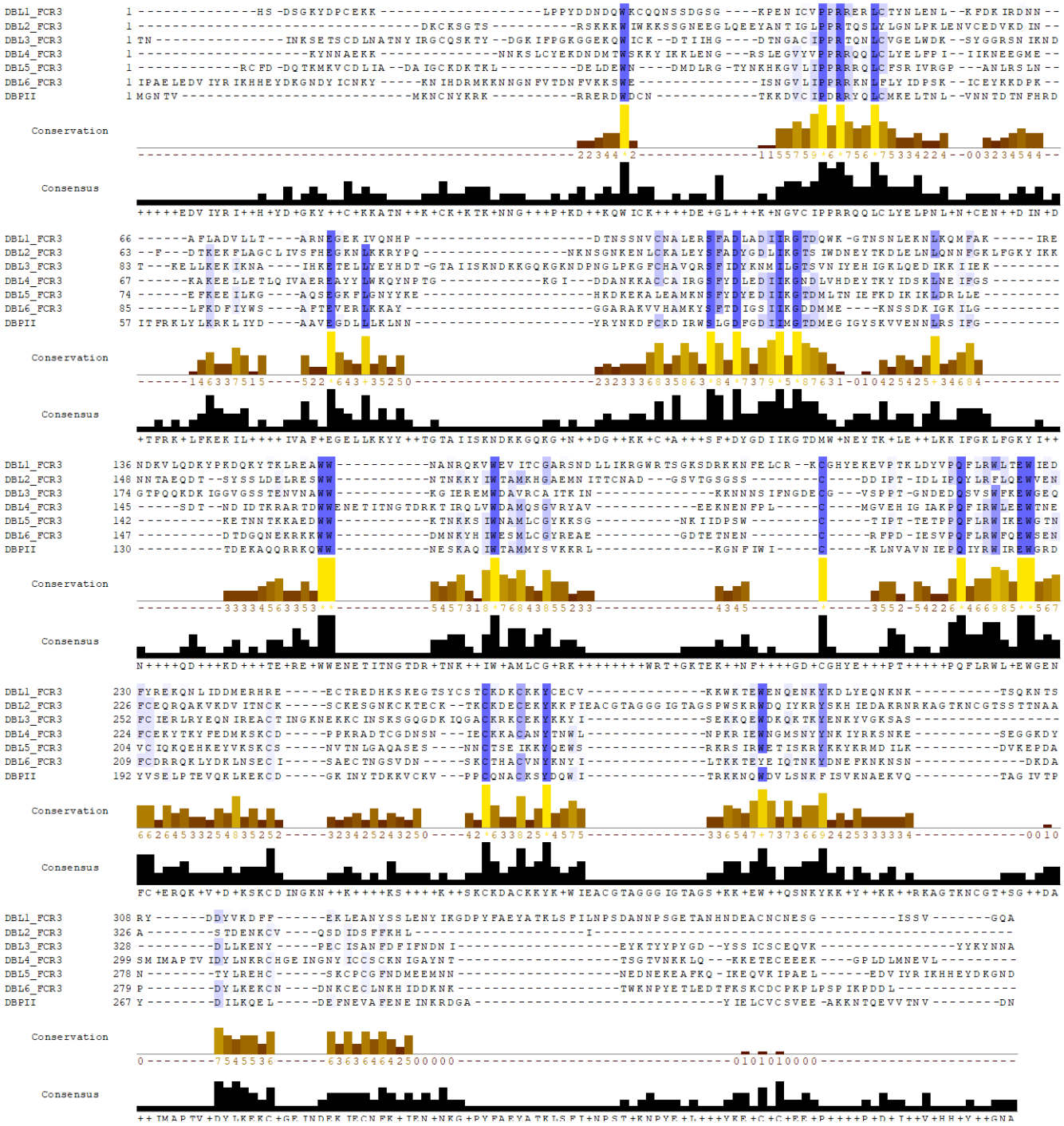

Figure 2.2. Alignment of DBL domains from VAR2CSA and PvDBP. Individual DBL domains from VAR2CSA (FCR3 allele) were aligned with the DBPII. Multiple alignments were produced with MAFFT version 7 using the L-INS-I algorithm under default parameters. Alignments were visualized and manually adjusted in Jalview. Dark blue shading indicates that >80% of the residues agree with the consensus sequence. Lighter and lightest shades indicate >60% and >40% agreement, respectively.

To determine whether immunization with DBPII can generate cross-reactive antibodies, we took advantage of two monoclonal antibodies, 3D10 and 2D10 (both IgG1), that developed following immunization with DBPII (218). We tested their reactivity to VAR2CSA and observed strong recognition with 3D10 with an endpoint titer of 0.86 μg/mL but much weaker recognition with 2D10 (Figure 2.3A). The 3D10 mAb also recognized individual recombinant DBL domains from VAR2CSA with the strongest reactivity against DBL5ε and ID1-ID2 (Figure 2.3B). This indicated that there was at least one epitope of DBPII that was shared with different domains of VAR2CSA.

Based on the cross-reactivity of 3D10 to VAR2CSA, we tested whether it recognized the protein expressed on the surface of iRBCs by IF assay. Mature forms of *P. falciparum* CS2 iRBCs that expressed VAR2CSA were fixed and stained with 3D10 and visualized by immunofluorescence (Figure 2.3C). We observed staining at or near the surface of iRBCs. The pattern of recognition was similar to that seen when iRBCs were co-stained with rabbit anti-VAR2CSA antibodies. Neither antibody stained uninfected red cells. Normal mouse serum and normal rabbit serum did not stain CS2 iRBCs. 3D10 also recognized live iRBCs (Figure 2.3D), as observed by live cell imaging ('Image Stream') with 3D10 and VAR2CSA antibodies co-localizing to the cell surface.

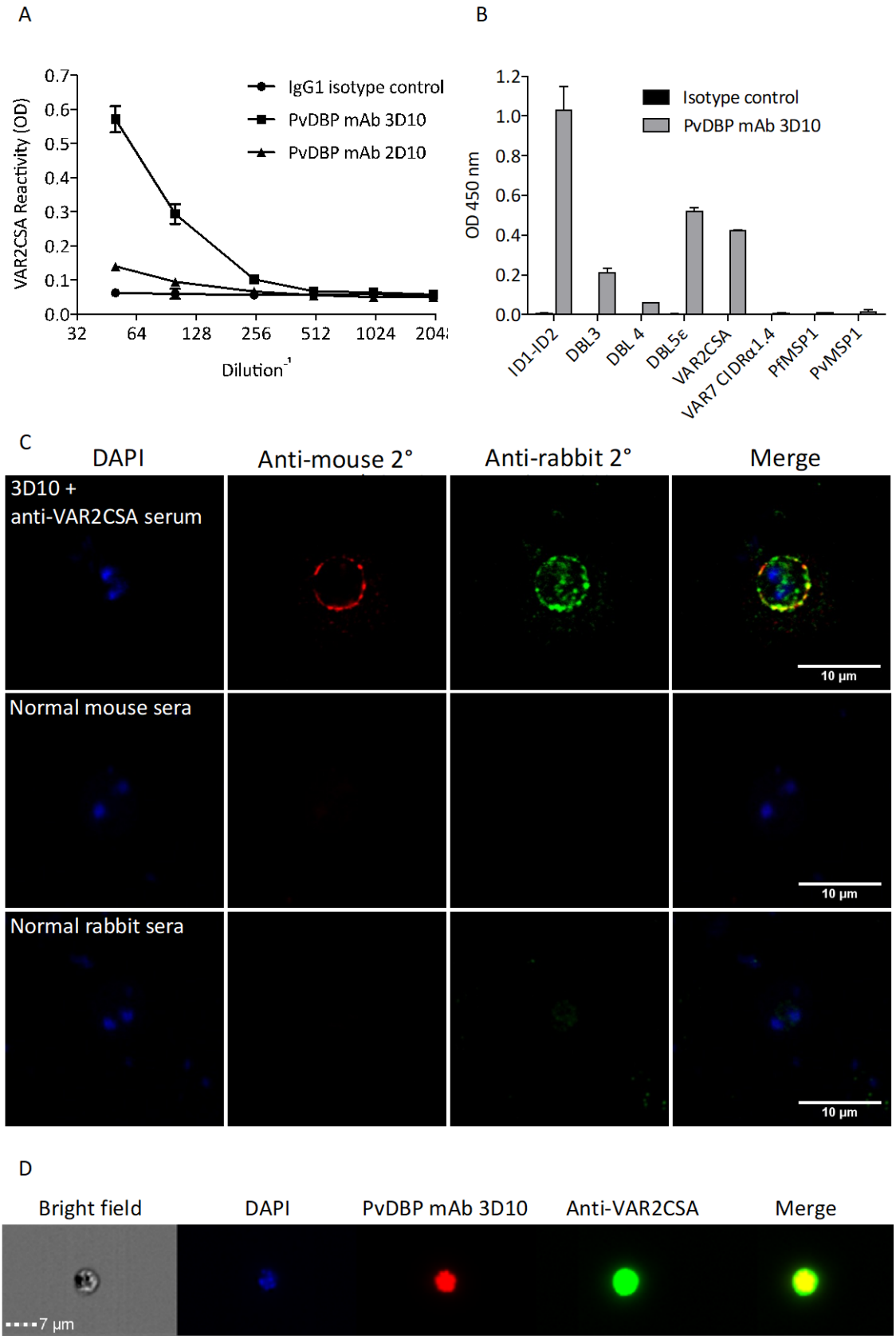
A
VAR2CSA Reactivity (OD)
IgG1 isotype control
PvDBP mAb 3D10
PvDBP mAb 2D10
Dilution⁻¹
B
OD 450 nm
Isotype control
PvDBP mAb 3D10
ID1-ID2
DBL3
DBL 4
DBL5ε
VAR2CSA
VAR7 CIDRα1.4
PfMSP1
PvMSP1
C
DAPI
Anti-mouse 2°
Anti-rabbit 2°
Merge
3D10 +
anti-VAR2CSA serum
Normal mouse sera
Normal rabbit sera
10 µm
D
Bright field
DAPI
PvDBP mAb 3D10
Anti-VAR2CSA
Merge
7 µm

Figure 2.3. A DBPII mouse monoclonal antibody recognizes VAR2CSA. (A) Titration of two DBPII mouse mAbs (3D10 and 2D10) and control IgG1 against full-length VAR2CSA (FCR3) by ELISA. The concentration of the first dilution (1/50 on the x-axis) of each antibody was 8.6 μg/mL. Data are mean OD values ± SD. (B) DBPII mAb 3D10 and the isotype control (both at 8.6 μg/mL) were tested against various recombinant DBL domains from VAR2CSA (ID1-ID2, DBL3X, DBL4, and DBL5ε), full-length VAR2CSA, *IT4var07* CIDRα1.4, PfMSP1 and PvMSP1 by ELISA, all coated at 0.5 μg/mL. (C) RBCs infected with mature CS2 parasites were fixed and co-stained with DAPI (blue), DBPII mAb 3D10, detected using a goat anti-mouse secondary (2°) antibody (red), and a rabbit polyclonal antibody to VAR2CSA, detected using a goat anti-rabbit secondary (2°) antibody (green). Normal mouse and normal rabbit sera were included as negative controls and are shown in the bottom two rows (D) Live cell images of a representative CS2 iRBC (bright field and DAPI) that shows co-staining of DBPII mAb 3D10 (red) and anti-VAR2CSA antibody (green).

Next, we quantified the population of cells recognized by 3D10 by flow cytometry (Figure 2.4). All strains were selected on CSA and >60% of iRBCs expressed VAR2CSA on the cell surface (Figure 2.4A, B). We observed that 9.1% of RBCs infected with CS2 parasites stained with 3D10, compared to the IgG1 isotype control (3.3%) (Figure 2.4C, D). While the overall percentage was low, the proportion of stained cells was higher with 3D10 compared to the isotype control and we observed high staining of individual cells recognized by the antibody. 3D10 recognized populations of trophozoites and schizonts whereas only 0.22% of RBCs enriched for rings were recognized (data not shown). 3D10 recognized a similar population of iRBCs from a placental isolate and NF54-CSA (Figure 2.4C, D), suggesting that the antibody to DBPII cross-reacts with multiple alleles of VAR2CSA. The small proportion of live stained cells compared to the fixed cells could indicate that the affinity of the cross-reactive antibodies is low, and the antibodies are sensitive to the washing during the flow procedure. Alternatively, the expression of the epitope recognized by 3D10 on the surface of iRBCs may be transient or the epitope is partially embedded within the plasma membrane.

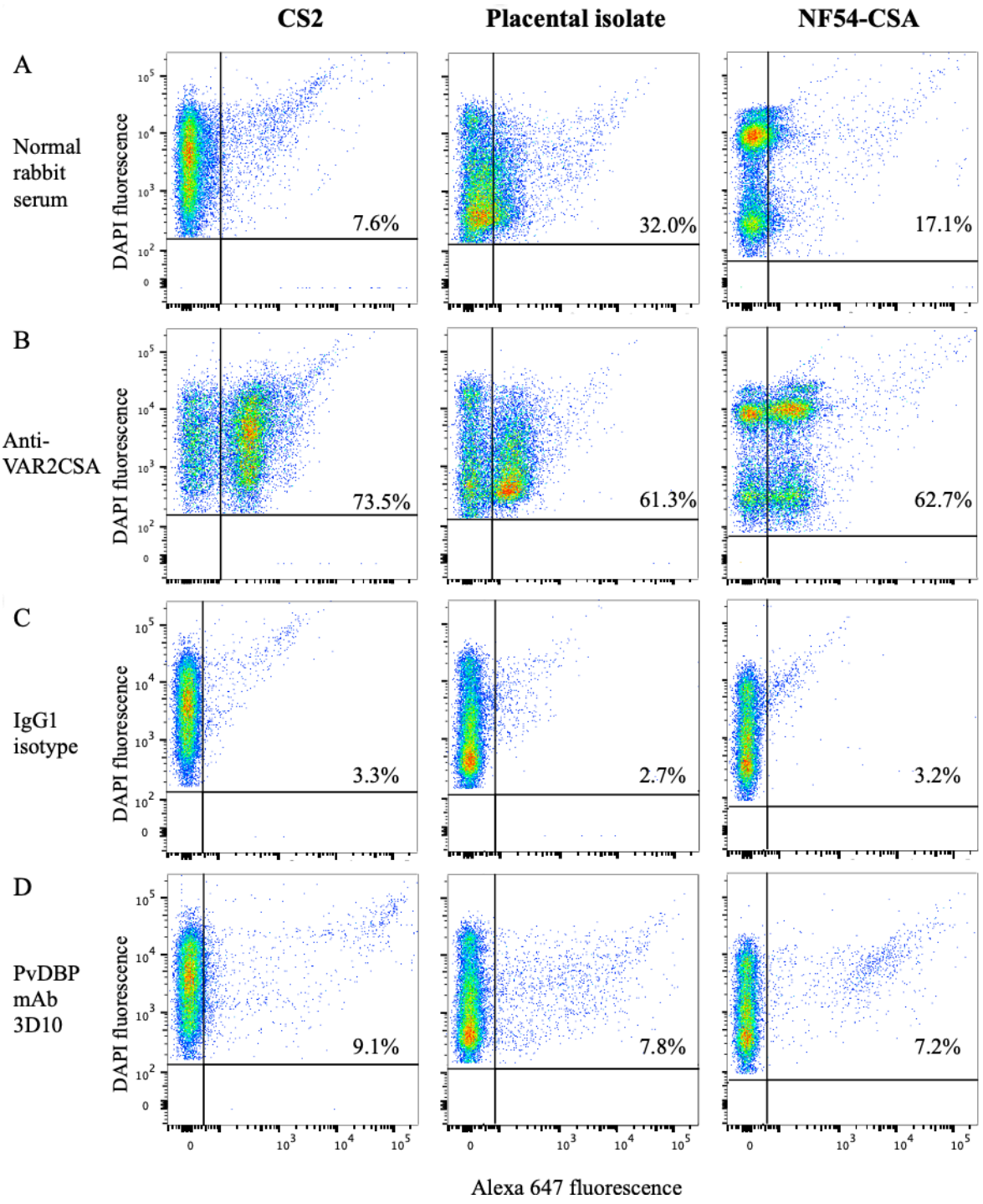

Figure. 2.4. DBPII mAb 3D10 recognizes live CS2 iRBCs. *P. falciparum* CS2, a placental isolate and NF54-CSA iRBCs were analyzed by flow cytometry. To verify the expression of VAR2CSA, iRBCs were stained with normal rabbit serum (A) and a polyclonal anti-VAR2CSA rabbit antibody (B), both at 1:40 dilution. All three strains were stained with the IgG1 isotype control (C) and DBPII 3D10 mAb (D), both at 143 µg/mL. The percent of iRBCs recognized by the antibody is indicated on each plot.

2.3.3 Inhibition of iRBC binding by DBPII mAb 3D10

To test the functional activity of 3D10, we asked whether it could block iRBC binding to CSA (Figure 2.5). Three parasite strains were tested that expressed high surface levels of VAR2CSA. Sera from primigravid and multigravid women from Uganda and soluble CSA were used as controls to measure inhibition of binding (Figure 2.5A). 3D10 inhibited binding of CS2 iRBCs to CSA by 32% relative to the IgG1 isotype control (Figure 2.5B). Binding inhibition, although partial, was also observed with the placental isolate and NF54-CSA (Figure 2.5C,D), suggesting that the epitope recognized by 3D10 may be conserved between falciparum strains. The mean percent inhibition across all experiments and strains (n=8 independent experiments) was 18.1% ± 3.0% SEM.

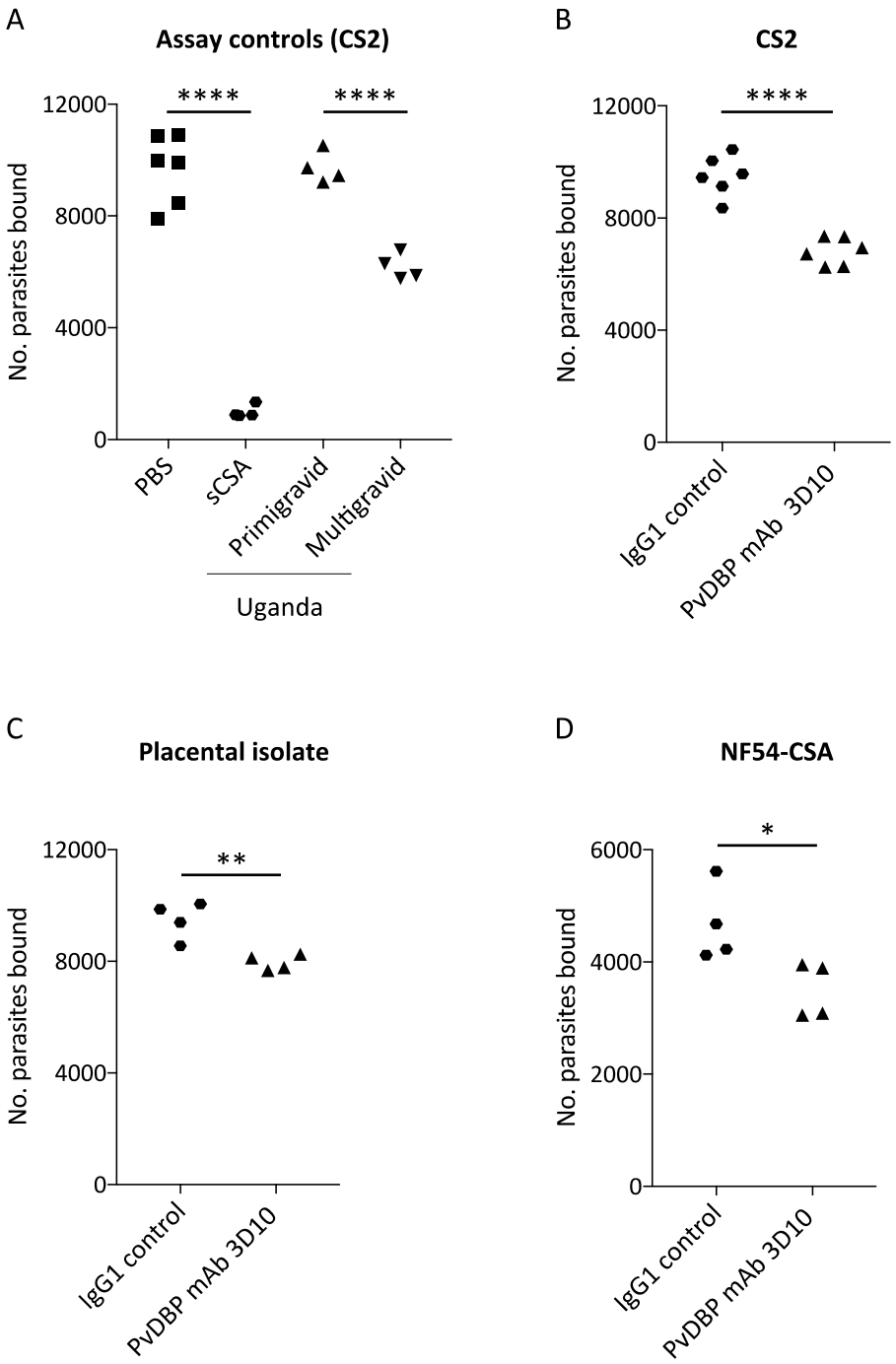

Figure 2.5. DBPII mAb 3D10 blocks adhesion of iRBCs to CSA. Controls for the IBA included CS2 iRBCs incubated with PBS alone, soluble CSA (sCSA), sera from primigravid and multigravid women from Uganda (A). DBPII mAb 3D10 was tested for inhibition of CS2 (B), a placental isolate (C), and NF54-CSA (D) iRBC binding to CSA. Results are expressed as the number of parasites bound to CSA from replicates of a representative experiment. Significance was determined using a Student's *t* test comparing. * $p < 0.05$, ** $p < 0.01$, **** $p < 0.0001$.

2.4 Discussion

This is the first demonstration of cross-species functional immune recognition of proteins involved in different virulence pathways from two divergent species of *Plasmodia*. Antibodies against the DBL domain from *P. vivax* PvDBP recognized DBL domains of *P. falciparum* VAR2CSA, which may contribute to cross-species immunity. We further showed that a PvDBP cross-reactive epitope is expressed on the surface of *P. falciparum* iRBCs, where it can sensitize the parasite to antibody-mediated inhibition of binding to CSA – the hallmark correlate of immunity to placental malaria. These findings are consistent with our previous findings that serum antibodies from Colombian men, women and children (with exposure to both *P. falciparum* and *P. vivax*) could inhibit binding of *P. falciparum* iRBCs to CSA (154). Here, we identified one source of these antibodies: exposure to PvDBP. Recently, PvDBP antibodies were associated with increased infant birth weight in a study from countries where both *P. vivax* and *P. falciparum* were prevalent, including Colombia and Brazil (225). We speculate that the increased birth weight in some infants is in response to cross-species protection against *P. falciparum*, leading to better pregnancy outcomes. This idea remains to be investigated in future studies.

Our findings are consistent with reports of broad antibody cross-reactivity between *P. falciparum* or *P. vivax* outside of pregnancy (177, 178, 226, 227), and several examples of antigen-specific reactivity between these two species. Sera from *P. vivax*-exposed individuals from Brazil recognized peptides from PfCLAG9 and conversely, antibodies raised against these peptides in mice recognized *P. vivax* iRBCs by IF assay (228). Cross-reactivity between orthologous proteins was reported for PfMSP5 and PvMSP5 (229), PfAMA-1 and PvAMA-1 (230), and recently, cross-boosting was demonstrated between Pvs48/45 and Pfs48/45 in mice (231). We provide the first evidence of cross-reactivity between non-orthologous proteins that are involved in different

biological pathways: cytoadherence and parasite invasion. Both pathways are essential for parasite survival during blood stage infection, which may have led to evolutionary conservation of specific epitopes in this protein family. Although the mechanism is not yet known, it is possible that binding of 3D10 to VAR2CSA blocks iRBC adhesion to CSA by steric hindrance. Based on our flow data, the target epitopes in VAR2CSA may be cryptic or exposed transiently, resulting in only a subset of iRBCs recognized by 3D10. However, this small proportion of cells was stained very strongly by the antibody, which could account for the partial inhibition of adhesion to CSA that we observed in the IBA.

Cross-reactivity among DBL domains in *P. falciparum* and *P. vivax* may extend beyond the ones characterized here. It will be important to map the target cross-reactive epitopes within all six domains of VAR2CSA and even other DBL proteins from *P. falciparum* that play a role in cytoadherence or invasion. It is also possible that the DBL domain of EBP2 can induce antibodies that recognize VAR2CSA or other DBL proteins from *P. falciparum*. Given their structural similarity (205, 232), PvDBP is likely not the sole determinant of cross-reactivity to VAR2CSA.

2.5 Conclusion

We discovered a novel mechanism that may lead to natural immunity to *P. falciparum* through cross-species recognition of a structurally related DBL domain from *P. vivax*. The specific epitopes in PvDBP that induce functional antibodies and inhibit parasite adhesion to CSA may be exploited as an approach to a vaccine against pregnancy-associated malaria and complement current vaccines in development that are based on domains of VAR2CSA.

Chapter 3: Antibodies to cryptic epitopes in distant homologues underpin a mechanism of heterologous immunity between *Plasmodium vivax* PvDBP and *Plasmodium falciparum* VAR2CSA

Data from this Chapter have been previously (233).

3.1 Introduction

Heterologous immunity can develop when prior exposure to one pathogen modulates the host immune response to pathogens of genetically diverse species. This form of immunity can be induced by vaccination or arise from natural infection, and lead to protective or deleterious outcomes following infection with a different organism. One of the classic examples of heterologous protection is the success of the cowpox vaccine to eradicate human smallpox. More recently, vaccination with the meningococcal B vaccine correlated with reduced incidence of gonorrhea (234, 235), and natural exposure to the non-tuberculous mycobacteria in the environment can induce heterologous immunity to *Mycobacterium tuberculosis* (236). This phenomenon can also be modeled in mice, where immunization or infection with one virus protects against heterologous viral challenge (237). For example, infection with influenza A virus can protect against challenge with RSV and vaccinia virus (238, 239) and immunization with adenovirus can protect against hepatitis C virus (240). Similarly, infection with Japanese Encephalitis Virus in mice can prime the immune response and promote rapid viral clearance following heterologous challenge with ZIKA virus (241).

Despite the evidence that cross-species immunity can be highly protective, it remains controversial whether this form of immunity plays a role in protection from malaria. Malaria is a parasitic disease caused by five species of *Plasmodium* with overlapping endemicity in many geographic areas. Population-based data from several regions where multiple species of

Plasmodium co-exist, such as South Asia and parts of Oceania, are consistent with heterologous immunity against *P. falciparum* following prior infection with *P. vivax* (226, 227, 242-244). However, the mechanism of heterologous immunity to malaria is not defined. In humans, T cells induced by vaccination with *P. falciparum* respond *in vitro* to *P. knowlesi* infected red blood cells, suggesting a role for the cellular arm of the immune system (185). In other studies, there is clearly heterologous cross-reactivity between antibodies as sera from patients infected with *P. vivax* cross-reacted with antigens from *P. falciparum* (170, 177, 178, 245, 246). These antibodies may cross-react with orthologous proteins involved in the same biological pathways in each species, such as PfMSP5/PvMSP5 (229), PfCLAG9/PvCLAG9 (228), PfAMA-1/PvAMA-1 (230), PfCSP/PvCSP and PfMSP-1/PvMSP-1 (247), and between Pfs48/45 and Pvs48/45 (231). However, functional activity of these cross-reactive antibodies was not reported.

We recently identified cross-species immune recognition between two homologous parasite proteins that are implicated in distinct biological pathways - *P. vivax* DBP and *P. falciparum* VAR2CSA (248). PvDBP is a protein expressed on the surface of merozoites that mediates invasion into red blood cells by binding to the DARC (10). VAR2CSA, on the other hand, is expressed by mature *P. falciparum* trophozoites and mediates sequestration of iRBCs in the placenta (121, 126, 129, 249). Sequestration is a common immune evasion mechanism thought to prevent destruction of iRBCs in the spleen and involves the interaction between certain antigenic variants of the PfEMP1 family expressed on the surface of iRBCs with specific host receptors in different tissues (250). In pregnancy, parasites express the PfEMP1 variant VAR2CSA which binds to CSA in the placenta. Placental sequestration is an important feature of malaria in pregnancy that can lead to poor outcomes for mother and baby, including stillbirth, preterm birth, low birth weight and maternal anemia and death (117-119).

Most studies that evaluated the acquisition of VAR2CSA antibodies have focused on women in sub-Saharan Africa, where *P. falciparum* is the dominant species (198). These studies showed parity-dependent anti-VAR2CSA antibody acquisition, which occurred following multiple malaria infections in pregnancy (121). We discovered an alternate route of anti-VAR2CSA antibody acquisition outside of pregnancy in areas where *P. vivax* and *P. falciparum* co-circulate (248). We showed that cross-reactivity is mediated by DBL domains, which are structurally-conserved domains present in many *Plasmodium* proteins, including VAR2CSA, which has 6 DBL domains (129) , and PvDBP, which has one (251). Antibodies against the DBPII from non-pregnant populations exposed to *P. vivax* recognized VAR2CSA by ELISA. Moreover, a mouse mAb against DBPII recognized VAR2CSA and blocked parasite adhesion to CSA *in vitro*.

Here, we probed the underlying mechanism of heterologous immunity to VAR2CSA. We identified a subdominant epitope in DBPII that mediates cross-reactivity to VAR2CSA and show that human antibodies purified against this epitope block iRBC adherence to CSA. Furthermore, both the human epitope-specific antibodies and the mouse mAb recognize overlapping, cryptic epitopes in VAR2CSA.

3.2 Methods

3.2.1 Human subjects

Approval for this study was granted by the Health Research Ethics Board of the University of Alberta in Canada (approval Pro00041720); the Comité de Ética of Instituto de Investigaciones Médicas of Universidad de Antioqua in Colombia (approvals 009-2013, 002-2015, 009-2016); the Ethics Committee of the Fundação Oswaldo Cruz, the Brazilian Health Ministry, and the Ethical

Committee of Research on Human Beings from the CPqRR/Fundação Oswaldo Cruz (reports 07/2009 and 26/2013; CAEE:50522115.7.0000.5091/05/2016), and the Higher Degrees, Research, and Ethics Committee in Uganda (HDREC approval 386). Participation in all studies was voluntary and each participant provided written consent.

Samples from individuals in Colombia, Brazil and Uganda were included in this study. In Souza, Brazil, samples were collected from individuals that were infected during a *P. vivax* outbreak in an otherwise malaria-free region (252). Samples from five individuals were tested in this study. Malaria-exposed individuals were recruited from the agricultural settlement of Rio Pardo, in the Brazilian Amazon to participate in a population-based open cohort study initiated in November 2008 (211). In this study, we included samples from individuals that were positive for exposure to *P. vivax* (based on PvMSP1 reactivity), but negative for *P. falciparum* exposure (based on PfMSP1 reactivity). Samples were also collected from unexposed Brazilians living in Belo Horizonte and used as negative controls. In Colombia, both symptomatic and asymptomatic men and children (including girls under 12 years of age) were recruited between 2013 and 2016 in the municipality of Puerto Libertador in the Department of Córdoba. Sera samples were collected in the community as part of a cross-sectional survey (asymptomatic cohort) and from individuals presenting to the clinic with suspected malaria (248). Sera samples from 50 unexposed individuals living in Medellín, Colombia were also collected and used as negative controls. In Bugiri, Uganda, plasma samples were collected from individuals over one year of age that presented to the clinic with suspected malaria, as part of another study (253). The samples used in this study were collected from male children and multigravid women, who were pregnant at the time of collection.

3.2.2 Mice

Mice used for the Sal 1 immunizations were purchased from Harlan Animal Research Laboratories and housed in the University of South Florida Animal Facility. Female BALB/c mice (6 – 8 weeks old) were used for immunizations. All procedures were approved by the Institutional Animal Care and Use Committee. Mice used for the DBL5ε immunizations were purchased from Charles River Laboratories and housed in the University of Alberta Animal Facility in a virus antibody-free room. Female BALB/c mice (6 – 8 weeks old) were used for immunizations. All procedures were approved by the University of Alberta Animal Care and Use Committee and mice were handled in accordance with the Canadian Council on Animal Care guidelines.

3.2.3 Synthetic peptide design

The SD1ss peptide was synthesized (Synpeptides Co.) with the following sequence: ASNTVMKNSNYKRKRRERDWDCNTKKDVCIPDRRYQLSMK. In this peptide, two of the cysteines (C_9 and C_{38}) were mutated to serine to ensure that only one disulphide bond could form. Thirty-one overlapping 20-mer peptides were designed to cover the entire DBL5ε domain of VAR2CSA (Mimotopes).

3.2.4 ELISAs

For indirect ELISAs, 96 well plates (catalogue no. 439454, Thermo Fisher Scientific) were coated with antigen in 1x phosphate-buffered saline (PBS) overnight at 4ºC (antigen concentrations are listed in Table S1). For ELISAs using peptides treated with DTT, the peptides were incubated with DTT (10 mM) at 56ºC for 10 min then added to the plate. Wells were blocked with 4% BSA (catalogue no. A7906, Sigma-Aldrich) for one hour at 37ºC followed by incubation

with the primary antibody for one hour at room temperature (RT) (antibody dilutions are listed in Table 3.1). After four washes with 1x PBST (0.01% Tween 20), an HRP-conjugated secondary antibody was added and the plate was incubated for one hour at RT (secondary antibody dilutions are listed in Table S1) (goat anti-rabbit HRP, catalogue no. 65-6120, Invitrogen; goat anti-mouse HRP, catalogue no. 170-6516, Biorad; goat anti-human HRP, catalogue no. ab98624, Abcam). The plate was again washed four times with 1x PBST before the developing reagent (TMB, catalogue no. T0440, Sigma-Aldrich) was added to each well. The reaction was stopped after 30 min at RT by addition of an equal amount of sulfuric acid (0.5 N) and the optical density (OD) of each well was measured at 450 nm. All samples were run in duplicate and the average OD for the antigen plus secondary antibody alone was subtracted from the OD of all samples.

Peptide competition ELISAs were performed as described for indirect ELISAs, except that the primary antibody was first incubated with a test peptide (SD1ss, 0.01, 0.1, and 1.0 μg/mL; all other peptides, 100 μg/mL) for 30 min at RT before being added to the plate.

Antibody competition ELISAs were also performed as described for the indirect ELISA, except that a competing antibody was added to the plate after blocking. The plate was then washed four times with 1x PBST and the detecting antibody was added. Following another set of washes, an HRP-conjugated secondary antibody directed against the detecting antibody was added.

Table 3.1 ELISA reagent details

Antigen	Antigen concentration (µg/mL)	Primary antibody	Primary antibody dilution	Secondary antibody dilution
SD1ss	1.0	3D10	Titration	1/3,000
		Sal 1 mouse IgG	5.0 µg/mL	
		Human sera	1/200	1/30,000
		Human IgG	5.0 µg/mL	
		Anti-VARCSA rabbit serum	1/750	1/3,000
DBPII	0.5	3D10	0.43 µg/mL	1/3,000
		Sal 1 mouse IgG	0.10 µg/mL	
		Human sera	1/100	1/40,000
		Human IgG	5.0 µg/mL	
C_{29} – K_{40}	5.0	3D10	4.3 µg/mL	1/3,000
VAR2CSA	1.0	3D10	8.6 µg/mL	1/3,000
		Sal 1 mouse IgG	5.0 µg/mL	
	0.5	Mouse serum	1/250	1/3,000
		Human sera	1/500*	1/6,000
		Human sera	1/1000	1/15,000
		Human IgG	5.0 µg/mL	
		Anti-VARCSA rabbit serum	1/750	1/3,000
		Anti-VARCSA rabbit serum	1/200**	1/3,000
EBP2	0.5	Human sera	1/200	1/40,000
		Human IgG	5.0 µg/mL	
PfMSP1	0.5	Human IgG	5.0 µg/mL	1/40,000
DBL5ε	0.5	3D10	4.0 µg/mL	1/3,000
DBL5ε peptides	5.0	3D10	0.86 µg/mL	1/3,000
		Human sera	1/200	1/40,000
		Anti-VARCSA rabbit serum	1/750	1/3,000

*Human sera were tested against VAR2CSA at a dilution of 1/500 in ELISAs performed in Brazil (Figure 2D).
**Rabbit sera were used at a dilution of 1/200 for antibody competition ELISAs (Figure 6C-E).

3.2.5 Immunization scheme

For the Sal 1 immunizations, 15 female BALB/c mice (6 – 8 weeks old) were immunized as previously described (254). Mice were given three doses of recombinant Sal 1 (25 µg/mouse)

emulsified in TitreMax Gold (catalogue no. T2684, Sigma) subcutaneously (s.c.) at day 0, 21 and 42. The final sera samples were collected three weeks after the last immunization.

For the DBL5ε immunizations, a female BALB/c (6 – 8 weeks old) mouse was immunized s.c. with recombinant DBL5ε in 2% Alhydrogel (CAS no. 21645-51-2, Brenntag Biosector) at day 0 (30 µg/mouse), day 21 (10 µg/mouse) and day 31 (10 µg/mouse) and serum was collected on day 45.

3.2.6 Sequencing of Brazilian isolate

Genomic DNA was extracted from 300 µL of whole blood using a genomic DNA purification kit (Puregene, Gentra Systems), according to the manufacturer's protocol. The DBPII region was amplified using the following primers: 5'- CCGTTATGAAGAACTGCAACTACA-3' and 5'- GAATGTGGCGGTGAATATCGAA-3'. The PCR product was isolated using the QIAquick PCR Purification Kit (catalogue no. 28104, Qiagen) and submitted for Sanger sequencing using the same primers used for PCR amplification.

3.2.7 Affinity purification

DBPII affinity purifications were performed using NHS-activated Sepharose beads (catalogue no. 17-0906-01, GE Healthcare) according to the manufacturer's guidelines. Beads (1.0 mL) were added to a filter column and washed with 13 mL ice cold HCl (1mM). Recombinant DBPII (1.7 mg) dissolved in coupling buffer (200 mM $NaHCO_3$, 500 mM NaCl, pH 8.3) was added to the column and incubated overnight at 4ºC. Flow-through was collected following centrifugation for 2 min at 500 x g for analysis of coupling efficiency. Any remaining active sites were deactivated by incubating the column for 2 hr at room temperature with 2 mL of deactivation

buffer (500 mM ethanolamine, 500 mM NaCl, pH 8.3). The column was then washed with 3 mL buffer 1 (100 mM Tris-HCl, 500 mM NaCl, pH 8.3), followed with 3 mL of buffer 2 (100 mM sodium acetate, 500 mM NaCl, pH 4.0). These washes were repeated three times before 5 mL of binding buffer (1x PBS) was flowed through the column. The column was prepared by washing with 3 mL elution buffer (100 mM glycine, pH 2.0), followed by 15 mL 1x PBS. Serum from men and children in Colombia exposed to *P. vivax* and *P. falciparum* was pooled (5 mL) and diluted 1:1 in 1x binding buffer, clarified using a 0.45 µm filter and was then loaded onto the column and incubated for 30 min at room temperature on a rocker. The column was washed with 9 mL of binding buffer until no protein was detected in the flow-through (measured using a NanoDrop). Bound antibodies were then eluted using 5 mL of elution buffer into tubes containing an equal volume of neutralization buffer (1M Tris-HCl, pH 9.0).

SD1ss affinity purifications were performed using NHS-activated HiTrap columns (catalogue no. 17-0716-01, GE Healthcare Life Sciences) according to the manufacturer's guidelines. Columns were acidified with HCl (1 mM) and coated with 1.0 mg of SD1ss in coupling buffer (200 mM $NaHCO_3$, 500 mM NaCl, pH 8.3). Unbound peptide or protein was then washed from the column using 3 column volumes of coupling buffer. Any remaining active sites were deactivated by flowing 2 mL of buffer A (500 mM ethanolamine, 500 nM NaCl, pH 8.3) through the column, followed by 2 mL of buffer B (100 mM acetate, 500 mM NaCl, pH 4.0) and then another 2 mL of buffer A. This was repeated six times, with a 30 min incubation in buffer A at RT after the third set of buffers was added. The column was then washed with 5 mL of 1x PBS, followed by 3 mL of elution buffer (0.1 M glycine-HCl, pH 2.0) and then another 10 mL of 1x PBS. Serum from men and children in Colombia exposed to *P. vivax* and *P. falciparum* was pooled (5 mL) and diluted 1:1 in 1x PBS, clarified using a 0.45 µm filter and loaded onto the column. The

sample was continuously run over the column at a flow rate of approximately 0.5 mL/min for one hour. The column was then washed with 1x PBS until no protein was detected in the flow-through (measured using a NanoDrop). Bound antibodies were then eluted using 5 mL of elution buffer into tubes containing an equal volume of neutralization buffer (1M Tris-HCl, pH 9.0).

Elution fractions from each affinity purification that contained protein were pooled and the buffer was exchanged with 1x PBS using an Amicon Ultra-4 centrifugal filter (catalogue no. UFC801024, Merck Millipore). Total IgG was then purified and the concentration was measured using a NanoDrop.

3.2.8 Purification of total IgG

Total IgG was purified from affinity-purified antibodies, pooled plasma or sera samples using a HiTrap Protein G HP column (catalogue no. 17-0404-03, GE Healthcare Life Sciences) according to the manufacturer's instructions. Briefly, the column was washed with 20 mL of 1x PBS before 1 mL of sera, plasma or affinity-purified antibodies was loaded onto the column. The column was then incubated for 1 hour at RT. The column was then washed with 1x PBS until there was no protein detected in the flow-through (measured using a NanoDrop). Bound IgG was eluted using 3 mL of elution buffer (0.1 M glycine-HCl, pH 9.0) into tubes containing an equal volume of neutralization buffer (1M Tris-HCl, pH 9.0). Elution fractions containing protein were pooled and the buffer was exchanged with 1x PBS using an Amicon Ultra-4 centrifugal filter and the concentration was measured using a NanoDrop.

3.2.9 *P. falciparum* culture

P. falciparum CS2 parasites were maintained in culture at 3% hematocrit in washed erythrocytes collected from O+ blood donors as described previously (221). Parasites were regularly selected for adhesion to CSA (catalogue no. C9819, Sigma-Aldrich) to enrich for parasites expressing VAR2CSA. Mature parasites were magnetically purified using the VarioMACS according to the manufacturer's instructions (LD columns, catalogue no. 130-042-901, Miltenyl Biotec).

3.2.10 IBAs

Ten spots were drawn in a semicircle around the outer edge of the bottom of a Petri dish (catalogue no. 351029, Corning). Each spot was coated with 20 µL CSA in 1x PBS (50 ug/mL) overnight at 4ºC in a humidified chamber. The spots were then blocked with 3% BSA in RPMI (catalogue no. 31800-022, Gibco Life Technologies) for one hour at 37ºC in a humidified chamber. Mature trophozoite stage *P. falciparum* CSA parasites were magnetically enriched using the VarioMACS and diluted to 1.0 x 10^7 cells/mL at 20% parasitemia in 3% BSA in RPMI containing uninfected red blood cells. The cells were then pelleted and the supernatant was replaced with either soluble CSA as a control (100 µg/mL) or antibodies diluted in 1x PBS (DBPII affinity-purified IgG, 100 µg/mL; SD1ss affinity-purified IgG, 90 µg/mL; total IgG from unexposed Colombians, 90 or 100 µg/mL to match concentration of affinity-purified IgG). The samples were then incubated for 30 min at RT and 20 µL was added to the CSA-coated spots. The plates were incubated for 15 min at RT. Plates were then placed on a rocker in a position such that PBS could be added to lower portion of the plate and not come into contact with the spots. 1x PBS (19 mL) was added to each plate and the rocker speed was slowly increased, while a further 6 mL of 1x

PBS was slowly added to the plate. The plates were washed for 8 min on the rocker before the PBS was aspirated from the plates and the remaining cells were fixed by slowly adding 10 mL of 1.5% glutaraldehyde and incubating at RT for 10 min. The cells were stained with 10 mL of 5% Giemsa for 5 min and washed twice with 10 mL of deionized water. To quantify the number of parasites on each spot, the entire spot was imaged using an EVOS FL Auto microscope (Invitrogen) with a 4x/0.13 phase objective lens. ImageJ was used to quantify the number of iRBC bound to each spot. All experiments include replicates across multiple plates.

3.2.11 Homology modeling

The 3D7 DBL5ε homology model was created as described previously (255). Briefly, the multiple alignment was submitted to HHpred server (256) and the best hit was selected based on score and structure resolution (VAR2CSA DBL3X, PBD ID: 3bqk). The model was then validated by submission to the ProQ server (257) and PyMol was used to generate figures (258).

3.2.12 Statistical analysis

Data were plotted using Prism software (version 8; GraphPad). Seroreactivity to different antigens was correlated using Spearman rank correlation (Figures 3.3 and 3.4). Comparisons of parasite counts in IBAs were made using Student's *t* test (Figures 3.5C and D) and comparisons of competition ELISA data were made using one-way ANOVA with multiple comparisons tests (Figures 3.6C-F and 3.7A).

3.3 Results

3.3.1 SD1ss contains the epitope in DBPII that is recognized by 3D10 and mediates cross-reactivity to VAR2CSA

We showed previously that the mAb against DBPII '3D10' cross-reacted with VAR2CSA and blocked parasite adhesion to CSA *in vitro* (248). The epitope recognized by 3D10 is predicted to localize to subdomain 1 (SD1) of DBPII based on mutational analysis of this domain and peptide library screening with the mAb (259, 260). We designed a synthetic peptide, 'SD1ss', that spans the 39 amino acid SD1 sequence and mutated the two outer cysteine residues to serines to ensure formation of a single disulphide bond (Figure 3.1A). We confirmed 3D10 recognition of SD1ss by ELISA and found that 3D10 had the same endpoint titre against DBPII and SD1ss (0.17 ng/mL) (Figure 3.1B).

We then tested the ability of the SD1ss peptide to block 3D10 recognition of DBPII using a competition ELISA. In this assay 3D10 was incubated with increasing concentrations of SD1ss then added to wells coated with DBPII (Figure 3.1C). As a negative control, 3D10 was incubated with C_{29}-K_{40} (at 1.0 µg/mL), a short peptide within SD1 that is not recognized by 3D10 (Figure 3.2). SD1ss blocked recognition of DBPII by 3D10 at a concentration of 1.0 µg/mL (Figure 3.1C), confirming that this peptide contains the epitope that mediates recognition of DBPII. Next, we performed a competition ELISA with full-length recombinant VAR2CSA as the capture antigen. When 3D10 was incubated with SD1ss (at 1.0 µg/mL), but not C_{29}-K_{40}, recognition of VAR2CSA was blocked (Figure 3.1D), showing that SD1ss contains an epitope that mediates cross-reactivity to VAR2CSA.

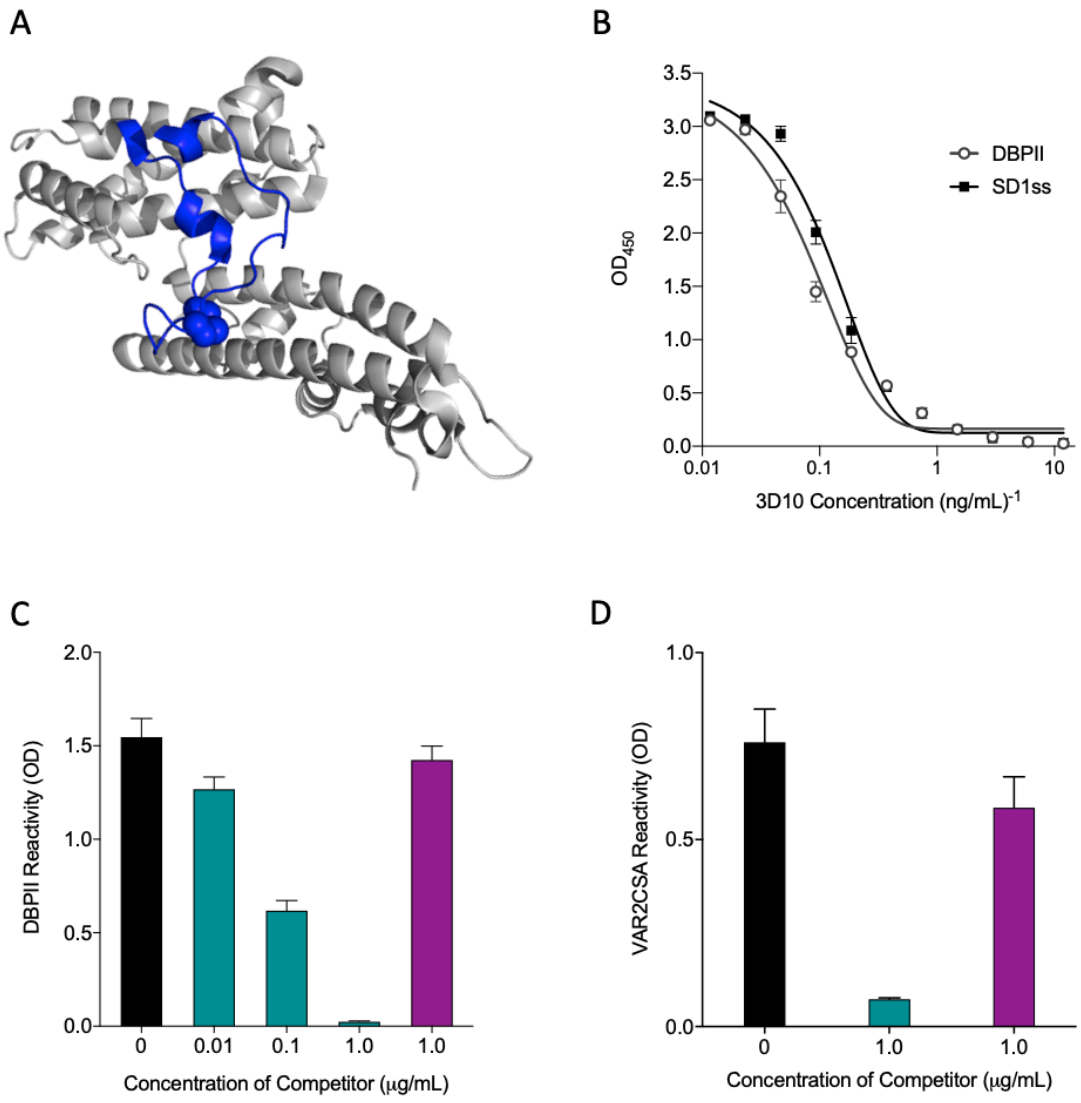

Figure 3.1. SD1ss contains an epitope in DBPII that is recognized by 3D10 and mediates cross-reactivity to VAR2CSA. (A) DBPII crystal structure (PDB ID: 4NUU) showing the SD1 region in blue. The disulphide bond in SD1ss is represented by space-filling spheres. (B) Titration of 3D10 against recombinant DBPII and synthetic SD1ss. (C and D) 3D10 was incubated alone (black bar), with SD1ss (teal bars) or the shorter peptide C_{29}-K_{40} (purple bars) before being adding to wells coated with DBPII (C) or VAR2CSA (D). Data are mean ± standard deviation (SD).

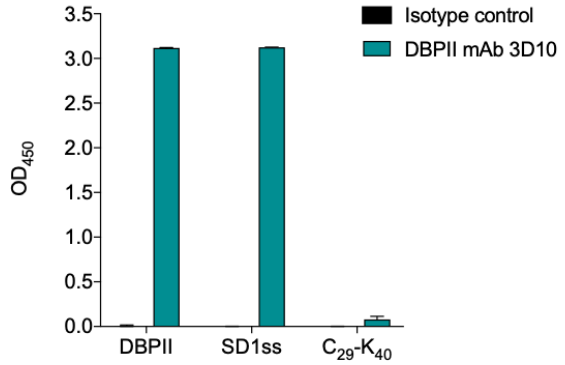

Figure 3.2. Peptide C_{29}-C_{40} is not recognized by 3D10. The 3D10 mAb did not recognize the C_{29}-C_{40} peptide within SD1. Data are mean ± SD.

3.3.2 SD1ss is a subdominant epitope in PvDBP

To test whether SD1ss is a dominant epitope in PvDBP, we generated and tested polyclonal sera to DBPII in BALB/c mice using the same strain of mice and the same allele of DBPII (Sal 1) that gave rise to the 3D10 mAb. Total IgG from mice immunized with Sal 1 DBPII recombinant protein did not recognize SD1ss by ELISA, despite high antibody titers to DBPII (Figure 3.3A). These antibodies also failed to recognize full-length VAR2CSA. These data demonstrate that SD1 is subdominant in this strain of mice and are consistent with the observation that of 7 mAbs generated to DBPII, only 3D10 recognizes the SD1 region (259, 260).

To investigate this in a human population, we tested sera from individuals infected during a *P. vivax* outbreak in Brazil that occurred in an otherwise malaria-free region (252). Serum from individuals who experienced *P. vivax* relapses developed a range of DBPII antibodies (Figure 3.3B) but failed to recognize SD1ss (Figure 3.3C). These human sera did not recognize VAR2CSA (Figure 3.3D), consistent with the mouse data that polyclonal antibodies against DBPII that lack specificity for SD1ss do not cross-react with VAR2CSA. It is possible that these sera failed to recognize SD1ss due to polymorphisms between the peptide sequence and the SD1 sequence in the outbreak clone. However, when we sequenced the SD1 region from *P. vivax* gDNA isolated from a patient during the outbreak, the sequence was 100% identical to SD1 in Sal 1, the strain used to design the SD1ss peptide. Furthermore, a BLASTp of the SD1 amino acid sequence was 100% identical to the top 100 *P. vivax* SD1 sequences from global isolates, suggesting that this region of DBPII is highly conserved and not under immune selection.

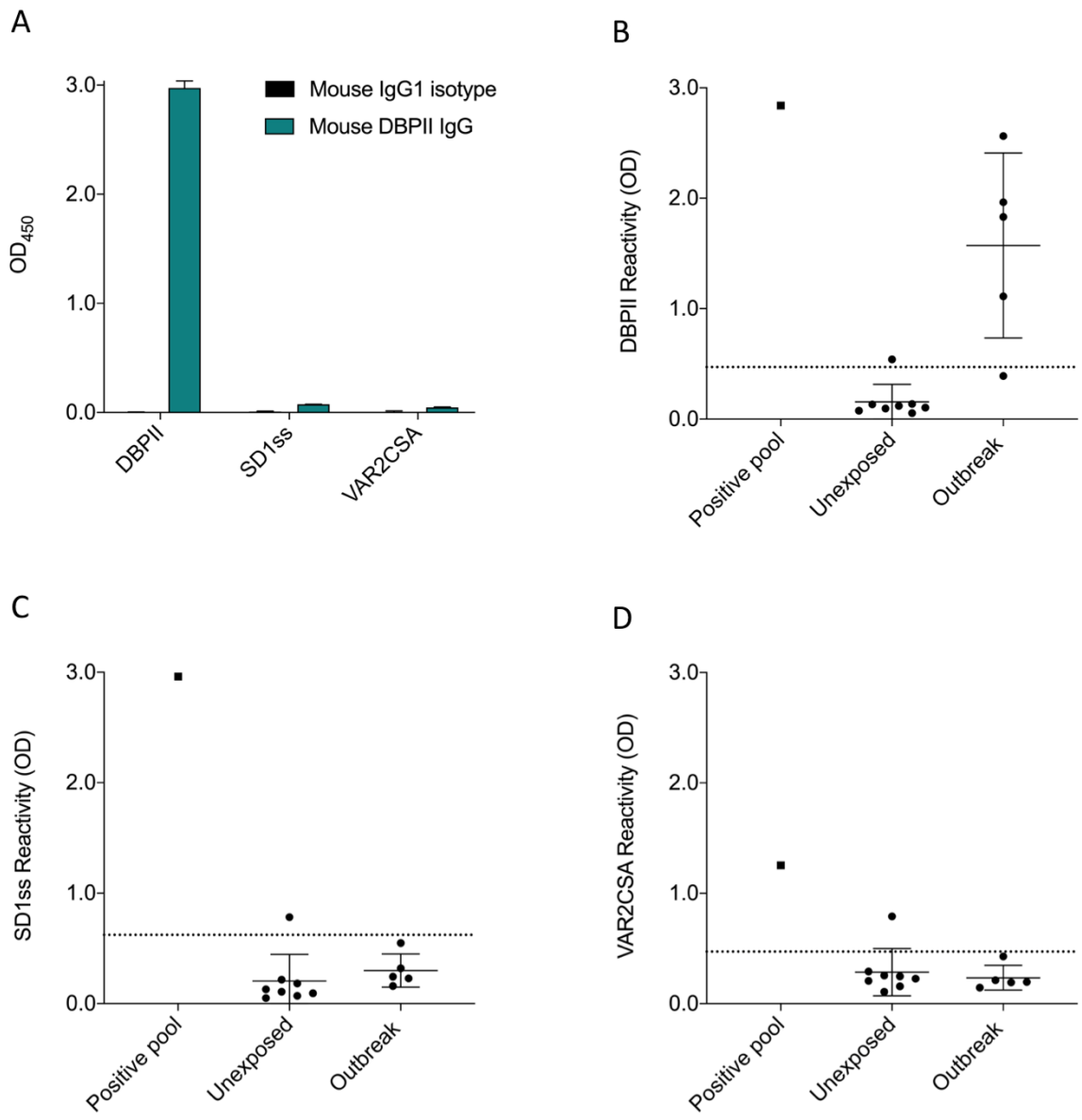

Figure 3.3. The SD1 domain of DBPII is subdominant. (A) Total IgG pooled from 15 mice immunized with the Sal 1 allele of DBPII was tested against DBPII, SD1ss and VAR2CSA by ELISA. IgG was tested at a concentration of 0.1 µg/mL against DBPII and 5.0 µg/mL against SD1ss and VAR2CSA. (B - D) Sera from individuals infected during an outbreak of *P. vivax* in a malaria-free region of Brazil were tested by ELISA against DBPII (B), SD1ss (C) and VAR2CSA (D). The cut-off was defined as 2 standard deviations above the mean OD of unexposed Brazilians tested against the same antigens. A pool of sera from individuals living in a malaria-endemic area of Brazil was included as a positive control. Data are mean ± SD.

We showed previously that *P. vivax*-exposed Brazilian men and children residing in Rio Pardo, a malaria-endemic area in the Amazon, had antibodies against VAR2CSA (248). Based on this finding, and the data above, we postulated that the SD1 epitope in PvDBP is poorly immunogenic. To address this, we tested sera from Brazilian men and children with life-long exposure to *P. vivax* for antibodies to SD1ss and DBPII. We observed that 78% had antibodies to DBPII whereas only 39% had antibodies to SD1ss. The antibody levels were correlated (r_s = 0.7014, p<0.0001; Figure 3.4A), but half of those who had DBPII antibodies did not have SD1ss antibodies. These findings are consistent with the mouse and outbreak data that exposure to DBPII does not always elicit an antibody response against SD1ss and confirms that this epitope in PvDBP is subdominant in human populations.

We then correlated the seroreactivity to DBPII and SD1ss with VAR2CSA reactivity and found that VAR2CSA antibody levels were correlated with both DBPII (r_s = 0.5443, p = 0.0002) and SD1ss (r_s = 0.6192, p<0.0001) (Figure 3.4B and 3.4C). To assess the specificity of these interactions, the sera were tested against another *P. vivax* merozoite protein, EBP2. This protein is a homologue of DBPII but the SD1-like region is significantly different compared to DBPII and the 3D10 mAb does not recognize this protein (232). Antibody levels against EBP2 did not correlate with VAR2CSA reactivity in this population (r_s = 0.2789, p = 0.0774; Figure 3.4D).

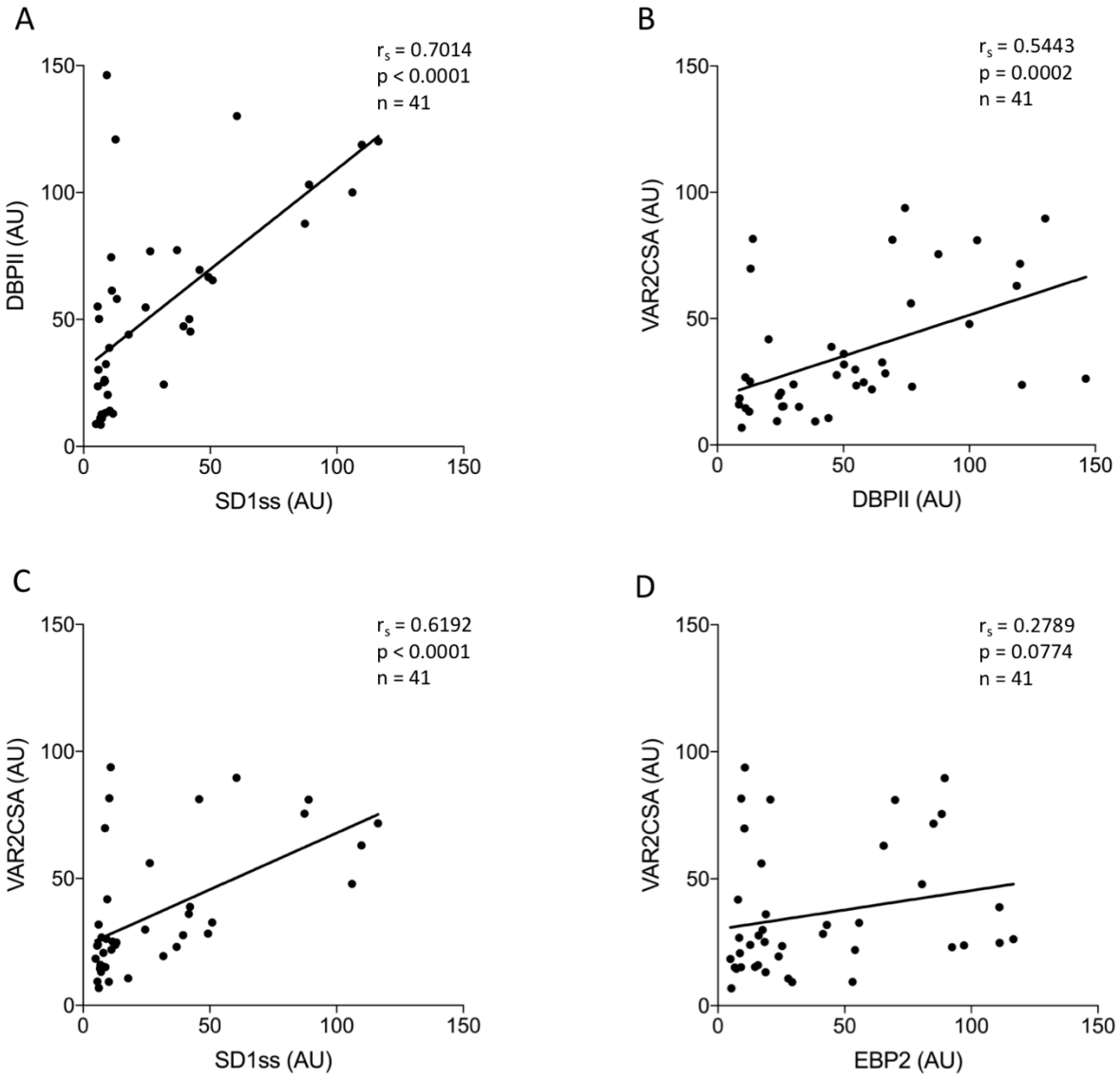

Figure 3.4. SD1ss antibodies correlate with VAR2CSA antibodies in sera from Brazilian men and children with exposure to *P. vivax* only. Individual sera from men and children from Rio Pardo, Brazil, were selected based on past exposure to *P. vivax* only. Sera were tested by ELISA for reactivity to DBPII, SD1ss, VAR2CSA, and EBP2. Antibody levels (ODs) were converted to arbitrary units (AU) based on the positive control included on every plate. Sera reactivity was correlated using Spearman rank correlation, r_s = Spearman rank coefficient.

We observed similar correlations of antibody levels in sera from men and children living in an area of Colombia endemic for both *P. vivax* and *P. falciparum* (Figure 3.5). These subjects were not selected based on past or current malaria infection and represent a more heterogeneous population in terms of malaria exposure. DBPII recognition was significantly correlated with SD1ss antibody levels (r_s = 0.5337, p<0.0001) and VAR2CSA antibodies correlated with both DBPII (r_s = 0.4046, p<0.0001) and SD1ss (r_s = 0.2353, p = 0.0028) antibody levels (Figure 3.5A-C). Again, there was no correlation between EPB2 and VAR2CSA antibody levels (r_s = 0.0472, p = 0.5372) (Figure 3.5D).

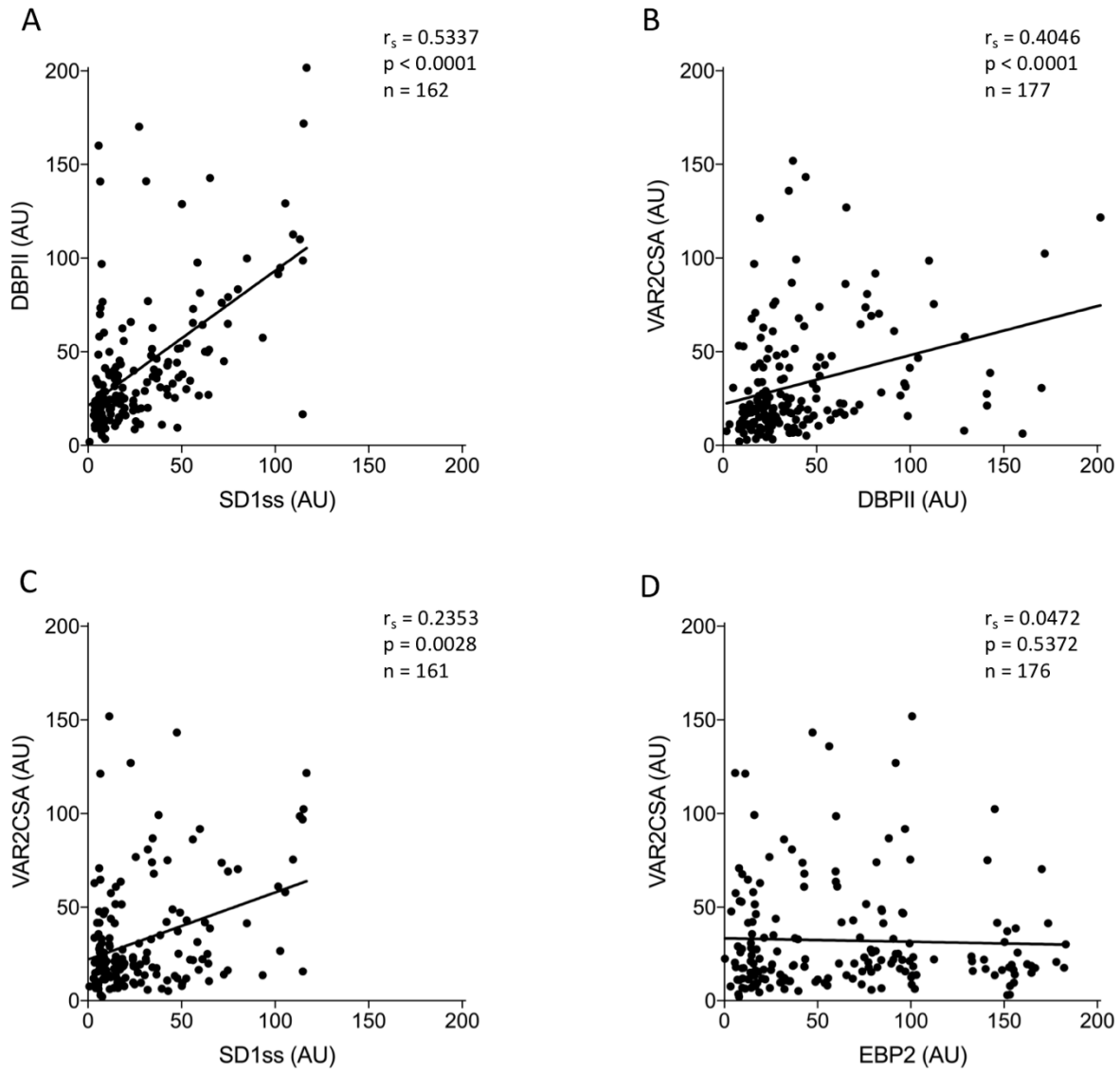

Figure 3.5. SD1ss antibodies correlate with VAR2CSA antibodies in sera from Colombian men and children. Sera from men and children living in a malaria-endemic area of Colombia were tested for reactivity to DBPII, SD1ss, VAR2CSA, and EBP2 by ELISA. Antibody levels (ODs) were converted to arbitrary units based on the positive control included on every plate. Sera reactivity was correlated using Spearman rank correlation, r_s = Spearman rank coefficient.

3.3.3 SD1ss–affinity purified human antibodies block parasite adhesion to CSA in vitro

Our data thus far suggest that antibodies to the epitope in PvDBP SD1 cross-react with VAR2CSA. To test this directly, we affinity-purified antibodies that recognize SD1ss from a pool of sera from non-pregnant populations in Colombia (men and children) exposed to *P. vivax* and *P. falciparum*. Similarly, we affinity-purified antibodies that recognize the entire DBPII recombinant protein. As expected from our immunogenicity data above, the DBPII affinity-purified antibodies recognized SD1ss very weakly (Figure 3.6A). They did recognize EBP2, presumably through shared epitopes in the DBL domain. In contrast, the SD1ss affinity-purified antibodies recognized DBPII but not EBP2, consistent with poor sequence conservation of the SD1-like region in EBP2. Neither of the purified antibodies recognized PfMSP1, an unrelated *P. falciparum* merozoite antigen. Both affinity-purified antibodies cross-reacted with VAR2CSA, and the reactivity of the SD1ss affinity-purified antibodies was higher compared to the DBPII affinity-purified antibodies (Figure 3.6B).

A critical question is whether the affinity-purified antibodies could protect against placental malaria. This can be measured *in vitro* using an inhibition of binding assay (IBA) to test if antibodies block parasite adhesion to CSA. Mature VAR2CSA-expressing *P. falciparum* CS2 trophozoites were incubated with the affinity-purified IgG, then added to immobilized CSA. The number of parasites bound per spot of CSA was quantified and compared to binding in the presence of IgG from a pool of unexposed Colombians as the negative control. We found that the DBPII-affinity purified IgG reduced parasite binding to CSA, but the effect was not significant (Figure 3.6C). However, SD1ss affinity-purified IgG blocked parasite adhesion to CSA and the effect was significant in three of four experiments (Figure 3.6D). The inhibition in these three experiments ranged from 32 – 45%.

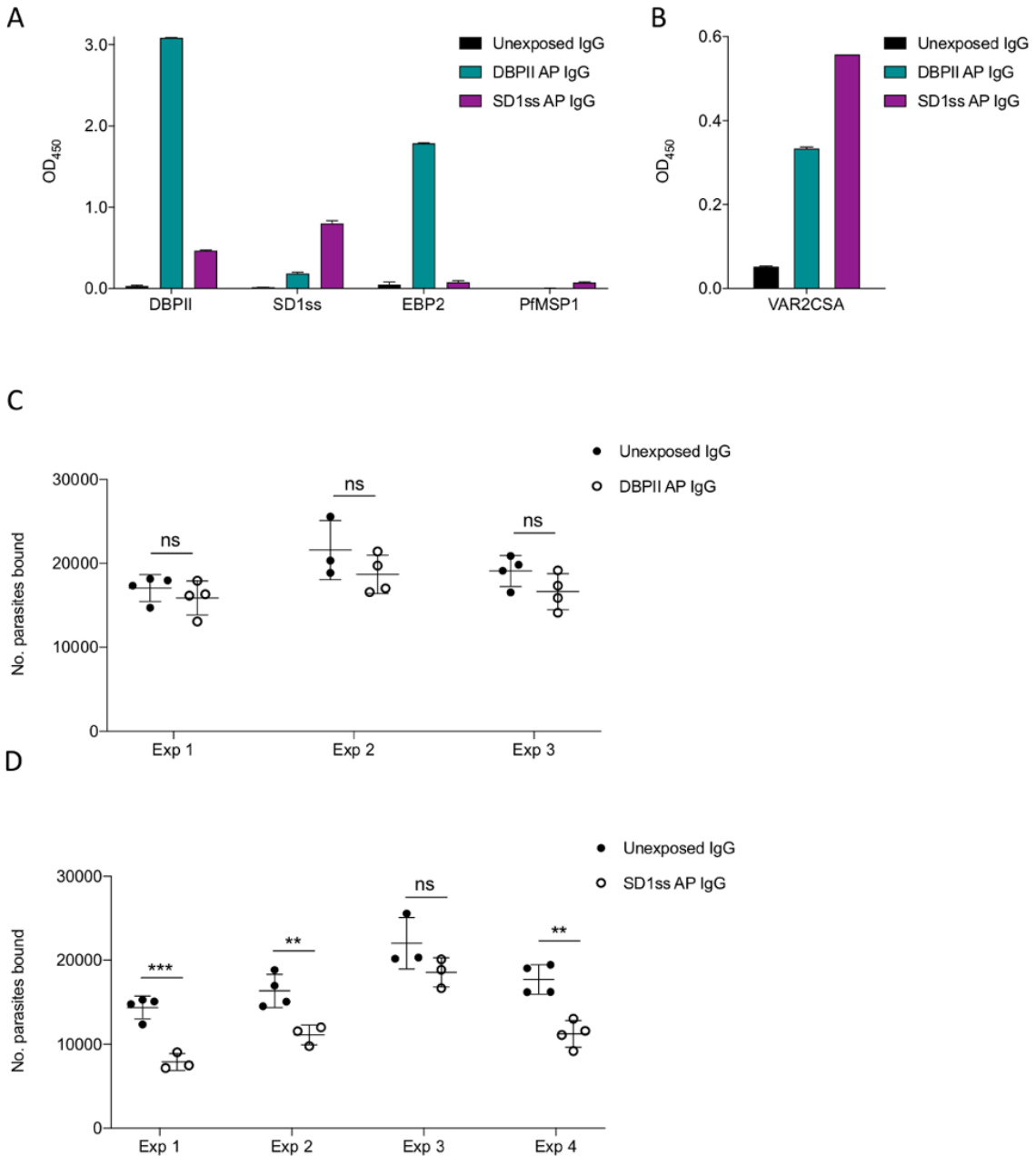

Figure 3.6. SD1ss-affinity purified antibodies recognize VAR2CSA and block iRBC adhesion to CSA. (A and B) Pooled sera from Colombian men and children were affinity-purified on DBPII or SD1ss. Total IgG purified from unexposed Colombians was used as a negative control. Antibodies were tested against various antigens by ELISA. (C and D) Affinity-purified DBPII (100 µg/mL) (C) and SD1ss (90 µg/mL) (D) antibodies were tested in the inhibition of binding assay using *P. falciparum* CS2 parasites expressing VAR2CSA. Data are from independent experiments. Data are mean ± SD and significance was determined using a Student's *t* test comparing unexposed Colombian IgG and affinity-purified IgG for each experiment. ** $p < 0.01$, *** $p < 0.001$, ns = not significant.

3.3.4 Antibodies to SD1 in PvDBP target cryptic epitopes in VAR2CSA

To better understand this mechanism of cross-species immunity, we investigated whether antibodies that developed following exposure to *P. falciparum* VAR2CSA would reciprocally recognize the epitope in PvDBP SD1. We first tested plasma collected from multigravid women from Uganda who were naturally exposed to VAR2CSA during pregnancy (Figure 3.7A). Despite high levels of VAR2CSA-specific antibodies, there was no recognition of SD1ss. Pooled sera from Ugandan children was included as a negative control. Sera from Colombian men and children that recognized both VAR2CSA and SD1ss was included as a positive control. To investigate this further, we tested serum from a rabbit that was immunized with recombinant VAR2CSA. Similar to the human sera, the rabbit serum did not recognize SD1ss (Figure 3.7B).

These data imply that cross-reactive antibodies (elicited against SD1) and VAR2CSA-induced antibodies recognize distinct epitopes in VAR2CSA. To test this further, we performed an antibody-based competition ELISA using the 3D10 mAb and VAR2CSA antibodies induced through immunization (in rabbits). Initially, rabbit anti-VAR2CSA serum or normal rabbit sera (NRS) (as a control) was added to wells coated with VAR2CSA. Then, the detecting antibody (anti-DBL5ε mouse serum, 3D10 mAb, or human SD1ss affinity-purified antibodies) was added. The rabbit anti-VAR2CSA antibody strongly blocked recognition by the anti-DBL5ε serum, compared to the NRS (Figure 3.7C), consistent with recognition of shared immunodominant epitopes by these sera. However, VAR2CSA rabbit antiserum could not block recognition of VAR2CSA by 3D10 (Figure 3.7D), demonstrating that the epitope on VAR2CSA recognized by 3D10 was not recognized by the polyclonal rabbit antiserum. Similarly, the rabbit polyclonal antiserum could not block recognition of VAR2CSA by human SD1ss affinity-purified antibodies (Figure 3.7E), demonstrating that, like 3D10, the epitope(s) on VAR2CSA recognized by human

antibodies that arose as a result of *P. vivax* exposure is distinct from those that are immunogenic in VAR2CSA. Thus, the epitope(s) on VAR2CSA recognized by 3D10 and by humans following *P. vivax* exposure are classical cryptic epitopes. To ask whether the human and mouse cryptic epitopes are the same, we tested whether SD1ss affinity-purified human antibodies could block recognition of 3D10 (Figure 3.7F). We demonstrated partial but significant blocking suggesting that these epitopes overlap but may not be identical.

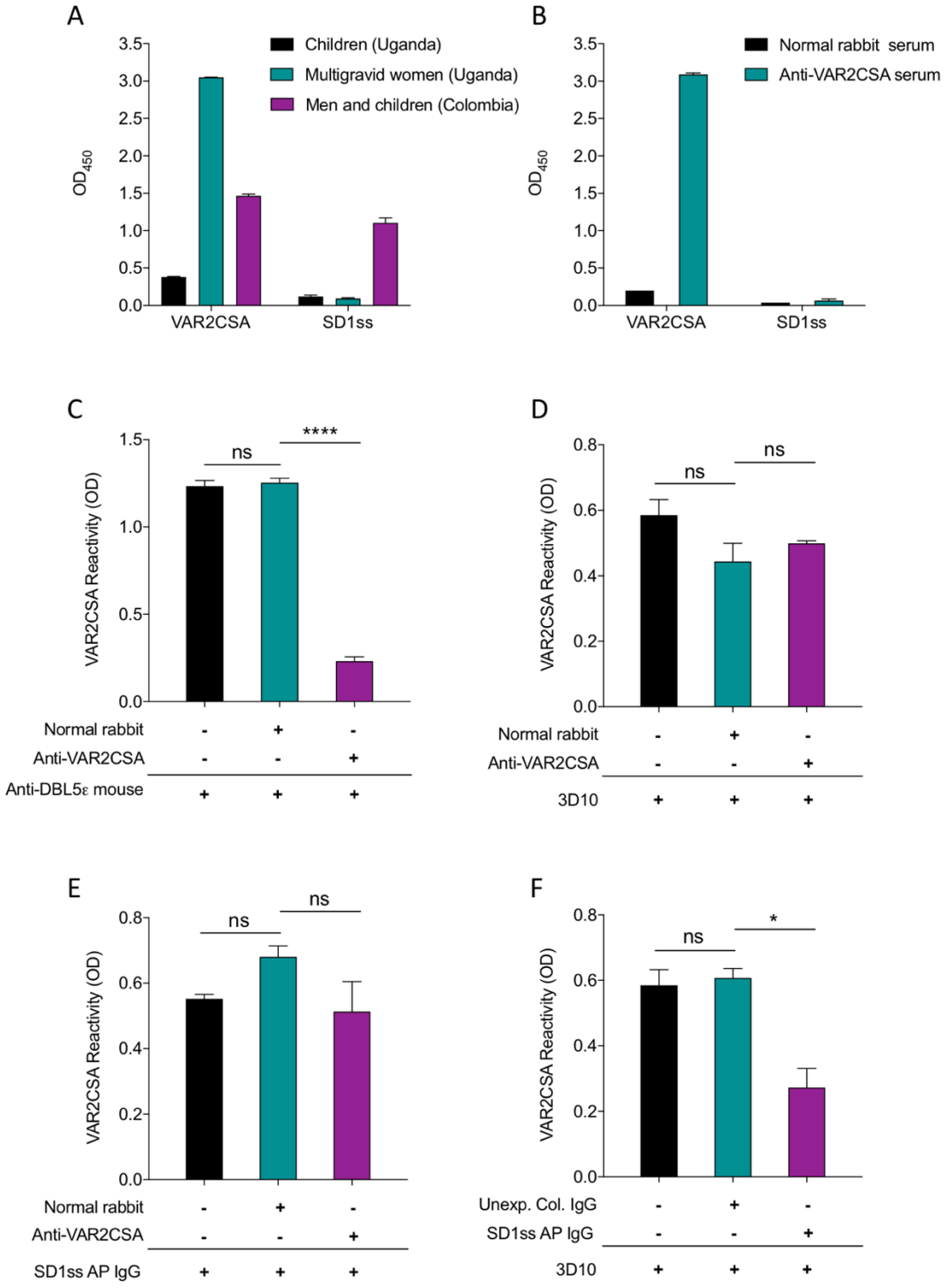

Figure 3.7. Epitopes in VAR2CSA recognized by vivax-derived antibodies are cryptic. (A) Pooled sera from Ugandan children and multigravid women were tested by ELISA against VAR2CSA and SD1ss. Sera from Colombian men and children were used as a positive control. (B) Anti-VAR2CSA rabbit sera was tested by ELISA against VAR2CSA and SD1ss. (C - F)

Competition ELISAs with VAR2CSA as the capture antigen and either anti-VAR2CSA rabbit sera (C-E) or human SD1ss-affinity purified antibodies (F) as the competing antibody. 3D10 (D, F), or human SD1ss-affinity purified antibodies (E) were added as the source of detection antibodies. Data are mean ± SD and significance was determined using a one-way ANOVA with multiple comparisons test. * $p < 0.05$, **** $p < 0.0001$, ns = not significant, AP = affinity purified.

3.3.5 Cryptic epitopes in the DBL5ε domain of VAR2CSA

VAR2CSA is a large multi-domain protein that could contain many target epitopes for the cross-reactive antibodies derived from SD1. We focused on mapping the epitopes in one domain, DBL5ε, as this domain is among the more conserved DBL domains in VAR2CSA and we showed previously that this domain is strongly recognized by the 3D10 mAb (248). We generated an array of overlapping peptides that span the DBL5ε domain and screened this array with 3D10 (Figure 3.8). Two peptides were strongly recognized (P20 and P23) while two others (P4 and P15) were weakly recognized. To validate these peptides further, we performed competition ELISAs and tested whether each peptide could compete out the recognition of DBL5ε by 3D10 (Figure 3.9A). Only P20 and P23 significantly reduced the recognition by 3D10. While the effect with each peptide was partial, there was no synergistic effect of combining the two peptides (Figure 3.9A).

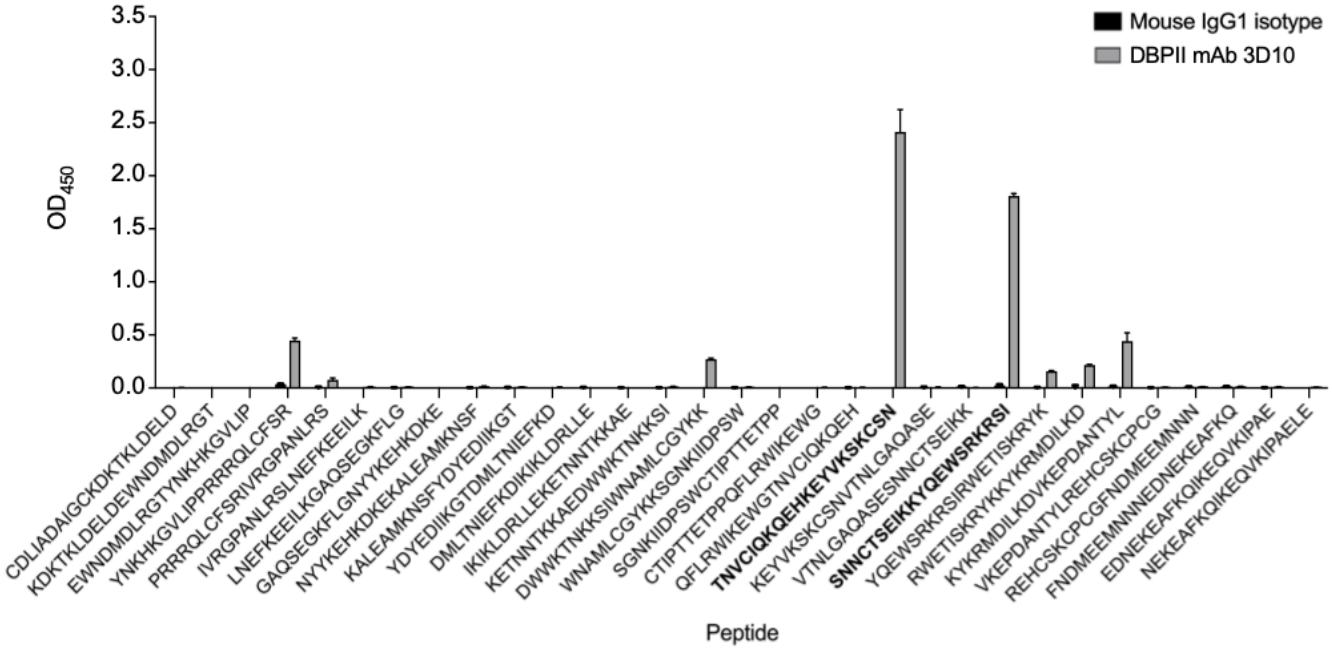

Figure 3.8. 3D10 recognizes epitopes in DBL5ε. An array of overlapping peptides that span DBL5ε was tested with the DBPII mAb 3D10 compared with a mouse IgG1 isotype control. P20 and P23 are in bold.

We next determined whether the epitopes in P20 and P23 were cryptic in DBL5ε. Whereas the pools of sera from Colombian and Brazilian men and children exposed only to *P. vivax* strongly recognized these same peptides (Figure 3.9B), they were not recognized by either the sera from Ugandan multigravid women (Figure 3.9C) or the rabbit immunized with VAR2CSA (Figure 3.9D).

To visualize the P20 and P23 epitopes within the protein structure of DBL5ε, we mapped the two peptide sequences onto a homology model of the DBL5ε (3D7) domain. Both peptides mapped to alpha helices in subdomain 3 (Figure 3.9E). These sites are distinct from the immunodominant epitopes recognized by sera from Tanzanian multigravid women (Figure 3.9F; blue) and rabbits immunized with VAR2CSA (200) and share no overlap with the putative CSA binding sequence in this domain (Figure 3.9E; yellow) (261).

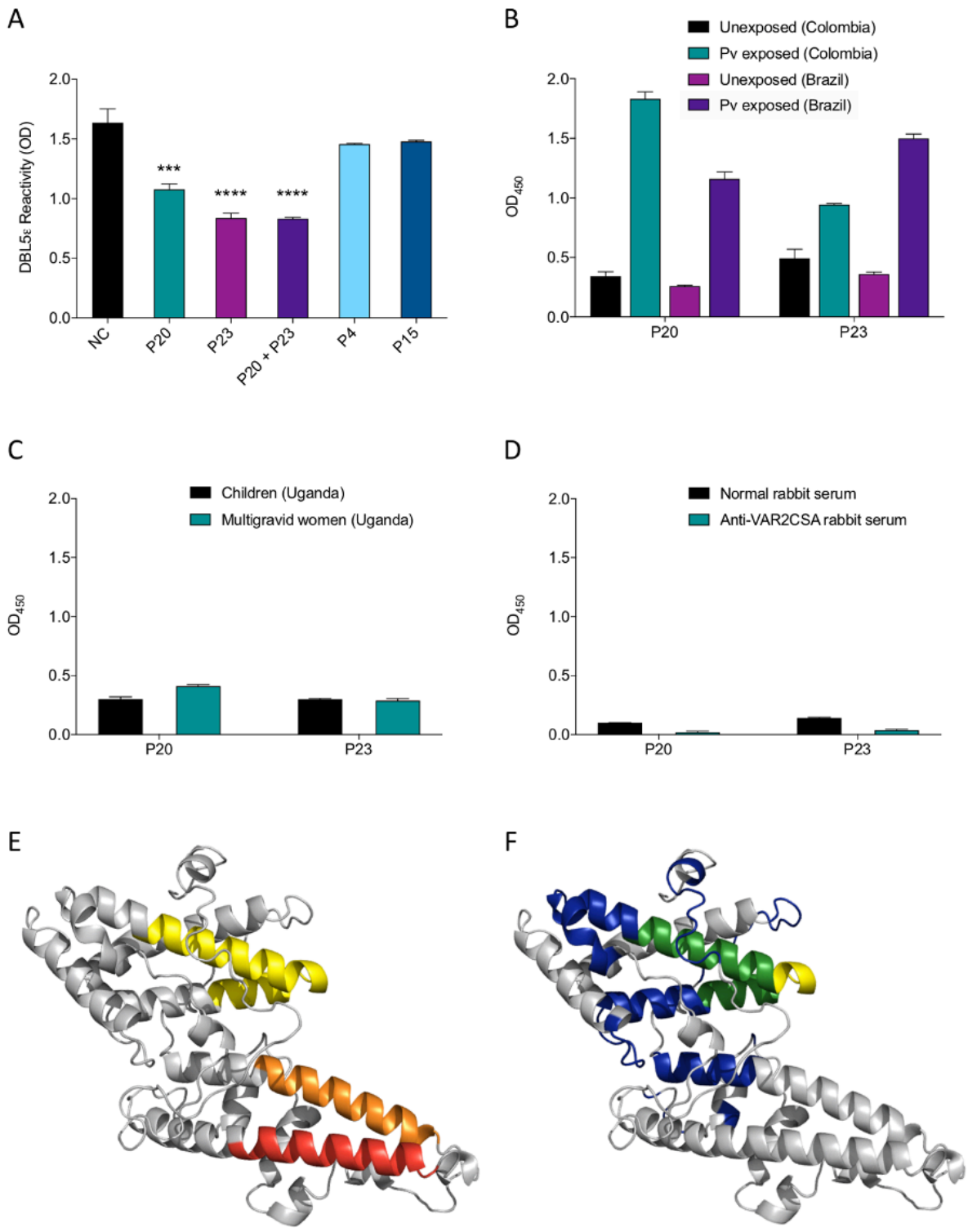

Figure 3.9. Recognition of specific peptides in the DBL5ε domain of VAR2CSA by vivax-derived antibodies. (A) Competition of 3D10 recognition of DBL5ε by individual peptides. 3D10 was incubated with peptides P20, P23, P20 and P23 in combination, P4, and P15 (all at 100 µg/mL) and added to a plate coated with DBL5ε protein. The OD of 3D10 preincubated with each peptide

was compared to the OD for the antibody alone (no competitor). NC = no competitor. (B - D) Recognition of P20 and P23 by sera from (B) Colombians and Brazilians exposed only to *P. vivax*, (C) children and multigravid women from Uganda and (D) rabbits immunized with full-length VAR2CSA was tested by ELISA. (E) Homology model of DBL5ε depicting P20 (orange), P23 (red), and the putative glycosaminoglycan binding site (yellow) (261). (F) Homology model of DBL5ε depicting the surface-exposed regions recognized by sera from multigravid African women (blue), some of which overlap with the putative glycosaminoglycan binding site (green) (261). Data are mean ± SD and significance was determined using a one-way ANOVA with multiple comparisons test (*** $p < 0.001$, **** $p < 0.0001$).

P20 nor P23 share only limited amino acid sequence homology with SD1ss; P20 contains two cysteine residues while P23 contains one cysteine as well as the motif 'RKR' which is important for recognition of SD1 by 3D10 (259, 260). We therefore investigated the possibility that 3D10 recognized a conformational epitope in these peptides. To test this, we measured 3D10 reactivity to each peptide after treatment with dithiothreitol (DTT), which would abolish disulphide bonding either within or between peptide molecules. When P20 and P23 were treated with DTT, 3D10 recognition was lost (Figure 3.10). Interestingly, 3D10 recognition of SD1ss was also reduced following treatment of the peptide with DTT, suggesting that the disulphide bond is important for recognition of the homologous epitopes.

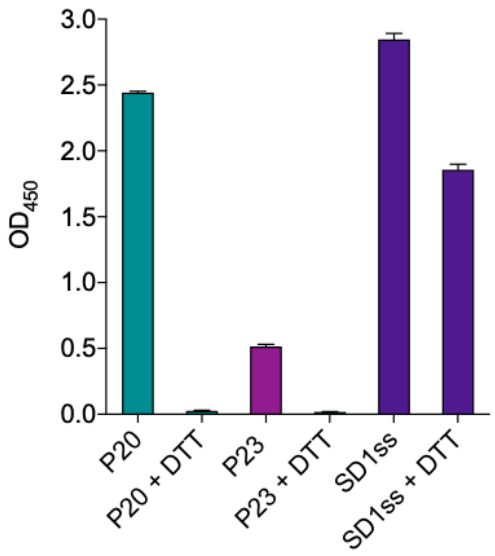

Figure 3.10. 3D10 recognizes conformational epitopes in P20, P23 and SD1ss. 3D10 recognition of P20 and P23 was lost when the peptides were treated with dithiothreitol (DTT). Recognition of SD1ss was reduced when the peptide was treated with DTT. Data are mean ± SD.

3.4 Discussion

We discovered a host defense mechanism in *Plasmodium* in which a subdominant epitope in the *P. vivax* antigen PvDBP elicits functional antibodies against cryptic epitopes in the distantly related *P. falciparum* homologue VAR2CSA. We mapped the epitope in PvDBP to SD1 and showed that human antibodies to this epitope recognized VAR2CSA and blocked parasite adhesion to CSA. Our data suggest that SD1 is subdominant in PvDBP by virtue of its poor immunogenicity in mice vaccinated with the Sal 1 allele of PvDBP and our findings that about half of individuals exposed to PvDBP do not develop SD1 antibodies. However, the levels of SD1 antibodies correlated with the levels VAR2CSA reactivity. This is consistent with findings from another study where volunteers were deliberately infected with the *P. vivax* Sal 1 strain and did not have cross-reactive antibodies to VAR2CSA (262). We expect that the Sal 1strain of PvDBP does not readily elicit SD1 antibodies in humans, as we observed in mice. While the mechanism that gives rise to SD1-specific antibodies during natural *P. vivax* infection is not known, certain alleles of PvDBP may adopt protein structures that preferentially expose SD1, or perhaps SD1 antibodies arise through affinity maturation following exposure to multiple, different PvDBP alleles. Alternatively, host genetic variability in HLA class II genes may also play a role in directing the antibody responses, as we reported previously for DBPII (212).

Antibodies to SD1 of PvDBP appear to have no protective value against *P. vivax* infection. The epitope is weakly immunogenic and antibodies that do arise, such as 3D10 in mice, do not inhibit binding to DARC or block *P. vivax* invasion of reticulocytes (218). Moreover, the amino acid sequence of SD1 is highly conserved, which is consistent with our interpretation that this subdomain is not under immune pressure. Likewise, our data strongly suggest that antibodies to SD1 target cryptic epitopes in VAR2CSA. Immune sera from rabbits immunized with VAR2CSA

failed to compete with the human SD1ss affinity-purified antibodies or the mouse 3D10 mAb for recognition sites on VAR2CSA. Yet the binding of SD1 antibodies to these cryptic epitopes can block parasite adhesion to CSA. We do not know whether the epitopes recognized by the vivax-derived antibodies are within the CSA binding sites of VAR2CSA or if the antibodies block adhesion by steric hindrance. However, the two peptides that we identified in the DBL5ε array map to sites distal to the predicted CSA binding sequence in this domain (261). They are also distinct from the immunodominant epitopes that were recognized by African multigravid women (200). Further work is needed to identify the target epitopes in other DBL domains of VAR2CSA and how they map to the three-dimensional structure of the full protein. To our knowledge this is the first demonstration of adhesion-blocking antibodies that target cryptic epitopes in VAR2CSA.

Antibodies can access cryptic epitopes through various mechanisms. Epitopes concealed within the head domain of the influenza A hemagglutinin protein are transiently exposed to antibodies during dynamic changes in the conformation of the trimer complex, through a process described as "breathing" (263-265). Similarly, several studies on dengue virus and West Nile virus revealed time- and temperature-dependent exposure of cryptic epitopes, reflecting the important role of structural dynamics in epitope accessibility (266-269). VAR2CSA forms a large globular complex that may undergo similar protein dynamics, exposing cryptic epitopes within intermediate protein conformations that arise during transport to the cell surface, post-translational modification/protein maturation, interaction with other knob proteins, or upon binding to CSA. The idea that these epitopes are exposed in only a subset of protein structures is consistent with our previous finding that the 3D10 mAb only recognized a small percentage of iRBCs that expressed native VAR2CSA on the cell surface (248).

The discovery of cryptic epitopes in VAR2CSA has direct applications for vaccine development against placental malaria. A significant obstacle to current vaccine strategies is the highly polymorphic nature of *var2csa* alleles (270), which impedes development of broadly neutralizing antibodies against diverse parasite strains. In a recent study of 247 *P. falciparum* isolates (271), 171 polymorphic loci were identified in the ID1-DBL2Xb sub-region that is included in two vaccines against pregnancy-associated malaria (191, 272). A different study identified 4 major domain clades in this region (193). The effects of these polymorphisms are highlighted by several reports that functional antibodies to VAR2CSA in different populations of African women are highly strain-specific, reflecting seroreactivity to immunodominant epitopes (273-275). Our finding that SD1 from *P. vivax* elicits protective antibodies against cryptic epitopes in VAR2CSA provides an alternative, yet complementary vaccine strategy that could circumvent this immune pressure.

Epitope-specific vaccines that direct the immune response to cryptic or subdominant epitopes are emerging as a viable strategy against many pathogens for which traditional vaccine approaches were unsuccessful (276, 277). These vaccine candidates include conserved epitopes in otherwise highly mutable viruses, such as HIV (278, 279), Ebola virus (280, 281), and influenza (263-265, 282, 283), as well as pathogenic bacteria, such as *Streptococcus pyogenes* (284), anthrax and *S. aureus* (276). A critical advantage is that many of these epitopes can induce broadly neutralizing, strain-transcending immunity by eliciting antibodies that cross-react with related but antigenically distinct pathogens (281, 284, 285).

3.5 Conclusions

We showed that antibodies to a highly conserved, subdominant epitope in *P. vivax* inhibited an unrelated virulence pathway in *P. falciparum in vitro*. It will be important in future clinical studies to determine whether these antibodies contribute to improved birth outcomes from *P. falciparum* placental malaria and to evaluate whether SD1 can elicit polyclonal neutralizing antibodies through immunization. While our data make SD1 an attractive epitope for future vaccine design, they also provide insight into an unusual mechanism of heterologous immunity to *Plasmodium* based on shared epitopes across the DBL protein family.

Chapter 4: Generation of a peptide vaccine against falciparum placental malaria based on a discontinuous epitope

Data from this Chapter have been previously published (286).

4.1. Introduction

Pregnancy-associated malaria caused by infection with the parasite *Plasmodium falciparum* can result in preterm birth, low birth weight babies, spontaneous abortion, and infant and maternal death (287). Despite ongoing efforts to develop a vaccine to prevent malaria in pregnancy, no effective vaccine exists. The leading vaccine candidates are based on VAR2CSA, a *P. falciparum* protein that mediates sequestration of infected red blood cells to the placenta (121, 126, 129, 186, 187, 249). While these vaccines show promise by eliciting strong antibodies to the homologous VAR2CSA allele, they failed to elicit broadly neutralizing antibodies against heterogeneous parasite strains due to extensive natural polymorphisms within VAR2CSA (186, 187, 190, 192). Polyvalent vaccines that include multiple alleles of VAR2CSA or new vaccines that target conserved epitopes are urgently needed.

We discovered an alternate source of antibodies to VAR2CSA that can be exploited for vaccine design. The source of these antibodies is an epitope shared between the Duffy binding-like (DBL) domain of the *P. vivax* Duffy binding protein (PvDBP), an invasion protein expressed by *P. vivax* merozoites, and the DBL domains of VAR2CSA (155). Despite sharing only 16–21% sequence homology, the DBL domains of VAR2CSA and PvDBP have shared epitopes that are targeted by cross-reactive antibodies elicited by natural exposure to *P. vivax* infection or through immunization with PvDBP (155, 233). A mouse monoclonal antibody (3D10 mAb) raised against the DBL domain of PvDBP recognized VAR2CSA and blocked parasite adhesion in an *in vitro* assay of placental malaria (155). When we investigated the cross-reactive target of 3D10, we found

that it recognized epitopes that were cryptic in VAR2CSA (233). Given the cryptic nature of these epitopes, they are unlikely to be under the same immune pressure as the more immunodominant epitopes in the protein. Therefore, identifying and targeting these epitopes in VAR2CSA may present a viable vaccine strategy against malaria in pregnancy. Targeting cryptic or subdominant epitopes has also been employed in the development of vaccine candidates for group A streptococcus (288), Ebola (280), and influenza (263-265).

Here, we designed an epitope-focused vaccine candidate against VAR2CSA based on the epitope that generated the 3D10 mAb. This epitope has been localized to the SD1 region of DBPII (233, 259, 260), and we used peptide arrays to refine the epitope to three discontinuous segments of SD1. Using a synthetic scaffold, we recapitulated this discontinuous epitope within a conformationally constrained peptide. Importantly, this peptide elicited antibodies in mice and a rabbit that recognized DBPII and cross-reacted with VAR2CSA. The cross-reactive rabbit antibodies also strongly recognized the surface of VAR2CSA-expressing iRBCs but did not block parasite adhesion to CSA or mediate opsonic phagocytosis *in vitro*. However, these findings represent an important step towards developing a cross-reactive vaccine candidate to target VAR2CSA.

4.2. Materials and Methods

4.2.1. Synthetic peptide design and conjugation

Peptides representing different regions of SD1 in DBPII (Figure 1) were synthesized (Synpeptides Co., Shanghai, China) based on the sequence from the Sal 1 allele of PvDBP. The SD1ss peptide was designed to cover the entire SD1 region, with one pair of cysteines (C_9 and C_{38}) mutated to serine to control disulfide bond formation. N_{10}-C_{22} was conjugated to diphtheria toxoid

(DT) using 6-maleimido-caproyl n-hydroxy succinimide (MCS) (Sigma, Oakville, Canada) (289). Briefly, MCS dissolved in dimethylformamide (DMF) (33.3 mg/mL) was added to a solution of DT in 0.1 M phosphate buffer (10 mg/mL) and mixed slowly at room temperature for 1 h. The modified carrier protein was then dialyzed against 0.1 M phosphate buffer containing 0.1 M ethylenediaminetetraacetic acid (EDTA) before mixing with the lyophilized N_{10}-C_{22} peptide (1.2 M excess of peptide). The conjugate was dialyzed overnight against 1X PBS and coupling was confirmed using SDS-PAGE analysis.

To more finely map the epitope, thirty-seven overlapping 10-mer linear peptides were designed (Pepscan, Amsterdam, Netherlands) to span the SD1 region of DBPII (Table 4.1). Chemically Linked Peptides on Scaffolds (CLIPS) technology was used to synthesize the $SD1_{CLIPS}$ peptide (C(T2-013)NYKRKRRERDWDCNTKKDVCIPDRRYQLC(T2-013)K(Aoa)), as previously described (290). The conformation of $SD1_{CLIPS}$ was constrained by first conjugating the outermost pair of cysteines (residues 1 and 30) using the T2-013 scaffold. The two interior cysteines (residues 14 and 21) were then deprotected and oxidized to form a disulfide bond. This peptide was conjugated to keyhole limpet hemocyanin (KLH) or bovine serum albumin (BSA) using a N-succinimidyl 4-formylbenzoate (S-4FB) linker via the C-terminal N-epsilon-aminooxyacetyl-L-lysine residue on the peptide (Pepscan, Amsterdam, Netherlands). Conjugation was monitored by adding 2-hydrazinpyridine to the carrier protein/peptide mixture. This reagent reacted with free S-4FB linkers on the carrier protein, producing a colored product, which allowed the reaction to be monitored over time. Excess peptide was removed by filtration.

Table 4.1 Peptides used for the Pepscan-based ELISA screen in Figure 3A and B.

Start (residue no.)	End (residue no.)	Native sequence	Mutated sequence
1	10	ASNTVMKNCN	ASNTV**AA**NCN
2	11	SNTVMKNCNY	SNTVM**AA**CNY
3	12	NTVMKNCNYK	NTVMK**AA**NYK
4	13	TVMKNCNYKR	TVMKN**AA**YKR
5	14	VMKNCNYKRK	VMKNC**AA**KRK
6	15	MKNCNYKRKR	MKNCN**AA**RKR
7	16	KNCNYKRKRR	KNCNY**AA**KRR
8	17	NCNYKRKRRE	NCNYK**AA**RRE
9	18	CNYKRKRRER	CNYKR**AA**RER
10	19	NYKRKRRERD	NYKRK**AA**ERD
11	20	YKRKRRERDW	YKRKR**AA**RDW
12	21	KRKRRERDWD	KRKRR**AA**DWD
13	22	RKRRERDWDC	RKRRE**AA**WDC
14	23	KRRERDWDCN	KRRER**AA**DCN
15	24	RRERDWDCNT	RRERD**AA**CNT
16	25	RERDWDCNTK	RERDW**AA**NTK
17	26	ERDWDCNTKK	ERDWD**AA**TKK
18	27	RDWDCNTKKD	RDWDC**AA**KKD
19	28	DWDCNTKKDV	DWDCN**AA**KDV
20	29	WDCNTKKDVC	WDCNT**AA**DVC
21	30	DCNTKKDVCI	DCNTK**AA**VCI
22	31	CNTKKDVCIP	CNTKK**AA**CIP
23	32	NTKKDVCIPD	NTKKD**AA**IPD
24	33	TKKDVCIPDR	TKKDV**AA**PDR
25	34	KKDVCIPDRR	KKDVC**AA**DRR
26	35	KDVCIPDRRY	KDVCI**AA**RRY
27	36	DVCIPDRRYQ	DVCIP**AA**RYQ
28	37	VCIPDRRYQL	VCIPD**AA**YQL
29	38	CIPDRRYQLC	CIPDR**AA**QLC
30	39	IPDRRYQLCM	IPDRR**AA**LCM
31	40	PDRRYQLCMK	PDRRY**AA**CMK
32	41	DRRYQLCMKE	DRRYQ**AA**MKE
33	42	RRYQLCMKEL	RRYQL**AA**KEL
34	43	RYQLCMKELT	RYQLC**AA**ELT
35	44	YQLCMKELTN	YQLCM**AA**LTN
36	45	QLCMKELTNL	QLCMK**AA**TNL
37	46	LCMKELTNLV	LCMKE**AA**NLV

4.2.2. Animal immunizations

For the (N_{10}-C_{22})-diphtheria toxoid (DT) immunizations, five female BALB/c mice (6 to 8 weeks old) were immunized subcutaneously with (N_{10}-C_{22})-DT or DT alone (30 µg/mouse) emulsified in Complete Freund's Adjuvant (CFA) (catalogue no. F5881; Sigma, Oakville, Canada) on day 1. On days 21 and 31, mice were boosted with the immunogen (10 µg/mouse) emulsified in Incomplete Freund's Adjuvant (IFA) (catalogue no. F5506; Sigma, Oakville, Canada) and the final sera samples were collected on day 45 via cardiac puncture under terminal anesthetic.

For the SD1$_{CLIPS}$-KLH immunizations, five female BALB/c mice (6 to 8 weeks old) were immunized subcutaneously with SD1$_{CLIPS}$-KLH or KLH alone (30 µg/mouse) emulsified in CFA on day 1. On days 21, 31, and 41, mice were boosted with the immunogen (10 µg/mouse on days 21 and 31, and 5 µg/mouse on day 41) emulsified in IFA. The final sera samples were collected on day 55 via cardiac puncture. All procedures were approved by the University of Alberta Animal Care and Use Committee (approval number: AUP00002124), and mice were handled in accordance with the Canadian Council on Animal Care Guidelines.

Rabbit antisera were generated commercially by ProSci Inc. (Poway, CA, USA). One rabbit was immunized with 160 µg of SD1$_{CLIPS}$-BSA in CFA followed by three boosts with 80 µg in IFA on days 14, 28, and 43 after the first immunization. The final bleed was collected on day 56.

4.2.3. ELISA

Indirect ELISAs were performed by coating 96-well plates (catalogue no. 439454; Thermo Fisher Scientific, Edmonton, Canada) with antigen diluted in 1X PBS, incubated overnight at 4 °C. Recombinant protein antigens were coated at 0.5 µg/mL, SD1ss was coated at 1.0 µg/mL, and all other synthetic peptides were coated at 5.0 µg/mL. Plates were blocked with 4% BSA (catalogue no. A7906; Sigma, Oakville, Canada) in 1X PBS for 1 h at 37 °C, then washed once

with 1× PBST (0.1% Tween 20). Primary antibody samples were diluted in PBS with 2% BSA to a total volume of 100 µL, added to wells , and incubated for 1 h at room temperature (RT). Plates were washed four times with 1× PBST, and 100 µL of horseradish peroxidase (HRP)-conjugated goat anti-mouse secondary antibody (1/3000) (catalogue no. 170-6516, Bio-Rad, Mississauga, Canada) was added to each well. After incubation for 1 h at RT, the plate was washed four times with 1X PBST, and 100 µL of 3,3′,5,5′-tetramethylbenzidine (TMB) (catalogue no. T0440; Sigma, Oakville, Canada) was added to each well. After incubation at RT for 30 min, the reaction was stopped by adding an equal amount of H_2SO_4 (0.5 N) to each well, and the optical density (OD) of individual wells was read at 450 nm. All samples were run in duplicate and the mean OD for each antigen alone plus secondary was subtracted from the OD of each sample.

Competition ELISAs were performed as above, except that primary antibodies were incubated with test peptides for 30 min at RT before addition to wells. To measure antibody avidity, ELISAs were performed using the same protocol for indirect ELISAs, except that 100 µL of 1 M NaSCN (catalogue no. 251410; Sigma, Oakville, Canada) or 1× PBS for control wells was added to each well following the primary antibody incubation. After a 10 min incubation at RT, the plates were washed four times with 1× PBST (0.1% Tween 20). The remaining steps were carried out as outlined for the indirect ELISA. Data represent samples tested in duplicate in at least two independent experiments.

The peptide library was screened by Pepscan-based ELISA (Pepscan, Amsterdam, Netherlands). Briefly, the peptide array was incubated with 3D10 or isotype control (0.2 µg/mL) overnight at 4°C then washed with 1X PBST. The array was then incubated with HRP-conjugated rabbit anti-mouse IgG (catalogue no. 6175-05, Southern Biotech, Birmingham, AL, USA) and

incubated for 1 h at 25 °C. After washing, 2,2′-azino-di-3-ethylbenzthiazoline sulfonate (ABTS) was added with 20 µL/mL of H_2O_2 (3%) and the color development was measured after 1 h.

4.2.4 Affinity purification

CNBr-activated Sepharose® 4B media (catalogue no. GE17-0430-01, Sigma, Oakville, ONT, Canada) was rehydrated in 10 mL HCl (1 mM) for 10 min then washed with approximately 200 mL of ice-cold HCl (1 mM). The media was transferred to a 15 mL conical tube, centrifuged and the supernatant was removed. The media was then resuspended in 10 mL of borate buffer (0.5 M NaCl, 0.2 M boric acid, pH 8.2) containing full-length recombinant VAR2CSA (1.0 mg), which was dialyzed against the borate buffer overnight at 4°C with three buffer changes. The media and antigen solution were incubated overnight at 4°C with end-over-end mixing. The remaining free active sites on the media were blocked by addition of 1 mL of Tris-HCl (1M, pH 8.0) and incubation for 2 hours at room temperature with end-over-end mixing. The beads were then washed extensively with borate buffer, followed by Tris-buffered saline (TBS, 20 mM Tris, 150 mM NaCl, pH 7.5) containing 0.1% NP-40.

Anti-SD1$_{CLIPS}$-BSA rabbit sera (10 mL) was pre-absorbed on AB+ washed RBCs for one hour on ice and added to the VAR2CSA-coated Sepharose® media. One milliliter NaCl (5 M), 0.1 mL 10% NP-40 and 0.5 mL Tris-HCl (1 M, pH 7.5) was added, and the solution was incubated overnight at 4°C with end-over-end mixing. The suspension was transferred to a polypropylene column (catalogue no. 208-3366-050, Caplugs, Rancho Dominguez, CA, USA) and the flowthrough was collected. The beads were then washed with 50 mL TBS containing 0.1% NP-40, followed by 70 mL of TBS. Bound antibodies were eluted with a total of 4 mL of glycine-HCl (100 mM, pH 2.5) in 0.5 mL aliquots divided into tubes containing 50 µL Tris-HCl (1 M, pH 8.0) to neutralize the solution. The aliquots were then combined, and the buffer was exchanged to 1X

PBS using an Amicon Ultra-4 centrifugal filter (catalogue no. UFC801024, Merck Millipore). The concentration of the eluted antibodies was measured using a NanoDrop.

4.2.5 Flow cytometry

Antibody reactivity to the surface of *P. falciparum* iRBCs was measured using flow cytometry, as described in Chapter 2, Section 2.9. IgG samples were tested at 40 µg/mL and detected with Alexa Fluor 647 conjugated goat anti-rabbit IgG (dilution 1/500, catalogue no. A21246, Life Technologies).

4.2.6 IBA

IBA experiments were carried out as described in Chapter 2, Section 2.10. IgG samples were tested at 100 µg/mL against three different parasites strains in at least two independent experiments each.

4.6.7 Opsonic phagocytosis

Opsonic phagocytosis experiments were carried out as described previously (291). Magnetically enriched mature *P. falciparum* iRBCs from *in vitro* culture were stained with ethidium bromide (EtBr) for 30 min at room temperature in the dark. The iRBCs were then washed twice with RPMI and resuspended at 1.25 x 10^8 cells/mL in RPMI. Twenty microlitres of the cell suspension was aliquoted to a separate tube for each antibody sample, centrifuged and the supernatant was removed. The pellet was then resuspended in the antibody solution in 1X PBS or in PBS alone for the negative control and incubated for 45 min at 37°C protected from light. The cells were washed once with RPMI, resuspended in 50 µL of pre-warmed THP-1 cell media and added to individual wells of a round-bottom 96 well plate containing 1.25 x 10^5 THP-1 cells in 100 µL of cell media. The plate was then incubated for 45 min at 37°C in a 5% CO_2 incubator.

The cell solution was transferred to a 1.5 mL tube, centrifuged and resuspended in 500 µL RBC lysis buffer. The cells were incubated for 10 min at room temperature with gentle agitation before being centrifuged and washed once, then resuspended in 2% FBS. EtBr-positive THP-1 cells were quantified by flow cytometry (Fortessa X20) and data analyzed with FlowJo version 7.6 (TreeStar, Ashland, USA).

4.2.8. Statistical analysis

Data were plotted and statistical significance was determined using a Kruskal-Wallis one-way ANOVA using Prism software (version 8; GraphPad, San Diego, CA, USA).

4.3. Results

4.3.1. N_{10}-C_{22} is the minimal epitope for 3D10 recognition, but does not elicit cross-reactive antibodies

In order to identify the minimal epitope for 3D10 recognition, we designed a number of synthetic peptides spanning the SD1 region of DBPII (Figure 4.1). In the native protein, this region contains four cysteine residues that form two disulfide bonds. We previously tried to recapitulate the native structure using a synthetic peptide, but based on mass spectrometry, the disulfide bonds did not form in the correct configuration (data not shown). Therefore, we designed a peptide called SD1ss, in which two of the cysteine residues were mutated to serines ('ss'), which allowed us to control the intramolecular disulfide bonding pattern. When we screened these peptides by ELISA; the regions nearest the amino terminus of SD1 (N_{10}-C_{29} and N_{10}-C_{22}) were strongly recognized by 3D10 (Figure 4.2A). The minimal epitope recognized by 3D10 was a 13 amino acid peptide called N_{10}-C_{22} that was recognized with an endpoint titer of 2.7 ng/mL, similar to the reactivity against the parent protein DBPII. This finding is supported by previous reports that 3D10 recognizes the

NXXRKR motif within this peptide (260, 292). Using a competition ELISA, this peptide was sufficient to block heterologous recognition of VAR2CSA by 3D10 (Figure 4.2B). When 3D10 was incubated with increasing concentrations of this peptide, N_{10}-C_{22} blocked recognition of VAR2CSA to a similar degree as SD1ss. The C_{29}-K_{40} peptide was included as a negative control for inhibition because 3D10 did not recognize this peptide (Figure 4.2A). Based on these results, we concluded that N_{10}-C_{22} represents the minimal epitope for homologous 3D10 recognition of DBPII and mediates heterologous recognition of VAR2CSA.

We next immunized five BALB/c mice with the N_{10}-C_{22} peptide conjugated to DT. The mice produced high levels of antibodies against N_{10}-C_{22}; however, the antibodies did not cross-react with VAR2CSA by ELISA (Figure 4.2C). This lack of cross-reactivity is not surprising, considering these antibodies also failed to recognize DBPII, the cognate protein from which the peptide was derived (Figure 4.2C).

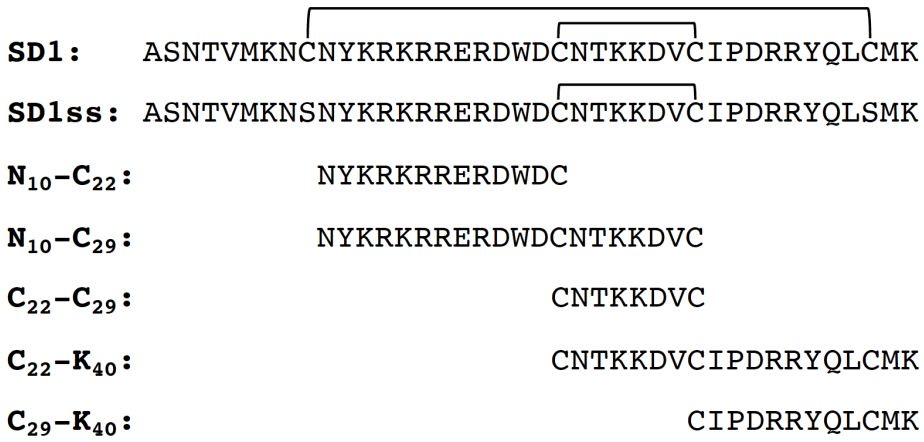

Figure 4.1. Synthetic peptides were designed to cover the subdomain 1 (SD1) region of DBPII. The subscript numbers indicate the amino acid position in the parent SD1 peptide. Disulfide bonds are noted with horizontal lines.

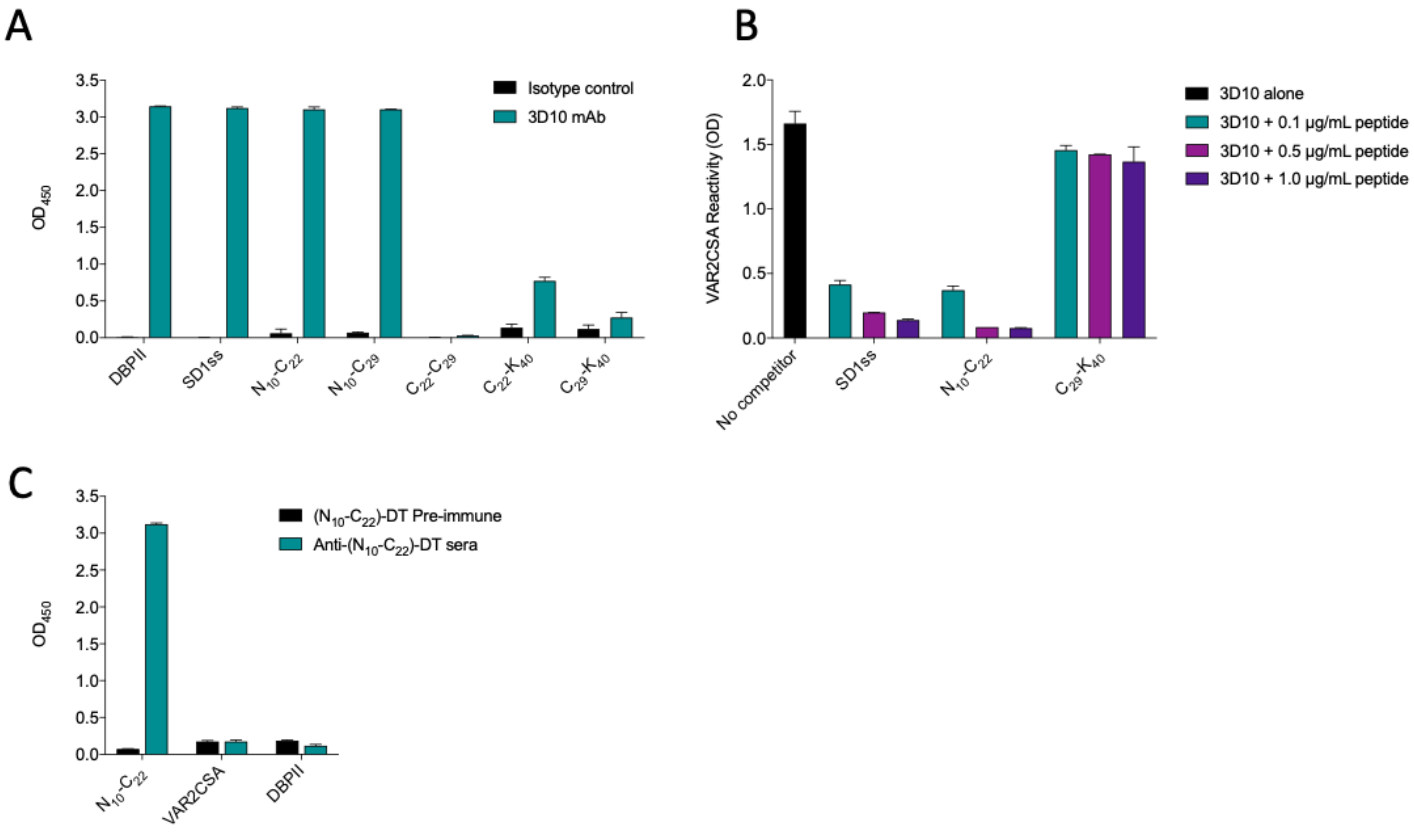

Figure 4.2. N_{10}-C_{22} is the minimal epitope for 3D10 recognition of DBPII and VAR2CSA but does not elicit cross-reactive antibodies in mice. (**A**) Synthetic peptides spanning the SD1 region of DBPII were screened with 3D10 by ELISA. Recombinant DBPII protein was included as a positive control. (**B**) 3D10 was incubated alone (black bar) or with increasing concentrations of SD1ss, N_{10}-C_{22}, or C_{29}-K_{40}, then added to wells coated with recombinant full-length VAR2CSA. (**C**) Pooled sera from mice (n = 5) before and after immunization with (N_{10}-C_{22})-DT were tested against N_{10}-C_{22}, VAR2CSA, and DBPII by ELISA. Data are mean ± standard deviation (SD).

4.3.2. 3D10 recognizes a discontinuous epitope in SD1

To map the recognition site of 3D10, we designed an array of 37 overlapping linear peptides spanning SD1 of DBPII (Table 4.1). We used a Pepscan-based ELISA for this screen because the peptides can be coated at a high concentration, which allows for identification of minor parts of the epitope that may not be detected using a conventional ELISA. We screened this library with 3D10 and found that it recognized peptides from three regions of SD1 (Figure 4.3A). These results suggested that the epitope is discontinuous. We then screened a library of these peptides where two residues in each peptide were mutated to alanine (Figure 4.3B). Several of these mutations resulted in a significant decrease in 3D10 recognition. These data further confirm that sequences within the two outer segments in particular are critical for 3D10 recognition.

In the native DBPII structure, there are two disulfide bonds that bring these regions in close proximity, allowing them to form the discontinuous epitope (Figure 4.3C). This presents a significant challenge for vaccine development as conformational epitopes are notoriously difficult to recapitulate with synthetic peptides (293).

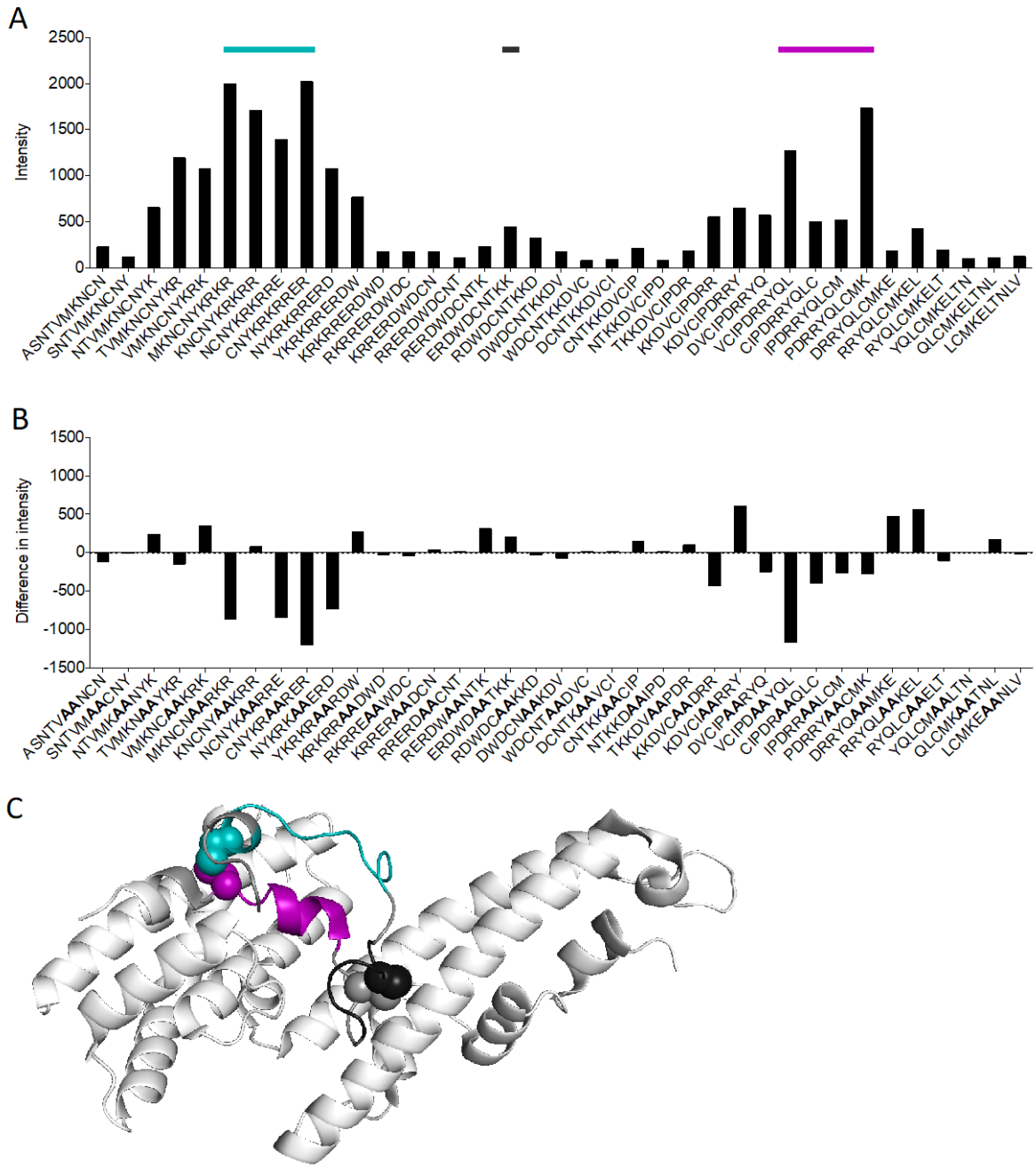

Figure 4.3. 3D10 recognizes a discontinuous epitope in SD1. (**A**) An overlapping peptide array spanning the SD1 region of DBPII was screened with 3D10. The colors of the lines above the bar graph correspond to the region of SD1 mapped to the structure in (C). (**B**) The intensity of 3D10 recognition of peptides with alanine substitutions (bolded) was subtracted from that of the native sequence. Negative values indicate that 3D10 recognition was decreased following alanine substitution. (**C**) The structure of SD1 was determined from a published crystal structure of DBPII that was adapted using PyMOL (PDB ID 4NUU). The cysteines involved in disulfide bonds are shown as space-filling spheres.

4.3.3. Immunization with SD1$_{CLIPS}$ elicited cross-reactive VAR2CSA antibodies

To recapitulate the immunogen that elicited the cross-reactive 3D10 mAb in DBPII, we designed a 31 amino acid peptide called SD1$_{CLIPS}$ that uses CLIPS technology to control bond formation and conformationally constrain the peptide to its native structure. Specifically, a synthetic scaffold was inserted in place of one of the disulfide bonds to ensure that the disulfide bond formed between the correct pair of cysteines (Figure 4.4A). After confirming that 3D10 recognized this peptide by ELISA (endpoint titer: 20.5 ng/mL), we immunized five BALB/c mice with SD1$_{CLIPS}$ conjugated to keyhole limpet hemocyanin (KLH). All mice produced high levels of antibodies against SD1$_{CLIPS}$ and 60% (3/5) of the mice also made antibodies that cross-reacted with VAR2CSA (Figure 4.4B). Although the titers of the anti-VAR2CSA antibodies were relatively low compared to those against SD1$_{CLIPS}$, these results demonstrate that a peptide immunogen successfully recapitulated a cross-reactive conformational epitope.

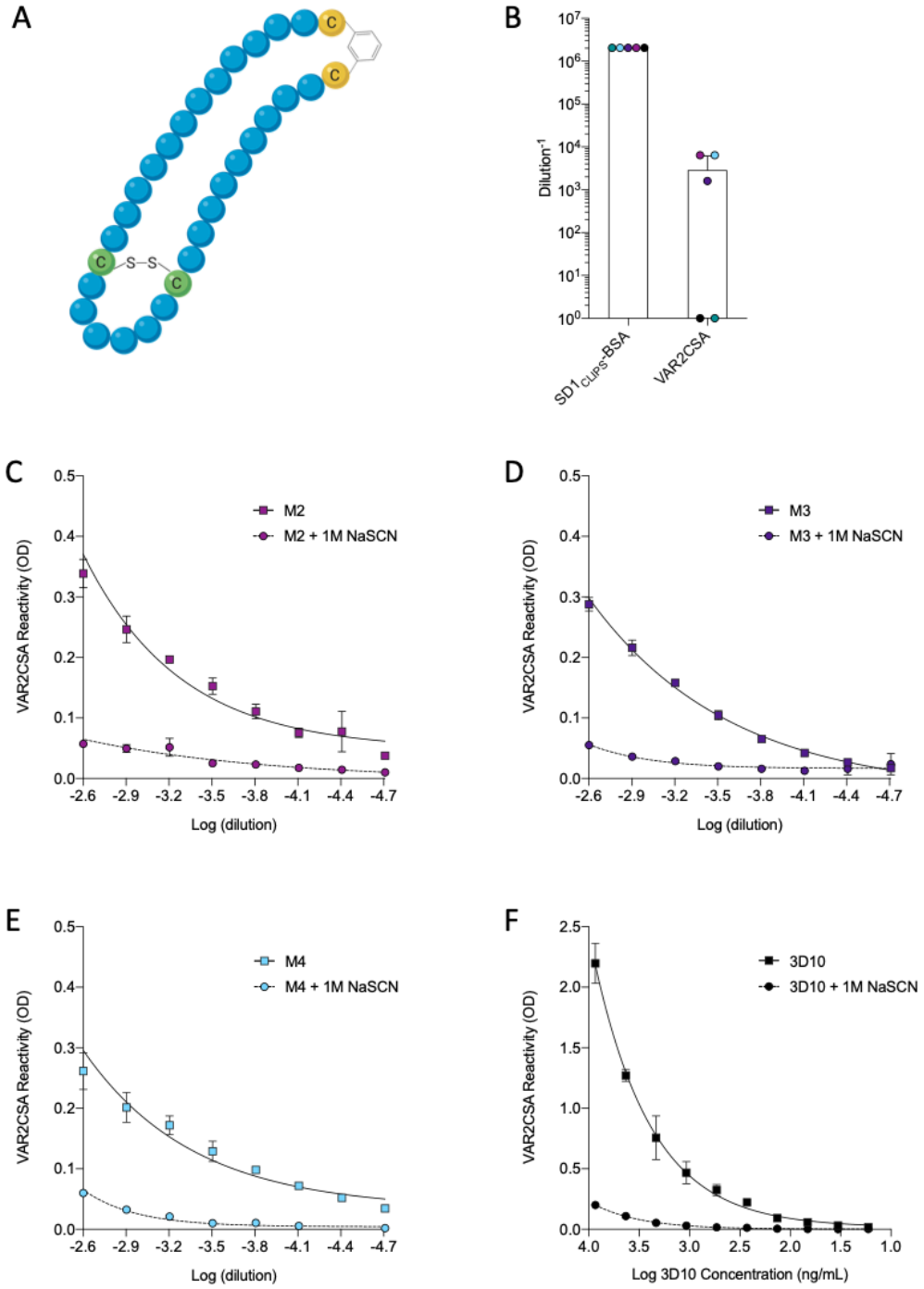

Figure 4.4. A conformationally constrained peptide encompassing the SD1 region of DBPII elicited antibodies that cross-react with VAR2CSA. (**A**) A synthetic 31 amino acid peptide of the SD1 region was designed using a chemical scaffold in place of one of the disulfide bonds. The cysteine residues that formed a disulfide bond are shown in green, and those involved in the chemical linkage are shown in yellow. (**B**) Endpoint titers for the individual mice immunized with SD1CLIPS-keyhole limpet hemocyanin (KLH) were measured against SD1CLIPS-bovine serum

albumin (BSA) and VAR2CSA by ELISA. Data from each individual mouse (M#) are represented by the same color throughout this and subsequent figures. Endpoint titers were calculated relative to the mean optical density (OD) of the matching pre-immune serum plus two standard deviations. (**C**–**F**) The avidity of the cross-reactive sera (**C–E**) and 3D10 (**F**) for VAR2CSA was determined by titrating the individual serum samples or 3D10 against VAR2CSA with and without the addition of 1 M NaSCN. Data are mean ± SD.

When we measured the avidity of the cross-reactive antibodies against VAR2CSA, the avidity was low compared to the avidity of the antibodies for their immunogen. Incubation with 1 M NaSCN significantly reduced antibody binding to VAR2CSA across a range of dilutions (Figure 4.4C–E), whereas there was little reduction in antibody binding to $SD1_{CLIPS}$ (Figure 4.5A–E). It is not uncommon for cross-reactive antibodies to have a lower avidity for the heterologous antigen. However, this does not negate the potential functional relevance of these antibodies. In fact, the avidity of these antibodies for VAR2CSA is similar to that of 3D10 (Figure 4.4F), which blocked VAR2CSA-expressing *P. falciparum* parasites from binding to the placental ligand *in vitro* (155).

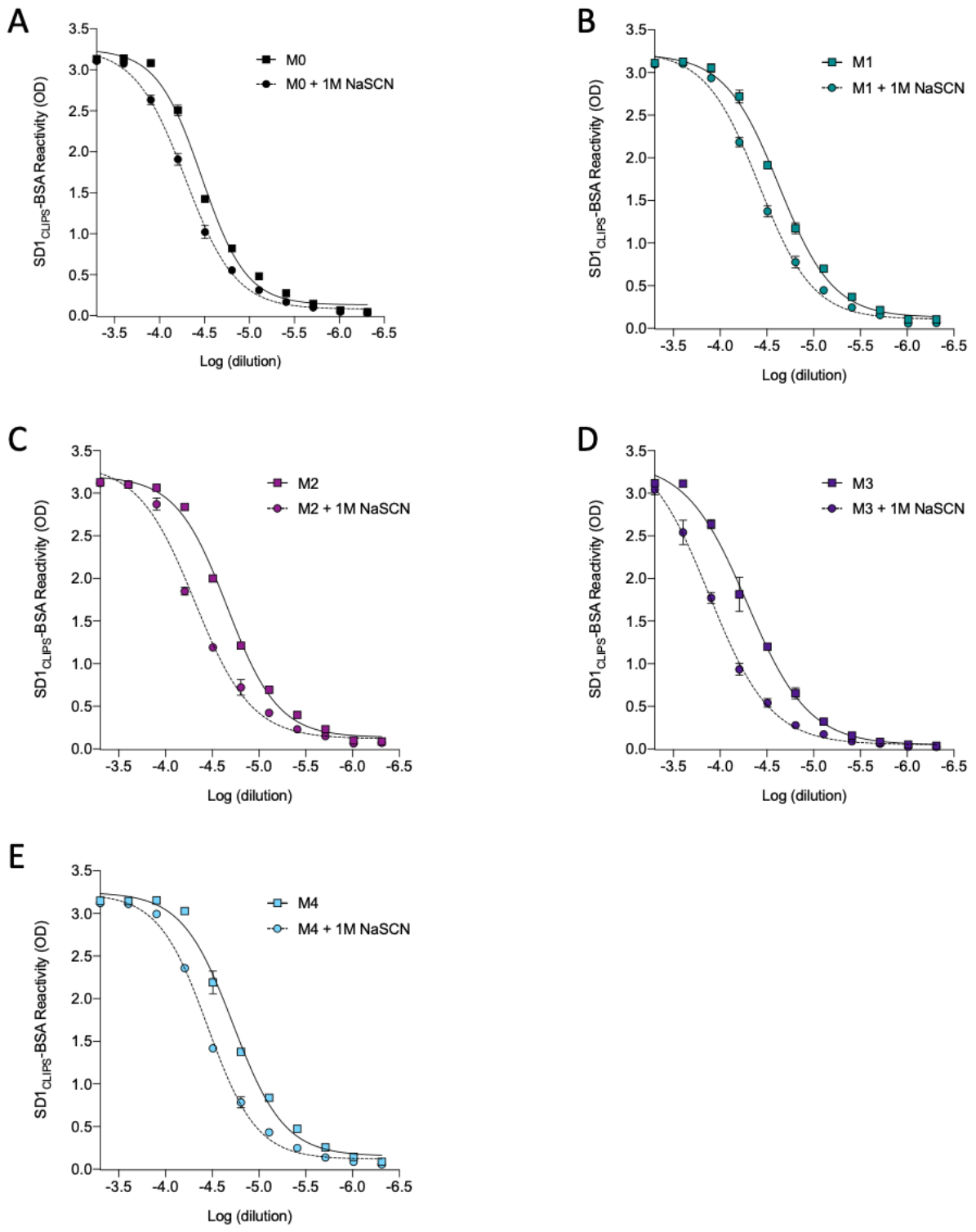

Figure 4.5. The avidity of individual mouse serum against SD1$_{CLIPS}$-BSA. (A-E) The avidity of individual serum samples for SD1$_{CLIPS}$-BSA was determined by titrating serum against this antigen with and without the addition of 1M NaSCN. Data are mean ± SD.

4.3.4. Fine specificity and avidity of anti-SD1$_{CLIPS}$ antibodies in individual mice

Despite making similar levels of antibodies against the SD1$_{CLIPS}$ immunogen, only three out of the five BALB/c mice made cross-reactive antibodies that recognized VAR2CSA. This prompted us to evaluate the fine specificity of the individual immune responses of each mouse for DBPII and the smaller peptides within the SD1 region. Sera from all of the mice recognized DBPII, N_{10}-C_{29}, C_{22}-K_{40}, and C_{22}-C_{29} at similarly high levels (Figure 4.6A). However, the mice had varying levels of antibodies against the shorter N_{10}-C_{22} and C_{29}-K_{40} peptides. For instance, serum from mouse M0 (black circles in Figure 4.6A) had an endpoint titer of 1/400 against N_{10}-C_{22} and did not recognize C_{29}-K_{40}, whereas serum from mouse M2 (light purple circles in Figure 4.6A) had an endpoint titer of over 1/200,000 against N_{10}- C_{22} and over 1/800,000 against C_{29}-K_{40}. Despite being of the same inbred strain of mouse, each of the five mice had a unique immune response to different regions of the SD1$_{CLIPS}$ immunogen.

There was no discernable difference in the recognition patterns of sera that cross-reacted with VAR2CSA (mice M2, M3, and M4) and sera that did not (mice M0 and M1). However, the cross-reactive sera had much lower avidity for DBPII than the non-cross-reactive sera (Figure 4.6B–F). This result is consistent with the avidity of 3D10 for DBPII, which is significantly lower compared to another DBPII monoclonal antibody, 2D10, which we showed previously does not cross-react with VAR2CSA (Figure 4.6G and H) (155). Together, these results suggest that antibodies against DBPII that cross-react with VAR2CSA exhibit low avidity against both of these proteins in immunized mice.

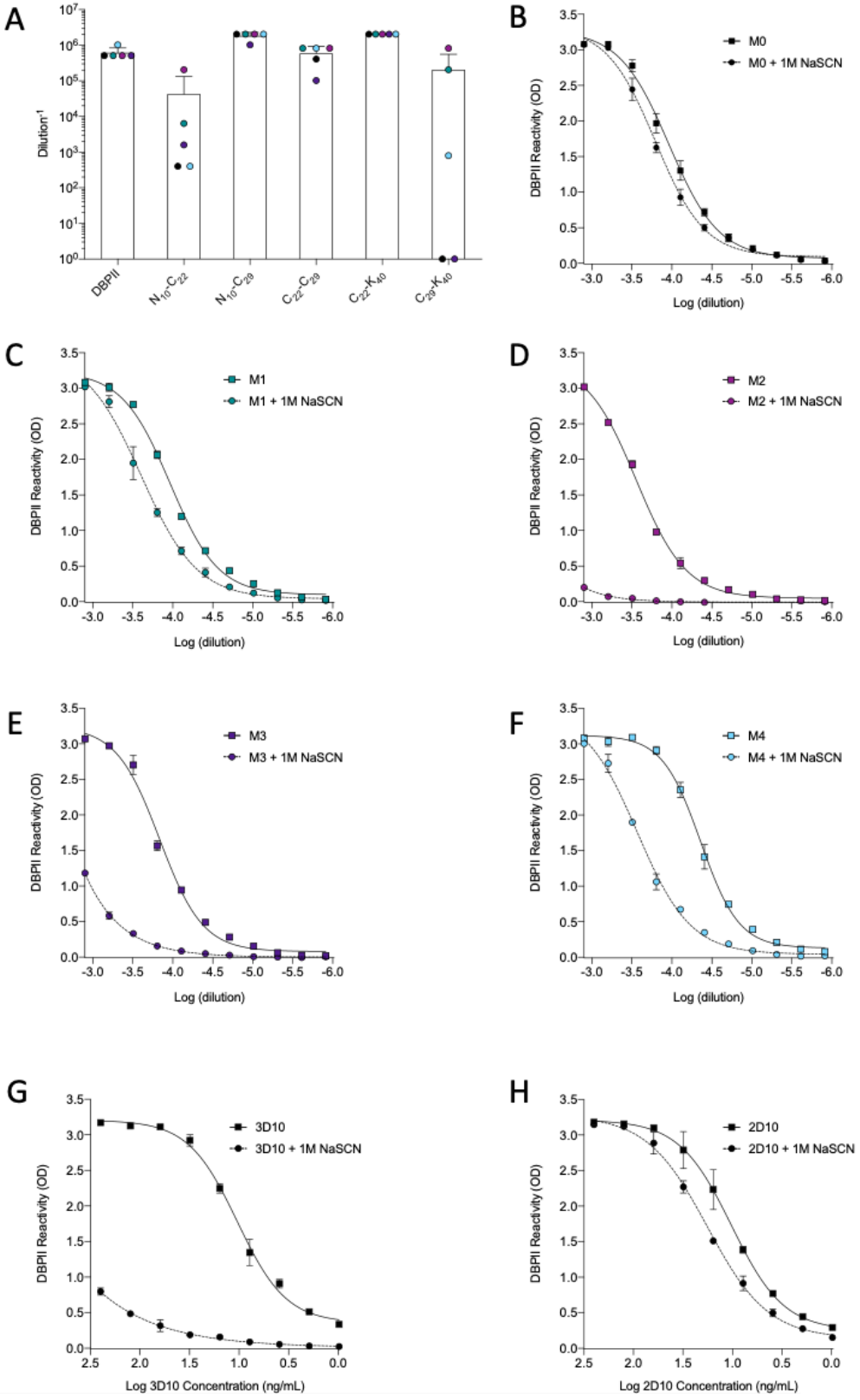
A
Dilution-1
DBPII
N10-C22
N10-C29
C22-C29
C22-K40
C29-K40
B
M0
M0 + 1M NaSCN
DBPII Reactivity (OD)
Log (dilution)
C
M1
M1 + 1M NaSCN
D
M2
M2 + 1M NaSCN
E
M3
M3 + 1M NaSCN
F
M4
M4 + 1M NaSCN
G
3D10
3D10 + 1M NaSCN
Log 3D10 Concentration (ng/mL)
H
2D10
2D10 + 1M NaSCN
Log 2D10 Concentration (ng/mL)

Figure 4.6. Cross-reactive sera that recognized VAR2CSA had low avidity against DBPII. (**A**) Endpoint titers for the individual mice immunized with SD1$_{CLIPS}$-KLH were measured against DBPII and the synthetic peptides spanning the SD1 region. Endpoint titers were calculated relative to the mean OD of the matching pre-immune serum plus two standard deviations. (**B**–**F**) The avidity of the individual serum samples for DBPII was determined by titrating against DBPII with and without the addition of 1 M NaSCN. (**G**–**H**) The avidity of 3D10 and 2D10 (a non-cross-reactive DBPII monoclonal antibody) against DBPII was determined by titrating the monoclonal antibodies against DBPII with or without the addition of 1 M NaSCN. Data are mean ± SD.

4.3.5. $SD1_{CLIPS}$ elicits cross-reactive antibodies in a rabbit

To determine if antibodies cross-reactive with VAR2CSA can be elicited in a different animal, we immunized a rabbit with the same $SD1_{CLIPS}$ peptide, only conjugated to BSA. This conjugate was highly immunogenic in the rabbit, with an endpoint titer against the peptide of 1/256,000 and very high avidity (Figure 4.7A). These antibodies also strongly recognized DBPII and, unlike the mouse serum, their avidity for DBPII was high (Figure 4.7B). Importantly, the serum also recognized VAR2CSA (Figure 4.7C), and consistent with the results from mice, these antibodies were not as strong (endpoint titer of 1/1600) and were of low avidity.

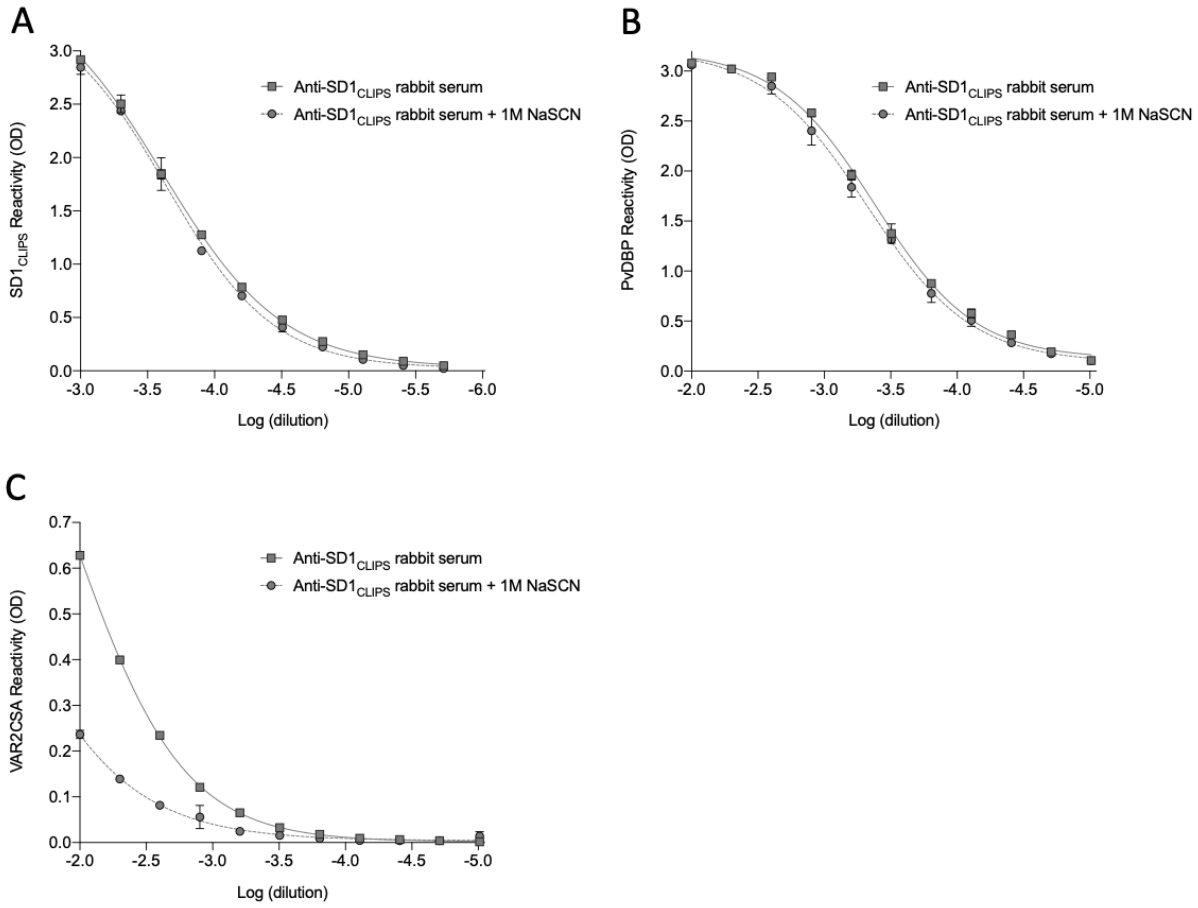

Figure 4.7. SD1$_{CLIPS}$ elicits cross-reactive antibodies in a rabbit. The avidity of the anti-SD1$_{CLIPS}$ rabbit serum against (**A**) SD1$_{CLIPS}$, (**B**) DBPII, and (**C**) VAR2CSA was determined by titrating the serum against the antigen with and without the addition of 1 M NaSCN. Data are mean ± SD.

The anti-SD1$_{CLIPS}$-BSA rabbit serum was also tested against a number of different *P. vivax* and *P. falciparum* antigens by ELISA. We found that the serum strongly recognized the N_{10}-C_{22} peptide encompassing an N terminal region of SD1 that was also strongly recognized by 3D10 (Figure 4.8A, 3D10 recognition: Figure 2.3B). Interestingly, the serum also recognized EBP2, which was not recognized by 3D10, although the recognition was not as strong as either DBPII or N_{10}-C_{22}. When we tested this serum against some of the DBL domains of VAR2CSA, DBL3X (OD: 1.5 ± 0.06 SD) was the most strongly recognized, followed by DBL4ε (OD: 0.7 ± 0.01 SD) and DBL5ε (OD: 0.5 ± 0.02 SD) (Figure 4.8B). The N-terminal region of VAR2CSA (DBL1-ID2 and ID1-ID2a) was not well recognized by the cross-reactive IgG (OD: 0.2 ± 0.02 SD for both), despite being the region that was most strongly recognized by 3D10 (OD: 1.0 ± 0.12 SD) (Figure 4.8C). Similarily, 3D10 did not recognize the non-pregnancy associated PfEMP1, VAR7, whereas the cross-reactive IgG recognized this antigen quite strongly (OD: 0.6 ± 0.01 SD). These results highlight potentially important differences in the recognition patterns between 3D10 and the cross-reactive IgG.

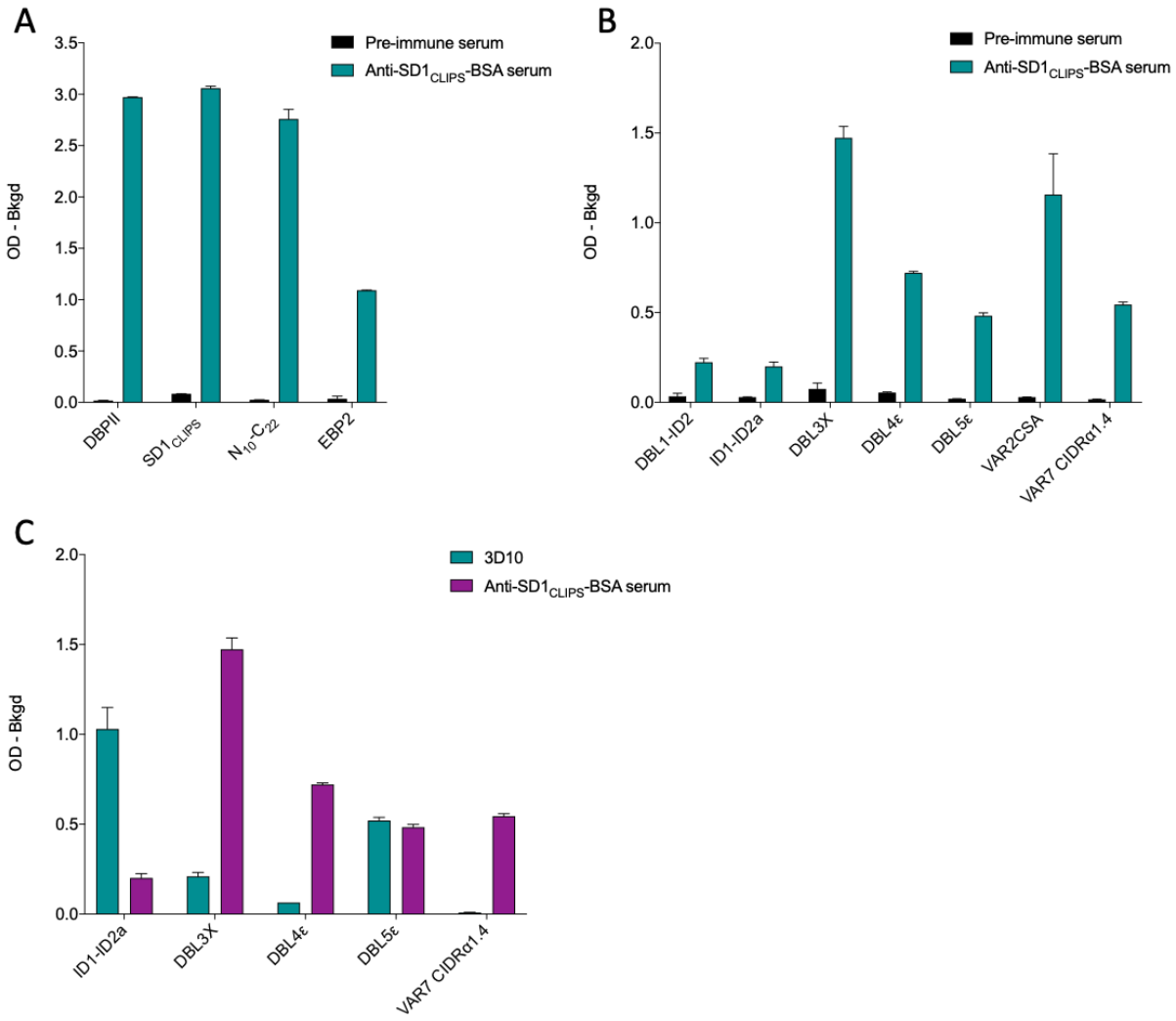

Figure 4.8. Serum from a rabbit immunized with SD1$_{CLIPS}$-BSA recognized *P. vivax* and *P. falciparum* antigens. The anti-SD1$_{CLIPS}$-BSA rabbit serum (dilution 1/200) was tested by ELISA against a number of (A) *P. vivax* and (B) *P. falciparum* antigens. Pre-immune serum was included as a negative control. (C) Data for 3D10 (8.6 µg/mL) and anti-SD1$_{CLIPS}$-BSA serum (dilution 1/200) against the DBL domains of VAR2CSA and the non-pregnancy associated PfEMP1 protein, VAR7 were combined. The reactivity was measured in separate experiments and the data were combined to facilitate comparison between the recognition profiles of the two different antibody samples. Data are mean ± SD.

In order to determine if the SD1$_{CLIPS}$-BSA immunizations elicited functional anti-VAR2CSA antibodies, the cross-reactive antibodies were affinity-purified from the rabbit serum using full-length VAR2CSA (Figure 4.9A). Evaluation by ELISA showed that the VAR2CSA reactivity of total IgG purified from the column flow through (flow through IgG) was reduced compared to that of the starting serum (anti-SD1$_{CLIPS}$ rabbit IgG), suggesting that the majority of the cross-reactive antibodies were purified from the serum (Figure 4.9B). These purified antibodies (cross-reactive IgG) recognized VAR2CSA (endpoint titre: 0.02 μg/mL), DBPII (endpoint titre: 1.25 μg/mL) and EBP2 (endpoint titre: 1.25 μg/mL) by ELISA (Figure 4.9B, C and D). Interestingly, the endpoint titres of the cross-reactive IgG were the same against both DBPII and EBP2, which is different from ELISAs with the starting serum where DBPII recognition (OD ± SD: 3.0 ± 0.02) was significantly stronger than EBP2 recognition (OD ± SD: 1.1 ± 0.01) (Figure 4.8A). Consistent with the results from 3D10 and the anti-SD1$_{CLIPS}$-BSA rabbit serum, the cross-reactive IgG recognition of VAR2CSA was significantly reduced following incubation with 1M NaSCN, indicating low antibody binding avidity (Figure 4.9C).

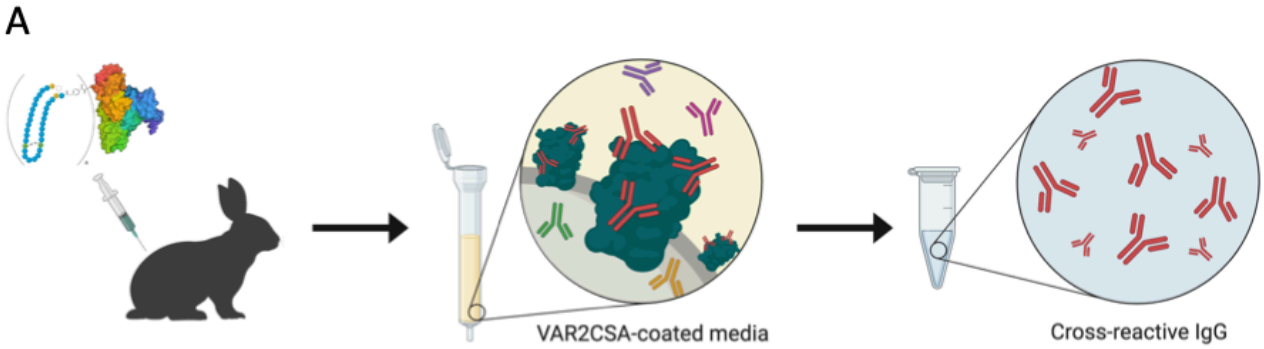
A
VAR2CSA-coated media
Cross-reactive IgG

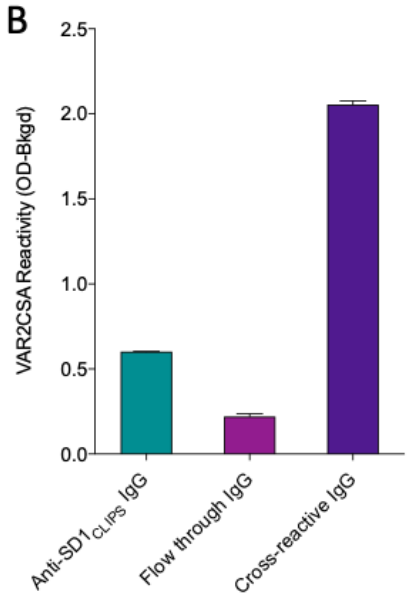
B
VAR2CSA Reactivity (OD-Bkgd)
2.5
2.0
1.5
1.0
0.5
0.0
Anti-SD1CLIPS IgG
Flow through IgG
Cross-reactive IgG

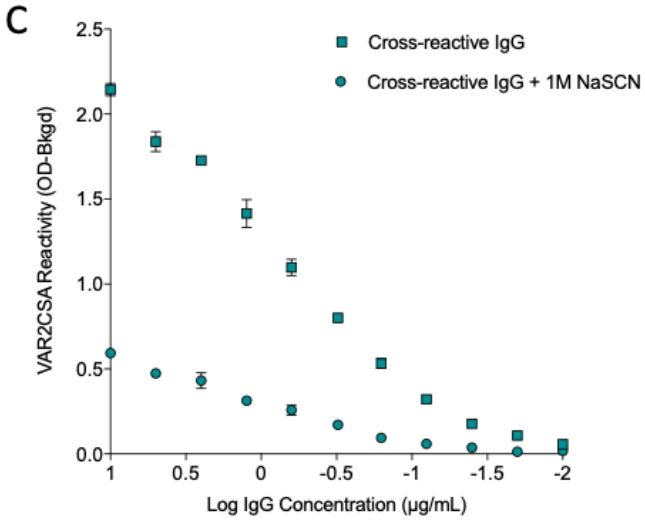
C
Cross-reactive IgG
Cross-reactive IgG + 1M NaSCN
VAR2CSA Reactivity (OD-Bkgd)
2.5
2.0
1.5
1.0
0.5
0.0
1
0.5
0
-0.5
-1
-1.5
-2
Log IgG Concentration (µg/mL)

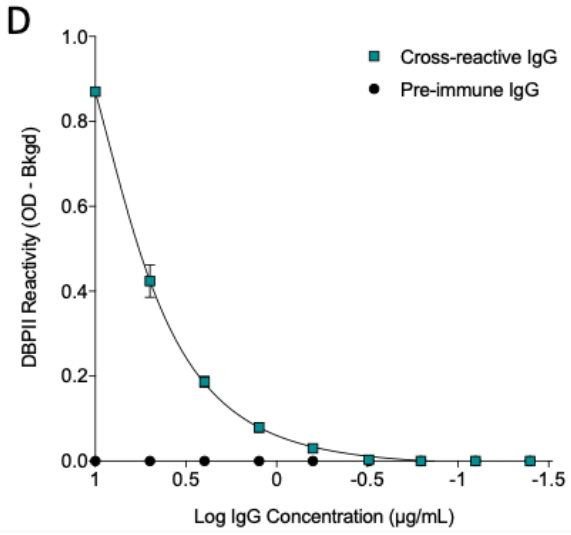
D
Cross-reactive IgG
Pre-immune IgG
DBPII Reactivity (OD - Bkgd)
1.0
0.8
0.6
0.4
0.2
0.0
1
0.5
0
-0.5
-1
-1.5
Log IgG Concentration (µg/mL)

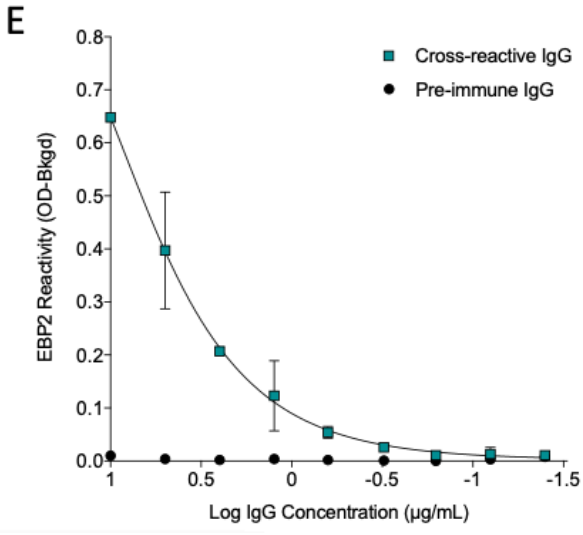
E
Cross-reactive IgG
Pre-immune IgG
EBP2 Reactivity (OD-Bkgd)
0.8
0.7
0.6
0.5
0.4
0.3
0.2
0.1
0.0
1
0.5
0
-0.5
-1
-1.5
Log IgG Concentration (µg/mL)

Figure 4.9. Cross-reactive antibodies were affinity-purified from anti-SD1$_{CLIPS}$ rabbit serum using full-length VAR2CSA. (A) Anti-SD1$_{CLIPS}$ rabbit serum was incubated with VAR2CSA-coated Sepharose, the unbound antibodies were washed from the column and the cross-reactive antibodies were eluted. (B) The reactivity of total IgG from the anti-SD1$_{CLIPS}$ rabbit serum (50 µg/mL), the flow through from the affinity-purification (50 µg/mL) and the cross-reactive antibodies (10 µg/mL) against VAR2CSA was measured by ELISA. (C) The avidity of the cross-reactive IgG against VAR2CSA was determined by titrating the antibodies against the antigen with and without the addition of 1 M NaSCN. The endpoint titres of the cross-reactive IgG against (D) DBPII, (E) EBP2 were measured by ELISA. Total IgG from the pre-immune rabbit serum was included as a negative control. Data are mean ± SD. Figure in (A) was made using BioRender.com.

4.3.6. Cross-reactive IgG recognized the surface of RBCs infected with three different strains of VAR2CSA-expressing *P. falciparum* parasites

Next, we determined if the cross-reactive IgG could recognize native VAR2CSA expressed on the surface of iRBCs. To test this, we used flow cytometry to quantify the cross-reactive IgG recognition of RBCs infected with three different strains of *P. falciparum* parasites. Interestingly, we found that the cross-reactive IgG displayed strain-transcending recognition of the surface of RBCs infected with all three strains of parasites. The highest percentage of iRBC recognition (95.6%) was observed with the placental isolate strain of *P. falciparum*, followed by the NF54-CSA (76.5%) and CS2 (68.1%) strains (Figure 4.10). Total IgG from the pre-immune rabbit serum and the affinity purification flow through were included as controls in all experiments and were run at the same concentration as the cross-reactive IgG (40 µg/mL).

Unexpectedly, in many of the flow experiments, a higher percentage of DAPI-negative RBCs were recognized by the cross-reactive IgG, compared to the pre-immune IgG and the flow through IgG. However, in all of these cases the percentage of DAPI-negative RBCs that were recognized was lower than the percentage of DAPI-positive RBCs that were recognized. We investigated this further by testing the cross-reactive IgG against uRBCs alone. Consistent with observations from previous flow experiments, a higher percentage of the uRBCs were recognized by the cross-reactive IgG (22.0%) compared to either the pre-immune IgG (1.26%) or the flow though IgG (1.11%) (Figure 4.11A). The reason for this non-specific staining is unknown, as all sera were pre-absorbed on AB+ human RBCs prior to affinity purification. However, the 22.0% of uRBCs recognized by the cross-reactive IgG could not account for the 68.1% to 95.6% of iRBCs that were recognized. The overall shift in the uRBC population stained with the cross-reactive IgG is also much lower than that observed in the iRBC population (Figure 4.11B). The relative difference in the median fluorescence intensity (MFI) between the uRBCs stained with the cross-reactive IgG

and the pre-immune IgG was 78.7 AU, while the relative difference between the iRBC populations stained with these same antibodies was 476.5 AU. Thus, despite there being some background recognition of uRBCs, most of the recognition was parasite antigen-specific.

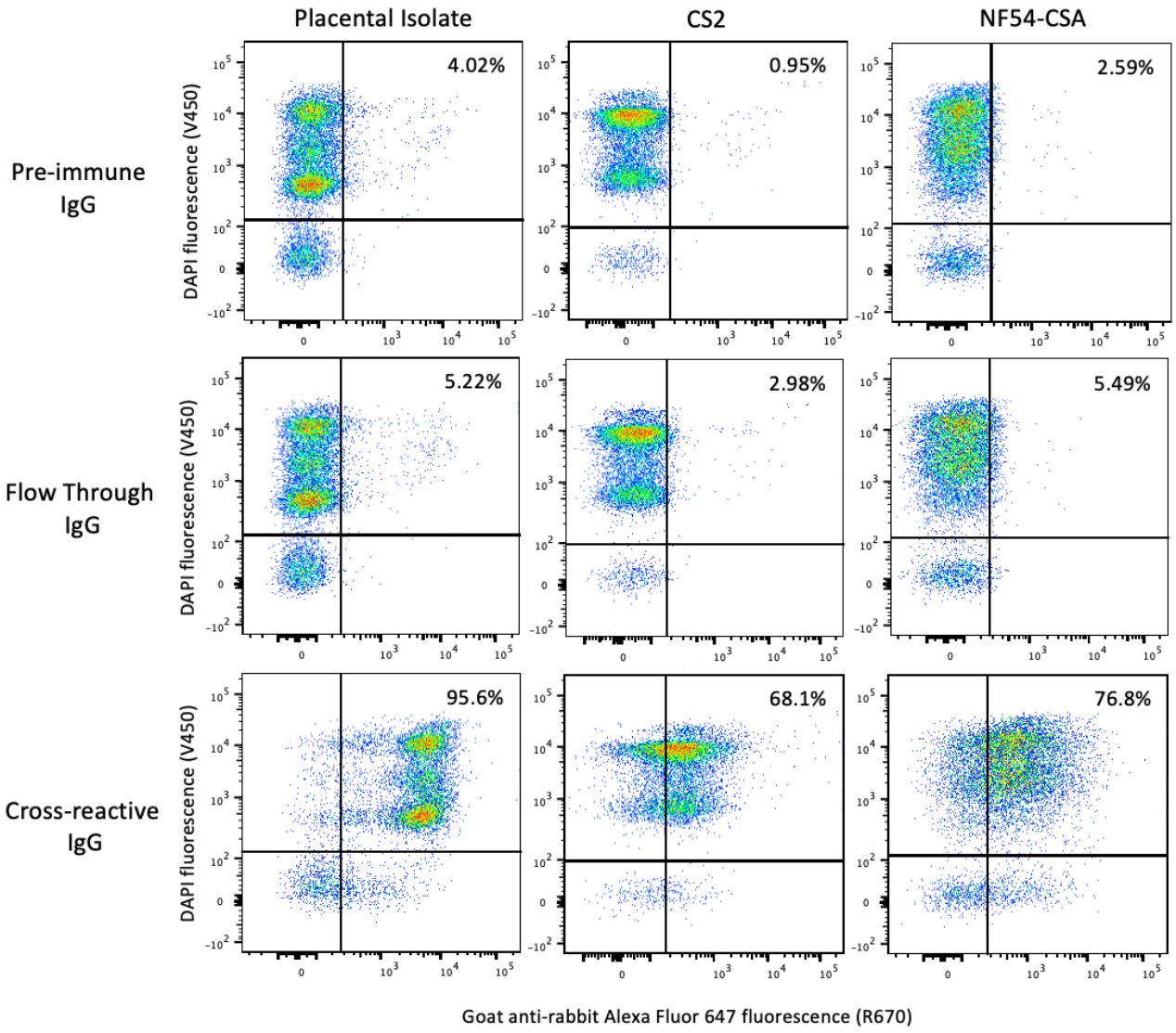

Figure 4.10. Cross-reactive IgG recognized the surface of VAR2CSA-expressing *P. falciparum* parasites. Mature trophozoites were incubated with cross-reactive IgG or total IgG purified from pre-immune rabbit serum or flow through from the affinity-purification. Antibodies bound to the surface of the iRBCs were detected using an Alexa Fluor 647-conjugated goat anti-rabbit IgG secondary antibody and parasite DNA was stained with DAPI. IgG were run at 40 µg/mL. Experiments with each parasite strain were repeated three times and representative plots are shown above. The percentage of iRBCs recognized by the IgG is indicated on each plot.

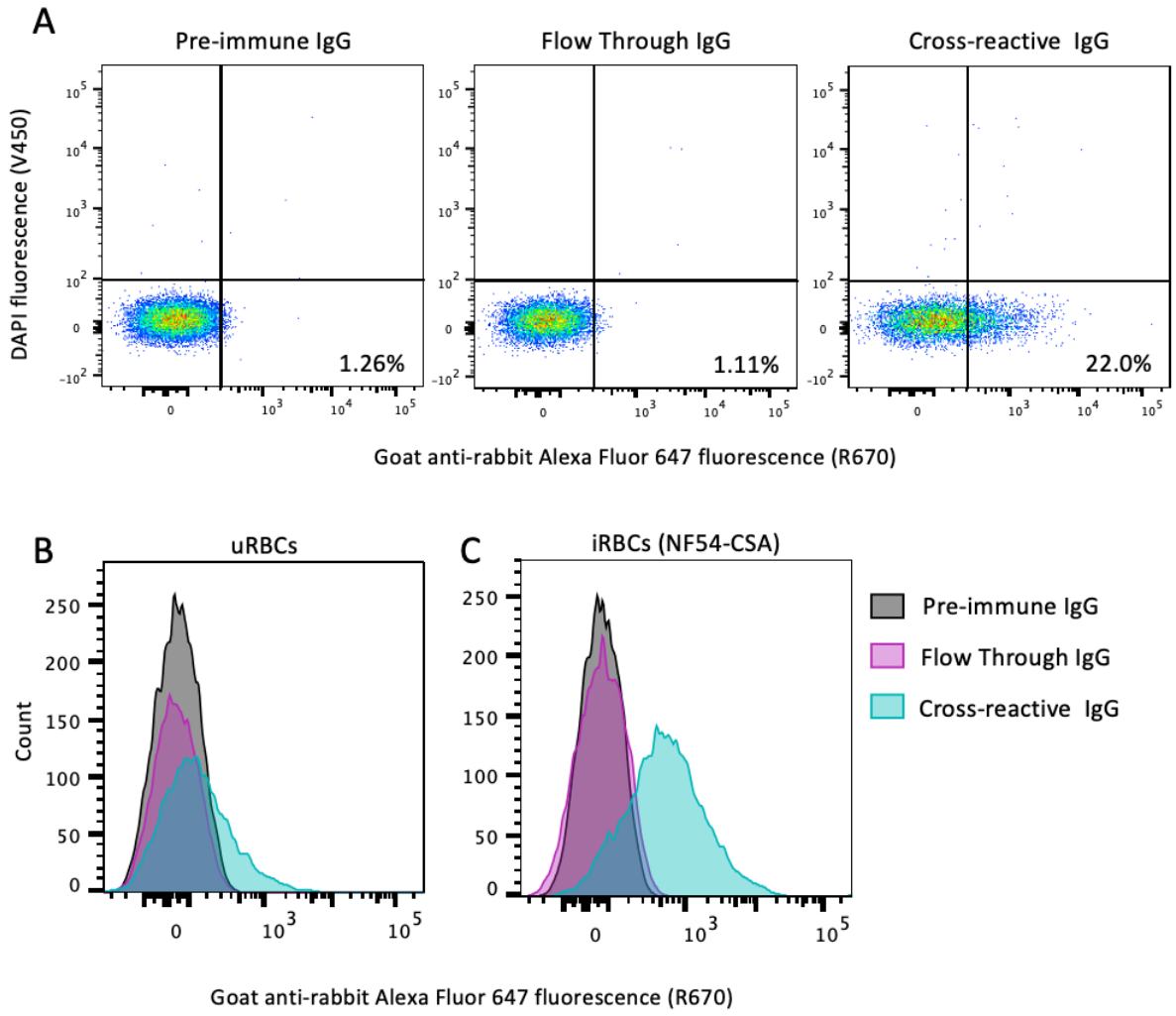

Figure 4.11. Cross-reactive IgG recognized a higher percentage of uRBCs than the pre-immune IgG or flow through IgG. (A) Pre-immune, flow through and cross-reactive IgG (40 µg/mL) recognition of uRBCs was quantified by flow cytometry. Rabbit IgG was detected using an Alexa Fluor 647 goat anti-rabbit secondary antibody and the percentage of RBCs recognized by the IgG is indicated on each plot. Histograms of uRBC (B) and iRBC (NF54-CSA) (C) populations stained with the different IgG samples were overlayed.

4.3.7. Cross-reactive IgG did not block parasite adhesion to CSA or mediate opsonic phagocytosis *in vitro*

Despite strongly recognizing the surface of VAR2CSA-expressing iRBC, the cross-reactive IgG did not block parasite binding to CSA *in vitro* (Figure 4.12A, C and E). The antibodies were tested in a minimum of two independent IBA experiments with each of the three strains of *P. falciparum* iRBCs. When the parasites were incubated with the cross-reactive IgG, there was no inhibition of CSA binding compared to pre-immune IgG. Two of the controls that were included in the IBAs were serum from a rabbit immunized with full-length VAR2CSA (FCR3 allele) and total IgG purified from this serum. These antibodies inhibited the CS2 parasite strain, which expresses the homologous FCR3 allele of VAR2CSA, from binding to CSA (Figure 4.12D). However, these antibodies did not block the placental isolate or NF54-CSA strains from binding to CSA (Figure 4.12B and F). There was also an unusual decrease in binding observed when the placental isolate strain was incubated with normal rabbit serum (Figure 4.12B). The reason for this background is unknown, but this was serum from a different rabbit than the one used in the experiments with CS2 and NF54-CSA parasites.

Human sera pools were also used as controls in these experiments. A pool of sera from individuals living in a malaria-free area of Colombia (unexposed Colombian sera) was used as a negative control and sera from multigravid women living in an area of Uganda that is holoendemic for malaria (Ugandan multigravid sera) was used as a positive control. The Ugandan multigravid sera displayed strain-transcending inhibitory activity against all three strains of *P. falciparum* (Figure 4.12B, D and F).

Placental Isolate

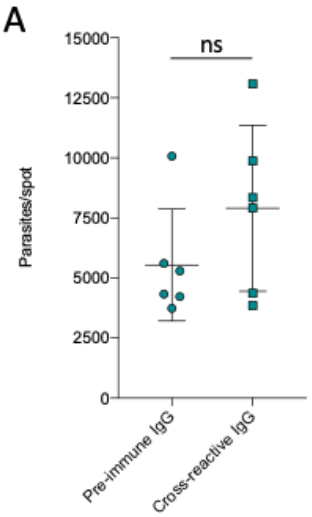

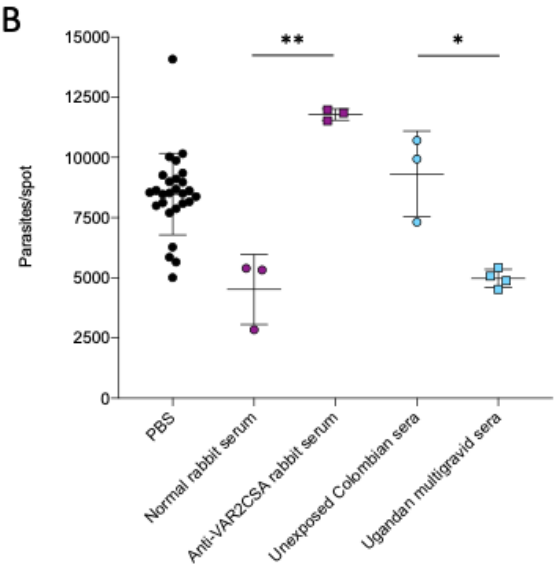

CS2

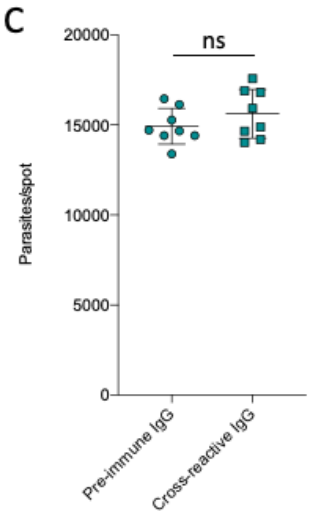

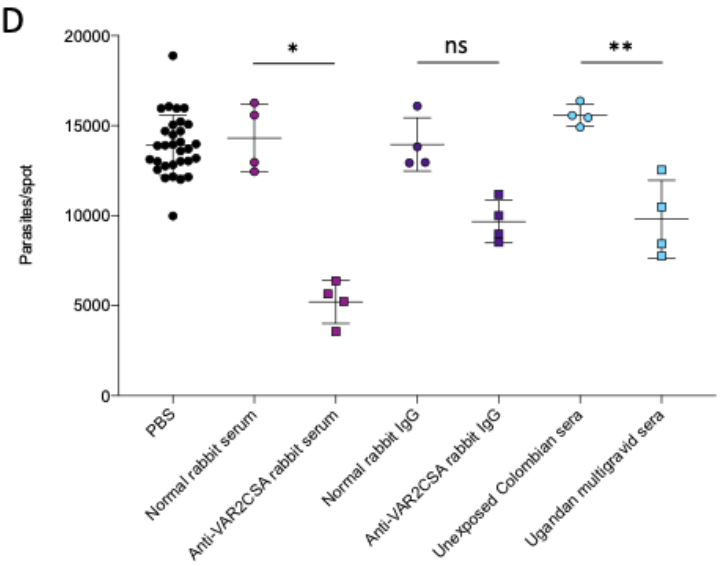

NF54-CSA

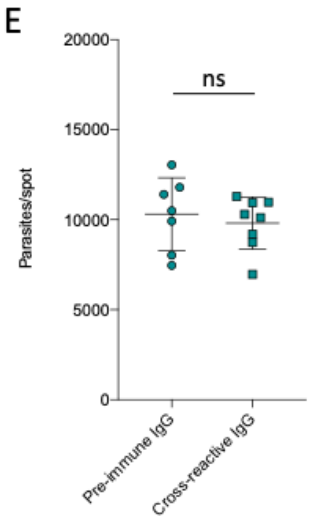

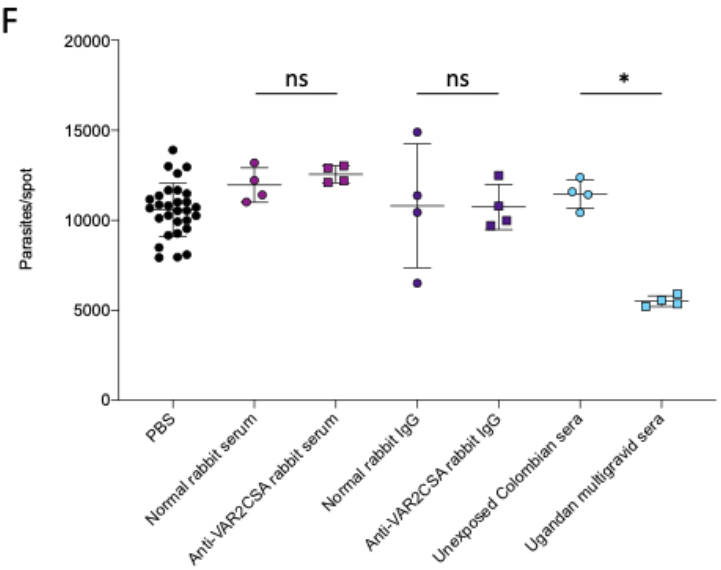

Figure 4.12. Cross-reactive IgG did not block parasite adhesion to CSA in vitro. Cross reactive IgG (teal squares) were incubated with RBCs infected with three different strains of *P. falciparum*: a placental isolate (A), CS2 (C) and NF54-CSA (E). Total IgG purified from pre-immune rabbit serum (teal circles) was used as a negative control and both IgG samples were used at 100 µg/mL. Assay controls were included with each of the parasite strains (B, D and F), including PBS alone (black circles), normal rabbit serum (light purple circles), anti-VAR2CSA rabbit serum (light purple squares), total IgG purified from normal rabbit serum (dark purple circles), total IgG from anti-VAR2CSA rabbit serum (dark purple squares), sera from unexposed Colombian individuals (blue circles) and sera from multigravid women from Uganda (blue squares). Sera samples were run at a 1/5 dilution and total IgG was run at 100 µg/mL. Data are the results of two experiments combined for each parasite strain and results are expressed as the number of parasites bound to each CSA-coated spot. In order to combine data from two separate experiments, the number of parasites bound to each spot was normalized using the mean number of parasites bound in the PBS condition in both experiments. Statistical significance was determined using a Kruskal-Wallis one-way ANOVA. Data are mean ± SD. *, $P < 0.05$; **, $P < 0.01$; ns, not significant.

To determine if the cross-reactive IgG could mediate phagocytosis, EtBr-stained iRBCs were incubated with the antibodies, then combined with human monocytes (THP-1 cells). Phagocytosis of iRBCs was quantified using flow cytometry by measuring the percentage of EtBr-positive monocytes (Figure 4.13). The percent phagocytosis in each sample was normalized to the positive control (anti-VAR2CSA rabbit serum) that was run in that experiment (Figure 4.13A). There was a small increase in phagocytosis with the cross-reactive IgG (20.4% ± 4.9% SD) compared to pre-immune IgG (15.3% ± 2.5% SD), but the difference was not statistically significant (Figure 4.13B).

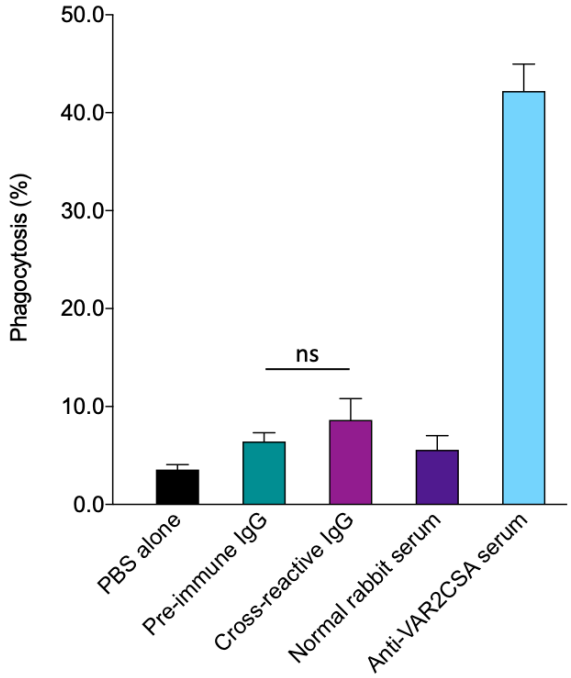

Figure 4.13. Cross-reactive IgG did not mediate opsonic phagocytosis of CS2 iRBCs. Incubation with the cross-reactive IgG did not significantly increase opsonic phagocytosis of CS2 iRBCs compared to pre-immune IgG. PBS alone and normal rabbit serum were included as negative controls, and anti-VAR2CSA rabbit serum was used as a positive control. Rabbit IgG was run at 150 µg/mL and serum samples were run at a 1/10 dilution. The data are from three independent opsonic phagocytosis experiments. Statistical significance was determined using a Kruskal-Wallis one-way ANOVA. Data are mean ± SD. ns, not significant.

4.4. Discussion

In this study, we used an epitope-focused vaccine to enhance the cross-reactivity that exists between DBPII and VAR2CSA. We designed a conformationally-constrained synthetic peptide that elicited an antibody response against not only its parent protein, DBPII, but also against a heterologous antigen, VAR2CSA. This immunogen was based on the recognition site of a monoclonal antibody that is cross-reactive against VAR2CSA (155). We initially mapped the minimal epitope to a 12 amino acid linear peptide within SD1. However, immunization with this peptide failed to elicit antibodies to DBPII and, not surprisingly, the antibodies did not cross-react with VAR2CSA. These results suggest that the linear N_{10}-C_{22} peptide is sufficient as an antigen for 3D10 recognition but is not a suitable immunogen to generate antibodies to the desired epitope in DBPII. It is also possible that immunization with this peptide elicited antibodies that recognized an unnatural epitope formed by the synthetic peptide that is not present in DBPII. Consistent with our results, others reported that 3D10 recognized a peptide from the same region of DBPII that overlapped with N_{10}-C_{22} by seven amino acids (260). However, this peptide also failed to elicit anti-DBPII antibodies.

The results of our peptide library screen expanded the minimal epitope to encompass three distinct segments of SD1 that are discontinuous yet constrained in the native protein by two disulfide bonds. To recapitulate this epitope, we designed the $SD1_{CLIPS}$ peptide that contains all regions of the discontinuous epitope and replaced one of the disulfide bonds with a synthetic scaffold. This allowed for control over bond formation in the peptide, constraining the bonding pattern to the structure in the parent protein. With this approach, we succeeded in generating the discontinuous epitope as it was in DBPII, overcoming a common challenge in peptide vaccine development.

While all mice immunized with SD1$_{CLIPS}$-KLH had high endpoint titers against the immunogen (<1/2.0 million), only three out of five mice made cross-reactive antibodies that recognized VAR2CSA. To better understand this, we evaluated the immune responses of the five mice to peptides from different regions of SD1 and found that no two mice had the same recognition profile. Certain peptides were recognized very strongly (endpoint titers <1/1.0 million) by sera from some mice but not others, revealing significant variation in the fine specificity of immune responses among the five mice. However, there was no discernable difference in the recognition patterns of the SD1 peptides between the sera samples that cross-reacted with VAR2CSA and those that did not.

In both the mice and the rabbit, the cross-reactive antibodies had low avidity for VAR2CSA. These experiments highlight a common feature of cross-reactive antibodies that lower avidity antibodies may be multispecific for similar but not identical epitopes in different antigens (293). There is evidence that people living in areas of high malaria transmission intensity develop lower avidity antibodies to some *P. falciparum* antigens, compared to those living in areas of low transmission intensity who develop relatively low titers of higher avidity antibodies (294, 295). This has been attributed to increased exposure to a highly diverse population of parasites in high transmission settings (294, 296) and/or impaired affinity maturation as a result of infection (297-299). Alternatively, lower avidity antibodies may reflect an adaptive advantage that allows the immune system to respond to antigens from different *P. falciparum* strains, as has been suggested for other pathogens (300). However, several studies demonstrated that higher avidity antibodies against blood stage *P. falciparum* antigens provided greater protection from severe (301) or clinical malaria (302). Importantly, in a retrospective case-control study and a longitudinal study in Cameroon, higher avidity anti-VAR2CSA antibodies were associated with protection from

malaria in pregnancy (145, 303). Thus, it is essential to explore ways to increase the avidity of these cross-reactive antibodies against VAR2CSA. Indeed, the low-avidity 3D10 antibody can block parasite binding to chondroitin sulfate A (CSA), but only when used at a high concentration (100 μg/mL) that is unlikely to be elicited through immunization (155).

In order to have a sufficiently high concentration of cross-reactive rabbit antibodies to evaluate in functional assays, we affinity-purified the cross-reactive IgG using full-length VAR2CSA. The cross-reactive antibodies that were purified strongly recognized the surface of RBCs infected with three different VAR2CSA-expressing *P. falciparum* strains. This result is very encouraging given the fact that 3D10 showed limited recognition of iRBCs by flow (7.2% - 9.1%), yet the cross-reactive IgG recognized a significant percentage of the population (68.1% - 95.6%) (Table 4.2). Additionally, the FCR3 allele of VAR2CSA was used to affinity-purify these antibodies, yet they displayed strain-transcending recognition of iRBCs, further indicating the presence of epitopes that are conserved across multiple alleles of VAR2CSA, which can be targeted by antibodies.

Despite strongly recognizing iRBCs by flow, the cross-reactive IgG did not block parasite adhesion to CSA *in vitro*. In contrast, 3D10 only recognized a small percentage of iRBCs yet blocked a significant number of the iRBCs from binding to CSA *in vitro*, albeit at a high concentration (Table 4.2). This suggests that the cross-reactive IgG and 3D10 antibodies recognize different epitopes in VAR2CSA. Consistent with this, there were significant differences between the cross-reactive IgG and 3D10 in the recognition of recombinant antigens (Table 4.2). Both antibodies recognized full-length VAR2CSA and DBPII by ELISA, but only the cross-reactive IgG recognized EBP2. Although homologous to PvDBP, EBP2 is not recognized by 3D10, likely because of the sequence variation between the SD1 domains of PvDBP and EBP2 (232). These

results highlight a key difference between these antibodies and suggests that the specificity of the cross-reactive antibodies elicited by SD1$_{CLIPS}$-BSA immunizations in the rabbit differs from that of 3D10.

Table 4.2. Summary of 3D10 and rabbit cross-reactive IgG data

Measure	**3D10**	**Cross-reactive IgG**
Recombinant protein recognition		
DBPII endpoint (μg/mL)	0.00043	1.25
EBP2 endpoint (μg/mL)	NR	1.25
VAR2CSA endpoint (μg/mL)	0.86	0.02
iRBC recognition		
Recognition of live CS2 iRBC (% positive)	9.1	68.1
Recognition of live NF54-CSA iRBC (% positive)	7.2	76.8
Recognition of live placental isolate iRBC (% positive)	7.8	95.6
Functionality		
Inhibition of iRBC binding to CSA (% inhibition ± SEM)*	18.1 ± 3.0	ND
Opsonic phagocytosis (% phagocytosis ± SD)*	ND	2.2 ± 1.4†

*Measured relative to negative control
†Not statistically significant
NR = no recognition
ND = not detected
SEM = standard error of the mean
SD = standard deviation

The most likely explanation for the lack of binding inhibition observed with the cross-reactive IgG is that these antibodies recognized cross-reactive, but non-inhibitory epitopes in VAR2CSA. The cross-reactive IgG likely bound to epitopes on VAR2CSA that are spatially distinct from those recognized by 3D10, which is able to block iRBC binding to CSA. It is possible that one of the inhibitory epitopes that 3D10 recognizes is in the DBL2X domain, which has been

defined as the minimal CSA binding domain (220, 304). In fact, 3D10 recognized recombinant ID1-DBL2X-ID2a more strongly than any other DBL domain (Figure 4.8C). However, the anti-SD1$_{CLIPS}$-BSA rabbit serum recognized this domain at a lower OD than any of the other domains that were tested (Figure 4.8B and C). It is important to note that the ODs for any given antigen cannot be directly compared between 3D10 and the anti-SD1$_{CLIPS}$-BSA rabbit serum. However, the relative recognition of the different DBL domains by each antibody or serum sample can shed light on the specificity of the antibodies.

A recently published cryo-electron microscopy structure of VAR2CSA (DBL1X-DBL4ε) bound to CSA provided crucial insight into the spatial relationships between the DBL domains within the full protein (304). The structure highlights the critical contributions that DBL1X and DBL2X make to the major CSA binding channel. As discussed previously, immunizations with the PAMVAC vaccine candidate, which is based on the DBL2X domain, led to high levels of inhibitory antibodies against homologous parasites, but failed to elicit antibodies with strain-transcending blocking activity *in vitro* (186, 192). Although refinement of this vaccine candidate is needed before it can progress in clinical trials, these data underscore the ability of antibodies targeting DBL2X to block parasite binding to CSA *in vitro*.

Publication of the structure of the CSA binding core of VAR2CSA also enabled the preliminary identification of structurally conserved SD1-like domains within the different DBL domains (Figure 4.14A). Interestingly, several residues in the SD1-like domain of DBL2X, which is structurally similar to the SD1 domain of PvDBP, are directly involved in binding to CSA (yellow residues in Figure 4.15B) (304). Although this needs to be confirmed experimentally, it seems plausible that 3D10 may block parasite binding to CSA by targeting this epitope. Furthermore, the fact that the non-inhibitory cross-reactive rabbit IgG does not recognize DBL2X

very strongly by ELISA could account for the lack of function observed with these antibodies. Based on the differences in recognition of the DBL2X domain between the cross-reactive IgG and 3D10, it may be useful to investigate a possible correlation between recognition of this domain with antibody blocking activity.

It is also possible that a subset of the cross-reactive IgG recognizes the same epitopes in VAR2CSA as 3D10, but the titre and/or avidity of these antibodies is too low to block binding in the IBA. Unlike 3D10, the cross-reactive IgG are polyclonal antibodies that could be recognizing many different epitopes within the VAR2CSA protein. Competition ELISAs were attempted to determine if the cross-reactive IgG could block VAR2CSA recognition by 3D10, but there was significant competition by the pre-immune IgG that could not be explained or prevented. These ELISAs are in the process of being optimized.

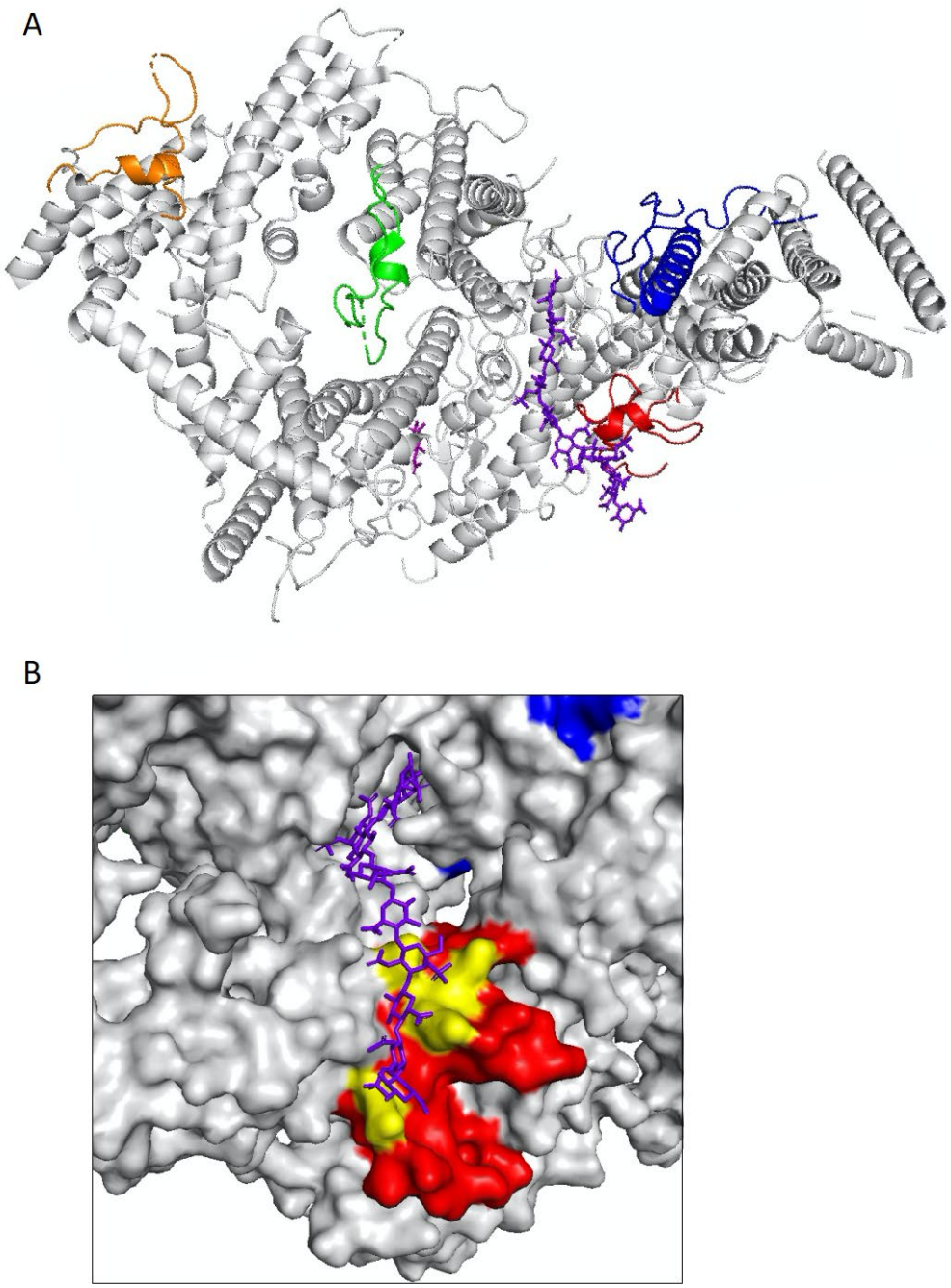

Figure 4.14. Cryo-electron microscopy structure of the CSA binding core of VAR2CSA. (A) The structure of the CSA binding core of VAR2CSA in complex with CSA (shown as dark purple lines in the major binding groove and light purple in the minor binding groove) was determined using cryo-electron microscopy in (304) (PDB accession no. 7JGH). Preliminary analysis of structural similarities between PvDBP and VAR2CSA revealed SD1-like domains in DBL1X (blue), DBL2X (red), DBL3X (orange) and DBL4ε (green) domains of VAR2CSA. (B) Four amino acids (N557, K561, K562 and N576, shown in yellow) in the SD1-like domain of DBL2X were shown to directly interact with the CSA moiety in the binding groove (304). Figures were generated in PyMol.

Anti-VAR2CSA antibodies are also purported to be protective by mediating opsonic phagocytosis of iRBCs (305, 306). Thus, we tested the ability of the cross-reactive IgG to mediate opsonic phagocytosis of iRBCs using a human monocyte cell line. However, consistent with experiments using 3D10, the cross-reactive IgG did not mediate phagocytosis of the CS2-iRBCs *in vitro*. We have not yet characterized the subclasses of the cross-reactive IgG but evaluating this could be informative for functional analysis of these antibodies. It may be the case that the antibodies target potentially functional epitopes on VAR2CSA, but that the Fc domain of the antibodies are unable to mediate phagocytosis. Additional antibody-mediated functions correlate with clinical protection and these need to be investigated with both the cross-reactive IgG and 3D10. These functions include antibody-mediated iRBC lysis by natural killer (NK) cells (307, 308) and antibody-mediated phagocytosis by neutrophils (reviewed in (309)).

In order to further develop this immunogen as a vaccine candidate, it is crucial to increase not only the avidity of the antibodies for VAR2CSA, but also the titers. This will hopefully increase the functional activity of these cross-reactive antibodies, since a high concentration of anti-VAR2CSA antibodies is required to block parasite adhesion to CSA *in vitro* (155, 233, 275, 310). We will use different methods to increase both the titer and avidity of the cross-reactive antibodies. For instance, we will employ different boosting schedules and/or adjuvant strategies that have been shown to increase the avidity of antibody responses against the sexual stage malaria antigen, Pfs25, and an HIV vaccine candidate (311, 312). We will also further investigate the epitopes in VAR2CSA that are targeted by these cross-reactive antibodies to inform optimal vaccine design.

4.5. Conclusions

Ultimately, our goal is to exploit the cross-reactive epitope in PvDBP that generates antibodies to shared epitopes in VAR2CSA. The structural peptide reported here provides a template for the

synthesis of a discontinuous conformational epitope from PvDBP that elicits cross-reactive antibodies to VAR2CSA. With further optimization to enhance immunogenicity and avidity, this peptide could be developed as a new vaccine candidate against placental malaria.

Chapter 5: Strategies to stimulate cross-reactive antibody responses in mice

5.1 Introduction

We previously demonstrated that a conformationally-constrained synthetic peptide based on a domain of PvDBP, called SD1$_{CLIPS}$, elicited cross-reactive antibodies that recognized native VAR2CSA. However, titres of the cross-reactive antibodies were low, and they were not consistently elicited in mice. Furthermore, following affinity-purification on VAR2CSA, the cross-reactive antibodies were unable to mediate opsonic phagocytosis or block iRBC binding to CSA *in vitro*. These results preclude SD1$_{CLIPS}$ from being a viable vaccine candidate in its current form. Here, we attempted to increase the cross-reactive antibody response by using different adjuvants and selectively boosting the antibodies that recognize the conserved epitope(s) using a heterologous prime/boost strategy.

Previous SD1$_{CLIPS}$ immunizations in both mice and rabbits were adjuvanted with Complete Freund's Adjuvant (CFA) for the primary immunization and Incomplete Freund's Adjuvant (IFA) for the subsequent boosts. However, as discussed previously, the cross-reactive antibody responses to these immunizations were inadequate. In an effort to improve these cross-reactive immune responses, we tested two additional adjuvants containing glucopyranosyl lipid adjuvant (GLA), both of which are approved for use in humans.

GLA is a potent synthetic TLR4 agonist and formulation as a stable oil-in-water emulsion (GLA-SE) enhances the immune response by prolonging antigen release (313-316). This adjuvant has recently been used in a number of clinical trials and has consistently elicited strong immune responses. In a recent phase 1 trial of a PvDBP-based vaccine candidate, adjuvantation with GLA-SE induced a robust, balanced Th1/Th2 immune response (317). Humoral responses to the immunizations were dominated by IgG1 antibodies and sera from vaccinees were able to block

PvDBP binding to DARC *in vitro*, in a strain-transcending manner. GLA-SE has also yielded promising results in a phase 1a/1b clinical trial of the P27A vaccine candidate (a peptide derived from the *P. falciparum* trophozoite exported protein 1 (PfTEX1)) (318). In pre-clinical studies of other blood stage antigens, such as *P. falciparum* merozoite surface protein 1 and 3 (PfMSP-1_{19}/PfMSP-3_{11}), PfMSP2, and the *P. falciparum* glutamate rich protein (PfGLURP), genetically conjugated to PfMSP3, formulation in GLA-SE resulted in enhanced immune responses compared to a number of other adjuvants (Reviewed in (319)). Similar findings were reported in studies of sexual stage vaccine candidates that were adjuvanted with GLA-SE (Reviewed in (319)). For example, in the evaluation of Pfs25, GLA-SE resulted in anti-Pfs25 IgG responses that were of higher titre and avidity compared to either aluminum hydroxide or aluminum hydroxide-GLA (320). Importantly, the antibodies generated through vaccination with Pfs25/GLA-SE also had higher transmission reducing activity in a standard membrane feeding assay, compared to those generated with the other adjuvants.

The other GLA containing adjuvant that we evaluated was GLA-LSQ, which is a liposomal formulation containing the saponin QS-21. Its' immunostimulatory effects are similar to GLA-SE, except that the addition of QS-21 acts as a NLR family pyrin domain containing 3 (NLRP3) inflammasome activator (321). The liposomal formulation also enhances the activation of antigen presenting cells (APCs) and better facilitates the formation of an antigen-releasing depot (322). In pre-clinical studies of a vaccine candidate based on the *P. falciparum* Cell-Traversal Protein for Ookinetes and Sporozoites (PfCelTOS), mice immunized using GLA-LSQ had lower parasite burdens in the liver following a *P. berghei* challenge, compared to mice that received GLA-SE (323). Additionally, adjuvantation of a Pfs25 vaccine candidate with GLA-LSQ resulted in higher antibody titres with a longer half-life compared to either Alhydrogel or CpG-SE (324).

Importantly for our work, immune responses to the VAR2CSA vaccine candidate, PAMVAC, adjuvanted with either GLA-LSQ or GLA-SE, were recently compared in a first-in-human phase 1a/1b trial (186). Sera from vaccinees that had received immunizations in GLA-SE had a higher anti-VAR2CSA IgG endpoint titre and higher blocking activity in the IBA, compared to sera from those immunized with GLA-LSQ. Interestingly, this is the opposite of what the authors reported in mice, where immunizations with GLA-LSQ resulted in antibodies with higher blocking activity than with GLA-SE. GLA-SE was also used in pre-clinical and clinical evaluation of the other leading VAR2CSA vaccine candidate, PRIMVAC. In rats, there was no significant difference between the immune responses elicited by PRIMVAC in GLA-SE or Alhydrogel (190). However, in clinical evaluation of this candidate, the authors reported higher anti-VAR2CSA antibody responses with GLA-SE compared to Alhydrogel (187). Furthermore, T cells isolated from individuals immunized with PRIMVAC in GLA-SE produced higher levels of IL2 and IL5.

Based on the promising findings in both pre-clinical and clinical evaluation of vaccine candidates using these adjuvants, we hypothesized that adjuvanting SD1$_{CLIPS}$-KLH with GLA-SE or GLA-LSQ may improve the cross-reactive antibody response compared to CFA/IFA.

Another approach that we took to increase the titre and functional activity of the cross-reactive antibodies was a heterologous prime/boost immunization schedule. By priming the immune system with SD1$_{CLIPS}$-KLH and boosting with VAR2CSA, we expected to specifically boost the antibodies targeting the anticipated cross-reactive epitopes. In theory, immunizations with SD1$_{CLIPS}$ would expand B cells that cross-react with conserved epitopes in VAR2CSA. Then when these epitopes are encountered in the heterologous VAR2CSA boost, these B cells could respond more quickly, resulting in a faster cross-reactive antibody response. It is important to note that we expected all mice to start making anti-VAR2CSA antibodies seven days following a boost

with this protein, regardless of their previous immunizations. However, we predicted that mice that had been immunized with SD1$_{CLIPS}$-KLH would generate an earlier anti-VAR2CSA antibody response compared to those that had been immunized with KLH (as the control). We also expected sera from the SD1$_{CLIPS}$-KLH immunized mice to have higher anti-VAR2CSA antibody titres and show increased recognition of native VAR2CSA, compared to mice that received KLH alone.

To test this, we gave mice two initial boosts with SD1$_{CLIPS}$-KLH or KLH alone, followed by recombinant VAR2CSA. Following the heterologous boost, we measured the titre of the cross-reactive antibodies, the timing at which the cross-reactive immune response was generated and the ability of the cross-reactive antibodies to recognize different alleles of VAR2CSA on the surface of iRBCs. To the best of my knowledge, there are no reports of a vaccine strategy using two distinct antigens to enhance an antibody response against a conserved epitope in the literature. However, an opinion piece was published that recommended taking this approach to dengue vaccine development (325). The authors argue that combining the two leading vaccine candidates using a heterologous prime/boost schedule would result in a broader and more effective immune response, which would help protect against all dengue serotypes. However, the goal in combining these vaccines is to elicit antibody responses against each of the different immunogens, rather than a shared conserved epitope, which is our objective.

Recently, there have been reports of an alternative heterologous prime/boost strategy in which the same immunogen is delivered using different vectors for the prime and boosts. For instance, a recent study using heterologous prime/boosts combining several different SARS-CoV-2 vaccine candidates gave promising results in mice (326). The authors tested sequential immunizations with different combinations of adenovirus-vectored, mRNA, recombinant subunit or inactivated virus vaccines. All of these candidates delivered a Spike protein-based immunogen

using different vectors, except the inactivated virus vaccine, which contained inactivated SARS-CoV-2 purified from Vero cells. Interestingly, sera from animals that had been immunized using the heterologous prime/boost approach had increased levels of neutralizing antibodies compared to a homologous prime/boost schedule (326). Similarly, heterologous prime/boost schedules were reported to improve immune responses to influenza (327), Ebola virus (328), cytomegalovirus (329) and HIV vaccine candidates (Reviewed in (330)). There is also a personalized cancer vaccine candidate in on-going phase I/II trials that uses an adenovirus vector for the priming immunization followed by a self-replicating RNA vector for the boost (ClinicalTrials.gov Identifier: NCT03639714). Although these vaccine strategies differ from our approach of using two unique immunogens, they are similar in that the use of different vectors likely results in diverse epitopes being presented to the immune system.

We also determined if exposure to VAR2CSA on the surface of iRBCs could boost or skew the cross-reactive antibody response following immunizations with SD1$_{CLIPS}$-KLH. Other than humanized mice, there are no small animals that can sustain a blood-stage *P. falciparum* infection. In our experiments, mice were essentially immunized with iRBCs expressing VAR2CSA, as the parasites were not able to establish an infection. Similar to the heterologous boost with recombinant VAR2CSA, we hypothesized that the cross-reactive antibody response elicited in mice immunized with SD1$_{CLIPS}$-KLH would be boosted and broadened following exposure to native VAR2CSA.

5.2 Methods

5.2.1 Animal Immunizations

For the SD1$_{CLIPS}$-KLH immunizations in Freund's adjuvant, five female BALB/c mice (6 to 8 weeks old) were immunized subcutaneously with SD1$_{CLIPS}$-KLH or KLH alone (30 µg/mouse) emulsified in Complete Freund's Adjuvant (CFA) (catalogue no. F5881; Sigma, Oakville, Canada) on day 1 (Table 5.1). On days 21, 31 and 45, mice were boosted with the immunogen (10 µg/mouse on days 21 and 31 and 5 µg/mouse on day 45) emulsified in Incomplete Freund's Adjuvant (IFA) (catalogue no. F5506; Sigma, Oakville, Canada). For the SD1$_{CLIPS}$-KLH immunizations in GLA-SE, five female BALB/c mice (6 to 8 weeks old) were immunized subcutaneously with SD1$_{CLIPS}$-KLH or KLH alone (30 µg/mouse on day 1, 10 µg/mouse on days 21 and 31 and 5 µg/mouse on day 45) in GLA-SE (5 µg/mouse GLA, 2% oil) (IDRI, Seattle, US) on days 1, 21, 31 and 45 of the experiment. For the SD1$_{CLIPS}$-KLH immunizations in GLA-LSQ, five female BALB/c mice (6 to 8 weeks old) were immunized subcutaneously with SD1$_{CLIPS}$-KLH or KLH alone (30 µg/mouse on day 1, 10 µg/mouse on days 21 and 31 and 5 µg/mouse on day 45) in GLA-LSQ (5 µg/mouse GLA and 2 µg/mouse QS21) (IDRI, Seattle, US) on days 1, 21, 31 and 45 of the experiment. The final sera samples from mice in all the groups were collected on day 59 via cardiac puncture.

For the heterologous prime/boost experiment, the immunogens were prepared as above for the SD1$_{CLIPS}$-KLH immunizations in GLA-SE. Immunizations to generate control sera using ID1-ID2a (kindly provided by Dr. Ali Salanti), VAR2CSA (kindly provided by Dr. Ali Salanti) or KLH were also prepared in GLA-SE. Mice were given immunizations on day 1 (30 µg/mouse for KLH and ID1-ID2a, 5 µg/mouse for VAR2CSA) and on days 21 and 31 (10 µg/mouse for KLH and ID1-ID2a, 3 µg/mouse for VAR2CSA). Female BALB/c mice (6 to 8 weeks old) were used in all of these immunizations and the details are listed in Table 5.1.

All procedures were approved by the University of Alberta Animal Care and Use Committee (approval number: AUP00002124), and mice were handled in accordance with the Canadian Council on Animal Care Guidelines.

Table 5.1. Heterologous prime/boost animal immunizations

		Day 1		Day 21		Day 31	
Group	**Mice, N**	**Immunogen**	**Dose* (g)**	**Immunogen**	**Dose* (g)**	**Immunogen**	**Dose* (g)**
$SD1_{CLIPS}$-KLH	7	$SD1_{CLIPS}$-KLH	30	$SD1_{CLIPS}$-KLH	10	$SD1_{CLIPS}$-KLH	10
$SD1_{CLIPS}$-KLH + VAR2CSA	7	$SD1_{CLIPS}$-KLH	30	$SD1_{CLIPS}$-KLH	10	VAR2CSA	3
KLH + VAR2CSA	7	KLH	30	KLH	10	VAR2CSA	3
ID1-ID2a	5	ID1-ID2a	30	ID1-ID2a	10	ID1-ID2a	10
VAR2CSA	5	VAR2CSA	5	VAR2CSA	3	VAR2CSA	3
KLH	4	KLH	30	KLH	10	KLH	10

*Dose of immunogen injected per mouse

5.2.2 ELISAs

ELISAs were carried out as described in section 4.2.3.

5.2.3 Flow cytometry

Flow cytometry experiments were carried out as described in section 2.2.9. Mouse sera were incubated with iRBC (0.5×10^6 cells/mL) at a 1/5 dilution, unless otherwise stated. Reactivity to the surface of the iRBCs was detected using Alexa Fluor 647 conjugated goat anti-mouse IgG (dilution 1/500, catalogue no. A21237, Life Technologies). The median fluorescent intensity (MFI) was calculated separately for the iRBC and uRBC populations in each sample and the MFI

of the uRBCs was subtracted from the MFI of the iRBCs. This subtraction was done to correct for the non-specific antibody binding to the surface of the RBCs that was observed in some samples.

5.2.3 Statistical analysis

Data were plotted and statistical significance was determined using a Kruskal-Wallis one-way ANOVA using Prism software (version 8; GraphPad, San Diego, CA, USA).

5.3 Results

5.3.1 Immunizations with SD1$_{CLIPS}$ in GLA-SE elicited a stronger cross-reactive antibody response than CFA/IFA or GLA-LSQ

We immunized mice with SD1$_{CLIPS}$-KLH or KLH alone in two different adjuvants in an attempt to increase the titre of cross-reactive antibodies elicited by these immunizations. Mice were immunized four times with SD1$_{CLIPS}$-KLH or KLH in CFA/IFA, GLA-SE or GLA-LSQ. Immunizations in all three of these adjuvants elicited a strong antibody response against the SD1$_{CLIPS}$ peptide (Figure 5.1A); however, there was significant background recognition of SD1$_{CLIPS}$ by sera from mice immunized with KLH in GLA-LSQ. This strange background recognition was also observed when the sera were tested against VAR2CSA by ELISA (Figure 5.1B), but the source of the background is unknown. SD1$_{CLIPS}$-KLH immunizations in GLA-SE elicited cross-reactive antibodies that recognized VAR2CSA in 3 out of 5 mice, compared to 1 out of 5 mice in the CFA/IFA group (Figure 5.1B). The ODs of the cross-reactive antibodies were also higher in the GLA-SE group compared to the CFA/IFA group, although endpoint titres have not been determined for these samples. Based on these results, we chose to use GLA-SE for subsequent immunization experiments.

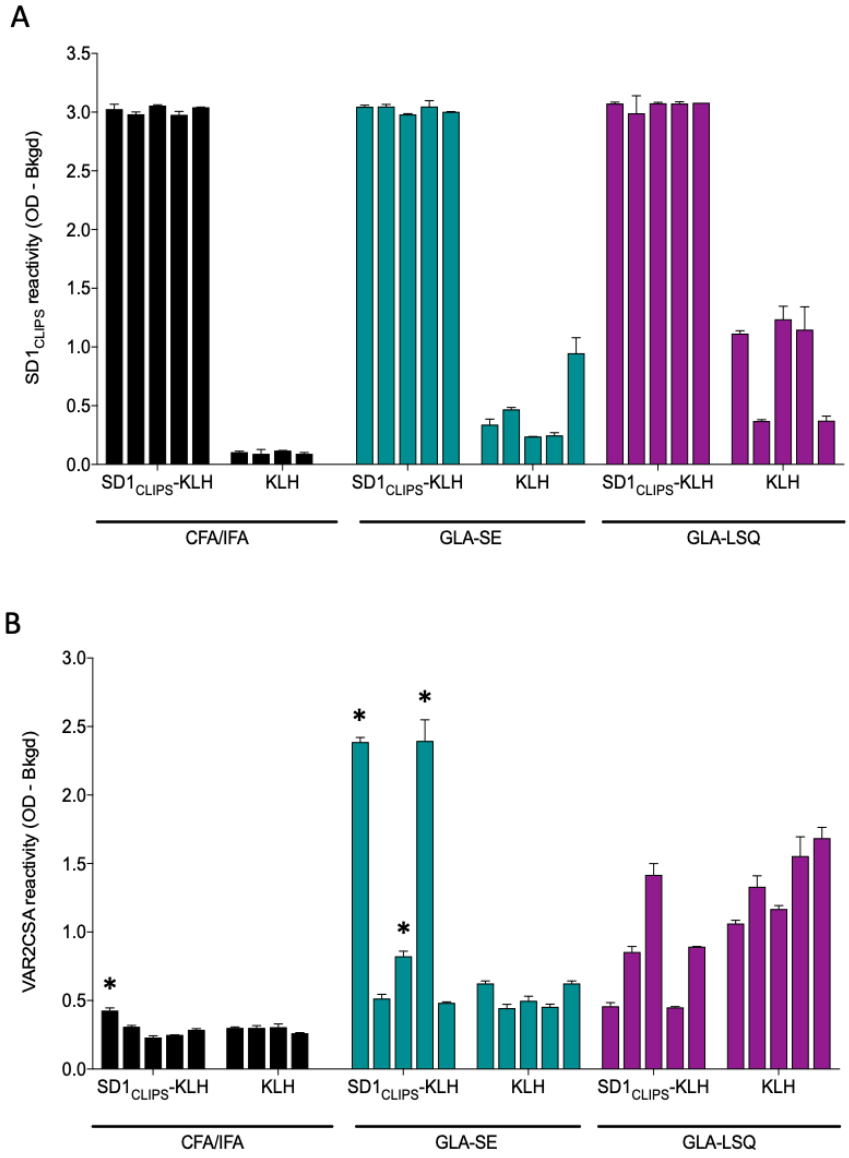

Figure 5.1. SD1$_{CLIPS}$-KLH immunizations with GLA-SE resulted in higher titres of cross-reactive antibodies compared to immunizations in CFA/IFA or GLA-LSQ. Sera from mice immunized with SD1$_{CLIPS}$-KLH or KLH in the three different adjuvants were tested against SD1$_{CLIPS}$ (A) and VAR2CSA (B) by ELISA. Sera were tested at a 1/250 dilution against SD1$_{CLIPS}$ and a 1/500 dilution against VAR2CSA. * Indicates a seropositive sample. A cut-off for each adjuvant group was calculated as the mean OD of the carrier protein controls + 2(SD). Data are mean ± SD.

5.3.2. Heterologous prime/boost immunizations did not increase anti-VAR2CSA antibody responses in mice

Previous immunizations with SD1$_{CLIPS}$ yielded low titres of cross-reactive antibodies. We hypothesized that by immunizing mice with SD1$_{CLIPS}$-KLH followed by recombinant VAR2CSA, we could specifically boost the cross-reactive antibodies. To test this hypothesis, we gave mice (n = 7) two immunizations with SD1$_{CLIPS}$-KLH, followed by an immunization with recombinant VAR2CSA, all formulated in GLA-SE. Two groups of mice (n = 7 in each group) were included as controls: one group was given three immunizations with SD1$_{CLIPS}$-KLH and another group was given two immunizations with KLH, followed by one immunization with VAR2CSA (Figure 5.2).

Sera from 6 out of the 7 mice that received three immunizations with SD1$_{CLIPS}$-KLH recognized SD1$_{CLIPS}$ very strongly by ELISA (endpoint titres: 1/10,240,000), while one mouse made lower levels of anti-SD1$_{CLIPS}$ antibodies (endpoint titre: 1/160,000) (Figure 5.3A). The mice that received two SD1$_{CLIPS}$-KLH immunizations followed by an immunization with VAR2CSA also generated very strong anti-SD1$_{CLIPS}$ antibody responses (endpoint titres ranged from 1/640,000 to 1/10,240,000). When we evaluated sera from these mice against VAR2CSA, we found that a final heterologous boost with VAR2CSA increased the anti-VAR2CSA antibody response in the mice relative to the group that received three immunizations of SD1$_{CLIPS}$-KLH (Figure 5.3B). In fact, only 2 of the 7 mice in the SD1$_{CLIPS}$-KLH group made cross-reactive antibodies that recognized VAR2CSA (endpoint titre: 1/1,500) whereas sera from all mice in both groups that received the heterologous VAR2CSA boost made antibodies that recognized VAR2CSA. When we compared the anti-VAR2CSA endpoint titres between these groups of mice, only mice that received KLH followed by VAR2CSA had significantly higher endpoint titres compared to sera from mice in the SD1$_{CLIPS}$-KLH alone group (Figure 5.3B). There was no statistically significant increase in anti-VAR2CSA endpoint titres between mice in the SD1$_{CLIPS}$-

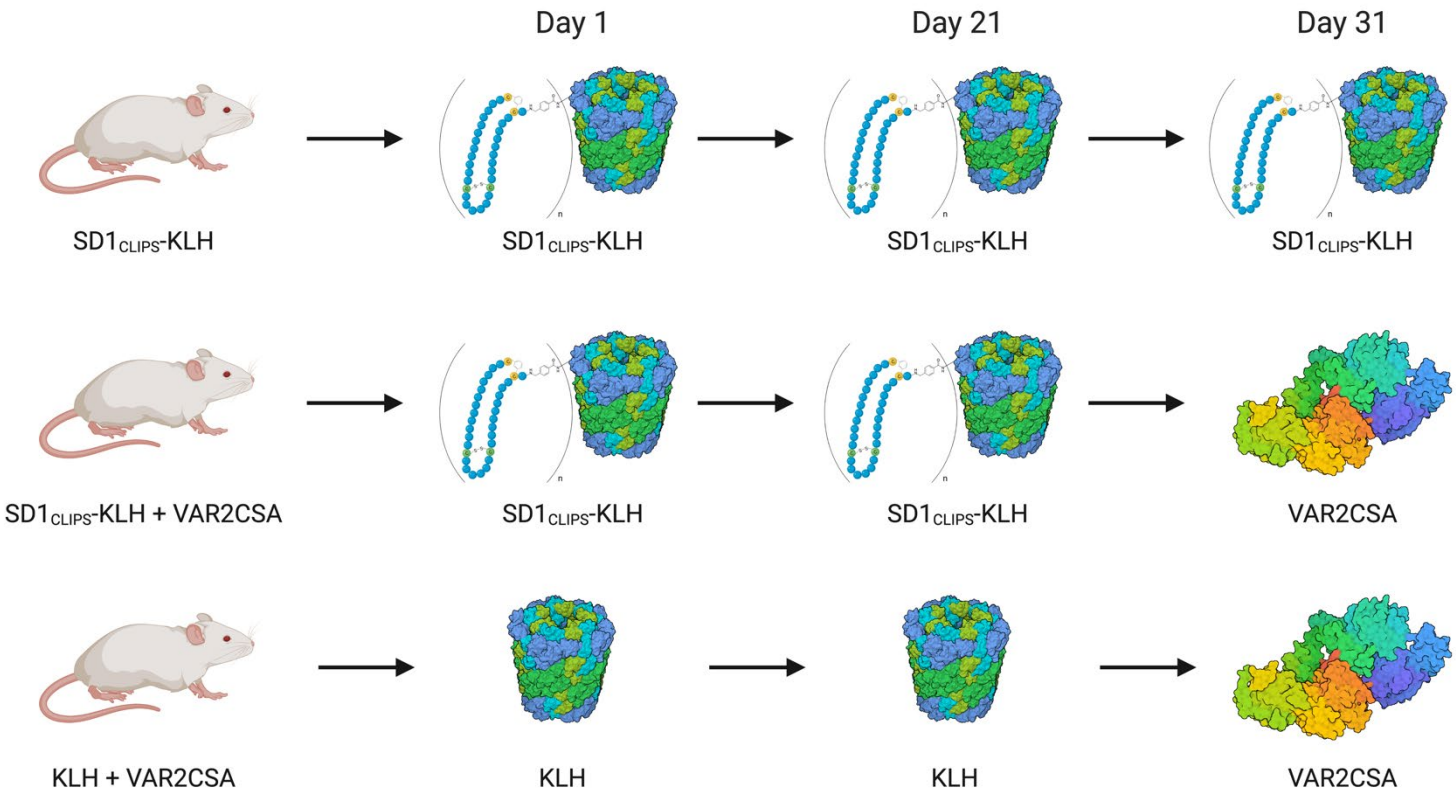

Figure 5.2. A heterologous prime/boost experiment using SD1$_{CLIPS}$-KLH and VAR2CSA was designed to enhance the cross-reactive antibody response. Female BALB/c mice (n= 7 per group) were immunized three times with immunogens formulated in GLA-SE. On days 1 and 21, mice were given either SD1$_{CLIPS}$-KLH or KLH (30 µg/mouse on day 1, 10 µg/mouse on day 21) and on day 31, mice were given either SD1$_{CLIPS}$-KLH (10 µg/mouse) or VAR2CSA (3 µg/mouse).

KLH + VAR2CSA group compared to mice in either the SD1$_{CLIPS}$-KLH alone or KLH + VAR2CSA groups. Although the difference between the SD1$_{CLIPS}$-KLH + VAR2CSA and the SD1$_{CLIPS}$-KLH alone group approached significance (p-value: 0.066).

To determine if the SD1$_{CLIPS}$-KLH immunizations primed the immune system to respond more rapidly to VAR2CSA, we collected sera 4 days (day 35 of the experiment) and 7 days (day 38 of the experiment) after the heterologous VAR2CSA boost. There was no difference in VAR2CSA recognition by sera from the SD1$_{CLIPS}$-KLH + VAR2CSA group of mice on day 35 compared to sera from the KLH + VAR2CSA group (Figure 5.3C). Surprisingly, on day 38, sera from 6 of the 7 mice in the KLH + VAR2CSA group recognized VAR2CSA, compared to only 4 of the 7 mice in the SD1$_{CLIPS}$-KLH + VAR2CSA group. These results suggest that the initial SD1$_{CLIPS}$-KLH immunizations did not prime the immune systems of the mice to target the conserved epitopes in VAR2CSA.

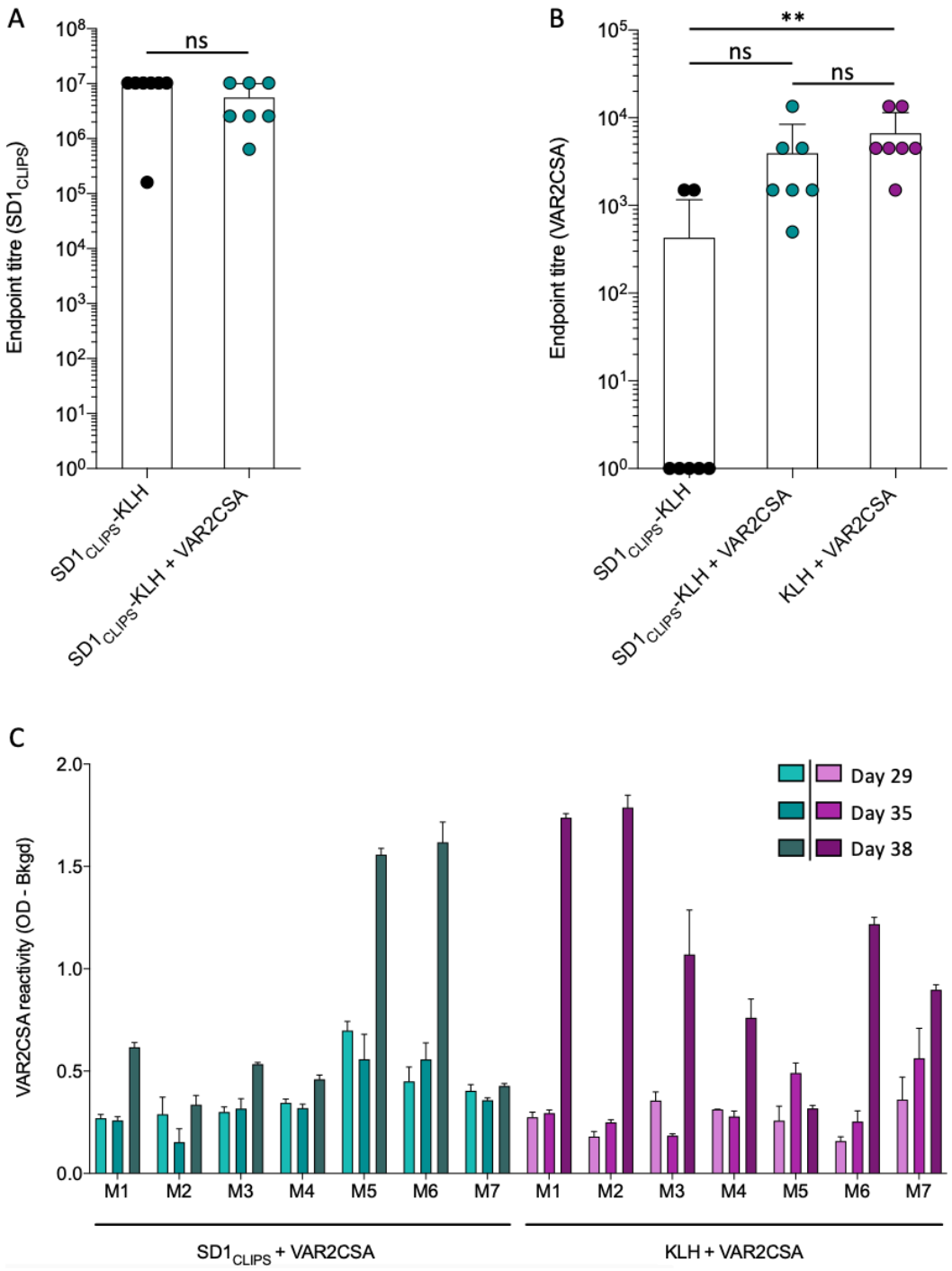

Figure 5.3. A heterologous boost with VAR2CSA following immunizations with SD1$_{CLIPS}$-KLH did not result in an increased cross-reactive antibody response. (A) Endpoint titres against the SD1$_{CLIPS}$ peptide were determined in both groups of mice that received SD1$_{CLIPS}$-KLH immunizations in GLA-SE. (B) VAR2CSA endpoint titres were measured in the three groups of mice. The cut-offs for the endpoint titres were defined as the mean OD-background plus 2 standard deviations of a pool of pre-immune sera from the appropriate group. (C) Sera samples from mice

in the SD1$_{CLIPS}$-KLH and KLH + VAR2CSA groups before (day 29, light teal and purple bars), 4 days after (day 35, teal and purple bars) and 7 days after (day 38, dark teal and purple bars) the heterologous boost were tested against VAR2CSA by ELISA. All sera samples were tested at a dilution of 1/250. Statistical significance was determined in (A) using a Kruskal-Wallis one-way ANOVA and in (B) using a Mann-Whitney test. Data are mean ± SD. **, $P < 0.01$; ns, not significant.

5.3.3 Sera from mice that received heterologous prime/boost immunizations did not recognize native VAR2CSA

To determine if $SD1_{CLIPS}$-KLH immunizations followed by a heterologous VAR2CSA boost directed the immune response against a conserved epitope in VAR2CSA, we tested the sera from these mice against two strains of *P. falciparum* parasites (Figure 5.4). Sera from mice in each of the cross-boosting groups outlined in Figure 5.1, as well as sera from mice that were immunized with the ID1-ID2a domain of VAR2CSA (PAMVAC vaccine candidate, FCR3 allele), full-length VAR2CSA (FCR3 allele) and KLH were tested against the CS2 and NF54-CSA strains of *P. falciparum* by flow.

When we tested these sera by flow there were no significant differences in the recognition of iRBCs between sera from any of the experimental groups (Figure 5.4). Reactivity to the surface of iRBCs varied significantly between different sera samples in the same experimental group and between the same sera in different experiments. This high degree of variability made it challenging to interpret the results of these experiments. For example, in experiment 1 with the CS2 iRBCs, the MFI of the uRBCs was higher than the MFI of the iRBCs in many of the samples, resulting in many negative calculated MFI values. While in experiment 2, all of the calculated MFI values were above zero, with the exception of one sample. However, this variability was not observed in the positive control sera. A pool of sera from mice that were immunized with VAR2CSA reacted strongly to the surface of CS2-iRBC (MFI = 253.0 and 261.3 in experiments 1 and 2, respectively), as did a pool of sera from mice immunized with ID1-ID2a (MFI = 146.3 and 154.1 in experiments 1 and 2, respectively), compared to a pool of pre-immune sera (MFI = 77.0 in experiment 2). Interestingly, the positive control sera did not consistently recognize the surface of NF54-CSA iRBCs, which express a different allele of VAR2CSA from the one used for immunizations.

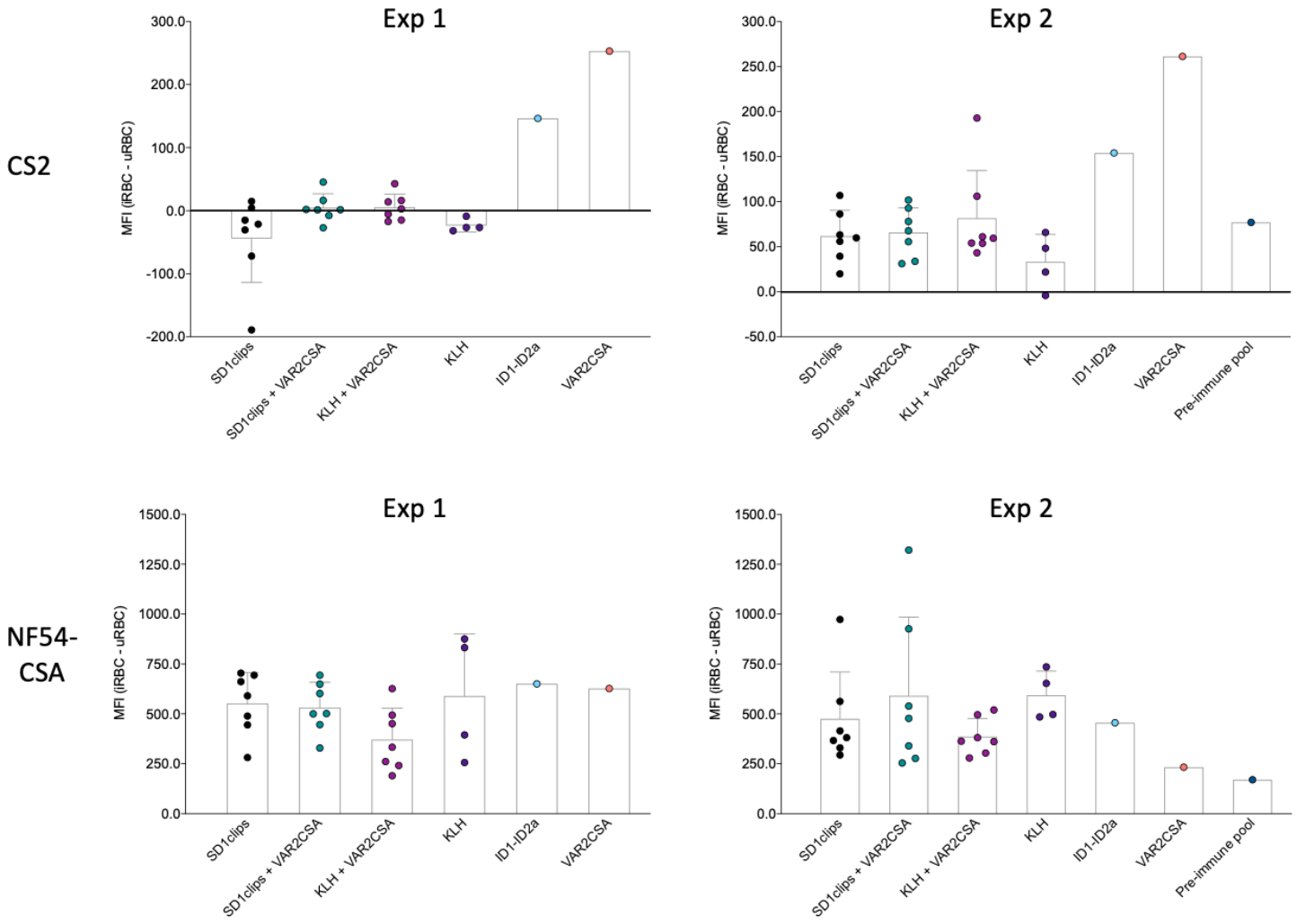

Figure 5.4. A heterologous VAR2CSA boost did not increase the cross-reactive antibody response in mice that had been immunized with SD1$_{CLIPS}$-KLH. Sera from individual mice were tested against mature CS2 and NF54-CSA *P. falciparum*-iRBC using flow cytometry in two independent experiments. Data are the MFI of the iRBC population minus the MFI of the uRBC population in each sample. Circles are data from individual serum samples and bars are mean ± SD. MFI, median fluorescent intensity.

5.3.4. Exposure to native VAR2CSA on the surface of iRBCs did not boost cross-reactive antibodies in mice

Sera were collected from mice immunized with SD1$_{CLIPS}$-KLH before (day 29), 7 days (day 38) and 14 days (Day 45) after an injection of VAR2CSA-expressing iRBCs. Although sera from mice in all groups showed increased recognition of VAR2CSA compared to pre-immune sera, the overall increase in the OD was quite small and was also observed in the KLH alone group (Figure 5.5). Importantly, there were no significant differences in VAR2CSA recognition between any of the groups.

Next, we tested sera from the individual mice in each group, 14 days following the injection of RBCs, against CS2 and NF54-CSA iRBCs by flow. The only statistically significant difference in the recognition of native VAR2CSA on the surface of iRBCs was observed between sera samples from mice immunized with SD1$_{CLIPS}$-KLH followed by uRBCs and mice immunized with KLH followed by NF54-CSA iRBCs (Figure 5.6A). Sera from mice that were immunized with SD1$_{CLIPS}$-KLH then uRBCs recognized NF54-CSA iRBCs more strongly than sera from mice immunized with KLH, followed by NF54-CSA iRBCs. The reason for this increased recognition is not known and its biological relevance is unclear. It is possible that antibodies against RBC membrane antigens were elicited in response to the injection with the uRBCs. However, if this was the case, we would expect to see equal recognition of the uRBC populations, which was not observed.

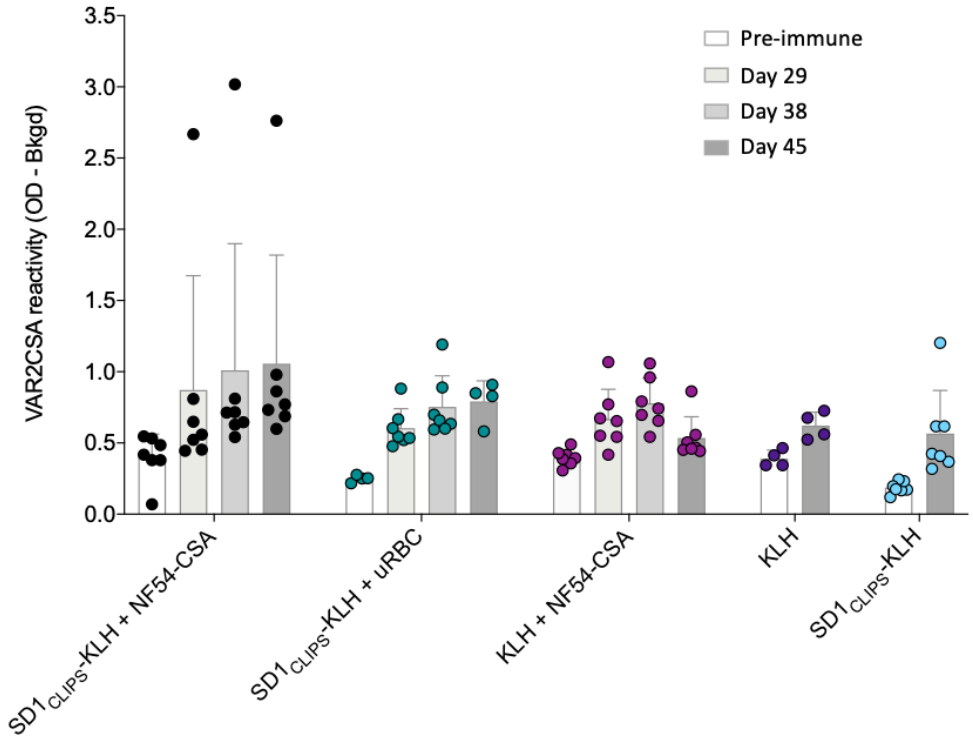

Figure 5.5 Exposure to native VAR2CSA on the surface of iRBCs did not increase VAR2CSA recognition by ELISA. Sera from mice in each of the cross-boosting groups were collected at different timepoints and tested against VAR2CSA by ELISA (dilution 1/250). Circles are data from individual mice and bars are mean ± SD.

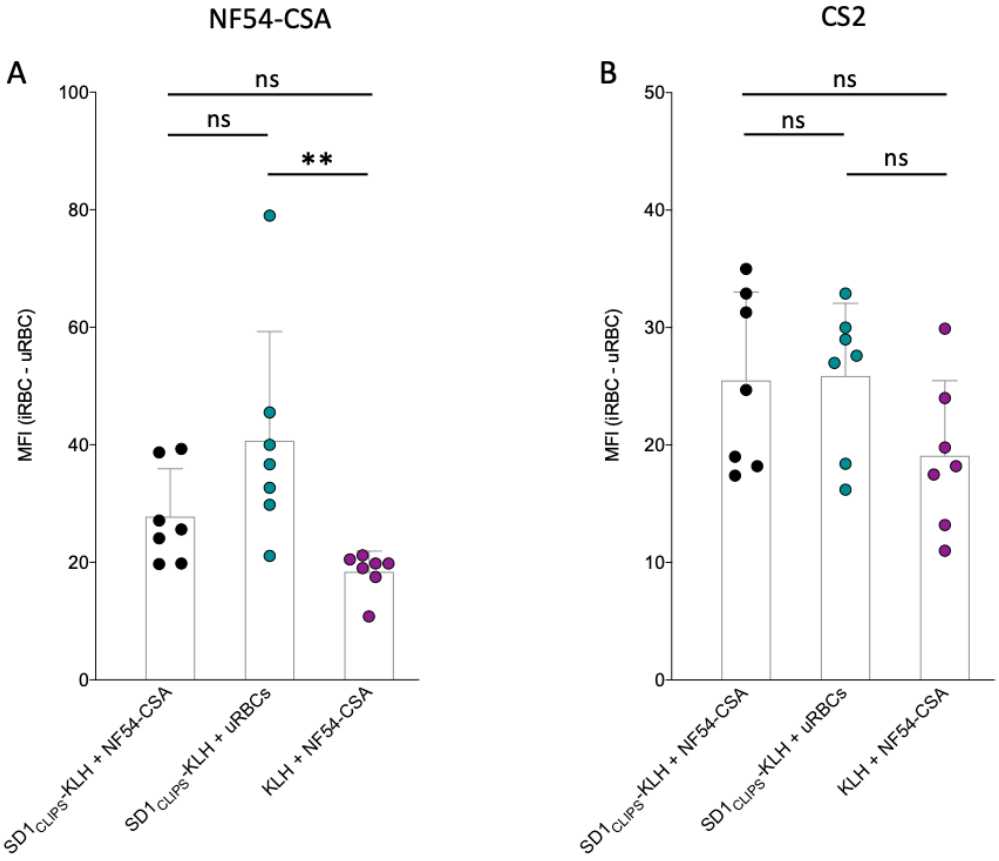

Figure 5.6 Immunization with NF54-CSA iRBCs did not enhance the cross-reactive antibody response in mice that were immunized with SD1$_{CLIPS}$-KLH. Sera from mice (dilution 1/5) were tested against (A) NF54-CSA and (B) CS2 iRBCs by flow cytometry. Circles represent individual mice and data were calculated as the MFI of the iRBC population minus the MFI of the uRBC population in each sample. Statistical significance was determined using a Kruskal-Wallis one-way ANOVA. Data are mean ± SD. **, $P < 0.01$; ns, not significant.

5.4 Discussion

In previous experiments, we achieved high antibody responses against SD1$_{CLIPS}$ using CFA and IFA in mice, but the endpoint titres of the cross-reactive antibodies were consistently low. Here, we tested two different adjuvants for their ability to increase the cross-reactive antibody response. We found that when SD1$_{CLIPS}$-KLH immunizations were formulated with GLA-SE, sera from mice had higher cross-reactive anti-VAR2CSA antibody titres, compared to those given in CFA/IFA or GLA-LSQ. However, inconsistency in the cross-reactive antibody responses is a challenge that we have yet to overcome. Using CFA/IFA, the number of mice in each group that made cross-reactive antibodies varied significantly between experiments, from 3/5 (60.0%) to 1/5 (20.0%) (Table 5.2). Using GLA-SE, a cross-reactive antibody response was elicited in 3/5 (60.0%) mice after 4 immunizations and in only 2/7 (28.5%) mice after 3 immunizations. As discussed in Chapter 4, analysis of the antibody responses that were elicited in mice immunized with SD1$_{CLIPS}$-KLH in CFA/IFA showed that the five mice each generated a unique immune response to the immunogen (Figure 4.6A). Although not surprising, these results underscore the variability in immune responses between individual animals. Going forward, it will be crucial to optimize the vaccine candidate to not only increase the cross-reactive antibody titres, but to ensure that they are consistently elicited in all animals. Given the genetic differences between strains of lab mice, it could also be important to test the vaccine candidates in different strains of mice, and potentially rats or rabbits as well.

Table 5.2. Summary of $SD1_{CLIPS}$ immunization data

Immunogen	Adjuvant	Mice, N	Immunizations, N	Anti-$SD1_{CLIPS}$ Ab, N (%)	Anti-VAR2CSA Ab, N (%)
$SD1_{CLIPS}$-KLH	CFA/IFA*	5	4	5 (100)	3 (60.0)
$SD1_{CLIPS}$-BSA	CFA/IFA*	4	4	4 (100)	2 (50.0)
$SD1_{CLIPS}$-KLH	CFA/IFA*	5	4	5 (100)	1 (20.0)
$SD1_{CLIPS}$-KLH	GLA-LSQ	5	4	5 (100)	0 (0.0)
$SD1_{CLIPS}$-KLH	GLA-SE	5	4	5 (100)	3 (60.0)
$SD1_{CLIPS}$-KLH	GLA-SE	7	3	7 (100)	2 (28.5)

*Initial immunization given in CFA, all boosts given in IFA.
Ab = antibodies

Previous experiments suggested that 3D10 recognized cryptic epitopes in VAR2CSA that are not exposed during natural infection or immunization with VAR2CSA (Discussed in Chapter 3). Because these epitopes are not under immune pressure, they are likely conserved in multiple alleles of VAR2CSA and targeting them may result in strain-transcending functional antibody responses, as was observed with 3D10. We hypothesized that immunizations with $SD1_{CLIPS}$-KLH would prime the immune system to target these cryptic epitopes upon exposure to recombinant or native VAR2CSA. This strategy has been successful in studies of a group A streptococcus vaccine candidate (288). Following immunizations with a peptide comprising a cryptic epitope from the M protein, a skin infection with the bacteria boosted antibodies targeting this epitope and even broadened the immune response. Similarly, we hypothesized that by immunizing mice with $SD1_{CLIPS}$-KLH followed by VAR2CSA, we could enhance the cross-reactive antibody response. However, the heterologous boost did not increase the speed at which the mice produced cross-reactive antibodies, nor did it increase the overall titres of the anti-VAR2CSA antibodies, compared to the control groups.

It is possible that the anti-VAR2CSA titres were lower in the cross-boosted mice because they were specifically boosted against the cross-reactive epitope, rather than the more immunodominant epitopes. However, this has yet to be investigated, as the epitopes in VAR2CSA that are targeted by the cross-reactive antibodies have not been identified. When we tested these sera by flow, there was no difference in the surface recognition between sera from the SD1$_{CLIPS}$-KLH + VAR2CSA immunized mice and the control mice. It is important to note that in flow experiments with both parasite strains, the variability in the surface recognition between sera samples from mice in the same experimental group made it difficult to interpret the data. It is also possible that the avidity of the cross-reactive antibodies differs between the groups, but this has not yet been investigated.

We also tested whether exposure to native VAR2CSA on the surface of iRBCs could enhance the cross-reactive antibody response in mice immunized with SD1$_{CLIPS}$-KLH. Similar to the heterologous prime/boost immunizations with recombinant VAR2CSA, exposure to native VAR2CSA on the surface of iRBCs did not increase the cross-reactive antibody response. It is important to note that in these experiments no mice made antibodies that recognized native VAR2CSA following injections with NF54-CSA iRBCs. Therefore, we cannot be sure that the injection with iRBCs provided enough VAR2CSA antigen to elicit an antibody response or boost the cross-reactive antibodies. Perhaps additional immunizations with iRBCs would help to increase the anti-VAR2CSA antibody response.

As discussed previously, the proportion of mice that produce a cross-reactive antibody response following SD1$_{CLIPS}$ immunization is inconsistent and often low. We also observed that only 2/7 mice made cross-reactive antibodies following 3 immunizations with SD1$_{CLIPS}$-KLH/GLA-SE in the control group of the heterologous prime/boost experiment. In previous

experiments, mice were given 4 immunizations with SD1$_{CLIPS}$-KLH, which generally resulted in a higher proportion of mice producing cross-reactive antibodies. In the previous experiment carried out with GLA-SE using 5 mice, 3 mice made cross-reactive antibodies. These data suggest that the epitope in SD1$_{CLIPS}$-KLH that elicits a cross-reactive antibody response is a subdominant epitope. It is possible that during the initial prime and boost immunizations, the B cell response is primarily focused on the immunodominant, non-cross-reactive epitopes. Then in subsequent boosts when there are high levels of antibodies targeting the immunodominant regions of SD1$_{CLIPS}$, the antibodies block B cell access to those epitopes and the response shifts to the more subdominant, cross-reactive epitopes. In fact, this has been described in studies of the immune response to the *P. falciparum* CSP protein in mice (331). During the initial boost when the overall level of antibodies against the immunogen is low, B cells primarily target the immunodominant epitopes. However, during subsequent boosts, high levels of antibodies were elicited against the immunodominant regions of the antigen, which blocked B cell access to these epitopes. This shifts the focus of the immune response and B cells that target the more subdominant epitopes are activated.

In the case of the heterologous prime/boost experiment, the initial boost with SD1$_{CLIPS}$ may not have elicited high enough anti-SD1$_{CLIPS}$ antibody titres to block B cell access to the immunodominant epitopes. This blockade would have led to the activation of only those B cells that recognized the immunodominant epitopes, rather than B cells targeting the subdominant cross-reactive epitopes in SD1$_{CLIPS}$. Then, when the mice were boosted with VAR2CSA, there were no primed cross-reactive B cells that could be boosted. Increasing the number of SD1$_{CLIPS}$-KLH immunizations to three, rather than two, prior to the VAR2CSA boost may improve the cross-reactive antibody response in the future.

The ideal approach is likely to re-design the SD1$_{CLIPS}$ peptide to make the cross-reactive epitope more immunodominant. All previous immunizations with SD1$_{CLIPS}$ elicited very strong anti-SD1$_{CLIPS}$ antibody responses. Thus, increasing the immunogenicity of the peptide overall is unlikely to improve the cross-reactive antibody response. However, designing an immunogen that focuses the immune response on the cross-reactive epitopes could be a viable approach. Evaluation of the immune responses of individual animals against peptides encompassing different regions of SD1$_{CLIPS}$ did not point to recognition of a particular epitope as being correlated with a cross-reactive antibody response (discussed in Chapter 4). However, further investigation of the target epitope(s) in VAR2CSA may inform modifications to SD1$_{CLIPS}$ that could improve the cross-reactive immune responses.

5.4 Conclusions

Here, we reported improved cross-reactive antibody responses to SD1$_{CLIPS}$-KLH using the adjuvant GLA-SE. Although the use of GLA-SE increased the anti-VAR2CSA titres in SD1$_{CLIPS}$-KLH immunized mice, these antibodies were still inconsistently elicited in the mice. We then tested a heterologous prime/boost schedule in an attempt to improve the cross-reactive immune response. However, immunizations with SD1$_{CLIPS}$-KLH did not enhance the anti-VAR2CSA antibody response following a boost with VAR2CSA, compared to mice immunized with KLH. These data suggest the need to redesign the SD1$_{CLIPS}$ peptide to strengthen the cross-reactive antibody response.

Chapter 6. Conclusions

Portions of this Chapter have been previously published (1).

6.1 Summary of research

The initial goal of this research was to investigate the unusual parity-independent acquisition of anti-VAR2CSA antibodies that we previously observed in populations in Colombia (154). This study linked the presence of anti-VAR2CSA antibodies in non-pregnant populations to the co-circulation of *P. vivax* and *P. falciparum* in this region and suggested immunological cross-reactivity between antigens from the two species.

Our first research objective was to identify a putative *P. vivax* antigen that mediates this cross-reactivity with VAR2CSA. *P. vivax* does not express any antigens that are VAR2CSA homologues. However, these parasites express the merozoite invasion ligand PvDBP, which contains a DBL domain that is a structurally-conserved domain found in a number of parasite antigens; there are six of these domains in VAR2CSA. We hypothesized that antibodies elicited against the DBL domain of the non-pregnancy associated PvDBP antigen cross-reacted with the DBL domains of VAR2CSA.

To further investigate this cross-reactivity, we obtained two monoclonal antibodies from collaborators that were raised against DBPII. One of the antibodies, 3D10, cross-reacted with VAR2CSA by ELISA, recognized a subset of iRBCs by flow and was able to block parasite adhesion to CSA *in vitro* (Chapter 2). The second monoclonal, 2D10, was not cross-reactive at all and indicated that there is a specific epitope in DBPII that mediates cross-reactivity. We also tested total IgG purified from sera from non-pregnant Colombian individuals exposed to *P. vivax* and found that they reduced parasite adhesion in the IBA. To the best of our knowledge, this was the

first description of cross-reactivity between non-orthologous antigens that mediate distinct biological functions: cytoadherence and parasite invasion.

In Chapter 3, we identified the putative epitopes in both PvDBP and VAR2CSA that mediated cross-reactivity between these antigens (Chapter 3). Based on scanning mutagenesis data from our collaborators (259) and ELISA experiments from our lab, we narrowed down the 3D10 recognition site to the SD1 region of DBPII. Interestingly, we found that SD1 in PvDBP was subdominant. A synthetic peptide encompassing this region, called SD1ss, was not recognized by antibodies elicited through vaccination with DBPII or through exposure to PvDBP during a natural infection in an outbreak setting. However, recognition of SD1ss was correlated with VAR2CSA recognition in sera from both Colombian and Brazilian non-pregnant populations exposed only to *P. vivax.* Furthermore, antibodies from a pool of sera from non-pregnant individuals in Colombia that were affinity-purified on SD1ss blocked parasite adhesion *in vitro*. Based on these findings, we speculate that several *P. vivax* infections or infections with certain strains of *P. vivax* may be necessary for the formation of antibodies against the SD1 region, however further study is needed.

We also tested whether the cross-reactivity between DBPII and VAR2CSA was reciprocal. We tested serum from a rabbit immunized with full-length VAR2CSA and a pool of sera from multigravid women from Uganda and found that neither recognized SD1ss by ELISA. Using antibody competition ELISAs, we also showed that 3D10 and the SD1ss affinity-purified antibodies recognized epitopes in VAR2CSA that were distinct from those recognized by antibodies elicited by immunizations with VAR2CSA. Taken together, these data suggest that the epitope(s) in VAR2CSA that are targeted by the cross-reactive antibodies are cryptic. Consistent with this, peptides identified by screening an overlapping peptide array of DBL5ε with 3D10 (P20 and P23) were not well recognized by anti-VAR2CSA rabbit serum or by sera from multigravid

women from Uganda. However, sera from Colombian and Brazilian individuals exposed to *P. vivax* recognized both P20 and P23. We also found that these peptides were spatially distinct from immunodominant epitopes that were identified previously on a homology model of DBL5ε, further supporting the cryptic nature of these epitopes. It is important to note that although the DBL5ε peptide array provided additional information about the epitopes that are recognized by 3D10, these results should be interpreted with caution, as linear peptides cannot recapitulate the secondary structures found in proteins.

Based on the findings in Chapters 2 and 3, we postulated that the immunological cross-reactivity between PvDBP and VAR2CSA could be exploited for the development of a placental malaria vaccine candidate. In theory, immunizations with the epitope that elicited 3D10 could generate a 3D10-like antibody response that would cross-react with VAR2CSA and potentially protect vaccinees against MiP. To inform vaccine design, we then focused on identifying the minimal epitope for 3D10 recognition in DBPII (Chapter 4). We narrowed down the recognition site to a 13 amino acid peptide (N_{10}-C_{22}) that was recognized by 3D10 as strongly as the entire SD1ss peptide. However, immunizations with N_{10}-C_{22} revealed that although sufficient for recognition by 3D10, this peptide could not elicit a 3D10-like antibody response in mice.

When we tested 3D10 against an overlapping peptide array of SD1, we found that three spatially distinct portions of the SD1 region were recognized. This suggested that the epitope recognized by 3D10 was discontinuous and conformational, revealing the importance of maintaining the native SD1 structure in the immunogen. SD1 contains approximately 40 amino acids that are structurally constrained by two disulfide bonds, making it a large, challenging peptide to synthesize. After attempting to synthesize it as a cyclic peptide ourselves, we designed a structurally-constrained peptide, called $SD1_{CLIPS}$, that was synthesized commercially.

Immunizations with this peptide (conjugated to either BSA or KLH) in mice and a rabbit elicited a cross-reactive antibody response that recognized recombinant VAR2CSA by ELISA.

In order to evaluate the function of the cross-reactive antibodies, we affinity-purified the antibodies on a column coated with VAR2CSA. Once purified, these cross-reactive IgG recognized native VAR2CSA on the surface of RBCs infected with 3 different *P. falciparum* strains. However, these antibodies did not block parasite adhesion to CSA or mediate opsonic phagocytosis *in vitro*. These results indicate that although the antibodies recognized cross-reactive epitopes in VAR2CSA, they were not the same epitopes that are targeted by 3D10, which can block parasite adhesion to CSA. Further analysis of the affinity-purified antibodies is needed before additional conclusions can be drawn. These include evaluating other potential functional activities, such as complement fixation, determining the isotypes of the cross-reactive antibodies and identifying the epitopes that they target in VAR2CSA.

Although immunizations with SD1$_{CLIPS}$ yielded promising results, the cross-reactive antibodies were regularly found at low titres in the sera, bound to VAR2CSA with low avidity and were inconsistently elicited in mice. These are all challenges that need to be addressed before SD1$_{CLIPS}$ could ever be a viable vaccine candidate. In Chapter 5, we attempted to enhance the cross-reactive immune response generated by SD1$_{CLIPS}$-KLH immunizations in mice. We tested two alternative adjuvants, GLA-SE and GLA-LSQ, both of which are approved for use in humans and yielded positive results in pre-clinical and clinical evaluations of several malaria vaccine candidates, including PAMVAC and PRIMVAC (186, 187). When adjuvanted with GLA-SE, SD1$_{CLIPS}$-KLH immunizations elicited higher titres of cross-reactive antibodies in mice, compared to either GLA-LSQ or CFA/IFA (the adjuvants that had been used in all previous immunizations).

However, the cross-reactive antibodies were still only elicited in 3/5 (60.0%) mice after 4 immunizations and in 2/7 (28.5%) mice after 3 immunizations.

We tried another approach to improve the cross-reactive antibody response using a heterologous prime/boost schedule with SD1$_{CLIPS}$-KLH followed by VAR2CSA. We hypothesized that cross-reactive B cells would be primed by the SD1$_{CLIPS}$ immunizations and then rapidly reactivated upon exposure to the cross-reactive epitope(s) in VAR2CSA. However, mice primed with SD1$_{CLIPS}$-KLH did not make anti-VAR2CSA antibodies any faster or at a higher titre than those primed with KLH. There was also no recognition of native VAR2CSA on the surface of iRBCs observed with sera from any group of mice in the heterologous prime/boost experiment.

Similar to the heterologous boost with recombinant VAR2CSA, we tested whether exposure to native VAR2CSA on the surface of iRBCs could boost or expand the cross-reactive antibodies generated against SD1$_{CLIPS}$-KLH. After mice were given two immunizations with SD1$_{CLIPS}$-KLH, they were injected with NF54-CSA iRBCs or uRBCs as a control. However, there were no cross-reactive antibodies generated in any of these mice, with the exception of one mouse that made anti-VAR2CSA antibodies after one SD1$_{CLIPS}$-KLH immunization.

Taken together, the results presented in this thesis suggest that there is potential to exploit the cross-reactivity between PvDBP and VAR2CSA for vaccine development, but that our current vaccine candidate and/or strategy needs to be improved.

6.2 Future directions

There are a number of different approaches that could be taken to further develop SD1$_{CLIPS}$ as a vaccine candidate. Likely the most promising approach is to redesign the immunogen based on the cross-reactive epitopes in VAR2CSA, providing these can be identified. There are a number

of ways to do this and we are already in the process of testing the cross-reactive antibodies against an overlapping peptide array of VAR2CSA. We also have a significant amount of empirical data regarding the specificity of 3D10 and the cross-reactive rabbit IgG. These data could be applied to the structural analysis of the cross-reactive epitopes within the structures of PvDBP, EBP2 and VAR2CSA to inform vaccine design.

Alternative types of immunogens should also be considered. For instance, recombinant DBPII can be mutated to make the SD1 region more immunodominant and elicit higher levels of cross-reactive antibodies. In fact, our collaborators previously designed genetically engineered DBPII proteins that contain mutations in many of the immunodominant regions (332). Two of these proteins, called DEKnull3 and DEKnull4, elicited cross-reactive antibodies in mice, although these data are preliminary (unpublished data).

6.3 Implications of research

Results of our study, as well as many others discussed in Chapter 1, suggest the possibility of targeting conserved epitopes in malaria parasite antigens through vaccination. However, to translate the observations spanning the last century into viable heterologous vaccine candidates, the conserved targets of immunity must be identified. Given that partial protection is observed in naturally exposed populations, we expect that multiple vaccine candidates will be needed to target different stages of the parasite's lifecycle. Cross-species vaccines that aim to prevent infection should target sporozoite antigens to inhibit hepatocyte invasion and development, while vaccines that target blood stage antigens could prevent severe disease. Gametocyte antigens are also attractive targets to prevent the onwards transmission of malaria. In Figure 6.1, we summarized findings from studies using human malaria parasite antigens that revealed potential cross-species vaccine targets from different parasite stages (1).

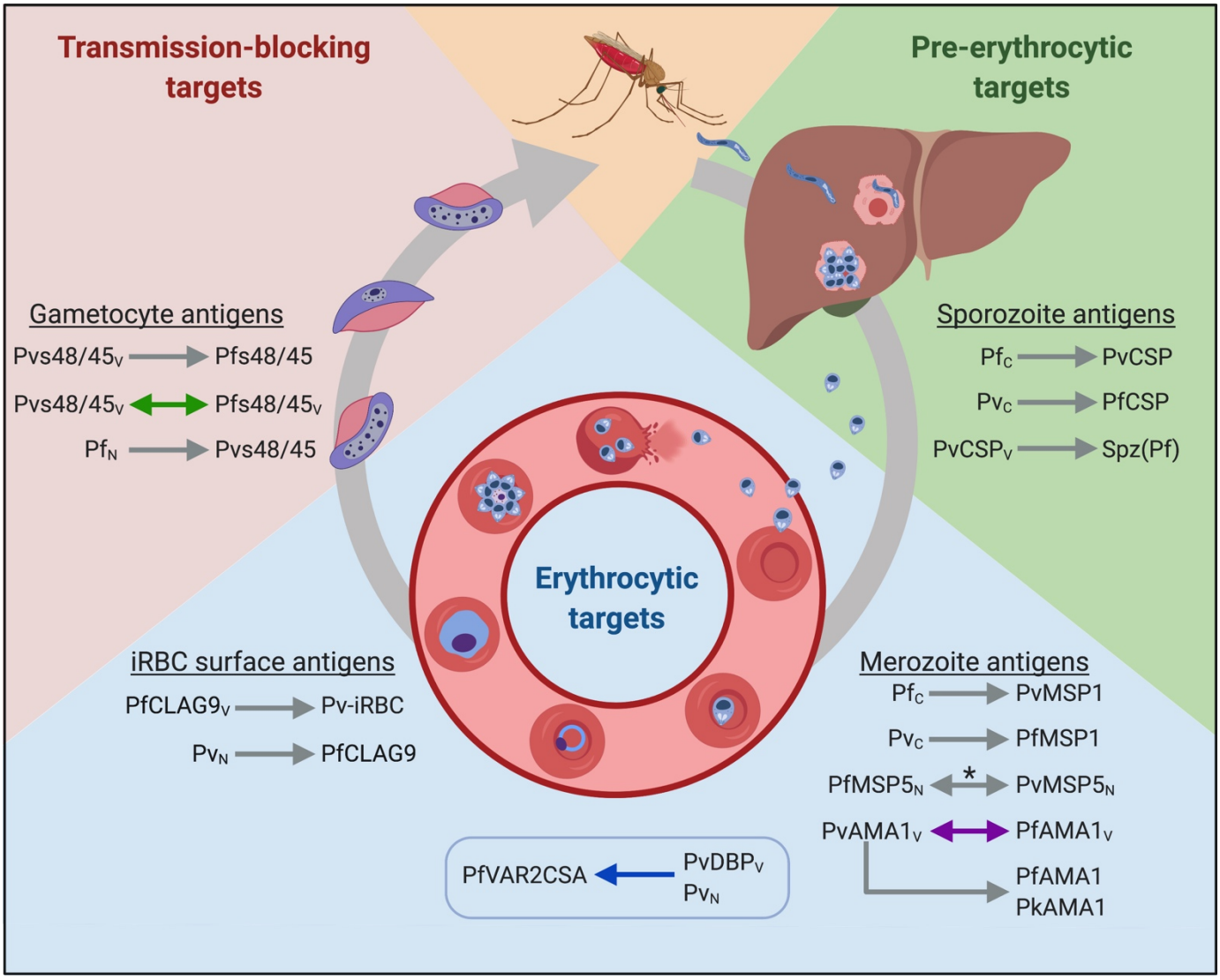

Figure 6.1. Putative cross-species vaccine candidates. Arrowheads indicate the direction of cross-reactivity and double arrowheads show reciprocal cross-reactivity. Grey arrows denote immunological cross-reactivity, but unknown functional activity, purple arrows denote that heterologous function was not demonstrated, blue arrows denote that heterologous function was demonstrated and green arrows denote cross-boosting following heterologous vaccination. The box indicates cross-stage, cross-species reactivity. Spz(Pf) = *P. falciparum* sporozoites. Subscript letters denote route of exposure to parasite or antigen; C = CHMI, V = exposure through vaccination, N = natural infection. Figure from (1).

It is conceivable that the whole parasite vaccine approach could replicate the partial cross-species immunity that has been observed in a number of studies (Reviewed in (1)). Parasites attenuated by irradiation, chemical treatment or genetic modification expose the immune system to a broad spectrum of antigens for that given stage, including antigens that are highly conserved across species (e.g. housekeeping antigens) and those which have conserved epitopes, which may by based on structural similarity (e.g. DBL domains). If these attenuated parasites can persist in vaccinated individuals and remain metabolically active (333), this creates an opportunity for sustained antigenic stimulation of either B or T cells with the potential for more robust protection from future infection.

An alternative vaccine approach, used in this thesis, is to define the conserved epitopes in related antigens from different species and focus the immune response on these epitopes. This hinges on the hypothesis that despite the extreme antigenic diversity in *Plasmodium*, there exist evolutionarily conserved epitopes that can elicit protective antibodies or stimulate cross-reactive T cells. Richie argued that selection pressure would favour antigenic diversity in species that infect the same host to avoid cross-species immunity that could eliminate both species (334). The continued scourge of malaria globally supports this tenet. However, based on data presented in this thesis and many of the studies described, we propose that conserved, cross-reactive epitopes may be more exposed in less virulent parasites and cryptic in more virulent ones. This could provide a competitive advantage for the benign parasite and ensure survival of the host.

It is clear from the analysis of *Plasmodium* genomes that the immunodominant antigens in all species are highly polymorphic. Yet if we consider the functions of these diverse antigens, they are largely restricted to the pathogenesis of a particular species. For instance, the PfEMP1 virulence factors mediate sequestration of iRBCs to different tissues as a mechanism of immune

evasion. Sequestration may have evolved to enhance the virulence of *P. falciparum* over other species that co-circulate in a given population and compete for the same host. But since the PfEMP1 family is unique to *P. falciparum* (and *P. reichenowi* in primates), the diversity among the members of the PfEMP1 family hinders the acquisition of strain-transcending immunity only within this species. This is also exemplified by the highly polymorphic proteins involved in erythrocyte invasion. *Plasmodium* species exhibit host cell tropism for different types of RBCs and evolved parasite ligands that bind to host receptors on those specific cells. In *P. vivax*, the PvDBP ligand interacts with DARC to invade reticulocytes and there is extensive diversity in the PvDBP domain that interacts with DARC. These polymorphisms are selected to evade immune responses that would block invasion of reticulocytes, yet they remain specific to *P. vivax* and do not impact other species that require different ligand-receptor interactions for invasion.

Despite the selection for variation in the immunodominant antigens within each species, many of these proteins evolved from ancestral homologues. The PfEMP1 and PvDBP proteins share a common protein architecture which includes DBL domains that may have conserved epitopes, which are essentially 'evolutionary relics.' These epitopes are probably not highly immunogenic and would induce antibodies with lower avidity toward their heterologous counterparts, as we observed with 3D10 and anti-SD1$_{CLIPS}$ sera. They may even be cryptic in some proteins, which could explain the non-reciprocal nature of cross-species immunity observed in our studies and so many other human and animal studies.

We suggest that vaccination can refine and amplify a cross-species immune response to target heterologous antigens. There are a number of potential vaccine targets identified already that elicit cross-reactive antibodies (Figure 6.1) and certainly new targets to discover (Figure 6.2). The first step to identify new cross-reactive B cell epitopes is to test sera for reactivity to

heterologous parasites (e.g. by IF assay or flow cytometry). Cross-reactive sera should then be assessed for functional activity against the heterologous parasite. This could involve testing the sera in various *in vitro* assays to measure effects on invasion, sequestration, transmission-blocking activity, etc. Most of these assays measure antibody function, with only indirect assays to measure T cell mediated responses (e.g. cytokine production) (335, 336). Even the more established antibody-based assays, such as the growth inhibition assay, vary in terms of validity and predictive value, and are largely antigen and strain-specific (337). Assays to measure adhesion-blocking activity also vary with the format; for example, the anti-adhesion activity of VAR2CSA antibodies varies significantly when compared between a static inhibition of binding assay, a flow-based assay, and a placental perfusion assay (338). Nevertheless, these assays can provide insight into the pathway blocked by those antibodies and generate hypotheses of which antigens are likely targets. Once the target protein is identified (through biochemical and/or immunological methods), antibodies specific to this antigen can be purified from the sera or generated as monoclonals (mAbs). These antibodies can be characterized in terms of their cross-reactivity (titers, avidity) and their functional activity against the heterologous parasite.

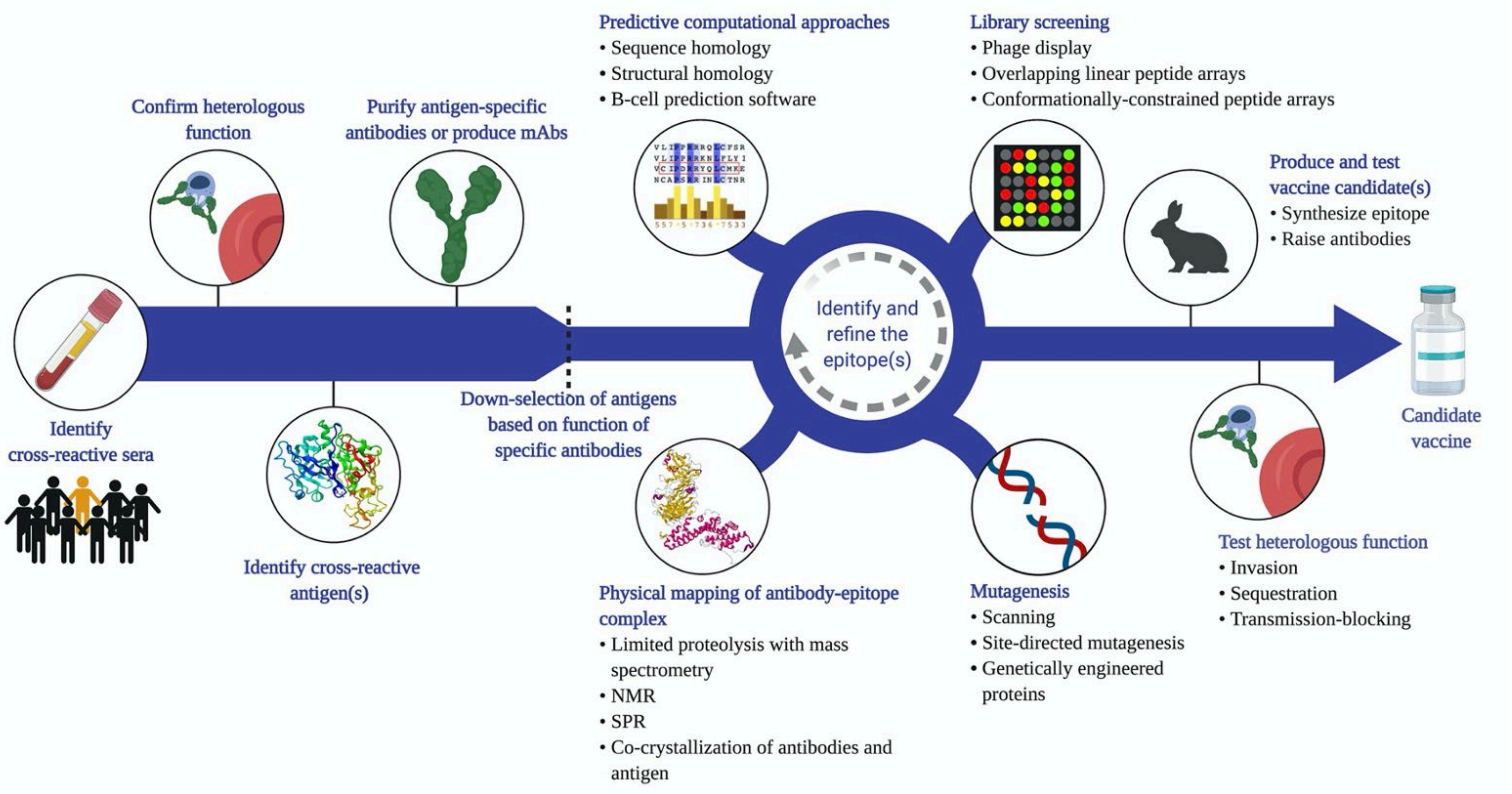

Figure 6.2 Proposed strategy to identify cross-species vaccine candidates based on cross-reactive B cell epitopes. Given that cross-species immunity is a rare event in naturally exposed populations, a large number of samples from endemic populations will need to be screened (e.g. by IF assay or flow cytometry) to identify sera that recognize heterologous parasites. Antibody function against the heterologous species should then be confirmed (e.g. invasion, cytoadherence, transmission-blocking assays), and the antigen that mediates this functional cross-reactivity identified. This can be achieved through a variety of methods, including depletion or competition experiments. Antigen-specific antibodies can be affinity-purified from sera, or monoclonal antibodies generated using PBMCs from naturally exposed individuals or from animals vaccinated with the antigen. Functional analysis of these antibodies can then be used to down-select candidate antigens before applying a variety of empirical approaches to map the cross-reactive epitope. Phage and peptide libraries can be screened with the cross-reactive antibodies. Mutagenesis techniques, such as site-directed mutagenesis or alanine scanning of recombinant proteins can map residues that are critical for antibody binding. Physical mapping, such as co-crystallization of the antigen-antibody complex, is another powerful approach to map the contact residues within the epitope. These experimental tools can be integrated with computational analysis of the antigens from each species. Once a putative cross-reactive epitope is identified, the next step is to generate a recombinant protein or synthetic peptide that recapitulates this epitope, raise epitope-specific antibodies in animals, and test for cross-reactivity and function in vitro. It is important to note that the process of identifying and refining the epitope is iterative and each approach can complement and inform the other to yield potent, functional cross-species antibodies. Created with Biorender.com, including crystal structures PDB accession numbers 1SME and 6R2S. Figure from (1).

To translate these findings into vaccine candidates, the cross-reactive epitope can be mapped using a variety of approaches. B cell epitopes may be linear but are more likely to be conformational if they represent structurally-related epitopes. Conformational epitopes are certainly more challenging to map but advances in structural and computational biology provide valuable tools that support rational vaccine design (reviewed in (339)). For example, cross-reactive human or mouse monoclonal antibodies can be co-crystallized with the target protein to map the epitope empirically (230). These antibodies can also be used to screen peptide libraries (conformationally-constrained or linear) or tested against mutant recombinant proteins to identify the epitope that mediates cross-reactivity. In parallel, computational approaches can be applied to protein databases to predict conserved epitopes. This technique was recently adopted to predict conserved linear and discontinuous epitopes in CSP and MSP-1 shared between the *P. falciparum* and *P. vivax* orthologues (247).

Computational modeling can also guide the design of vaccine candidates to enhance immunogenicity and to elicit broadly neutralizing antibodies. Computational simulations of affinity maturation applied to the antibody response to *P. falciparum* AMA-1 revealed that polyvalent vaccines promoted cross-reactive antibody responses to shared epitopes (across strains; AMA-1 from different species was not included) (340). In future, entire proteomes and epitope libraries spanning the evolutionary spectrum of Plasmodia can be probed using artificial intelligence and machine learning to discover targets of cross-species epitopes. It is important to note that the process of identifying and refining the epitope is iterative and each approach can complement and inform the other.

Once a cross-species epitope is mapped, the next step is to reproduce the epitope synthetically such that it can elicit functional antibodies or protective cellular responses against

the heterologous epitopes in other species. This can be achieved with engineered recombinant proteins that expose the epitope preferentially (e.g. (341)), linear epitopes conjugated to carrier peptides, and for conformational epitopes, this is feasible with the use of peptide scaffolds that restrict the conformation of peptides as immunogens (e.g. Chapter 4). An alternative delivery platform is the use of transgenic parasites from one species engineered to express antigens from a different species (342). The success of these approaches will depend on the fine specificity of the antibodies and their avidity for the heterologous epitopes. The avidity of cross-species antibodies observed in human and animal infections is generally low but different immunization strategies can be adopted to promote affinity-maturation, including the choice of adjuvant, delivery platform, dosing, and boosting schemes (37). As such, several rounds of identification, design and testing may be required to produce potent, functional cross-species antibodies.

One outstanding question is whether these immune responses would be boosted by natural infection with heterologous species. This may depend on a number of variables including the intensity of parasite transmission, host genetics, and immune regulation. We hypothesize that if the epitope is truly cross-reactive, then memory B or T cells will be expanded by exposure to the heterologous epitope even if it is not immunogenic in that species. This phenomenon was recently reported for a cryptic epitope in group A *Streptococcus* where immunization with the conserved peptide was boosted by natural infection with different bacterial strains (288). Similar vaccine strategies are being adopted against cryptic epitopes in Ebola antigens (280), and toward the development of a universal influenza vaccine (263-265).

The challenges facing the current VAR2CSA based vaccine candidates, PRIMVAC and PAMVAC, underscore the need for vaccine strategies to focus on identifying and targeting conserved epitopes in parasite antigens. In phase 1a/1b clinical trials of both of these candidates,

surface recognition of iRBCs and CSA binding inhibition were observed when sera from vaccinees were tested against parasites expressing the same allele of *var2csa* that was used in the vaccine; however, there was little recognition of parasites expressing a heterologous allele of VAR2CSA and no blocking activity was observed (186, 187, 192). Both of these candidates include DBL domains near the N terminus of VAR2CSA that are known to be polymorphic among field isolates (193). It is likely that the polymorphic nature of VAR2CSA will continue to impede efforts to produce vaccines that elicit a strain-transcending immune response. In fact, this type of vaccine strategy which presents naturally immunodominant, polymorphic epitopes will likely continue to fail to produce strain-transcending immunity when faced with the high degree of antigenic polymorphisms in *Plasmodium* parasites (73).

6.4 Challenges of implementing a placental malaria vaccine

Beyond the biological challenges associated with developing a placental malaria vaccine, there are other factors that need to be considered. For instance, a vaccine to prevent malaria infection in pregnancy would need to be given to girls before they reach child-bearing age and protection would need to extend throughout the next 2 to 3 decades. An ideal vaccine would elicit and sustain a high anti-VAR2CSA IgG response through the formation of long-lasting plasma cells and memory B and T cells. If a vaccine was able to achieve this response, the logical target population would be girls below the age of five who are covered by the World Health Organization's Expanded Programme on Immunization (EPI). This program was established in 1977 with the goal of achieving universal vaccination. However, program expansion has stalled in recent years, coverage varies drastically between countries and the data on vaccine coverage is often of poor quality (343). Despite these challenges, inclusion in the EPI would likely ensure the

highest coverage, with a target population of 15 million girls per year in sub-Saharan Africa and 22.5 million in South-East Asia (344). The Pan American Health Organization has a similar immunization program in South America, which reached over 90% of the target population for several vaccines in 2019 (345). Fitting into an already existing immunization program is ideal, as no new vaccine schedule is needed and this should reduce program costs for endemic countries. However, inclusion into these programs requires that robust, long-lasting immunity be achieved through vaccination in early childhood.

An alternative implementation strategy is to include the vaccine in a program targeting adolescent girls, such as the human papillomavirus vaccine program. This program targets approximately 30 million girls annually between the ages of 11-12 in malaria-endemic areas (346). However, at present this program either has not been implemented in many African countries or its coverage is falling significantly short of its target (347). Targeting an older cohort of girls reduces the longevity of the response that is needed. However, it still must be sustained over many years and may require further boosting in early adulthood to ensure protective immunity is attained.

Inclusion into either of these immunization programs requires that the malaria vaccine does not interfere with the current vaccines and that the number and timing of boosts required conforms to that of the existing immunizations. It is also important to consider that because *P. falciparum* only expresses VAR2CSA when it infects a pregnant woman, an infection outside of pregnancy will likely not boost the immune response elicited by a vaccine based on VAR2CSA. If the vaccine was similar to the two leading candidates, which are based on the polymorphic DBL domains of VAR2CSA, it would be unlikely to generate an immune response against epitopes conserved in other PfEMP1 antigens. Therefore, depending on the longevity of the response elicited by the

vaccine, it may be necessary to boost women before their first pregnancy (when possible) and maybe even between pregnancies, especially in low-transmission settings.

In low-transmission settings, people receive less than ten infectious mosquito bites per year, so it is likely that a woman could give birth multiple times before being exposed to MiP (348). While this is clearly beneficial in most cases, pregnant women are at increased risk of severe malaria in these settings, due to their relatively limited exposure to the parasite and therefore low immunity (349). In fact, in low-transmission settings, women of all parities are susceptible to severe malaria infection during pregnancy (350). Thus, pregnant women in low-transmission settings represent a particularly vulnerable population, and special consideration must be given when implementing a vaccine to prevent MiP in these settings. For instance, the relatively low natural exposure to VAR2CSA may necessitate additional boosting through immunization that is not required in high-transmission settings.

6.5 Concluding remarks

Efforts to eradicate malaria have been on-going for decades and while there have been monumental achievements in the control of the disease, there is still a long way to go. One of the missing pieces in the fight against malaria is a safe, efficacious vaccine that can either reduce morbidity and mortality or prevent infection or transmission altogether. The slow progress in developing a malaria vaccine underscores the many challenges with a traditional vaccine approach. We need to consider alternative, yet complementary strategies. Thus, exploiting rare immune mechanisms like cross-species immunity are worthy of consideration and with our current tools, this is more amenable than ever before. We don't expect this approach to yield a vaccine that provides sterile immunity to malaria; but if we could emulate the reduction in disease severity

observed with heterologous infections in humans and in animal studies, this vaccine could reduce mortality in the most vulnerable populations and allow natural, strain-transcending immunity to develop.

References

1. Mitran CJ, Yanow SK. 2020. The Case for Exploiting Cross-Species Epitopes in Malaria Vaccine Design. Front Immunol 11:335.

2. WHO. 2020. World Malaria Report. Geneva.

3. Sutherland CJ, Tanomsing N, Nolder D, Oguike M, Jennison C, Pukrittayakamee S, Dolecek C, Hien TT, do Rosario VE, Arez AP, Pinto J, Michon P, Escalante AA, Nosten F, Burke M, Lee R, Blaze M, Otto TD, Barnwell JW, Pain A, Williams J, White NJ, Day NP, Snounou G, Lockhart PJ, Chiodini PL, Imwong M, Polley SD. 2010. Two nonrecombining sympatric forms of the human malaria parasite Plasmodium ovale occur globally. J Infect Dis 201:1544-50.

4. Ansari HR, Templeton TJ, Subudhi AK, Ramaprasad A, Tang J, Lu F, Naeem R, Hashish Y, Oguike MC, Benavente ED, Clark TG, Sutherland CJ, Barnwell JW, Culleton R, Cao J, Pain A. 2016. Genome-scale comparison of expanded gene families in Plasmodium ovale wallikeri and Plasmodium ovale curtisi with Plasmodium malariae and with other Plasmodium species. Int J Parasitol 46:685-96.

5. Twohig KA, Pfeffer DA, Baird JK, Price RN, Zimmerman PA, Hay SI, Gething PW, Battle KE, Howes RE. 2019. Growing evidence of Plasmodium vivax across malaria-endemic Africa. PLoS Negl Trop Dis 13:e0007140.

6. Price RN, Commons RJ, Battle KE, Thriemer K, Mendis K. 2020. Plasmodium vivax in the Era of the Shrinking P. falciparum Map. Trends Parasitol 36:560-570.

7. Simonetti AB. 1996. The biology of malarial parasite in the mosquito--a review. Mem Inst Oswaldo Cruz 91:519-41.

8. CDC. 2020. Malaria Biology - Lifecycle, *on* Centers for Disease Control. Accessed

9. Meis JF, Ponnudurai T, Mons B, van Belkum A, van Eerd PM, Druilhe P, Schellekens H. 1990. Plasmodium falciparum: studies on mature exoerythrocytic forms in the liver of the chimpanzee, Pan troglodytes. Exp Parasitol 70:1-11.

10. Miller LH, Mason SJ, Clyde DF, McGinniss MH. 1976. The resistance factor to Plasmodium vivax in blacks. The Duffy-blood-group genotype, FyFy. N Engl J Med 295:302-4.

11. Miller LH, Mason SJ, Dvorak JA, McGinniss MH, Rothman IK. 1975. Erythrocyte receptors for (Plasmodium knowlesi) malaria: Duffy blood group determinants. Science 189:561-3.

12. Horuk R, Chitnis CE, Darbonne WC, Colby TJ, Rybicki A, Hadley TJ, Miller LH. 1993. A receptor for the malarial parasite Plasmodium vivax: the erythrocyte chemokine receptor. Science 261:1182-4.

13. Chitnis CE, Miller LH. 1994. Identification of the erythrocyte binding domains of Plasmodium vivax and Plasmodium knowlesi proteins involved in erythrocyte invasion. J Exp Med 180:497-506.

14. VanBuskirk KM, Sevova E, Adams JH. 2004. Conserved residues in the Plasmodium vivax Duffy-binding protein ligand domain are critical for erythrocyte receptor recognition. Proc Natl Acad Sci U S A 101:15754-9.

15. Iyer J, Gruner AC, Renia L, Snounou G, Preiser PR. 2007. Invasion of host cells by malaria parasites: a tale of two protein families. Mol Microbiol 65:231-49.

16. Aguilar R, Magallon-Tejada A, Achtman AH, Moraleda C, Joice R, Cistero P, Li Wai Suen CS, Nhabomba A, Macete E, Mueller I, Marti M, Alonso PL, Menendez C, Schofield L, Mayor A. 2014. Molecular evidence for the localization of Plasmodium falciparum immature gametocytes in bone marrow. Blood 123:959-66.

17. Joice R, Nilsson SK, Montgomery J, Dankwa S, Egan E, Morahan B, Seydel KB, Bertuccini L, Alano P, Williamson KC, Duraisingh MT, Taylor TE, Milner DA, Marti M. 2014. Plasmodium falciparum transmission stages accumulate in the human bone marrow. Sci Transl Med 6:244re5.

18. Neveu G, Richard C, Dupuy F, Behera P, Volpe F, Subramani PA, Marcel-Zerrougui B, Vallin P, Andrieu M, Minz AM, Azar N, Martins RM, Lorthiois A, Gazeau F, Lopez-Rubio JJ, Mazier D, Silva AKA, Satpathi S, Wassmer SC, Verdier F, Lavazec C. 2020. Plasmodium falciparum sexual parasites develop in human erythroblasts and affect erythropoiesis. Blood 136:1381-1393.

19. Howes RE, Battle KE, Mendis KN, Smith DL, Cibulskis RE, Baird JK, Hay SI. 2016. Global Epidemiology of Plasmodium vivax. Am J Trop Med Hyg 95:15-34.

20. Markus MB. 2011. The hypnozoite concept, with particular reference to malaria. Parasitol Res 108:247-52.

21. Ntumngia FB, Thomson-Luque R, Pires CV, Adams JH. 2016. The role of the human Duffy antigen receptor for chemokines in malaria susceptibility: current opinions and future treatment prospects. J Receptor Ligand Channel Res 9:1-11.

22. Long CA, Zavala F. 2017. Immune Responses in Malaria. Cold Spring Harb Perspect Med 7.

23. Mideo N, Reece SE, Smith AL, Metcalf CJ. 2013. The Cinderella syndrome: why do malaria-infected cells burst at midnight? Trends Parasitol 29:10-6.

24. Marsh K, Kinyanjui S. 2006. Immune effector mechanisms in malaria. Parasite Immunol 28:51-60.

25. Tran TM, Li S, Doumbo S, Doumtabe D, Huang CY, Dia S, Bathily A, Sangala J, Kone Y, Traore A, Niangaly M, Dara C, Kayentao K, Ongoiba A, Doumbo OK, Traore B,

Crompton PD. 2013. An intensive longitudinal cohort study of Malian children and adults reveals no evidence of acquired immunity to Plasmodium falciparum infection. Clin Infect Dis 57:40-7.

26. mal ERACGoD, Diagnostics. 2011. A research agenda for malaria eradication: diagnoses and diagnostics. PLoS Med 8:e1000396.

27. Ouedraogo AL, Bousema T, de Vlas SJ, Cuzin-Ouattara N, Verhave JP, Drakeley C, Luty AJ, Sauerwein R. 2010. The plasticity of Plasmodium falciparum gametocytaemia in relation to age in Burkina Faso. Malar J 9:281.

28. Kwiatkowski D. 1990. Tumour necrosis factor, fever and fatality in falciparum malaria. Immunol Lett 25:213-6.

29. Taverne J, Tavernier J, Fiers W, Playfair JH. 1987. Recombinant tumour necrosis factor inhibits malaria parasites in vivo but not in vitro. Clin Exp Immunol 67:1-4.

30. Couper KN, Blount DG, Riley EM. 2008. IL-10: the master regulator of immunity to infection. J Immunol 180:5771-7.

31. Lyke KE, Burges R, Cissoko Y, Sangare L, Dao M, Diarra I, Kone A, Harley R, Plowe CV, Doumbo OK, Sztein MB. 2004. Serum levels of the proinflammatory cytokines interleukin-1 beta (IL-1beta), IL-6, IL-8, IL-10, tumor necrosis factor alpha, and IL-12(p70) in Malian children with severe Plasmodium falciparum malaria and matched uncomplicated malaria or healthy controls. Infect Immun 72:5630-7.

32. Moore KW, de Waal Malefyt R, Coffman RL, O'Garra A. 2001. Interleukin-10 and the interleukin-10 receptor. Annu Rev Immunol 19:683-765.

33. Prakash D, Fesel C, Jain R, Cazenave PA, Mishra GC, Pied S. 2006. Clusters of cytokines determine malaria severity in Plasmodium falciparum-infected patients from endemic areas of Central India. J Infect Dis 194:198-207.

34. Kurtzhals JA, Adabayeri V, Goka BQ, Akanmori BD, Oliver-Commey JO, Nkrumah FK, Behr C, Hviid L. 1998. Low plasma concentrations of interleukin 10 in severe malarial anaemia compared with cerebral and uncomplicated malaria. Lancet 351:1768-72.

35. Awandare GA, Goka B, Boeuf P, Tetteh JK, Kurtzhals JA, Behr C, Akanmori BD. 2006. Increased levels of inflammatory mediators in children with severe Plasmodium falciparum malaria with respiratory distress. J Infect Dis 194:1438-46.

36. Anonymous. 2018. World Malaria Report. World Health Organization, Geneva.

37. Draper SJ, Sack BK, King CR, Nielsen CM, Rayner JC, Higgins MK, Long CA, Seder RA. 2018. Malaria Vaccines: Recent Advances and New Horizons. Cell Host Microbe 24:43-56.

38. Kurtovic L, Behet MC, Feng G, Reiling L, Chelimo K, Dent AE, Mueller I, Kazura JW, Sauerwein RW, Fowkes FJI, Beeson JG. 2018. Human antibodies activate complement against Plasmodium falciparum sporozoites, and are associated with protection against malaria in children. BMC Med 16:61.

39. Weiss WR, Jiang CG. 2012. Protective CD8+ T lymphocytes in primates immunized with malaria sporozoites. PLoS One 7:e31247.

40. Zaidi I, Diallo H, Conteh S, Robbins Y, Kolasny J, Orr-Gonzalez S, Carter D, Butler B, Lambert L, Brickley E, Morrison R, Sissoko M, Healy SA, Sim BKL, Doumbo OK, Hoffman SL, Duffy PE. 2017. gammadelta T Cells Are Required for the Induction of Sterile Immunity during Irradiated Sporozoite Vaccinations. J Immunol 199:3781-3788.

41. Doolan DL, Hoffman SL. 2000. The complexity of protective immunity against liver-stage malaria. J Immunol 165:1453-62.

42. Good MF, Doolan DL. 1999. Immune effector mechanisms in malaria. Curr Opin Immunol 11:412-9.

43. Schofield L, Villaquiran J, Ferreira A, Schellekens H, Nussenzweig R, Nussenzweig V. 1987. Gamma interferon, CD8+ T cells and antibodies required for immunity to malaria sporozoites. Nature 330:664-6.

44. Epstein JE, Paolino KM, Richie TL, Sedegah M, Singer A, Ruben AJ, Chakravarty S, Stafford A, Ruck RC, Eappen AG, Li T, Billingsley PF, Manoj A, Silva JC, Moser K, Nielsen R, Tosh D, Cicatelli S, Ganeshan H, Case J, Padilla D, Davidson S, Garver L, Saverino E, Murshedkar T, Gunasekera A, Twomey PS, Reyes S, Moon JE, James ER, Kc N, Li M, Abot E, Belmonte A, Hauns K, Belmonte M, Huang J, Vasquez C, Remich S, Carrington M, Abebe Y, Tillman A, Hickey B, Regules J, Villasante E, Sim BKL, Hoffman SL. 2017. Protection against Plasmodium falciparum malaria by PfSPZ Vaccine. JCI Insight 2:e89154.

45. Epstein JE, Tewari K, Lyke KE, Sim BK, Billingsley PF, Laurens MB, Gunasekera A, Chakravarty S, James ER, Sedegah M, Richman A, Velmurugan S, Reyes S, Li M, Tucker K, Ahumada A, Ruben AJ, Li T, Stafford R, Eappen AG, Tamminga C, Bennett JW, Ockenhouse CF, Murphy JR, Komisar J, Thomas N, Loyevsky M, Birkett A, Plowe CV, Loucq C, Edelman R, Richie TL, Seder RA, Hoffman SL. 2011. Live attenuated malaria vaccine designed to protect through hepatic CD8(+) T cell immunity. Science 334:475-80.

46. Ishizuka AS, Lyke KE, DeZure A, Berry AA, Richie TL, Mendoza FH, Enama ME, Gordon IJ, Chang LJ, Sarwar UN, Zephir KL, Holman LA, James ER, Billingsley PF, Gunasekera A, Chakravarty S, Manoj A, Li M, Ruben AJ, Li T, Eappen AG, Stafford RE, K CN, Murshedkar T, DeCederfelt H, Plummer SH, Hendel CS, Novik L, Costner PJ, Saunders JG, Laurens MB, Plowe CV, Flynn B, Whalen WR, Todd JP, Noor J, Rao S, Sierra-Davidson K, Lynn GM, Epstein JE, Kemp MA, Fahle GA, Mikolajczak SA, Fishbaugher M, Sack BK, Kappe SH, Davidson SA, Garver LS, Bjorkstrom NK, Nason

MC, et al. 2016. Protection against malaria at 1 year and immune correlates following PfSPZ vaccination. Nat Med 22:614-23.

47. Mordmuller B, Surat G, Lagler H, Chakravarty S, Ishizuka AS, Lalremruata A, Gmeiner M, Campo JJ, Esen M, Ruben AJ, Held J, Calle CL, Mengue JB, Gebru T, Ibanez J, Sulyok M, James ER, Billingsley PF, Natasha KC, Manoj A, Murshedkar T, Gunasekera A, Eappen AG, Li T, Stafford RE, Li M, Felgner PL, Seder RA, Richie TL, Sim BK, Hoffman SL, Kremsner PG. 2017. Sterile protection against human malaria by chemoattenuated PfSPZ vaccine. Nature 542:445-449.

48. Seder RA, Chang LJ, Enama ME, Zephir KL, Sarwar UN, Gordon IJ, Holman LA, James ER, Billingsley PF, Gunasekera A, Richman A, Chakravarty S, Manoj A, Velmurugan S, Li M, Ruben AJ, Li T, Eappen AG, Stafford RE, Plummer SH, Hendel CS, Novik L, Costner PJ, Mendoza FH, Saunders JG, Nason MC, Richardson JH, Murphy J, Davidson SA, Richie TL, Sedegah M, Sutamihardja A, Fahle GA, Lyke KE, Laurens MB, Roederer M, Tewari K, Epstein JE, Sim BK, Ledgerwood JE, Graham BS, Hoffman SL, Team VRCS. 2013. Protection against malaria by intravenous immunization with a nonreplicating sporozoite vaccine. Science 341:1359-65.

49. Lyke KE, Ishizuka AS, Berry AA, Chakravarty S, DeZure A, Enama ME, James ER, Billingsley PF, Gunasekera A, Manoj A, Li M, Ruben AJ, Li T, Eappen AG, Stafford RE, Kc N, Murshedkar T, Mendoza FH, Gordon IJ, Zephir KL, Holman LA, Plummer SH, Hendel CS, Novik L, Costner PJ, Saunders JG, Berkowitz NM, Flynn BJ, Nason MC, Garver LS, Laurens MB, Plowe CV, Richie TL, Graham BS, Roederer M, Sim BK, Ledgerwood JE, Hoffman SL, Seder RA. 2017. Attenuated PfSPZ Vaccine induces strain-transcending T cells and durable protection against heterologous controlled human malaria infection. Proc Natl Acad Sci U S A 114:2711-2716.

50. Roestenberg M, McCall M, Hopman J, Wiersma J, Luty AJ, van Gemert GJ, van de Vegte-Bolmer M, van Schaijk B, Teelen K, Arens T, Spaarman L, de Mast Q, Roeffen W, Snounou G, Renia L, van der Ven A, Hermsen CC, Sauerwein R. 2009. Protection against a malaria challenge by sporozoite inoculation. N Engl J Med 361:468-77.

51. Bijker EM, Teirlinck AC, Schats R, van Gemert GJ, van de Vegte-Bolmer M, van Lieshout L, IntHout J, Hermsen CC, Scholzen A, Visser LG, Sauerwein RW. 2014. Cytotoxic markers associate with protection against malaria in human volunteers immunized with Plasmodium falciparum sporozoites. J Infect Dis 210:1605-15.

52. Sissoko MS, Healy SA, Katile A, Omaswa F, Zaidi I, Gabriel EE, Kamate B, Samake Y, Guindo MA, Dolo A, Niangaly A, Niare K, Zeguime A, Sissoko K, Diallo H, Thera I, Ding K, Fay MP, O'Connell EM, Nutman TB, Wong-Madden S, Murshedkar T, Ruben AJ, Li M, Abebe Y, Manoj A, Gunasekera A, Chakravarty S, Sim BKL, Billingsley PF, James ER, Walther M, Richie TL, Hoffman SL, Doumbo O, Duffy PE. 2017. Safety and efficacy of PfSPZ Vaccine against Plasmodium falciparum via direct venous inoculation in healthy malaria-exposed adults in Mali: a randomised, double-blind phase 1 trial. Lancet Infect Dis 17:498-509.

53. Duffy PE, Patrick Gorres J. 2020. Malaria vaccines since 2000: progress, priorities, products. NPJ Vaccines 5:48.

54. Cockburn IA, Seder RA. 2018. Malaria prevention: from immunological concepts to effective vaccines and protective antibodies. Nat Immunol 19:1199-1211.

55. Fernandez-Ruiz D, Ng WY, Holz LE, Ma JZ, Zaid A, Wong YC, Lau LS, Mollard V, Cozijnsen A, Collins N, Li J, Davey GM, Kato Y, Devi S, Skandari R, Pauley M, Manton JH, Godfrey DI, Braun A, Tay SS, Tan PS, Bowen DG, Koch-Nolte F, Rissiek B, Carbone FR, Crabb BS, Lahoud M, Cockburn IA, Mueller SN, Bertolino P, McFadden GI, Caminschi I, Heath WR. 2016. Liver-Resident Memory CD8(+) T Cells Form a Front-Line Defense against Malaria Liver-Stage Infection. Immunity 45:889-902.

56. Tse SW, Radtke AJ, Espinosa DA, Cockburn IA, Zavala F. 2014. The chemokine receptor CXCR6 is required for the maintenance of liver memory CD8(+) T cells specific for infectious pathogens. J Infect Dis 210:1508-16.

57. Laurens MB. 2019. RTS,S/AS01 vaccine (Mosquirix): an overview. Hum Vaccin Immunother doi:10.1080/21645515.2019.1669415:1-10.

58. Olotu A, Fegan G, Wambua J, Nyangweso G, Leach A, Lievens M, Kaslow DC, Njuguna P, Marsh K, Bejon P. 2016. Seven-Year Efficacy of RTS,S/AS01 Malaria Vaccine among Young African Children. N Engl J Med 374:2519-29.

59. Arora N, L CA, Pannu AK. 2021. Towards Eradication of Malaria: Is the WHO's RTS,S/AS01 Vaccination Effective Enough? Risk Manag Healthc Policy 14:1033-1039.

60. Neafsey DE, Juraska M, Bedford T, Benkeser D, Valim C, Griggs A, Lievens M, Abdulla S, Adjei S, Agbenyega T, Agnandji ST, Aide P, Anderson S, Ansong D, Aponte JJ, Asante KP, Bejon P, Birkett AJ, Bruls M, Connolly KM, D'Alessandro U, Dobano C, Gesase S, Greenwood B, Grimsby J, Tinto H, Hamel MJ, Hoffman I, Kamthunzi P, Kariuki S, Kremsner PG, Leach A, Lell B, Lennon NJ, Lusingu J, Marsh K, Martinson F, Molel JT, Moss EL, Njuguna P, Ockenhouse CF, Ogutu BR, Otieno W, Otieno L, Otieno K, Owusu-Agyei S, Park DJ, Pelle K, Robbins D, Russ C, et al. 2015. Genetic Diversity and Protective Efficacy of the RTS,S/AS01 Malaria Vaccine. N Engl J Med 373:2025-2037.

61. Bongfen SE, Ntsama PM, Offner S, Smith T, Felger I, Tanner M, Alonso P, Nebie I, Romero JF, Silvie O, Torgler R, Corradin G. 2009. The N-terminal domain of Plasmodium falciparum circumsporozoite protein represents a target of protective immunity. Vaccine 27:328-35.

62. Rts SCTP. 2015. Efficacy and safety of RTS,S/AS01 malaria vaccine with or without a booster dose in infants and children in Africa: final results of a phase 3, individually randomised, controlled trial. Lancet 386:31-45.

63. Moris P, Jongert E, van der Most RG. 2018. Characterization of T-cell immune responses in clinical trials of the candidate RTS,S malaria vaccine. Hum Vaccin Immunother 14:17-27.

64. Cohen S, Mc GI, Carrington S. 1961. Gamma-globulin and acquired immunity to human malaria. Nature 192:733-7.

65. Crompton PD, Kayala MA, Traore B, Kayentao K, Ongoiba A, Weiss GE, Molina DM, Burk CR, Waisberg M, Jasinskas A, Tan X, Doumbo S, Doumtabe D, Kone Y, Narum DL, Liang X, Doumbo OK, Miller LH, Doolan DL, Baldi P, Felgner PL, Pierce SK. 2010. A prospective analysis of the Ab response to Plasmodium falciparum before and after a malaria season by protein microarray. Proc Natl Acad Sci U S A 107:6958-63.

66. Teo A, Feng G, Brown GV, Beeson JG, Rogerson SJ. 2016. Functional Antibodies and Protection against Blood-stage Malaria. Trends Parasitol 32:887-898.

67. Fowkes FJ, Richards JS, Simpson JA, Beeson JG. 2010. The relationship between anti-merozoite antibodies and incidence of Plasmodium falciparum malaria: A systematic review and meta-analysis. PLoS Med 7:e1000218.

68. Beeson JG, Drew DR, Boyle MJ, Feng G, Fowkes FJ, Richards JS. 2016. Merozoite surface proteins in red blood cell invasion, immunity and vaccines against malaria. FEMS Microbiol Rev 40:343-72.

69. Richards JS, Arumugam TU, Reiling L, Healer J, Hodder AN, Fowkes FJ, Cross N, Langer C, Takeo S, Uboldi AD, Thompson JK, Gilson PR, Coppel RL, Siba PM, King CL, Torii M, Chitnis CE, Narum DL, Mueller I, Crabb BS, Cowman AF, Tsuboi T, Beeson JG. 2013. Identification and prioritization of merozoite antigens as targets of protective human immunity to Plasmodium falciparum malaria for vaccine and biomarker development. J Immunol 191:795-809.

70. Weiss GE, Gilson PR, Taechalertpaisarn T, Tham WH, de Jong NW, Harvey KL, Fowkes FJ, Barlow PN, Rayner JC, Wright GJ, Cowman AF, Crabb BS. 2015. Revealing the sequence and resulting cellular morphology of receptor-ligand interactions during Plasmodium falciparum invasion of erythrocytes. PLoS Pathog 11:e1004670.

71. Thera MA, Doumbo OK, Coulibaly D, Laurens MB, Ouattara A, Kone AK, Guindo AB, Traore K, Traore I, Kouriba B, Diallo DA, Diarra I, Daou M, Dolo A, Tolo Y, Sissoko MS, Niangaly A, Sissoko M, Takala-Harrison S, Lyke KE, Wu Y, Blackwelder WC, Godeaux O, Vekemans J, Dubois MC, Ballou WR, Cohen J, Thompson D, Dube T, Soisson L, Diggs CL, House B, Lanar DE, Dutta S, Heppner DG, Jr., Plowe CV. 2011. A field trial to assess a blood-stage malaria vaccine. N Engl J Med 365:1004-13.

72. Chan JA, Fowkes FJ, Beeson JG. 2014. Surface antigens of Plasmodium falciparum-infected erythrocytes as immune targets and malaria vaccine candidates. Cell Mol Life Sci 71:3633-57.

73. Stanisic DI, Barry AE, Good MF. 2013. Escaping the immune system: How the malaria parasite makes vaccine development a challenge. Trends Parasitol 29:612-22.

74. Troye-Blomberg M, Worku S, Tangteerawatana P, Jamshaid R, Soderstrom K, Elghazali G, Moretta L, Hammarstrom M, Mincheva-Nilsson L. 1999. Human gamma delta T cells that inhibit the in vitro growth of the asexual blood stages of the Plasmodium falciparum parasite express cytolytic and proinflammatory molecules. Scand J Immunol 50:642-50.

75. Worku S, Bjorkman A, Troye-Blomberg M, Jemaneh L, Farnert A, Christensson B. 1997. Lymphocyte activation and subset redistribution in the peripheral blood in acute malaria illness: distinct gammadelta+ T cell patterns in Plasmodium falciparum and P. vivax infections. Clin Exp Immunol 108:34-41.

76. Junqueira C, Barbosa CRR, Costa PAC, Teixeira-Carvalho A, Castro G, Sen Santara S, Barbosa RP, Dotiwala F, Pereira DB, Antonelli LR, Lieberman J, Gazzinelli RT. 2018. Cytotoxic CD8(+) T cells recognize and kill Plasmodium vivax-infected reticulocytes. Nat Med 24:1330-1336.

77. Junqueira C, Polidoro RB, Castro G, Absalon S, Liang Z, Sen Santara S, Crespo A, Pereira DB, Gazzinelli RT, Dvorin JD, Lieberman J. 2021. gammadelta T cells suppress Plasmodium falciparum blood-stage infection by direct killing and phagocytosis. Nat Immunol 22:347-357.

78. Hviid L, Jensen AT. 2015. PfEMP1 - A Parasite Protein Family of Key Importance in Plasmodium falciparum Malaria Immunity and Pathogenesis. Adv Parasitol 88:51-84.

79. Auburn S, Getachew S, Pearson RD, Amato R, Miotto O, Trimarsanto H, Zhu SJ, Rumaseb A, Marfurt J, Noviyanti R, Grigg MJ, Barber B, William T, Goncalves SM, Drury E, Sriprawat K, Anstey NM, Nosten F, Petros B, Aseffa A, McVean G, Kwiatkowski DP, Price RN. 2019. Genomic Analysis of Plasmodium vivax in Southern Ethiopia Reveals Selective Pressures in Multiple Parasite Mechanisms. J Infect Dis 220:1738-1749.

80. Chen SB, Wang Y, Kassegne K, Xu B, Shen HM, Chen JH. 2017. Whole-genome sequencing of a Plasmodium vivax clinical isolate exhibits geographical characteristics and high genetic variation in China-Myanmar border area. BMC Genomics 18:131.

81. Ford A, Kepple D, Abagero BR, Connors J, Pearson R, Auburn S, Getachew S, Ford C, Gunalan K, Miller LH, Janies DA, Rayner JC, Yan G, Yewhalaw D, Lo E. 2020. Whole genome sequencing of Plasmodium vivax isolates reveals frequent sequence and structural polymorphisms in erythrocyte binding genes. PLoS Negl Trop Dis 14:e0008234.

82. Miller LH, Baruch DI, Marsh K, Doumbo OK. 2002. The pathogenic basis of malaria. Nature 415:673-9.

83. Fried M, Duffy PE. 1996. Adherence of Plasmodium falciparum to chondroitin sulfate A in the human placenta. Science 272:1502-4.

84. Rasti N, Wahlgren M, Chen Q. 2004. Molecular aspects of malaria pathogenesis. FEMS Immunol Med Microbiol 41:9-26.

85. Reeder JC, Cowman AF, Davern KM, Beeson JG, Thompson JK, Rogerson SJ, Brown GV. 1999. The adhesion of Plasmodium falciparum-infected erythrocytes to chondroitin sulfate A is mediated by P. falciparum erythrocyte membrane protein 1. Proc Natl Acad Sci U S A 96:5198-202.

86. Lavazec C. 2017. Molecular mechanisms of deformability of Plasmodium-infected erythrocytes. Curr Opin Microbiol 40:138-144.

87. Mohandas N, Gallagher PG. 2008. Red cell membrane: past, present, and future. Blood 112:3939-48.

88. Baruch DI, Pasloske BL, Singh HB, Bi X, Ma XC, Feldman M, Taraschi TF, Howard RJ. 1995. Cloning the P. falciparum gene encoding PfEMP1, a malarial variant antigen and adherence receptor on the surface of parasitized human erythrocytes. Cell 82:77-87.

89. Smith JD, Chitnis CE, Craig AG, Roberts DJ, Hudson-Taylor DE, Peterson DS, Pinches R, Newbold CI, Miller LH. 1995. Switches in expression of Plasmodium falciparum var genes correlate with changes in antigenic and cytoadherent phenotypes of infected erythrocytes. Cell 82:101-10.

90. Su XZ, Heatwole VM, Wertheimer SP, Guinet F, Herrfeldt JA, Peterson DS, Ravetch JA, Wellems TE. 1995. The large diverse gene family var encodes proteins involved in cytoadherence and antigenic variation of Plasmodium falciparum-infected erythrocytes. Cell 82:89-100.

91. Baruch DI, Gormely JA, Ma C, Howard RJ, Pasloske BL. 1996. Plasmodium falciparum erythrocyte membrane protein 1 is a parasitized erythrocyte receptor for adherence to CD36, thrombospondin, and intercellular adhesion molecule 1. Proc Natl Acad Sci U S A 93:3497-502.

92. Duraisingh MT, Voss TS, Marty AJ, Duffy MF, Good RT, Thompson JK, Freitas-Junior LH, Scherf A, Crabb BS, Cowman AF. 2005. Heterochromatin silencing and locus repositioning linked to regulation of virulence genes in Plasmodium falciparum. Cell 121:13-24.

93. Freitas-Junior LH, Hernandez-Rivas R, Ralph SA, Montiel-Condado D, Ruvalcaba-Salazar OK, Rojas-Meza AP, Mancio-Silva L, Leal-Silvestre RJ, Gontijo AM, Shorte S, Scherf A. 2005. Telomeric heterochromatin propagation and histone acetylation control mutually exclusive expression of antigenic variation genes in malaria parasites. Cell 121:25-36.

94. Tonkin CJ, Carret CK, Duraisingh MT, Voss TS, Ralph SA, Hommel M, Duffy MF, Silva LM, Scherf A, Ivens A, Speed TP, Beeson JG, Cowman AF. 2009. Sir2 paralogues cooperate to regulate virulence genes and antigenic variation in Plasmodium falciparum. PLoS Biol 7:e84.

95. Lopez-Rubio JJ, Mancio-Silva L, Scherf A. 2009. Genome-wide analysis of heterochromatin associates clonally variant gene regulation with perinuclear repressive centers in malaria parasites. Cell Host Microbe 5:179-90.

96. Ralph SA, Scherf A. 2005. The epigenetic control of antigenic variation in Plasmodium falciparum. Curr Opin Microbiol 8:434-40.

97. Scherf A, Riviere L, Lopez-Rubio JJ. 2008. SnapShot: var gene expression in the malaria parasite. Cell 134:190.

98. Scherf A, Hernandez-Rivas R, Buffet P, Bottius E, Benatar C, Pouvelle B, Gysin J, Lanzer M. 1998. Antigenic variation in malaria: in situ switching, relaxed and mutually exclusive transcription of var genes during intra-erythrocytic development in Plasmodium falciparum. EMBO J 17:5418-26.

99. Schieck E, Pfahler JM, Sanchez CP, Lanzer M. 2007. Nuclear run-on analysis of var gene expression in Plasmodium falciparum. Mol Biochem Parasitol 153:207-12.

100. Lopez-Rubio JJ, Gontijo AM, Nunes MC, Issar N, Hernandez Rivas R, Scherf A. 2007. 5' flanking region of var genes nucleate histone modification patterns linked to phenotypic inheritance of virulence traits in malaria parasites. Mol Microbiol 66:1296-305.

101. Volz JC, Bartfai R, Petter M, Langer C, Josling GA, Tsuboi T, Schwach F, Baum J, Rayner JC, Stunnenberg HG, Duffy MF, Cowman AF. 2012. PfSET10, a Plasmodium falciparum methyltransferase, maintains the active var gene in a poised state during parasite division. Cell Host Microbe 11:7-18.

102. Roberts DJ, Craig AG, Berendt AR, Pinches R, Nash G, Marsh K, Newbold CI. 1992. Rapid switching to multiple antigenic and adhesive phenotypes in malaria. Nature 357:689-92.

103. Brown KN, Brown IN. 1965. Immunity to malaria: antigenic variation in chronic infections of Plasmodium knowlesi. Nature 208:1286-8.

104. Barnwell JW, Howard RJ, Coon HG, Miller LH. 1983. Splenic requirement for antigenic variation and expression of the variant antigen on the erythrocyte membrane in cloned Plasmodium knowlesi malaria. Infect Immun 40:985-94.

105. Barnwell JW, Howard RJ, Miller LH. 1982. Altered expression of Plasmodium knowlesi variant antigen on the erythrocyte membrane in splenectomized rhesus monkeys. J Immunol 128:224-6.

106. Wang CW, Mwakalinga SB, Sutherland CJ, Schwank S, Sharp S, Hermsen CC, Sauerwein RW, Theander TG, Lavstsen T. 2010. Identification of a major rif transcript common to gametocytes and sporozoites of Plasmodium falciparum. Malar J 9:147.

107. Wang CW, Hermsen CC, Sauerwein RW, Arnot DE, Theander TG, Lavstsen T. 2009. The Plasmodium falciparum var gene transcription strategy at the onset of blood stage infection in a human volunteer. Parasitol Int 58:478-80.

108. Lavstsen T, Magistrado P, Hermsen CC, Salanti A, Jensen AT, Sauerwein R, Hviid L, Theander TG, Staalsoe T. 2005. Expression of Plasmodium falciparum erythrocyte membrane protein 1 in experimentally infected humans. Malar J 4:21.

109. Desai M, ter Kuile FO, Nosten F, McGready R, Asamoa K, Brabin B, Newman RD. 2007. Epidemiology and burden of malaria in pregnancy. Lancet Infect Dis 7:93-104.

110. Guyatt HL, Snow RW. 2004. Impact of malaria during pregnancy on low birth weight in sub-Saharan Africa. Clin Microbiol Rev 17:760-9, table of contents.

111. Akuze J, Blencowe H, Waiswa P, Baschieri A, Gordeev VS, Kwesiga D, Fisker AB, Thysen SM, Rodrigues A, Biks GA, Abebe SM, Gelaye KA, Mengistu MY, Geremew BM, Delele TG, Tesega AK, Yitayew TA, Kasasa S, Galiwango E, Natukwatsa D, Kajungu D, Enuameh YA, Nettey OE, Dzabeng F, Amenga-Etego S, Newton SK, Tawiah C, Asante KP, Owusu-Agyei S, Alam N, Haider MM, Imam A, Mahmud K, Cousens S, Lawn JE, Every Newborn ISCG. 2020. Randomised comparison of two household survey modules for measuring stillbirths and neonatal deaths in five countries: the Every Newborn-INDEPTH study. Lancet Glob Health 8:e555-e566.

112. Moore KA, Simpson JA, Scoullar MJL, McGready R, Fowkes FJI. 2017. Quantification of the association between malaria in pregnancy and stillbirth: a systematic review and meta-analysis. Lancet Glob Health 5:e1101-e1112.

113. Muehlenbachs A, Mutabingwa TK, Edmonds S, Fried M, Duffy PE. 2006. Hypertension and maternal-fetal conflict during placental malaria. PLoS Med 3:e446.

114. Ndao CT, Dumont A, Fievet N, Doucoure S, Gaye A, Lehesran JY. 2009. Placental malarial infection as a risk factor for hypertensive disorders during pregnancy in Africa: a case-control study in an urban area of Senegal, West Africa. Am J Epidemiol 170:847-53.

115. Shulman CE, Graham WJ, Jilo H, Lowe BS, New L, Obiero J, Snow RW, Marsh K. 1996. Malaria is an important cause of anaemia in primigravidae: evidence from a district hospital in coastal Kenya. Trans R Soc Trop Med Hyg 90:535-9.

116. Verhoeff FH, Brabin BJ, Chimsuku L, Kazembe P, Broadhead RL. 1999. An analysis of the determinants of anaemia in pregnant women in rural Malawi--a basis for action. Ann Trop Med Parasitol 93:119-33.

117. Ahmed R, Singh N, ter Kuile FO, Bharti PK, Singh PP, Desai M, Udhayakumar V, Terlouw DJ. 2014. Placental infections with histologically confirmed Plasmodium falciparum are associated with adverse birth outcomes in India: a cross-sectional study. Malar J 13:232.

118. Brabin BJ, Romagosa C, Abdelgalil S, Menendez C, Verhoeff FH, McGready R, Fletcher KA, Owens S, D'Alessandro U, Nosten F, Fischer PR, Ordi J. 2004. The sick placenta-the role of malaria. Placenta 25:359-78.

119. Rogerson SJ, Hviid L, Duffy PE, Leke RF, Taylor DW. 2007. Malaria in pregnancy: pathogenesis and immunity. Lancet Infect Dis 7:105-17.

120. Tuikue Ndam NG, Salanti A, Bertin G, Dahlback M, Fievet N, Turner L, Gaye A, Theander T, Deloron P. 2005. High level of var2csa transcription by Plasmodium falciparum isolated from the placenta. J Infect Dis 192:331-5.

121. Salanti A, Dahlback M, Turner L, Nielsen MA, Barfod L, Magistrado P, Jensen AT, Lavstsen T, Ofori MF, Marsh K, Hviid L, Theander TG. 2004. Evidence for the involvement of VAR2CSA in pregnancy-associated malaria. J Exp Med 200:1197-203.

122. Achur RN, Valiyaveettil M, Alkhalil A, Ockenhouse CF, Gowda DC. 2000. Characterization of proteoglycans of human placenta and identification of unique chondroitin sulfate proteoglycans of the intervillous spaces that mediate the adherence of Plasmodium falciparum-infected erythrocytes to the placenta. J Biol Chem 275:40344-56.

123. Agbor-Enoh ST, Achur RN, Valiyaveettil M, Leke R, Taylor DW, Gowda DC. 2003. Chondroitin sulfate proteoglycan expression and binding of Plasmodium falciparum-infected erythrocytes in the human placenta during pregnancy. Infect Immun 71:2455-61.

124. Gysin J, Pouvelle B, Fievet N, Scherf A, Lepolard C. 1999. Ex vivo desequestration of Plasmodium falciparum-infected erythrocytes from human placenta by chondroitin sulfate A. Infect Immun 67:6596-602.

125. Maubert B, Guilbert LJ, Deloron P. 1997. Cytoadherence of Plasmodium falciparum to intercellular adhesion molecule 1 and chondroitin-4-sulfate expressed by the syncytiotrophoblast in the human placenta. Infect Immun 65:1251-7.

126. Gamain B, Trimnell AR, Scheidig C, Scherf A, Miller LH, Smith JD. 2005. Identification of multiple chondroitin sulfate A (CSA)-binding domains in the var2CSA gene transcribed in CSA-binding parasites. J Infect Dis 191:1010-3.

127. Duffy MF, Byrne TJ, Elliott SR, Wilson DW, Rogerson SJ, Beeson JG, Noviyanti R, Brown GV. 2005. Broad analysis reveals a consistent pattern of var gene transcription in Plasmodium falciparum repeatedly selected for a defined adhesion phenotype. Mol Microbiol 56:774-88.

128. Elliott SR, Duffy MF, Byrne TJ, Beeson JG, Mann EJ, Wilson DW, Rogerson SJ, Brown GV. 2005. Cross-reactive surface epitopes on chondroitin sulfate A-adherent Plasmodium falciparum-infected erythrocytes are associated with transcription of var2csa. Infect Immun 73:2848-56.

129. Salanti A, Staalsoe T, Lavstsen T, Jensen AT, Sowa MP, Arnot DE, Hviid L, Theander TG. 2003. Selective upregulation of a single distinctly structured var gene in chondroitin sulphate A-adhering Plasmodium falciparum involved in pregnancy-associated malaria. Mol Microbiol 49:179-91.

130. Viebig NK, Gamain B, Scheidig C, Lepolard C, Przyborski J, Lanzer M, Gysin J, Scherf A. 2005. A single member of the Plasmodium falciparum var multigene family determines cytoadhesion to the placental receptor chondroitin sulphate A. EMBO Rep 6:775-81.

131. Salanti A, Clausen TM, Agerbaek MO, Al Nakouzi N, Dahlback M, Oo HZ, Lee S, Gustavsson T, Rich JR, Hedberg BJ, Mao Y, Barington L, Pereira MA, LoBello J, Endo M, Fazli L, Soden J, Wang CK, Sander AF, Dagil R, Thrane S, Holst PJ, Meng L, Favero F, Weiss GJ, Nielsen MA, Freeth J, Nielsen TO, Zaia J, Tran NL, Trent J, Babcook JS, Theander TG, Sorensen PH, Daugaard M. 2015. Targeting Human Cancer by a Glycosaminoglycan Binding Malaria Protein. Cancer Cell 28:500-514.

132. Baston-Bust DM, Gotte M, Janni W, Krussel JS, Hess AP. 2010. Syndecan-1 knock-down in decidualized human endometrial stromal cells leads to significant changes in cytokine and angiogenic factor expression patterns. Reprod Biol Endocrinol 8:133.

133. Nordmaj MA, Roberts ME, Sachse ES, Dagil R, Andersen AP, Skeltved N, Grunddal KV, Erdogan SM, Choudhary S, Gustsavsson T, Orum-Madsen MS, Moskalev I, Tian W, Yang Z, Clausen TM, Theander TG, Daugaard M, Nielsen MA, Salanti A. 2021. Development of a bispecific immune engager using a recombinant malaria protein. Cell Death Dis 12:353.

134. Clausen TM, Pereira MA, Al Nakouzi N, Oo HZ, Agerbaek MO, Lee S, Orum-Madsen MS, Kristensen AR, El-Naggar A, Grandgenett PM, Grem JL, Hollingsworth MA, Holst PJ, Theander T, Sorensen PH, Daugaard M, Salanti A. 2016. Oncofetal Chondroitin Sulfate Glycosaminoglycans Are Key Players in Integrin Signaling and Tumor Cell Motility. Mol Cancer Res 14:1288-1299.

135. Bang-Christensen SR, Pedersen RS, Pereira MA, Clausen TM, Loppke C, Sand NT, Ahrens TD, Jorgensen AM, Lim YC, Goksoyr L, Choudhary S, Gustavsson T, Dagil R, Daugaard M, Sander AF, Torp MH, Sogaard M, Theander TG, Ostrup O, Lassen U, Hamerlik P, Salanti A, Agerbaek MO. 2019. Capture and Detection of Circulating Glioma Cells Using the Recombinant VAR2CSA Malaria Protein. Cells 8.

136. Clausen TM, Kumar G, Ibsen EK, Orum-Madsen MS, Hurtado-Coll A, Gustavsson T, Agerbaek MO, Gatto F, Todenhofer T, Basso U, Knowles MA, Sanchez-Carbayo M, Salanti A, Black PC, Daugaard M. 2020. A simple method for detecting oncofetal chondroitin sulfate glycosaminoglycans in bladder cancer urine. Cell Death Discov 6:65.

137. Sand NT, Petersen TB, Bang-Christensen SR, Ahrens TD, Loppke C, Jorgensen AM, Gustavsson T, Choudhary S, Theander TG, Salanti A, Agerbaek MO. 2020. Optimization of rVAR2-Based Isolation of Cancer Cells in Blood for Building a Robust Assay for Clinical Detection of Circulating Tumor Cells. Int J Mol Sci 21.

138. Zhao K, Cheng G, Zhang B, Li D, Han J, Chen J, Wang B, Li M, Xiao T, Le A, Sun B, Jin Z, Zhang J, Fan X. 2020. Targeting delivery of partial VAR2CSA peptide guided N-2-Hydroxypropyl trimethyl ammonium chloride chitosan nanoparticles for multiple cancer types. Mater Sci Eng C Mater Biol Appl 106:110171.

139. Clausen TM, Christoffersen S, Dahlback M, Langkilde AE, Jensen KE, Resende M, Agerbaek MO, Andersen D, Berisha B, Ditlev SB, Pinto VV, Nielsen MA, Theander TG, Larsen S, Salanti A. 2012. Structural and functional insight into how the Plasmodium falciparum VAR2CSA protein mediates binding to chondroitin sulfate A in placental malaria. J Biol Chem 287:23332-45.

140. Hviid L, Salanti A. 2007. VAR2CSA and protective immunity against pregnancy-associated Plasmodium falciparum malaria. Parasitology 134:1871-6.

141. O'Neil-Dunne I, Achur RN, Agbor-Enoh ST, Valiyaveettil M, Naik RS, Ockenhouse CF, Zhou A, Megnekou R, Leke R, Taylor DW, Gowda DC. 2001. Gravidity-dependent production of antibodies that inhibit binding of Plasmodium falciparum-infected erythrocytes to placental chondroitin sulfate proteoglycan during pregnancy. Infect Immun 69:7487-92.

142. Tuikue Ndam NG, Salanti A, Le-Hesran JY, Cottrell G, Fievet N, Turner L, Sow S, Dangou JM, Theander T, Deloron P. 2006. Dynamics of anti-VAR2CSA immunoglobulin G response in a cohort of senegalese pregnant women. J Infect Dis 193:713-20.

143. Babakhanyan A, Leke RG, Salanti A, Bobbili N, Gwanmesia P, Leke RJ, Quakyi IA, Chen JJ, Taylor DW. 2014. The antibody response of pregnant Cameroonian women to VAR2CSA ID1-ID2a, a small recombinant protein containing the CSA-binding site. PLoS One 9:e88173.

144. Dechavanne S, Srivastava A, Gangnard S, Nunes-Silva S, Dechavanne C, Fievet N, Deloron P, Chene A, Gamain B. 2015. Parity-dependent recognition of DBL1X-3X suggests an important role of the VAR2CSA high-affinity CSA-binding region in the development of the humoral response against placental malaria. Infect Immun 83:2466-74.

145. Tutterrow YL, Salanti A, Avril M, Smith JD, Pagano IS, Ako S, Fogako J, Leke RG, Taylor DW. 2012. High avidity antibodies to full-length VAR2CSA correlate with absence of placental malaria. PLoS One 7:e40049.

146. Tornyigah B, d'Almeida T, Escriou G, Viwami F, Fievet N, Luty AJF, Massougbodji A, Nielsen MA, Deloron P, Tuikue Ndam N. 2021. Plasmodium falciparum VAR2CSA-Specific IgG Subclass Responses Reflect Protection Against Low Birth Weight and Pregnancy-Associated Malaria. Front Immunol 12:610305.

147. Ndam NT, Denoeud-Ndam L, Doritchamou J, Viwami F, Salanti A, Nielsen MA, Fievet N, Massougbodji A, Luty AJ, Deloron P. 2015. Protective Antibodies against Placental Malaria and Poor Outcomes during Pregnancy, Benin. Emerg Infect Dis 21:813-23.

148. Fried M, Nosten F, Brockman A, Brabin BJ, Duffy PE. 1998. Maternal antibodies block malaria. Nature 395:851-2.

149. Ataide R, Mwapasa V, Molyneux ME, Meshnick SR, Rogerson SJ. 2011. Antibodies that induce phagocytosis of malaria infected erythrocytes: effect of HIV infection and correlation with clinical outcomes. PLoS One 6:e22491.

150. Jaworowski A, Fernandes LA, Yosaatmadja F, Feng G, Mwapasa V, Molyneux ME, Meshnick SR, Lewis J, Rogerson SJ. 2009. Relationship between human immunodeficiency virus type 1 coinfection, anemia, and levels and function of antibodies to variant surface antigens in pregnancy-associated malaria. Clin Vaccine Immunol 16:312-9.

151. Keen J, Serghides L, Ayi K, Patel SN, Ayisi J, van Eijk A, Steketee R, Udhayakumar V, Kain KC. 2007. HIV impairs opsonic phagocytic clearance of pregnancy-associated malaria parasites. PLoS Med 4:e181.

152. Gavina K, Gnidehou S, Arango E, Hamel-Martineau C, Mitran C, Agudelo O, Lopez C, Karidio A, Banman S, Carmona-Fonseca J, Salanti A, Tuikue Ndam N, Hawkes M, Maestre A, Yanow SK. 2018. Clinical Outcomes of Submicroscopic Infections and Correlates of Protection of VAR2CSA Antibodies in a Longitudinal Study of Pregnant Women in Colombia. Infect Immun 86.

153. Cutts JC, Agius PA, Zaw L, Powell R, Moore K, Draper B, Simpson JA, Fowkes FJI. 2020. Pregnancy-specific malarial immunity and risk of malaria in pregnancy and adverse birth outcomes: a systematic review. BMC Med 18:14.

154. Gnidehou S, Doritchamou J, Arango EM, Cabrera A, Arroyo MI, Kain KC, Ndam NT, Maestre A, Yanow SK. 2014. Functional antibodies against VAR2CSA in nonpregnant populations from colombia exposed to Plasmodium falciparum and Plasmodium vivax. Infect Immun 82:2565-73.

155. Gnidehou S, Mitran CJ, Arango E, Banman S, Mena A, Medawar E, Lima BAS, Doritchamou J, Rajwani J, Jin A, Gavina K, Ntumngia F, Duffy P, Narum D, Ndam NT, Nielsen MA, Salanti A, Kano FS, Carvalho LH, Adams JH, Maestre A, Good MF, Yanow SK. 2019. Cross-Species Immune Recognition Between Plasmodium vivax Duffy Binding Protein Antibodies and the Plasmodium falciparum Surface Antigen VAR2CSA. J Infect Dis 219:110-120.

156. Adegnika AA, Verweij JJ, Agnandji ST, Chai SK, Breitling LP, Ramharter M, Frolich M, Issifou S, Kremsner PG, Yazdanbakhsh M. 2006. Microscopic and sub-microscopic Plasmodium falciparum infection, but not inflammation caused by infection, is associated with low birth weight. Am J Trop Med Hyg 75:798-803.

157. Cohee LM, Kalilani-Phiri L, Boudova S, Joshi S, Mukadam R, Seydel KB, Mawindo P, Thesing P, Kamiza S, Makwakwa K, Muehlenbachs A, Taylor TE, Laufer MK. 2014. Submicroscopic malaria infection during pregnancy and the impact of intermittent preventive treatment. Malar J 13:274.

158. Cottrell G, Moussiliou A, Luty AJ, Cot M, Fievet N, Massougbodji A, Deloron P, Tuikue Ndam N. 2015. Submicroscopic Plasmodium falciparum Infections Are Associated With Maternal Anemia, Premature Births, and Low Birth Weight. Clin Infect Dis 60:1481-8.

159. Malhotra I, Dent A, Mungai P, Muchiri E, King CL. 2005. Real-time quantitative PCR for determining the burden of Plasmodium falciparum parasites during pregnancy and infancy. J Clin Microbiol 43:3630-5.

160. Mayor A, Moro L, Aguilar R, Bardaji A, Cistero P, Serra-Casas E, Sigauque B, Alonso PL, Ordi J, Menendez C. 2012. How hidden can malaria be in pregnant women? Diagnosis by microscopy, placental histology, polymerase chain reaction and detection of histidine-rich protein 2 in plasma. Clin Infect Dis 54:1561-8.

161. Mohammed AH, Salih MM, Elhassan EM, Mohmmed AA, Elzaki SE, El-Sayed BB, Adam I. 2013. Submicroscopic Plasmodium falciparum malaria and low birth weight in an area of unstable malaria transmission in Central Sudan. Malar J 12:172.

162. Arango EM, Samuel R, Agudelo OM, Carmona-Fonseca J, Maestre A, Yanow SK. 2013. Molecular detection of malaria at delivery reveals a high frequency of submicroscopic infections and associated placental damage in pregnant women from northwest Colombia. Am J Trop Med Hyg 89:178-83.

163. Agudelo OM, Aristizabal BH, Yanow SK, Arango E, Carmona-Fonseca J, Maestre A. 2014. Submicroscopic infection of placenta by Plasmodium produces Th1/Th2 cytokine imbalance, inflammation and hypoxia in women from north-west Colombia. Malar J 13:122.

164. McGready R, Davison BB, Stepniewska K, Cho T, Shee H, Brockman A, Udomsangpetch R, Looareesuwan S, White NJ, Meshnick SR, Nosten F. 2004. The effects of Plasmodium falciparum and P. vivax infections on placental histopathology in an area of low malaria transmission. Am J Trop Med Hyg 70:398-407.

165. Parekh FK, Davison BB, Gamboa D, Hernandez J, Branch OH. 2010. Placental histopathologic changes associated with subclinical malaria infection and its impact on the fetal environment. Am J Trop Med Hyg 83:973-80.

166. Stanisic DI, Moore KA, Baiwog F, Ura A, Clapham C, King CL, Siba PM, Beeson JG, Mueller I, Fowkes FJ, Rogerson SJ. 2015. Risk factors for malaria and adverse birth outcomes in a prospective cohort of pregnant women resident in a high malaria transmission area of Papua New Guinea. Trans R Soc Trop Med Hyg 109:313-24.

167. Singh N, Bharti PK, Singh MP, Singh R, Yeboah-Antwi K, Desai M, Udhayakumar V, Muniyandi M, Hamer DH, Wylie BJ. 2015. What is the burden of submicroscopic malaria in pregnancy in central India? Pathog Glob Health 109:30-8.

168. Bardaji A, Martinez-Espinosa FE, Arevalo-Herrera M, Padilla N, Kochar S, Ome-Kaius M, Botto-Menezes C, Castellanos ME, Kochar DK, Kochar SK, Betuela I, Mueller I, Rogerson S, Chitnis C, Hans D, Menegon M, Severini C, Del Portillo H, Dobano C,

Mayor A, Ordi J, Piqueras M, Sanz S, Wahlgren M, Slutsker L, Desai M, Menendez C, PregVax Study G. 2017. Burden and impact of Plasmodium vivax in pregnancy: A multi-centre prospective observational study. PLoS Negl Trop Dis 11:e0005606.

169. Kingsbury AN. 1927. Some investigations of malarial fevers. IV. The complement fixation reaction. Trans R Soc Trop Med Hyg 20:359-364.

170. Mayer MM, Heidelberger M. 1946. Studies in human malaria; complement-fixation reactions. J Immunol 54:89-102.

171. Taliaferro WH, Taliaferro, L. G. and Fisher, A. B. . 1927. A precipitin test in malaria. J Prev Med 1:343 - 357.

172. Taliaferro WHaT, L. G. 1928. A precipitin test in malaria. (2nd Rept.). J Prev Med 2:147-167.

173. Taliaferro WH. 1929. The Immunology of Parasitic Infections. The Century Co. , New York.

174. Row R. 1931. Preciptin reaction in malarial sera. Trans R Soc Trop Med Hyg 24:623-7.

175. Tobie JE, Coatney GR. 1961. Fluorescent antibody staining of human malaria parasites. Exp Parasitol 11:128-32.

176. Tobie JE, Kuvin SF, Contacos PG, Coatney GR, Evans CB. 1962. Fluorescent antibody studies on cross reactions between human and simian malaria in normal volunteers. Am J Trop Med Hyg 11:589-96.

177. Diggs CL, Sadun EH. 1965. Serological Cross Reactivity between Plasmodium Vivax and Plasmodium Falciparum as Determined by a Modified Fluorescent Antibody Test. Exp Parasitol 16:217-23.

178. Kumar N, Folgar JP, Lubega P. 1992. Recognition of Plasmodium falciparum asexual stage antigens by antibodies in sera from people exposed to Plasmodium vivax. Am J Trop Med Hyg 47:422-8.

179. Kumar N, Zhao Y, Graves P, Perez Folgar J, Maloy L, Zheng H. 1990. Human immune response directed against Plasmodium falciparum heat shock-related proteins. Infect Immun 58:1408-14.

180. Tsuji M, Mattei D, Nussenzweig RS, Eichinger D, Zavala F. 1994. Demonstration of heat-shock protein 70 in the sporozoite stage of malaria parasites. Parasitol Res 80:16-21.

181. el-Nahal HM. 1967. Serological cross-reaction between rodent malaria parasites as determined by the indirect immunofluorescent technique. Bull World Health Organ 36:423-9.

182. Grun JL, Weidanz WP. 1983. Antibody-independent immunity to reinfection malaria in B-cell-deficient mice. Infect Immun 41:1197-204.

183. Sedegah M, Weiss WW, Hoffman SL. 2007. Cross-protection between attenuated Plasmodium berghei and P. yoelii sporozoites. Parasite Immunol 29:559-65.

184. Butler NS, Schmidt NW, Vaughan AM, Aly AS, Kappe SH, Harty JT. 2011. Superior antimalarial immunity after vaccination with late liver stage-arresting genetically attenuated parasites. Cell Host Microbe 9:451-62.

185. Stanisic DI, Fink J, Mayer J, Coghill S, Gore L, Liu XQ, El-Deeb I, Rodriguez IB, Powell J, Willemsen NM, De SL, Ho MF, Hoffman SL, Gerrard J, Good MF. 2018. Vaccination with chemically attenuated Plasmodium falciparum asexual blood-stage parasites induces parasite-specific cellular immune responses in malaria-naive volunteers: a pilot study. BMC Med 16:184.

186. Mordmuller B, Sulyok M, Egger-Adam D, Resende M, de Jongh WA, Jensen MH, Smedegaard HH, Ditlev SB, Soegaard M, Poulsen L, Dyring C, Calle CL, Knoblich A, Ibanez J, Esen M, Deloron P, Ndam N, Issifou S, Houard S, Howard RF, Reed SG, Leroy O, Luty AJF, Theander TG, Kremsner PG, Salanti A, Nielsen MA. 2019. First-in-human, Randomized, Double-blind Clinical Trial of Differentially Adjuvanted PAMVAC, A Vaccine Candidate to Prevent Pregnancy-associated Malaria. Clin Infect Dis 69:1509-1516.

187. Sirima SB, Richert L, Chene A, Konate AT, Campion C, Dechavanne S, Semblat JP, Benhamouda N, Bahuaud M, Loulergue P, Ouedraogo A, Nebie I, Kabore M, Kargougou D, Barry A, Ouattara SM, Boilet V, Allais F, Roguet G, Havelange N, Lopez-Perez E, Kuppers A, Konate E, Roussillon C, Kante M, Belarbi L, Diarra A, Henry N, Soulama I, Ouedraogo A, Esperou H, Leroy O, Batteux F, Tartour E, Viebig NK, Thiebaut R, Launay O, Gamain B. 2020. PRIMVAC vaccine adjuvanted with Alhydrogel or GLA-SE to prevent placental malaria: a first-in-human, randomised, double-blind, placebo-controlled study. Lancet Infect Dis 20:585-597.

188. Bigey P, Gnidehou S, Doritchamou J, Quiviger M, Viwami F, Couturier A, Salanti A, Nielsen MA, Scherman D, Deloron P, Tuikue Ndam N. 2011. The NTS-DBL2X region of VAR2CSA induces cross-reactive antibodies that inhibit adhesion of several Plasmodium falciparum isolates to chondroitin sulfate A. J Infect Dis 204:1125-33.

189. Chene A, Gangnard S, Dechavanne C, Dechavanne S, Srivastava A, Tetard M, Hundt S, Leroy O, Havelange N, Viebig NK, Gamain B. 2018. Down-selection of the VAR2CSA DBL1-2 expressed in E. coli as a lead antigen for placental malaria vaccine development. NPJ Vaccines 3:28.

190. Chene A, Gangnard S, Guadall A, Ginisty H, Leroy O, Havelange N, Viebig NK, Gamain B. 2019. Preclinical immunogenicity and safety of the cGMP-grade placental malaria vaccine PRIMVAC. EBioMedicine 42:145-156.

191. Dahlback M, Jorgensen LM, Nielsen MA, Clausen TM, Ditlev SB, Resende M, Pinto VV, Arnot DE, Theander TG, Salanti A. 2011. The chondroitin sulfate A-binding site of the VAR2CSA protein involves multiple N-terminal domains. J Biol Chem 286:15908-17.

192. Gamain B, Chene A, Viebig NK, Tuikue Ndam N, Nielsen MA. 2021. Progress and Insights Toward an Effective Placental Malaria Vaccine. Front Immunol 12:634508.

193. Benavente ED, Oresegun DR, de Sessions PF, Walker EM, Roper C, Dombrowski JG, de Souza RM, Marinho CRF, Sutherland CJ, Hibberd ML, Mohareb F, Baker DA, Clark TG, Campino S. 2018. Global genetic diversity of var2csa in Plasmodium falciparum with implications for malaria in pregnancy and vaccine development. Sci Rep 8:15429.

194. Patel JC, Hathaway NJ, Parobek CM, Thwai KL, Madanitsa M, Khairallah C, Kalilani-Phiri L, Mwapasa V, Massougbodji A, Fievet N, Bailey JA, Ter Kuile FO, Deloron P, Engel SM, Taylor SM, Juliano JJ, Tuikue Ndam N, Meshnick SR. 2017. Increased risk of low birth weight in women with placental malaria associated with P. falciparum VAR2CSA clade. Sci Rep 7:7768.

195. Good MF, Stanisic D, Xu H, Elliott S, Wykes M. 2004. The immunological challenge to developing a vaccine to the blood stages of malaria parasites. Immunol Rev 201:254-67.

196. Anonymous. 2014. The contribution of malaria control to maternal and newborn health. World Health Organization on behalf of the Roll Back Malaria Partnership Secretariat, Geneva.

197. Duffy PE. 2007. Plasmodium in the placenta: parasites, parity, protection, prevention and possibly preeclampsia. Parasitology 134:1877-81.

198. Ataide R, Mayor A, Rogerson SJ. 2014. Malaria, primigravidae, and antibodies: knowledge gained and future perspectives. Trends Parasitol 30:85-94.

199. Duffy PE, Fried M. 2003. Antibodies that inhibit Plasmodium falciparum adhesion to chondroitin sulfate A are associated with increased birth weight and the gestational age of newborns. Infect Immun 71:6620-3.

200. Andersen P, Nielsen MA, Resende M, Rask TS, Dahlback M, Theander T, Lund O, Salanti A. 2008. Structural insight into epitopes in the pregnancy-associated malaria protein VAR2CSA. PLoS Pathog 4:e42.

201. Beeson JG, Ndungu F, Persson KE, Chesson JM, Kelly GL, Uyoga S, Hallamore SL, Williams TN, Reeder JC, Brown GV, Marsh K. 2007. Antibodies among men and children to placental-binding Plasmodium falciparum-infected erythrocytes that express var2csa. Am J Trop Med Hyg 77:22-8.

202. Fodjo BA, Atemnkeng N, Esemu L, Yuosembom EK, Quakyi IA, Tchinda VH, Smith J, Salanti A, Bigoga J, Taylor DW, Leke RG, Babakhanyan A. 2016. Antibody responses to

the full-length VAR2CSA and its DBL domains in Cameroonian children and teenagers. Malar J 15:532.

203. Oleinikov AV, Voronkova VV, Frye IT, Amos E, Morrison R, Fried M, Duffy PE. 2012. A plasma survey using 38 PfEMP1 domains reveals frequent recognition of the Plasmodium falciparum antigen VAR2CSA among young Tanzanian children. PLoS One 7:e31011.

204. Adams JH, Sim BK, Dolan SA, Fang X, Kaslow DC, Miller LH. 1992. A family of erythrocyte binding proteins of malaria parasites. Proc Natl Acad Sci U S A 89:7085-9.

205. Hester J, Chan ER, Menard D, Mercereau-Puijalon O, Barnwell J, Zimmerman PA, Serre D. 2013. De novo assembly of a field isolate genome reveals novel Plasmodium vivax erythrocyte invasion genes. PLoS Negl Trop Dis 7:e2569.

206. Howell DP, Samudrala R, Smith JD. 2006. Disguising itself--insights into Plasmodium falciparum binding and immune evasion from the DBL crystal structure. Mol Biochem Parasitol 148:1-9.

207. Choe H, Moore MJ, Owens CM, Wright PL, Vasilieva N, Li W, Singh AP, Shakri R, Chitnis CE, Farzan M. 2005. Sulphated tyrosines mediate association of chemokines and Plasmodium vivax Duffy binding protein with the Duffy antigen/receptor for chemokines (DARC). Mol Microbiol 55:1413-22.

208. Tran TM, Oliveira-Ferreira J, Moreno A, Santos F, Yazdani SS, Chitnis CE, Altman JD, Meyer EV, Barnwell JW, Galinski MR. 2005. Comparison of IgG reactivities to Plasmodium vivax merozoite invasion antigens in a Brazilian Amazon population. Am J Trop Med Hyg 73:244-55.

209. Rodriguez JC, Uribe GA, Araujo RM, Narvaez PC, Valencia SH. 2011. Epidemiology and control of malaria in Colombia. Mem Inst Oswaldo Cruz 106 Suppl 1:114-22.

210. Naranjo-Diaz N, Rosero DA, Rua-Uribe G, Luckhart S, Correa MM. 2013. Abundance, behavior and entomological inoculation rates of anthropophilic anophelines from a primary Colombian malaria endemic area. Parasit Vectors 6:61.

211. Kano FS, Sanchez BA, Sousa TN, Tang ML, Saliba J, Oliveira FM, Nogueira PA, Goncalves AQ, Fontes CJ, Soares IS, Brito CF, Rocha RS, Carvalho LH. 2012. Plasmodium vivax Duffy binding protein: baseline antibody responses and parasite polymorphisms in a well-consolidated settlement of the Amazon Region. Trop Med Int Health 17:989-1000.

212. Kano FS, Souza-Silva FA, Torres LM, Lima BA, Sousa TN, Alves JR, Rocha RS, Fontes CJ, Sanchez BA, Adams JH, Brito CF, Pires DE, Ascher DB, Sell AM, Carvalho LH. 2016. The Presence, Persistence and Functional Properties of Plasmodium vivax Duffy Binding Protein II Antibodies Are Influenced by HLA Class II Allelic Variants. PLoS Negl Trop Dis 10:e0005177.

213. Gavina K, Arango E, larrotta CA, Maestre A, Yanow SK. 2017. A sensitive species-specific reverse transcription real-time PCR method for detection of Plasmodium falciparum and Plasmodium vivax. Parasite Epidemiology and Control 2:70-76.

214. Sousa TN, Kano FS, Brito CF, Carvalho LH. 2014. The Duffy binding protein as a key target for a Plasmodium vivax vaccine: lessons from the Brazilian Amazon. Mem Inst Oswaldo Cruz 0:25-30.

215. Mangold KA, Manson RU, Koay ES, Stephens L, Regner M, Thomson RB, Jr., Peterson LR, Kaul KL. 2005. Real-time PCR for detection and identification of Plasmodium spp. J Clin Microbiol 43:2435-40.

216. Turner L, Lavstsen T, Berger SS, Wang CW, Petersen JE, Avril M, Brazier AJ, Freeth J, Jespersen JS, Nielsen MA, Magistrado P, Lusingu J, Smith JD, Higgins MK, Theander TG. 2013. Severe malaria is associated with parasite binding to endothelial protein C receptor. Nature 498:502-5.

217. Khunrae P, Dahlback M, Nielsen MA, Andersen G, Ditlev SB, Resende M, Pinto VV, Theander TG, Higgins MK, Salanti A. 2010. Full-length recombinant Plasmodium falciparum VAR2CSA binds specifically to CSPG and induces potent parasite adhesion-blocking antibodies. J Mol Biol 397:826-34.

218. Ntumngia FB, Schloegel J, Barnes SJ, McHenry AM, Singh S, King CL, Adams JH. 2012. Conserved and variant epitopes of Plasmodium vivax Duffy binding protein as targets of inhibitory monoclonal antibodies. Infect Immun 80:1203-8.

219. Cham GK, Kurtis J, Lusingu J, Theander TG, Jensen AT, Turner L. 2008. A semi-automated multiplex high-throughput assay for measuring IgG antibodies against Plasmodium falciparum erythrocyte membrane protein 1 (PfEMP1) domains in small volumes of plasma. Malar J 7:108.

220. Nielsen MA, Resende M, de Jongh WA, Ditlev SB, Mordmuller B, Houard S, Ndam NT, Agerbaek MO, Hamborg M, Massougbodji A, Issifou S, Strobaek A, Poulsen L, Leroy O, Kremsner PG, Chippaux JP, Luty AJ, Deloron P, Theander TG, Dyring C, Salanti A. 2015. The Influence of Sub-Unit Composition and Expression System on the Functional Antibody Response in the Development of a VAR2CSA Based Plasmodium falciparum Placental Malaria Vaccine. PLoS One 10:e0135406.

221. Trager W, Jensen JB. 1976. Human malaria parasites in continuous culture. Science 193:673-5.

222. Srivastava A, Gangnard S, Round A, Dechavanne S, Juillerat A, Raynal B, Faure G, Baron B, Ramboarina S, Singh SK, Belrhali H, England P, Lewit-Bentley A, Scherf A, Bentley GA, Gamain B. 2010. Full-length extracellular region of the var2CSA variant of PfEMP1 is required for specific, high-affinity binding to CSA. Proc Natl Acad Sci U S A 107:4884-9.

223. Wipasa J, Suphavilai C, Okell LC, Cook J, Corran PH, Thaikla K, Liewsaree W, Riley EM, Hafalla JC. 2010. Long-lived antibody and B Cell memory responses to the human malaria parasites, Plasmodium falciparum and Plasmodium vivax. PLoS Pathog 6:e1000770.

224. Wang Q, Zhao Z, Zhang X, Li X, Zhu M, Li P, Yang Z, Wang Y, Yan G, Shang H, Cao Y, Fan Q, Cui L. 2016. Naturally Acquired Antibody Responses to Plasmodium vivax and Plasmodium falciparum Merozoite Surface Protein 1 (MSP1) C-Terminal 19 kDa Domains in an Area of Unstable Malaria Transmission in Southeast Asia. PLoS One 11:e0151900.

225. Requena P, Arevalo-Herrera M, Menegon M, Martinez-Espinosa FE, Padilla N, Botto-Menezes C, Malheiro A, Hans D, Castellanos ME, Robinson L, Samol P, Kochar S, Kochar SK, Kochar DK, Desai M, Sanz S, Quinto L, Mayor A, Rogerson S, Mueller I, Severini C, Del Portillo HA, Bardaji A, Chitnis CC, Menendez C, Dobano C. 2017. Naturally Acquired Binding-Inhibitory Antibodies to Plasmodium vivax Duffy Binding Protein in Pregnant Women Are Associated with Higher Birth Weight in a Multicenter Study. Front Immunol 8:163.

226. Nagao Y, Kimura-Sato M, Chavalitshewinkoon-Petmitr P, Thongrungkiat S, Wilairatana P, Ishida T, Tan-Ariya P, de Souza JB, Krudsood S, Looareesuwan S. 2008. Suppression of Plasmodium falciparum by serum collected from a case of Plasmodium vivax infection. Malar J 7:113.

227. Chuangchaiya S, Jangpatarapongsa K, Chootong P, Sirichaisinthop J, Sattabongkot J, Pattanapanyasat K, Chotivanich K, Troye-Blomberg M, Cui L, Udomsangpetch R. 2010. Immune response to Plasmodium vivax has a potential to reduce malaria severity. Clin Exp Immunol 160:233-9.

228. Costa JD, Zanchi FB, Rodrigues FL, Honda ER, Katsuragawa TH, Pereira DB, Taborda RL, Tada MS, Ferreira Rde G, Pereira-da-Silva LH. 2013. Cross-reactive anti-PfCLAG9 antibodies in the sera of asymptomatic parasite carriers of Plasmodium vivax. Mem Inst Oswaldo Cruz 108:98-105.

229. Woodberry T, Minigo G, Piera KA, Hanley JC, de Silva HD, Salwati E, Kenangalem E, Tjitra E, Coppel RL, Price RN, Anstey NM, Plebanski M. 2008. Antibodies to Plasmodium falciparum and Plasmodium vivax merozoite surface protein 5 in Indonesia: species-specific and cross-reactive responses. J Infect Dis 198:134-42.

230. Igonet S, Vulliez-Le Normand B, Faure G, Riottot MM, Kocken CH, Thomas AW, Bentley GA. 2007. Cross-reactivity studies of an anti-Plasmodium vivax apical membrane antigen 1 monoclonal antibody: binding and structural characterisation. J Mol Biol 366:1523-37.

231. Cao Y, Bansal GP, Merino K, Kumar N. 2016. Immunological Cross-Reactivity between Malaria Vaccine Target Antigen P48/45 in Plasmodium vivax and P. falciparum and Cross-Boosting of Immune Responses. PLoS One 11:e0158212.

232. Ntumngia FB, Thomson-Luque R, Torres Lde M, Gunalan K, Carvalho LH, Adams JH. 2016. A Novel Erythrocyte Binding Protein of Plasmodium vivax Suggests an Alternate Invasion Pathway into Duffy-Positive Reticulocytes. MBio 7.

233. Mitran CJ, Mena A, Gnidehou S, Banman S, Arango E, Lima BAS, Lugo H, Ganesan A, Salanti A, Mbonye AK, Ntumngia F, Barakat K, Adams JH, Kano FS, Carvalho LH, Maestre AE, Good MF, Yanow SK. 2019. Antibodies to Cryptic Epitopes in Distant Homologues Underpin a Mechanism of Heterologous Immunity between Plasmodium vivax PvDBP and Plasmodium falciparum VAR2CSA. mBio 10.

234. Petousis-Harris H, Paynter J, Morgan J, Saxton P, McArdle B, Goodyear-Smith F, Black S. 2017. Effectiveness of a group B outer membrane vesicle meningococcal vaccine against gonorrhoea in New Zealand: a retrospective case-control study. The Lancet 390:1603-1610.

235. Paynter J, Goodyear-Smith F, Morgan J, Saxton P, Black S, Petousis-Harris H. 2019. Effectiveness of a Group B Outer Membrane Vesicle Meningococcal Vaccine in Preventing Hospitalization from Gonorrhea in New Zealand: A Retrospective Cohort Study. Vaccines (Basel) 7.

236. Lin MY, Reddy TB, Arend SM, Friggen AH, Franken KL, van Meijgaarden KE, Verduyn MJ, Schoolnik GK, Klein MR, Ottenhoff TH. 2009. Cross-reactive immunity to Mycobacterium tuberculosis DosR regulon-encoded antigens in individuals infected with environmental, nontuberculous mycobacteria. Infect Immun 77:5071-9.

237. Welsh RM, Che JW, Brehm MA, Selin LK. 2010. Heterologous immunity between viruses. Immunol Rev 235:244-66.

238. Chen HD, Fraire AE, Joris I, Welsh RM, Selin LK. 2003. Specific history of heterologous virus infections determines anti-viral immunity and immunopathology in the lung. Am J Pathol 163:1341-55.

239. Walzl G, Tafuro S, Moss P, Openshaw PJ, Hussell T. 2000. Influenza virus lung infection protects from respiratory syncytial virus-induced immunopathology. J Exp Med 192:1317-26.

240. Agrawal B, Gupta N, Vedi S, Singh S, Li W, Garg S, Li J, Kumar R. 2019. Heterologous Immunity between Adenoviruses and Hepatitis C Virus (HCV): Recombinant Adenovirus Vaccine Vectors Containing Antigens from Unrelated Pathogens Induce Cross-Reactive Immunity Against HCV Antigens. Cells 8.

241. Saron WAA, Rathore APS, Ting L, Ooi EE, Low J, Abraham SN, St John AL. 2018. Flavivirus serocomplex cross-reactive immunity is protective by activating heterologous memory CD4 T cells. Sci Adv 4:eaar4297.

242. Maitland K, Williams TN, Newbold CI. 1997. Plasmodium vevax and P. falciparum: Biological interactions and the possibility of cross-species immunity. Parasitol Today 13:227-31.

243. Gunewardena DM, Carter R, Mendis KN. 1994. Patterns of acquired anti-malarial immunity in Sri Lanka. Mem Inst Oswaldo Cruz 89 Suppl 2:63-5.

244. Bruce MC, Donnelly CA, Alpers MP, Galinski MR, Barnwell JW, Walliker D, Day KP. 2000. Cross-species interactions between malaria parasites in humans. Science 287:845-8.

245. Kingsbury AN. 1927. Some investigations of malarial fevers. IV - The complement fixation reaction. Transactions of The Royal Society of Tropical Medicine and Hygiene 19:359 - 364.

246. Row R. 1931. Precipitin Reaction in Malarial Sera. Transactions of the Royal Society of Tropical Medicine and Hygiene 24.

247. Hall CE, Hagan LM, Bergmann-Leitner E, Tosh DM, Bennett JW, Regules JA, Chuang I, Angov E, Dutta S, Chattopadhyay D, Yadava A. 2019. Mosquito Bite-Induced Controlled Human Malaria Infection with Plasmodium vivax or P. falciparum Generates Immune Responses to Homologous and Heterologous Preerythrocytic and Erythrocytic Antigens. Infect Immun 87.

248. Gnidehou S, Mitran CJ, Arango E, Banman S, Mena A, Medawar E, Lima BAS, Doritchamou J, Rajwani J, Jin A, Gavina K, Ntumngia F, Duffy PE, Narum D, Ndam NT, Nielsen MA, Salanti A, Kano FS, Carvalho LH, Adams JH, Maestre A, Good MF, Yanow SK. 2019. Cross-species immune recognition between Plasmodium vivax Duffy binding protein antibodies and the Plasmodium falciparum surface antigen VAR2CSA. The Journal of Infectious Diseases doi:10.1093/infdis/jiy467.

249. Fried M, Domingo GJ, Gowda CD, Mutabingwa TK, Duffy PE. 2006. Plasmodium falciparum: chondroitin sulfate A is the major receptor for adhesion of parasitized erythrocytes in the placenta. Exp Parasitol 113:36-42.

250. Smith JD, Rowe JA, Higgins MK, Lavstsen T. 2013. Malaria's deadly grip: cytoadhesion of Plasmodium falciparum-infected erythrocytes. Cell Microbiol 15:1976-83.

251. Kappe SH, Noe AR, Fraser TS, Blair PL, Adams JH. 1998. A family of chimeric erythrocyte binding proteins of malaria parasites. Proc Natl Acad Sci U S A 95:1230-5.

252. Ceravolo IP, Sanchez BA, Sousa TN, Guerra BM, Soares IS, Braga EM, McHenry AM, Adams JH, Brito CF, Carvalho LH. 2009. Naturally acquired inhibitory antibodies to Plasmodium vivax Duffy binding protein are short-lived and allele-specific following a single malaria infection. Clin Exp Immunol 156:502-10.

253. Mitran CJ, Mbonye AK, Hawkes M, Yanow SK. 2018. Using Reference Quantitative Polymerase Chain Reaction to Assess the Clinical Performance of the Paracheck-Pf (R) Rapid Diagnostic Test in a Field Setting in Uganda. American Journal of Tropical Medicine and Hygiene 99:357-359.

254. Ntumngia FB, Barnes SJ, McHenry AM, George MT, Schloegel J, Adams JH. 2014. Immunogenicity of a synthetic vaccine based on Plasmodium vivax Duffy binding protein region II. Clin Vaccine Immunol 21:1215-23.

255. Gnidehou S, Jessen L, Gangnard S, Ermont C, Triqui C, Quiviger M, Guitard J, Lund O, Deloron P, Ndam NT. 2010. Insight into antigenic diversity of VAR2CSA-DBL5epsilon domain from multiple Plasmodium falciparum placental isolates. PLoS One 5.

256. Soding J, Biegert A, Lupas AN. 2005. The HHpred interactive server for protein homology detection and structure prediction. Nucleic Acids Res 33:W244-8.

257. Wallner B, Elofsson A. 2003. Can correct protein models be identified? Protein Science 12:1073-1086.

258. Delano W. 2002. The Pymol Molecular Graphics System.

259. Chen E, Salinas ND, Huang Y, Ntumngia F, Plasencia MD, Gross ML, Adams JH, Tolia NH. 2016. Broadly neutralizing epitopes in the Plasmodium vivax vaccine candidate Duffy Binding Protein. Proc Natl Acad Sci U S A 113:6277-82.

260. George MT, Schloegel JL, Ntumngia FB, Barnes SJ, King CL, Casey JL, Foley M, Adams JH. 2019. Identification of an Immunogenic Broadly Inhibitory Surface Epitope of the Plasmodium vivax Duffy Binding Protein Ligand Domain. mSphere 4.

261. Resende M, Nielsen MA, Dahlback M, Ditlev SB, Andersen P, Sander AF, Ndam NT, Theander TG, Salanti A. 2008. Identification of glycosaminoglycan binding regions in the Plasmodium falciparum encoded placental sequestration ligand, VAR2CSA. Malar J 7:104.

262. Lopez-Perez M, Larsen MD, Bayarri-Olmos R, Ampomah P, Stevenson L, Arevalo-Herrera M, Herrera S, Hviid L. 2018. IgG Responses to the Plasmodium falciparum Antigen VAR2CSA in Colombia Are Restricted to Pregnancy and Are Not Induced by Exposure to Plasmodium vivax. Infect Immun 86.

263. Bajic G, Maron MJ, Adachi Y, Onodera T, McCarthy KR, McGee CE, Sempowski GD, Takahashi Y, Kelsoe G, Kuraoka M, Schmidt AG. 2019. Influenza Antigen Engineering Focuses Immune Responses to a Subdominant but Broadly Protective Viral Epitope. Cell Host Microbe 25:827-835 e6.

264. Bangaru S, Lang S, Schotsaert M, Vanderven HA, Zhu X, Kose N, Bombardi R, Finn JA, Kent SJ, Gilchuk P, Gilchuk I, Turner HL, Garcia-Sastre A, Li S, Ward AB, Wilson IA, Crowe JE, Jr. 2019. A Site of Vulnerability on the Influenza Virus Hemagglutinin Head Domain Trimer Interface. Cell 177:1136-1152 e18.

265. Watanabe A, McCarthy KR, Kuraoka M, Schmidt AG, Adachi Y, Onodera T, Tonouchi K, Caradonna TM, Bajic G, Song S, McGee CE, Sempowski GD, Feng F, Urick P, Kepler TB, Takahashi Y, Harrison SC, Kelsoe G. 2019. Antibodies to a Conserved

Influenza Head Interface Epitope Protect by an IgG Subtype-Dependent Mechanism. Cell 177:1124-1135 e16.

266. Li J, Watterson D, Chang CW, Che XY, Li XQ, Ericsson DJ, Qiu LW, Cai JP, Chen J, Fry SR, Cheung STM, Cooper MA, Young PR, Kobe B. 2018. Structural and Functional Characterization of a Cross-Reactive Dengue Virus Neutralizing Antibody that Recognizes a Cryptic Epitope. Structure 26:51-+.

267. Dowd KA, Jost CA, Durbin AP, Whitehead SS, Pierson TC. 2011. A dynamic landscape for antibody binding modulates antibody-mediated neutralization of West Nile virus. PLoS Pathog 7:e1002111.

268. Lok SM, Kostyuchenko V, Nybakken GE, Holdaway HA, Battisti AJ, Sukupolvi-Petty S, Sedlak D, Fremont DH, Chipman PR, Roehrig JT, Diamond MS, Kuhn RJ, Rossmann MG. 2008. Binding of a neutralizing antibody to dengue virus alters the arrangement of surface glycoproteins. Nat Struct Mol Biol 15:312-7.

269. Pierson TC, Diamond MS. 2012. Degrees of maturity: the complex structure and biology of flaviviruses. Curr Opin Virol 2:168-75.

270. Bockhorst J, Lu F, Janes JH, Keebler J, Gamain B, Awadalla P, Su XZ, Samudrala R, Jojic N, Smith JD. 2007. Structural polymorphism and diversifying selection on the pregnancy malaria vaccine candidate VAR2CSA. Mol Biochem Parasitol 155:103-12.

271. Bordbar B, Tuikue Ndam N, Renard E, Jafari-Guemouri S, Tavul L, Jennison C, Gnidehou S, Tahar R, Gamboa D, Bendezu J, Menard D, Barry AE, Deloron P, Sabbagh A. 2014. Genetic diversity of VAR2CSA ID1-DBL2Xb in worldwide Plasmodium falciparum populations: impact on vaccine design for placental malaria. Infect Genet Evol 25:81-92.

272. Mordmuller B, Sulyok M, Egger-Adam D, Resende M, de Jongh WA, Jensen MH, Smedegaard HH, Ditlev SB, Soegaard M, Poulsen L, Dyring C, Calle CL, Knoblich A, Ibanez J, Esen M, Deloron P, Ndam N, Issifou S, Houard S, Howard RF, Reed SG, Leroy O, Luty AJF, Theander TG, Kremsner PG, Salanti A, Nielsen MA. 2019. First-in-human, randomized, double-blind clinical trial of differentially adjuvanted PAMVAC, a vaccine candidate to prevent pregnancy-associated malaria. Clin Infect Dis doi:10.1093/cid/ciy1140.

273. Beeson JG, Elliott SR, Hommel M. 2008. Polymorphic and conserved targets of antibodies against Plasmodium falciparum during pregnancy. J Infect Dis 197:1350-1; author reply 1351-2.

274. Doritchamou J, Teo A, Morrison R, Arora G, Kwan J, Manzella-Lapeira J, Medina-Maldonado S, Langhorne J, Hviid L, Narum DL, Dicko A, Fried M, Duffy PE. 2019. Functional Antibodies against Placental Malaria Parasites Are Variant Dependent and Differ by Geographic Region. Infect Immun 87.

275. Doritchamou JY, Herrera R, Aebig JA, Morrison R, Nguyen V, Reiter K, Shimp RL, MacDonald NJ, Narum DL, Fried M, Duffy PE. 2016. VAR2CSA Domain-Specific Analysis of Naturally Acquired Functional Antibodies to Plasmodium falciparum Placental Malaria. J Infect Dis 214:577-86.

276. Oscherwitz J. 2016. The promise and challenge of epitope-focused vaccines. Hum Vaccin Immunother 12:2113-2116.

277. Good MF, Yanow SK. 2016. Cryptic epitope for antibodies should not be forgotten in vaccine design. Expert Rev Vaccines 15:675-6.

278. Kaplan G, Roitburd-Berman A, Lewis GK, Gershoni JM. 2016. Range of CD4-Bound Conformations of HIV-1 gp120, as Defined Using Conditional CD4-Induced Antibodies. J Virol 90:4481-4493.

279. Lertjuthaporn S, Cicala C, Van Ryk D, Liu M, Yolitz J, Wei D, Nawaz F, Doyle A, Horowitch B, Park C, Lu S, Lou Y, Wang S, Pan R, Jiang X, Villinger F, Byrareddy SN, Santangelo PJ, Morris L, Wibmer CK, Biris K, Mason RD, Gorman J, Hiatt J, Martinelli E, Roederer M, Fujikawa D, Gorini G, Franchini G, Arakelyan A, Ansari AA, Pattanapanyasat K, Kong XP, Fauci AS, Arthos J. 2018. Select gp120 V2 domain specific antibodies derived from HIV and SIV infection and vaccination inhibit gp120 binding to alpha4beta7. PLoS Pathog 14:e1007278.

280. Mitchell DAJ, Dupuy LC, Sanchez-Lockhart M, Palacios G, Back JW, Shimanovskaya K, Chaudhury S, Ripoll DR, Wallqvist A, Schmaljohn CS. 2017. Epitope mapping of Ebola virus dominant and subdominant glycoprotein epitopes facilitates construction of an epitope-based DNA vaccine able to focus the antibody response in mice. Hum Vaccin Immunother 13:2883-2893.

281. West BR, Moyer CL, King LB, Fusco ML, Milligan JC, Hui S, Saphire EO. 2018. Structural Basis of Pan-Ebolavirus Neutralization by a Human Antibody against a Conserved, yet Cryptic Epitope. Mbio 9.

282. Lee YJ, Yu JE, Kim P, Lee JY, Cheong YC, Lee YJ, Chang J, Seong BL. 2018. Eliciting unnatural immune responses by activating cryptic epitopes in viral antigens. FASEB J 32:4658-4669.

283. Ekiert DC, Bhabha G, Elsliger MA, Friesen RH, Jongeneelen M, Throsby M, Goudsmit J, Wilson IA. 2009. Antibody recognition of a highly conserved influenza virus epitope. Science 324:246-51.

284. Ozberk V, Pandey M, Good MF. 2018. Contribution of cryptic epitopes in designing a group A streptococcal vaccine. Hum Vaccin Immunother 14:2034-2052.

285. Stiasny K, Kiermayr S, Holzmann H, Heinz FX. 2006. Cryptic properties of a cluster of dominant flavivirus cross-reactive antigenic sites. J Virol 80:9557-68.

286. Mitran CJ, Higa LM, Good MF, Yanow SK. 2020. Generation of a Peptide Vaccine Candidate against Falciparum Placental Malaria Based on a Discontinuous Epitope. Vaccines (Basel) 8.

287. Fried M, Duffy PE. 1998. Maternal malaria and parasite adhesion. J Mol Med (Berl) 76:162-71.

288. Pandey M, Ozberk V, Langshaw EL, Calcutt A, Powell J, Batzloff MR, Rivera-Hernandez T, Good MF. 2018. Skin infection boosts memory B-cells specific for a cryptic vaccine epitope of group A streptococcus and broadens the immune response to enhance vaccine efficacy. NPJ Vaccines 3:15.

289. Jones GL, Edmundson HM, Spencer L, Gale J, Saul A. 1989. The use of maleimidocaproyloxysuccinimide to prepare malarial peptide carrier immunogens. Immunogenicity of the linking region. J Immunol Methods 123:211-6.

290. Timmerman P, Puijk WC, Meloen RH. 2007. Functional reconstruction and synthetic mimicry of a conformational epitope using CLIPS technology. J Mol Recognit 20:283-99.

291. Quintana MDP, Anabire NG, Hviid L. 2020. Measuring Naturally Acquired Phagocytosis-Inducing Antibodies to Plasmodium falciparum Parasites by a Flow Cytometry-Based Assay. J Vis Exp doi:10.3791/61538.

292. Chen SW, Van Regenmortel MH, Pellequer JL. 2009. Structure-activity relationships in peptide-antibody complexes: implications for epitope prediction and development of synthetic peptide vaccines. Curr Med Chem 16:953-64.

293. Van Regenmortel MH. 2009. What is a B-cell epitope? Methods Mol Biol 524:3-20.

294. Amoah LE, Abagna HB, Akyea-Mensah K, Lo AC, Kusi KA, Gyan BA. 2018. Characterization of anti-EBA175RIII-V in asymptomatic adults and children living in communities in the Greater Accra Region of Ghana with varying malaria transmission intensities. BMC Immunol 19:34.

295. Ssewanyana I, Arinaitwe E, Nankabirwa JI, Yeka A, Sullivan R, Kamya MR, Rosenthal PJ, Dorsey G, Mayanja-Kizza H, Drakeley C, Greenhouse B, Tetteh KK. 2017. Avidity of anti-malarial antibodies inversely related to transmission intensity at three sites in Uganda. Malar J 16:67.

296. Adjah J, Fiadzoe B, Ayanful-Torgby R, Amoah LE. 2018. Seasonal variations in Plasmodium falciparum genetic diversity and multiplicity of infection in asymptomatic children living in southern Ghana. BMC Infect Dis 18:432.

297. Anders RF. 1986. Multiple cross-reactivities amongst antigens of Plasmodium falciparum impair the development of protective immunity against malaria. Parasite Immunol 8:529-39.

298. Cadman ET, Abdallah AY, Voisine C, Sponaas AM, Corran P, Lamb T, Brown D, Ndungu F, Langhorne J. 2008. Alterations of splenic architecture in malaria are induced independently of Toll-like receptors 2, 4, and 9 or MyD88 and may affect antibody affinity. Infect Immun 76:3924-31.

299. Ibison F, Olotu A, Muema DM, Mwacharo J, Ohuma E, Kimani D, Marsh K, Bejon P, Ndungu FM. 2012. Lack of avidity maturation of merozoite antigen-specific antibodies with increasing exposure to Plasmodium falciparum amongst children and adults exposed to endemic malaria in Kenya. PLoS One 7:e52939.

300. Jain D, Salunke DM. 2019. Antibody specificity and promiscuity. Biochem J 476:433-447.

301. Leoratti FM, Durlacher RR, Lacerda MV, Alecrim MG, Ferreira AW, Sanchez MC, Moraes SL. 2008. Pattern of humoral immune response to Plasmodium falciparum blood stages in individuals presenting different clinical expressions of malaria. Malar J 7:186.

302. Ferreira MU, Kimura EA, De Souza JM, Katzin AM. 1996. The isotype composition and avidity of naturally acquired anti-Plasmodium falciparum antibodies: differential patterns in clinically immune Africans and Amazonian patients. Am J Trop Med Hyg 55:315-23.

303. Babakhanyan A, Fang R, Wey A, Salanti A, Sama G, Efundem C, Leke RJ, Chen JJ, Leke RG, Taylor DW. 2015. Comparison of the specificity of antibodies to VAR2CSA in Cameroonian multigravidae with and without placental malaria: a retrospective case-control study. Malar J 14:480.

304. Ma R, Lian T, Huang R, Renn JP, Petersen JD, Zimmerberg J, Duffy PE, Tolia NH. 2021. Structural basis for placental malaria mediated by Plasmodium falciparum VAR2CSA. Nat Microbiol 6:380-391.

305. Ataide R, Hasang W, Wilson DW, Beeson JG, Mwapasa V, Molyneux ME, Meshnick SR, Rogerson SJ. 2010. Using an improved phagocytosis assay to evaluate the effect of HIV on specific antibodies to pregnancy-associated malaria. PLoS One 5:e10807.

306. Hommel M, Chan JA, Umbers AJ, Langer C, Rogerson SJ, Smith JD, Beeson JG. 2018. Evaluating antibody functional activity and strain-specificity of vaccine candidates for malaria in pregnancy using in vitro phagocytosis assays. Parasit Vectors 11:69.

307. Arora G, Hart GT, Manzella-Lapeira J, Doritchamou JY, Narum DL, Thomas LM, Brzostowski J, Rajagopalan S, Doumbo OK, Traore B, Miller LH, Pierce SK, Duffy PE, Crompton PD, Desai SA, Long EO. 2018. NK cells inhibit Plasmodium falciparum growth in red blood cells via antibody-dependent cellular cytotoxicity. Elife 7.

308. Hart GT, Tran TM, Theorell J, Schlums H, Arora G, Rajagopalan S, Sangala ADJ, Welsh KJ, Traore B, Pierce SK, Crompton PD, Bryceson YT, Long EO. 2019. Adaptive NK cells in people exposed to Plasmodium falciparum correlate with protection from malaria. J Exp Med 216:1280-1290.

309. Aitken EH, Alemu A, Rogerson SJ. 2018. Neutrophils and Malaria. Front Immunol 9:3005.

310. Saveria T, Oleinikov AV, Wiliamson K, Chaturvedi R, Lograsso J, Keitany GJ, Fried M, Duffy P. 2013. Antibodies to Escherichia coli-expressed C-terminal domains of Plasmodium falciparum variant surface antigen 2-chondroitin sulfate A (VAR2CSA) inhibit binding of CSA-adherent parasites to placental tissue. Infect Immun 81:1031-9.

311. Thompson EA, Ols S, Miura K, Rausch K, Narum DL, Spangberg M, Juraska M, Wille-Reece U, Weiner A, Howard RF, Long CA, Duffy PE, Johnston L, O'Neil CP, Lore K. 2018. TLR-adjuvanted nanoparticle vaccines differentially influence the quality and longevity of responses to malaria antigen Pfs25. JCI Insight 3.

312. Phillips B, Van Rompay KKA, Rodriguez-Nieves J, Lorin C, Koutsoukos M, Tomai M, Fox CB, Eudailey J, Dennis M, Alam SM, Hudgens M, Fouda G, Pollara J, Moody A, Shen X, Ferrari G, Permar S, De Paris K. 2018. Adjuvant-Dependent Enhancement of HIV Env-Specific Antibody Responses in Infant Rhesus Macaques. J Virol 92.

313. Anderson RC, Fox CB, Dutill TS, Shaverdian N, Evers TL, Poshusta GR, Chesko J, Coler RN, Friede M, Reed SG, Vedvick TS. 2010. Physicochemical characterization and biological activity of synthetic TLR4 agonist formulations. Colloids Surf B Biointerfaces 75:123-32.

314. Coler RN, Baldwin SL, Shaverdian N, Bertholet S, Reed SJ, Raman VS, Lu X, DeVos J, Hancock K, Katz JM, Vedvick TS, Duthie MS, Clegg CH, Van Hoeven N, Reed SG. 2010. A synthetic adjuvant to enhance and expand immune responses to influenza vaccines. PLoS One 5:e13677.

315. Orr MT, Duthie MS, Windish HP, Lucas EA, Guderian JA, Hudson TE, Shaverdian N, O'Donnell J, Desbien AL, Reed SG, Coler RN. 2013. MyD88 and TRIF synergistic interaction is required for TH1-cell polarization with a synthetic TLR4 agonist adjuvant. Eur J Immunol 43:2398-408.

316. Windish HP, Duthie MS, Misquith A, Ireton G, Lucas E, Laurance JD, Bailor RH, Coler RN, Reed SG. 2011. Protection of mice from Mycobacterium tuberculosis by ID87/GLA-SE, a novel tuberculosis subunit vaccine candidate. Vaccine 29:7842-8.

317. Singh K, Mukherjee P, Shakri AR, Singh A, Pandey G, Bakshi M, Uppal G, Jena R, Rawat A, Kumar P, Bhardwaj R, Yazdani SS, Hans D, Mehta S, Srinivasan A, Anil K, Madhusudhan RL, Patel J, Singh A, Rao R, Gangireddy S, Patil R, Kaviraj S, Singh S, Carter D, Reed S, Kaslow DC, Birkett A, Chauhan VS, Chitnis CE. 2018. Malaria vaccine candidate based on Duffy-binding protein elicits strain transcending functional antibodies in a Phase I trial. NPJ Vaccines 3:48.

318. Steiner-Monard V, Kamaka K, Karoui O, Roethlisberger S, Audran R, Daubenberger C, Fayet-Mello A, Erdmann-Voisin A, Felger I, Geiger K, Govender L, Houard S, Huber E, Mayor C, Mkindi C, Portevin D, Rusch S, Schmidlin S, Tiendrebeogo RW, Theisen M, Thierry AC, Vallotton L, Corradin G, Leroy O, Abdulla S, Shekalaghe S, Genton B,

Spertini F, Jongo SA. 2019. The Candidate Blood-stage Malaria Vaccine P27A Induces a Robust Humoral Response in a Fast Track to the Field Phase 1 Trial in Exposed and Nonexposed Volunteers. Clin Infect Dis 68:466-474.

319. Pirahmadi S, Zakeri S, Djadid ND, Mehrizi AA. 2021. A review of combination adjuvants for malaria vaccines: a promising approach for vaccine development. Int J Parasitol doi:10.1016/j.ijpara.2021.01.006.

320. Patra KP, Li F, Carter D, Gregory JA, Baga S, Reed SG, Mayfield SP, Vinetz JM. 2015. Alga-produced malaria transmission-blocking vaccine candidate Pfs25 formulated with a human use-compatible potent adjuvant induces high-affinity antibodies that block Plasmodium falciparum infection of mosquitoes. Infect Immun 83:1799-808.

321. Marty-Roix R, Vladimer GI, Pouliot K, Weng D, Buglione-Corbett R, West K, MacMicking JD, Chee JD, Wang S, Lu S, Lien E. 2016. Identification of QS-21 as an Inflammasome-activating Molecular Component of Saponin Adjuvants. J Biol Chem 291:1123-36.

322. Perrie Y, Crofts F, Devitt A, Griffiths HR, Kastner E, Nadella V. 2016. Designing liposomal adjuvants for the next generation of vaccines. Adv Drug Deliv Rev 99:85-96.

323. Espinosa DA, Vega-Rodriguez J, Flores-Garcia Y, Noe AR, Munoz C, Coleman R, Bruck T, Haney K, Stevens A, Retallack D, Allen J, Vedvick TS, Fox CB, Reed SG, Howard RF, Salman AM, Janse CJ, Khan SM, Zavala F, Gutierrez GM. 2017. The Plasmodium falciparum Cell-Traversal Protein for Ookinetes and Sporozoites as a Candidate for Preerythrocytic and Transmission-Blocking Vaccines. Infect Immun 85.

324. Radtke AJ, Anderson CF, Riteau N, Rausch K, Scaria P, Kelnhofer ER, Howard RF, Sher A, Germain RN, Duffy P. 2017. Adjuvant and carrier protein-dependent T-cell priming promotes a robust antibody response against the Plasmodium falciparum Pfs25 vaccine candidate. Sci Rep 7:40312.

325. Macias A, Ruiz-Palacios G, Ramos-Castaneda J. 2020. Combine dengue vaccines to optimize effectiveness. Vaccine 38:4801-4804.

326. He Q, Mao Q, An C, Zhang J, Gao F, Bian L, Li C, Liang Z, Xu M, Wang J. 2021. Heterologous prime-boost: breaking the protective immune response bottleneck of COVID-19 vaccine candidates. Emerg Microbes Infect 10:629-637.

327. Wang S, Parker C, Taaffe J, Solorzano A, Garcia-Sastre A, Lu S. 2008. Heterologous HA DNA vaccine prime--inactivated influenza vaccine boost is more effective than using DNA or inactivated vaccine alone in eliciting antibody responses against H1 or H3 serotype influenza viruses. Vaccine 26:3626-33.

328. Powlson J, Wright D, Zeltina A, Giza M, Nielsen M, Rampling T, Venkatrakaman N, Bowden TA, Hill AVS, Ewer KJ. 2019. Characterization of Antigenic MHC-Class-I-Restricted T Cell Epitopes in the Glycoprotein of Ebolavirus. Cell Rep 29:2537-2545 e3.

329. Gil A, Shen S, Coley S, Gibson L, Diamond DJ, Wang S, Lu S. 2013. DNA vaccine prime followed by boost with live attenuated virus significantly improves antigen-specific T cell responses against human cytomegalovirus. Hum Vaccin Immunother 9:2120-32.

330. Excler JL, Kim JH. 2019. Novel prime-boost vaccine strategies against HIV-1. Expert Rev Vaccines 18:765-779.

331. McNamara HA, Idris AH, Sutton HJ, Vistein R, Flynn BJ, Cai Y, Wiehe K, Lyke KE, Chatterjee D, Kc N, Chakravarty S, Lee Sim BK, Hoffman SL, Bonsignori M, Seder RA, Cockburn IA. 2020. Antibody Feedback Limits the Expansion of B Cell Responses to Malaria Vaccination but Drives Diversification of the Humoral Response. Cell Host Microbe 28:572-585 e7.

332. Ntumngia FB, Pires CV, Barnes SJ, George MT, Thomson-Luque R, Kano FS, Alves JRS, Urusova D, Pereira DB, Tolia NH, King CL, Carvalho LH, Adams JH. 2017. An engineered vaccine of the Plasmodium vivax Duffy binding protein enhances induction of broadly neutralizing antibodies. Sci Rep 7:13779.

333. Good MF, Reiman JM, Rodriguez IB, Ito K, Yanow SK, El-Deeb IM, Batzloff MR, Stanisic DI, Engwerda C, Spithill T, Hoffman SL, Lee M, McPhun V. 2013. Cross-species malaria immunity induced by chemically attenuated parasites. J Clin Invest doi:10.1172/JCI66634.

334. Richie TL. 1988. Interactions between malaria parasites infecting the same vertebrate host. Parasitology 96 (Pt 3):607-39.

335. Flaxman A, Ewer KJ. 2018. Methods for Measuring T-Cell Memory to Vaccination: From Mouse to Man. Vaccines (Basel) 6.

336. McCall MBB, Kremsner PG, Mordmuller B. 2018. Correlating efficacy and immunogenicity in malaria vaccine trials. Semin Immunol 39:52-64.

337. Duncan CJ, Hill AV, Ellis RD. 2012. Can growth inhibition assays (GIA) predict blood-stage malaria vaccine efficacy? Hum Vaccin Immunother 8:706-14.

338. Pehrson C, Heno KK, Adams Y, Resende M, Mathiesen L, Soegaard M, de Jongh WA, Theander TG, Salanti A, Nielsen MA. 2017. Comparison of functional assays used in the clinical development of a placental malaria vaccine. Vaccine 35:610-618.

339. Ahmad TA, Eweida AE, Sheweita SA. 2016. B-cell epitope mapping for the design of vaccines and effective diagnostics. Trials in Vaccinology 5:71-83.

340. Chaudhury S, Reifman J, Wallqvist A. 2014. Simulation of B cell affinity maturation explains enhanced antibody cross-reactivity induced by the polyvalent malaria vaccine AMA1. J Immunol 193:2073-86.

341. Ntumngia FB, Adams JH. 2012. Design and immunogenicity of a novel synthetic antigen based on the ligand domain of the Plasmodium vivax duffy binding protein. Clin Vaccine Immunol 19:30-6.

342. Mendes AM, Machado M, Goncalves-Rosa N, Reuling IJ, Foquet L, Marques C, Salman AM, Yang ASP, Moser KA, Dwivedi A, Hermsen CC, Jimenez-Diaz B, Viera S, Santos JM, Albuquerque I, Bhatia SN, Bial J, Angulo-Barturen I, Silva JC, Leroux-Roels G, Janse CJ, Khan SM, Mota MM, Sauerwein RW, Prudencio M. 2018. A Plasmodium berghei sporozoite-based vaccination platform against human malaria. NPJ Vaccines 3:33.

343. Harrison K, Rahimi N, Danovaro-Holliday MC. 2020. Factors limiting data quality in the expanded programme on immunization in low and middle-income countries: A scoping review. Vaccine 38:4652-4663.

344. Keja K, Chan C, Hayden G, Henderson RH. 1988. Expanded programme on immunization. World Health Stat Q 41:59-63.

345. PAHO. 2020. Immunization Data and Statistics. https://www.paho.org/en/topics/immunization/immunization-data-and-statistics. Accessed

346. WHO. 2020. Policy and Decision-making for HPV Vaccine Introduction. http://www.who.int/immunization/hpv/deliver/en/. Accessed

347. Bruni L, Diaz M, Barrionuevo-Rosas L, Herrero R, Bray F, Bosch FX, de Sanjose S, Castellsague X. 2016. Global estimates of human papillomavirus vaccination coverage by region and income level: a pooled analysis. Lancet Glob Health 4:e453-63.

348. Organization WH. 2018. MALARIA SURVEILLANCE, MONITORING & EVALUATION: A REFERENCE MANUAL.

349. Duffy P, Desowitz RS. 2001. Pregnancy malaria throughout history: Dangerous labors. In Malaria in pregnancy: Deadly parasite, susceptible host. *In* Duffy P, Fried, M (ed). Taylor & Francis, New York.

350. Nosten F, ter Kuile F, Maelankirri L, Decludt B, White NJ. 1991. Malaria during pregnancy in an area of unstable endemicity. Trans R Soc Trop Med Hyg 85:424-9.